

# Topics in Applied Physics – Volume 110

Rainer Behrisch, Wolfgang Eckstein (Eds.)

---

*Sputtering by Particle Bombardment,  
Experiments and Computer Calculations  
from Threshold to MeV Energies*

---

Reprint of the book chapter **”Sputtering Yields”**

by W. Eckstein published in:  
Sputtering by Particle Bombardment, Experiments and Computer  
Calculations from Threshold to MeV Energies  
R. Behrisch and W. Eckstein (Eds.)  
Springer, Berlin 2007, pp. 33 - 186.

The original publication is available at [www.springerlink.com](http://www.springerlink.com)

**Springer**

Berlin Heidelberg New York  
Barcelona Budapest Hong Kong  
London Milan Paris  
Santa Clara Singapore Tokyo

**2007**

ISBN 987-3-540-44500-5

# Sputtering Yields

W. Eckstein

Max-Planck-Institut für Plasmaphysik, Boltzmannstr.2, D-85748 Garching,  
Germany wge@ipp.mpg.de

**Abstract.** Sputtering is caused by collision cascades initiated by energetic ions or neutrals incident on a solid or liquid target. The sputtering yield,  $Y$ , i.e. the average number of atoms removed from a target per incident particle (atom or ion), is the most global value in sputtering. It depends on the target material, on the species of bombarding particles and their energy and the angle of incidence. Most experimental and calculated results have been determined for amorphous and polycrystalline targets but also values for single crystal targets are available. An extensive comparison of experimental and calculated yield values are provided and the accuracies of these values are discussed. The sputtering yields of multicomponent systems depend on the bombarding fluence and show sometimes a complicated behaviour.

## 1 Experimental Methods

Several conditions have to be fulfilled for achieving reliable and reproducible results [1,2]:

- a) The beam of incident particles (ions or neutrals) should have a well defined energy with a small energy width (important especially at low energies) and a small angular divergence (important at grazing incidence). The beam should be mass-analyzed, especially for light ions, in order to separate different species such as molecular ions from atomic ions and especially particles with very different masses. The incident fluence should be measured accurately, which affords the knowledge of the ion current.
- b) For elemental targets the impurity content in the target should be negligible, especially if impurities have masses very different from the investigated element. Due to the dependence of the yield on the angle of incidence the target should be flat. An initially polished surface will, however, generally become rough during particle bombardment [3,4]. Implantation of the bombarding species into the target will also modify the yield; therefore a measurement of the yield versus the incident fluence is valuable to show the difference between low fluence and steady state (saturation). Most targets are not amorphous and the crystal grains are not randomly oriented. The target structure, if not a single crystal, should be checked to have an idea about any texture of the target. For a sputtering measurement at a target consisting of a thin film on a substrate, the film should be thick enough, that the underlying substrate does not modify the collision cascade in the film.

c) The vacuum conditions should be good enough, that adsorption of residual gas species on the target during bombardment is negligible. This is of special importance if the yields are low such as for light incident ions and for oxide and nitride forming elements. The general condition is, that the arrival number and the sticking probability of these rest gas species per unit time must be smaller than the corresponding arrival of beam species times the sputtering yield of the gas species.

For the determination the sputtering yield the incident fluence and the removed target material have to be measured. The incident fluence is usually determined by the incident charge, the removed material by several methods [2]:

a) Mass change.

The amount of material removed from an elemental target can be determined by the measured mass change,  $\Delta m$ , giving for the sputtering yield

$$Y = \frac{\Delta m}{M_2 n_1} N_0 \quad (1)$$

where  $M_2$  is the target atomic mass,  $n_1$  is the number of incident projectile ions (atoms), and  $N_0$  is the Avogadro number. This formula is only correct, if implantation and trapping of bombarding projectiles [4,5] into the target is negligible. This is justified for light ions implanted into a target of heavy atoms, if their concentration stays low during bombardment and if the light ions do not accumulate in the target, i.e. diffusion into the bulk can be neglected. The mass change of a thin film evaporated on a quartz crystal oscillator can be determined by a frequency change of the oscillator [6–8]. Other problems are the weighing of the bombarded target outside the bombarding vacuum chamber due to adsorption of water or oxygen at the surface, adsorption of gaseous species inside the vacuum chamber, and surface roughness.

b) Thickness change.

The amount of material removed can be determined by the measurement of the thickness change of a thin film, for example, with Rutherford backscattering [9,10]. The measured areal density before and after bombardment give the yield. Other methods are x-ray analysis, nuclear reaction analysis, methods using electrons such as an electron microprobe or transmission electron microscopy, mechanical methods such as the measurement of crater depth, and changes in interference colours. Changes in electrical resistivity have been applied to thin metal films and wires [11,12]. Thin metal films have been sputtered until a hole appeared [13]. Possible errors are forward sputtering and a nonuniform current density distribution.

c) Collection of sputtered material.

Another procedure to determine the amount of atoms removed is a measurement of the sputtered material by collecting it on catcher foils. Possible errors are an incomplete collection of sputtered material due to a limited

solid angle (smaller than half space), incomplete sticking, backscattering and sputtering of the deposited films. This is especially important for high energy sputtered atoms at oblique incidence bombardment. Another very sensitive technique is neutron activation of the collected material or of the target [14,15].

d) Field ion microscopy.

This method allows counting of the atoms sputtered from a tip, but a problem appears for the determination of the incident ion fluence [16,17]. An array of tips was used.

e) Spectroscopy method.

A plasma column in front of the target is may be used for exciting the sputtered neutrals. Specific emission lines are observed [18]. The method needs knowledge about the plasma, and for the calculation of the excitation rate it relies on an atomic data base as ADAS [19]. The method is fast and very sensitive.

With these techniques a large amount of sputtering yield data have been accumulated for many ion-target combinations, mostly for polycrystalline targets.

## 2 Calculational Methods

Several efforts have been made to calculate sputtering yields for amorphous, polycrystalline and single crystal targets [20–23]. Besides the analytic approach by *Sigmund* [20,21] many sputtering yields have been calculated with computer programs based on the binary collision approximation, see Chapter by Eckstein and Urbassek . A large number of yields have been provided mainly by *Yamamura* [24,25] with his program ACAT [26] and by *Eckstein* [27] with the program TRIM.SP [28,29]. These authors use different interaction potentials, Yamamura the Nakagawa-Yamamura potential [30], Eckstein the KrC (WHB) potential [31]. For the surface binding energy [29] the heat of sublimation is applied. A comparison for the energy dependence of the sputtering yield of silver bombarded with Ar calculated with different interaction potentials is shown in Fig. 1. Whereas the KrC, ZBL, and Moliere (correction factor to the screening length,  $ca=0.8$ ) potentials give nearly the same results, however, Moliere (with  $ca=1$ ) and Nakagawa-Yamamura potentials show larger yields at higher bombarding energies. For comparison also sputtering yields determined by the analytic theory are given; these values are generally higher than the yields obtained by computer programs. In the threshold region the differences in the yield calculated with the different potentials are more pronounced due to the differences of the potentials at large interatomic distances.

For the inelastic energy loss an equipartition of the Lindhard-Scharff and the Oen-Robinson models is used in some computer simulations (see Chapter

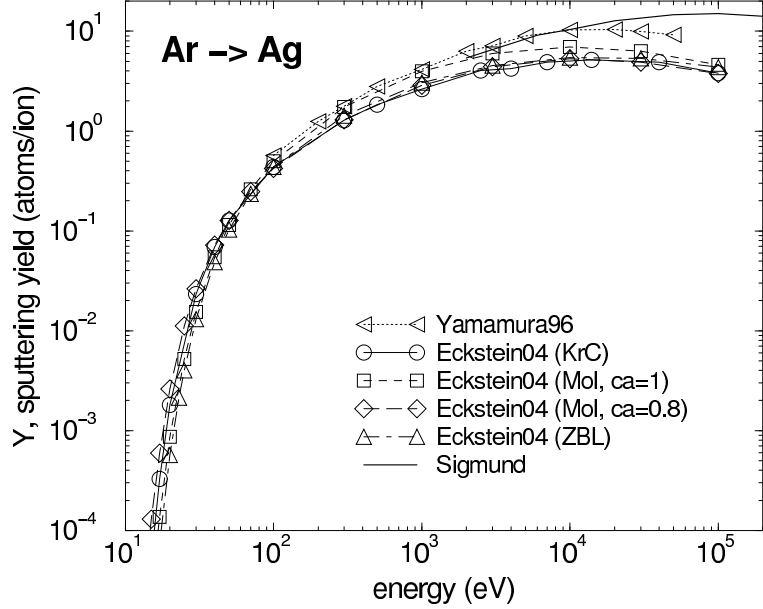


**Fig. 1.** Calculated energy dependence of the sputtering yield at normal incidence for the bombardment of Ag with Ar for different interaction potentials ( $ca$  is a correction factor to the screening length) calculated by Yamamura [24,25] and by Eckstein [32]. The curve from the analytic theory (Sigmund) is taken from [2]. Lines are drawn to guide the eye

by Eckstein, Urbassek). The influence of inelastic energy losses in the calculated sputtering yields is shown in Fig. 2. As expected the effect of the inelastic energy loss is smallest in the keV energy range and increases with higher and lower incident energies. The relative small effect may be a justification for the neglect of the inelastic energy loss in the analytic theory.

No assumptions are made to improve agreement with experimental data. Only for light ions Yamamura introduced small corrections in the screening length [24,25] in the interaction potential, which he supported by theoretical arguments [33].

The static BCA programs allow the determination of sputtering yields under the assumption that the target composition is not changed during bombardment. This applies for selfbombardment, hydrogen and noble gas bombardment, as long as trapping of these species can be regarded as negligible. In most other cases, such as, for example, for metal atom bombardment of carbon the target composition is changed in the implantation range. Then the yield will change with bombarding time or ion fluence. In these cases a dynamic program such as TRIDYN [29,34,35] has to be applied. An exception is the bombardment with a low fluence (negligible target change).

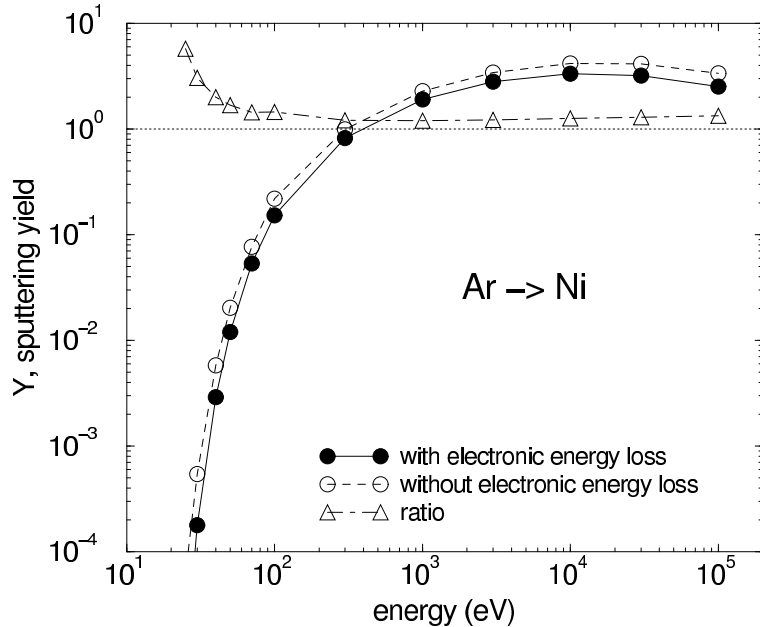


**Fig. 2.** Calculated energy dependence of the sputtering yield at normal incidence for the bombardment of Ni with Ar with and without inelastic energy loss calculated with TRIM.SP [32]. Lines are drawn to guide the eye

### 3 Mono-atomic Targets

As bombarding particles mainly hydrogen isotopes and noble gases have been used. The implicit assumption is, that target composition changes due to bombardment as for example by implantation are negligible. All other examples are discussed in sections 4 to 8. Experimental data up to 1981 were presented in the review by *Andersen and Bay* [2]. Since that time computer simulation has provided many values [24,25,36]. Collection of sputtering yields for special materials for the nuclear fusion community can be found in [37–41].

#### 3.1 Energy Dependence of the Sputtering Yield at Normal Incidence

For the survey of the many experimental and calculated sputtering yields at normal incidence the following procedure has been adopted. The calculated values have been fitted by an empirical formula and will be compared with experimental data, see 3.3. The reasoning for this procedure is the following: The experimental data often cover only a limited energy range between the threshold energy and at least 10 keV, whereas missing values can be obtained by calculations. Another point is, possible systematic deviations between calculated and experimental data will show up more clearly. In experiments the

target surface roughness (which may change even with ion fluence) is usually not known, whereas in calculations a nearly flat surface is assumed. Due to the increase of the sputtering yield with an increasing angle of incidence (with respect to the surface normal) the experimental data at normal incidence should generally give a somewhat higher value than the calculated values (up to a factor of two). On the other side, simulations may suffer from insufficiently accurate interaction potentials or inelastic energy losses.

The procedure applied here is different from the fitting by *Yamamura* [24,25] and *Janev* [42], who used the available experimental data and some calculated values for the fitting. In the last mentioned paper the authors derived a unified analytic representation for the sputtering yields, which is not convenient for practical purposes.

### 3.2 Fitting

Many formulae have been proposed to describe the energy dependence of the sputtering yield at normal incidence, see [43] and the literature in this paper. In this book the energy dependence of sputtering yields calculated for normal incidence has been fitted with the formula proposed by *Eckstein* and *Preuss* [44], which gives generally a better description of the available yield values; it was also used in [41]:

$$Y(E_0) = q s_n^{KrC}(\varepsilon_L) \frac{\left(\frac{E_0}{E_{th}} - 1\right)^\mu}{\lambda/w(\varepsilon_L) + \left(\frac{E_0}{E_{th}} - 1\right)^\mu} \quad (2)$$

with the nuclear stopping power for the KrC (WKB) potential [43]

$$\begin{aligned} s_n^{KrC}(\varepsilon_L) &= \frac{0.5 \ln(1 + 1.2288\varepsilon_L)}{w(\varepsilon_L)} \quad \text{with} \\ w(\varepsilon_L) &= \varepsilon_L + 0.1728\sqrt{\varepsilon_L} + 0.008\varepsilon_L^{0.1504} \end{aligned} \quad , \quad (3)$$

the reduced energy

$$\varepsilon_L = E_0 \frac{M_2}{M_1 + M_2} \frac{a_L}{Z_1 Z_2 e^2} = E_0 / \varepsilon \quad (4)$$

and the Lindhard screening length [45]

$$a_L = \left(\frac{9\pi^2}{128}\right)^{1/3} a_B \left(Z_1^{2/3} + Z_2^{2/3}\right)^{-1/2}, \quad a_B = 0.0529177 \text{ nm} \quad (5)$$

where  $a_B$  is the Bohr radius.  $Z_1$ ,  $Z_2$ , and  $M_1$ ,  $M_2$  are the atomic numbers and the atomic masses of the projectile and target atom, respectively. The threshold energy  $E_{th}$  and the values  $q$ ,  $\lambda$  and  $\mu$  are fitting parameters. The value  $\varepsilon$  is used in tables 1 to 9.

The proportionality of the yield,  $Y$ , to the nuclear stopping power is adopted from analytic theory [20,21].  $q$  describes the absolute yield,  $\lambda$  triggers the onset of the decrease of the sputtering yield at low energies towards the threshold, and  $\mu$  is assigned in order to describe the strength of this decrease. The fitting parameters  $\lambda$ ,  $q$ ,  $\mu$  and  $E_{th}$  are obtained by a procedure based on Bayesian statistics, which provides a region of confidence and the corresponding errors [44].

For the fitting of the calculated sputtering yields mainly the values by *Yamamura* [24,25] and *Eckstein* [32,36] are used. Both datasets agree mostly reasonably well, see Fig. 3, but in some cases deviations up to a factor of two occur. In many cases additional values of the sputtering yield have been calculated [32] to get a reasonable fit to lower energies or to extend the fit to higher energies, where experimental data were available.

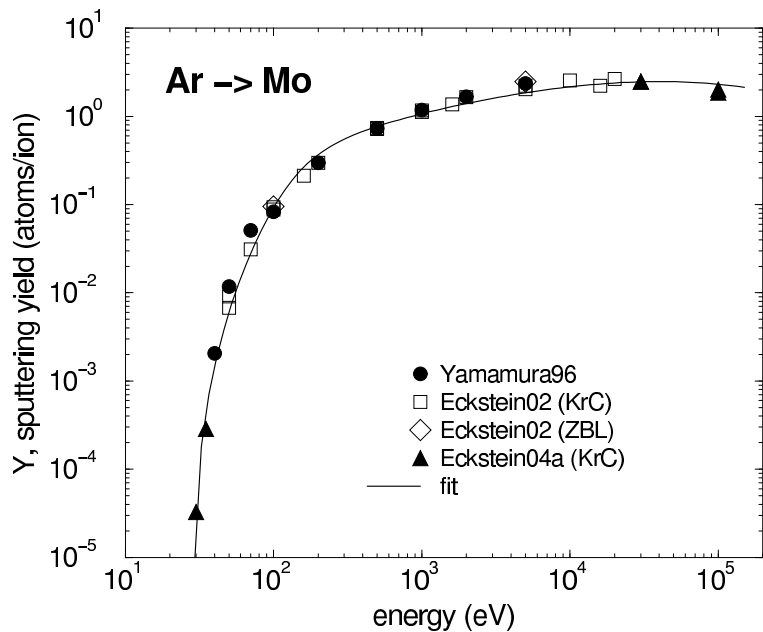


**Fig. 3.** Energy dependence of the sputtering yield at normal incidence for the bombardment of Mo with Ar calculated by Yamamura [24,25] and by Eckstein [32,36]

The fitting parameters for the calculated values are given in Tables 1- 9 (Appendix) together with  $\varepsilon$ ,  $E_{sb}$  and  $E_{sb}/\gamma$ .  $E_{sb}$  is the surface binding energy, and  $\gamma = 4M_1 M_2 / (M_1 + M_2)^2$  is the energy transfer factor,  $M_1$  and  $M_2$  are the atomic masses of the projectile and target atom, respectively. Tables 25 - 28 give a list of sputtering yields and the corresponding references not shown in the figures.

### 3.3 Comparison of Calculated Values with Experimental Data

For each ion - target combination, where experimental data are available, figures were produced as shown in Figs. 4-63. Each figure shows the algebraic fit for the energy dependence of the calculated sputtering yield values and the experimental data points measured by different authors at normal incidence for polycrystalline or amorphous materials. In cases, where only calculated values are available, fit curves for several incident ions are shown in one figure. The different plots have not always the same energy and yield scales. Usually, the energy scale for the light ions, hydrogen and helium, reaches up to 20 keV, whereas for the heavy ions the energy scale reaches up to 200 keV. In some cases the energy scale has been extended, if measured data at higher energies are available. The yield scale has a lower limit of  $10^{-4}$ , the upper limit depends on the data. Experimental data for single crystals have not been included in these plots because of possible channeling effects; the same applies for bombardment with nonvolatile ion species due to fluence dependent results (Tables 29 to 31), and to ion species which form stable compounds with target atoms such as oxides.

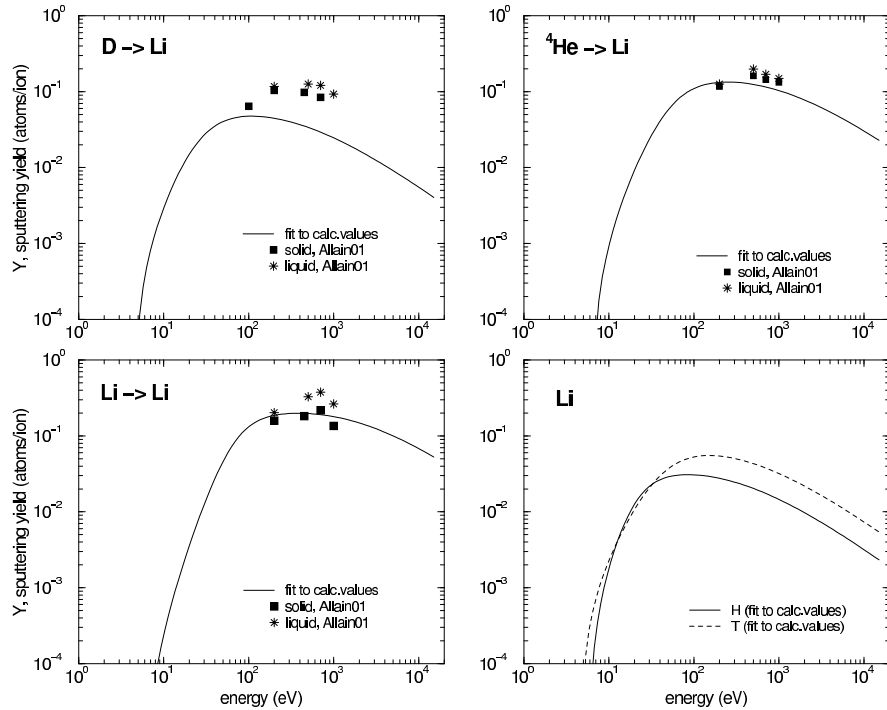


**Fig. 4.** Energy dependence of sputtering yields of Li for bombardment at normal incidence with D,  ${}^4\text{He}$ , Li [46] and H and T

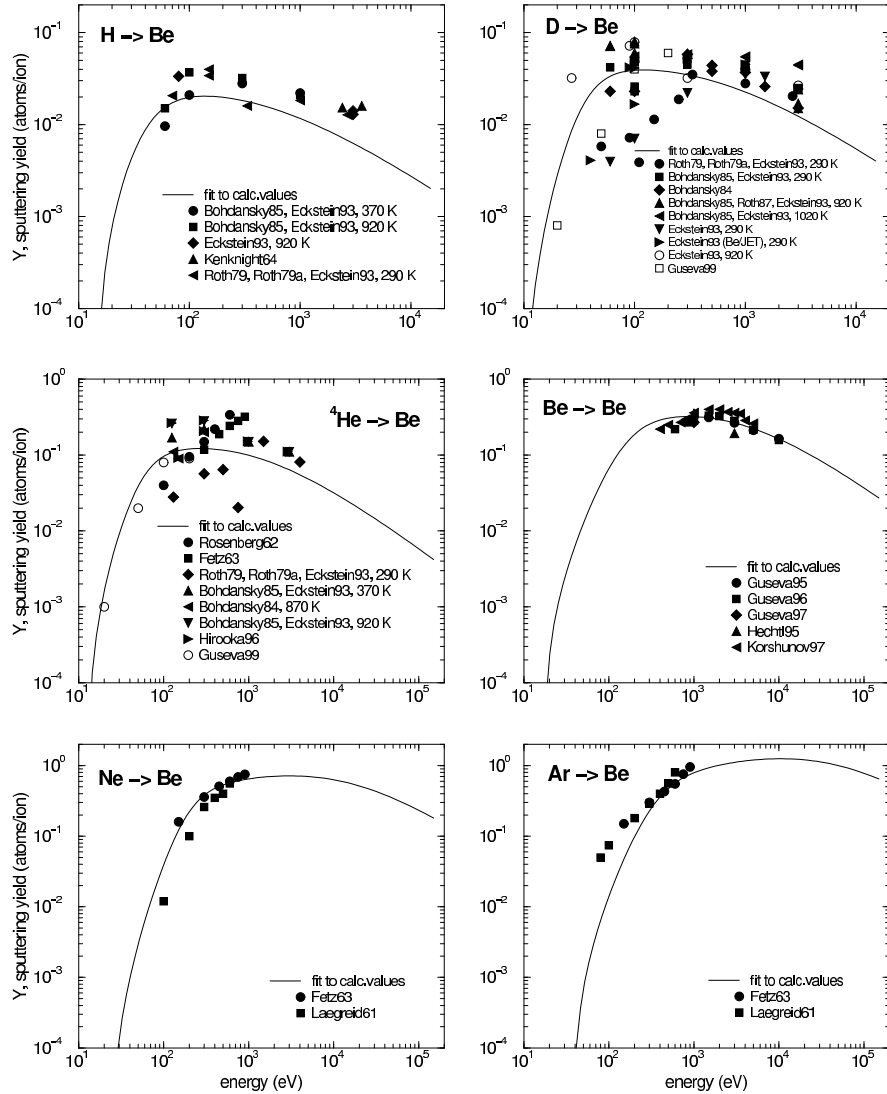


**Fig. 5.** Energy dependence of sputtering yields of Be for bombardment at normal incidence [47] with H [27,48–51], D [16,27,48,50–53],  ${}^4\text{He}$  [16,17,48,50,51,54–57], Be [58–62], Ne [55,63] and Ar [55,63]. Several authors in one line mean the same data in different publications

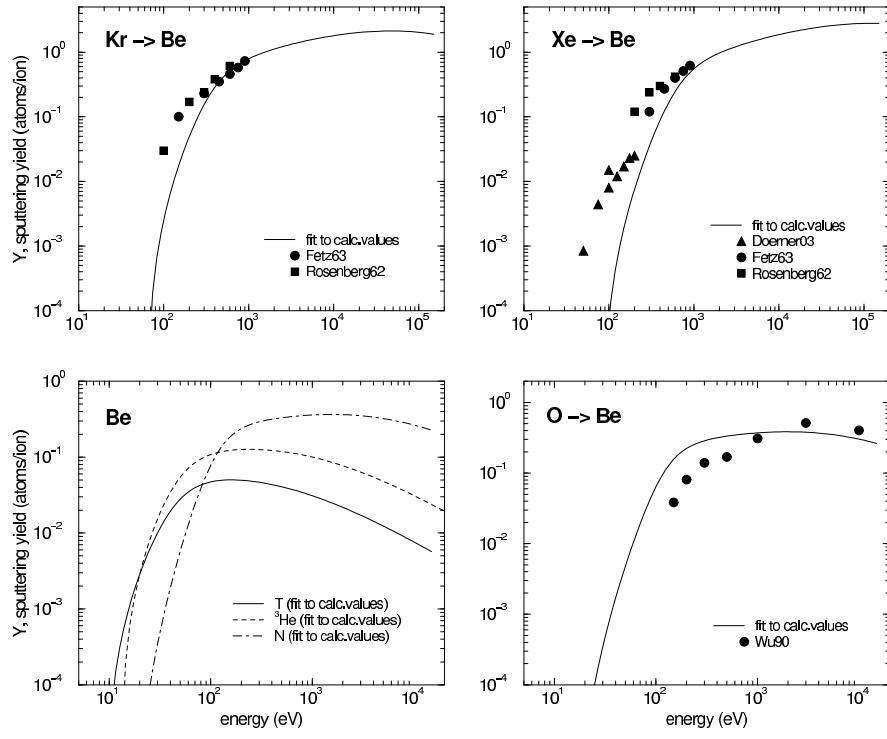


**Fig. 6.** Energy dependence of sputtering yields of Be for bombardment at normal incidence with Kr [54,55], Xe [18,54,55], T and  ${}^3\text{He}$  and N, and O [64]

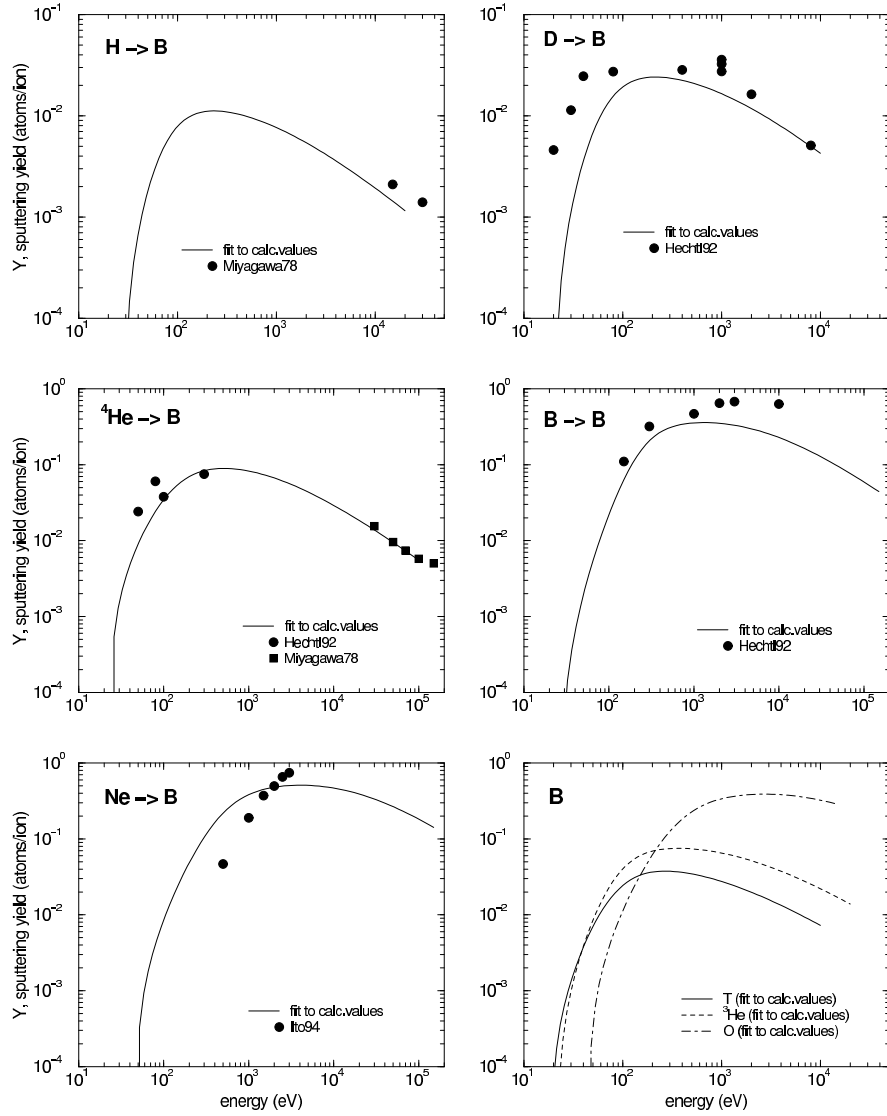


**Fig. 7.** Energy dependence of sputtering yields of B for bombardment at normal incidence with H [65], D [27,66],  ${}^4\text{He}$  [27,65,66], B [27,66], Ne [67], and T,  ${}^3\text{He}$ , O (only low fluence)

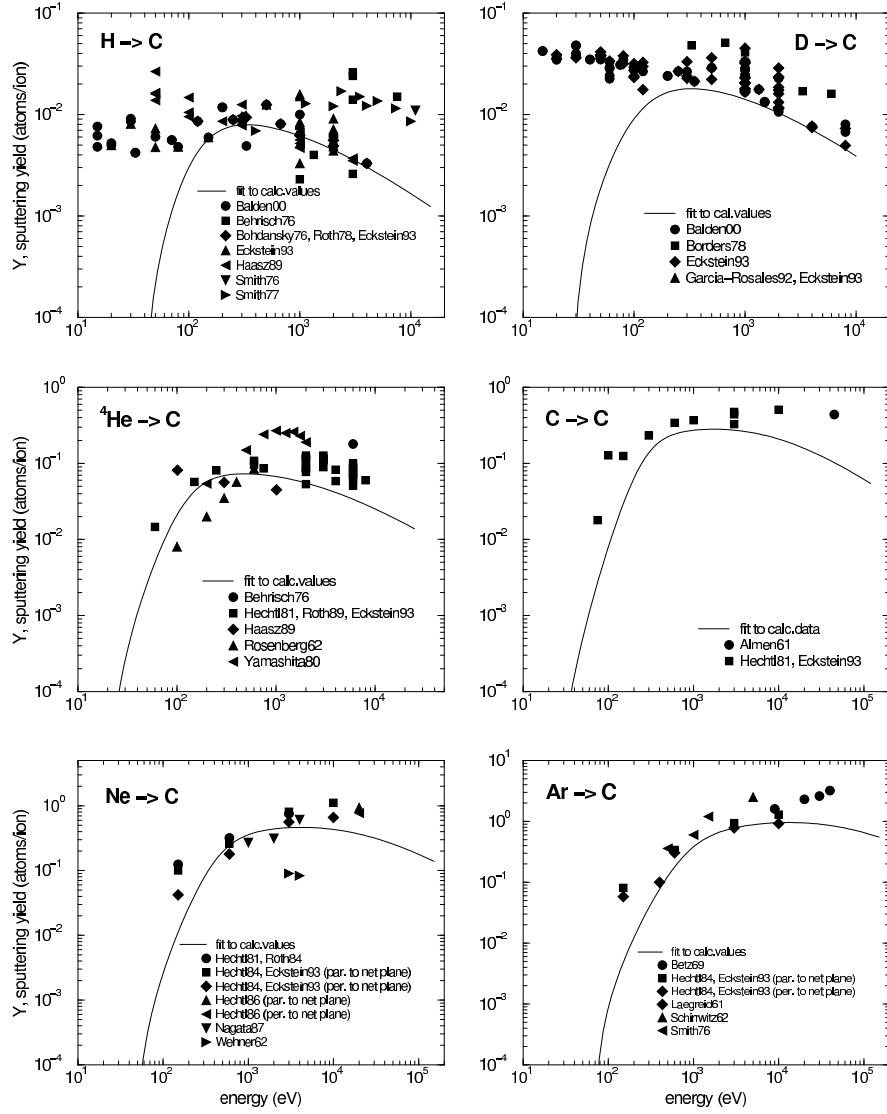


**Fig. 8.** Energy dependence of sputtering yields of C for bombardment at normal incidence with H [27,68–74], D [27,74–76],  ${}^4\text{He}$  [27,54,68,72,73,77,78], C [27,78–83], Ne [27,78,80,84–87], and Ar [27,63,70,85,88,89]

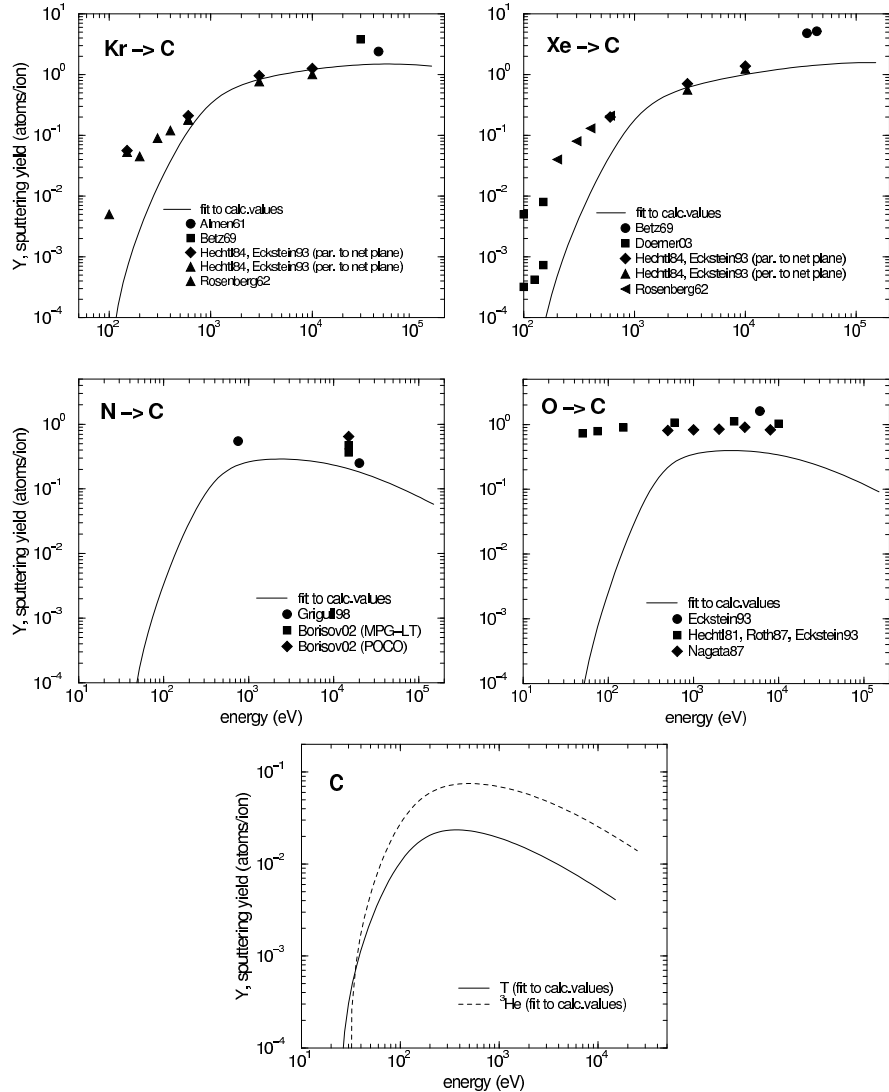


**Fig. 9.** Energy dependence of sputtering yields of C for bombardment at normal incidence with Kr [27,54,85,89,90], Xe [18,27,54,85,89], N [91–93], O [27,53,78,80,87], and T,  ${}^3\text{He}$

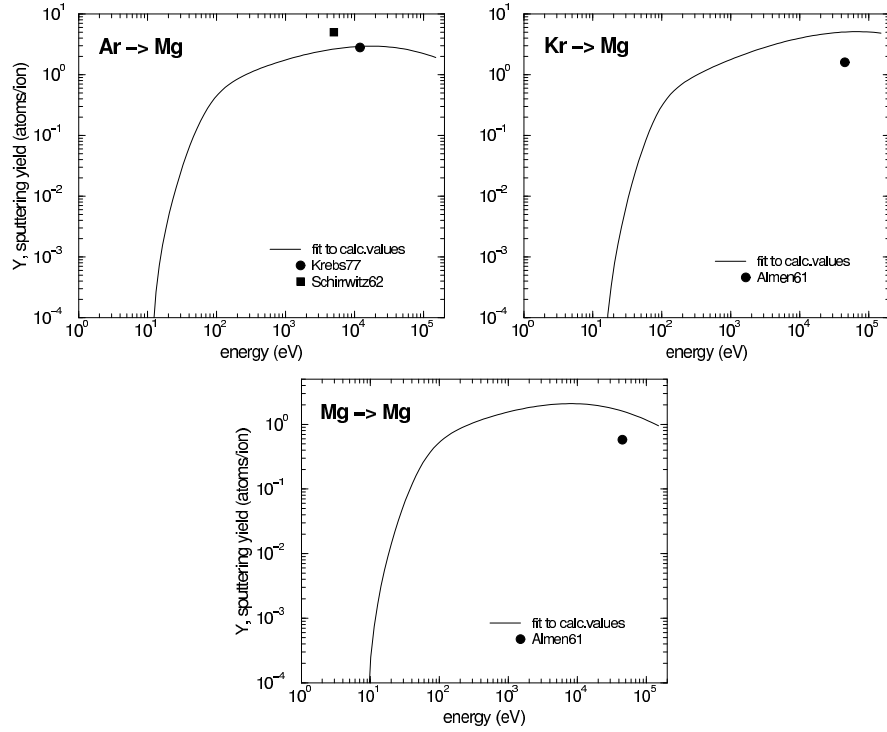


**Fig. 10.** Energy dependence of sputtering yields of Mg for bombardment at normal incidence with Ar [88,94], Kr [90], and Mg [79]

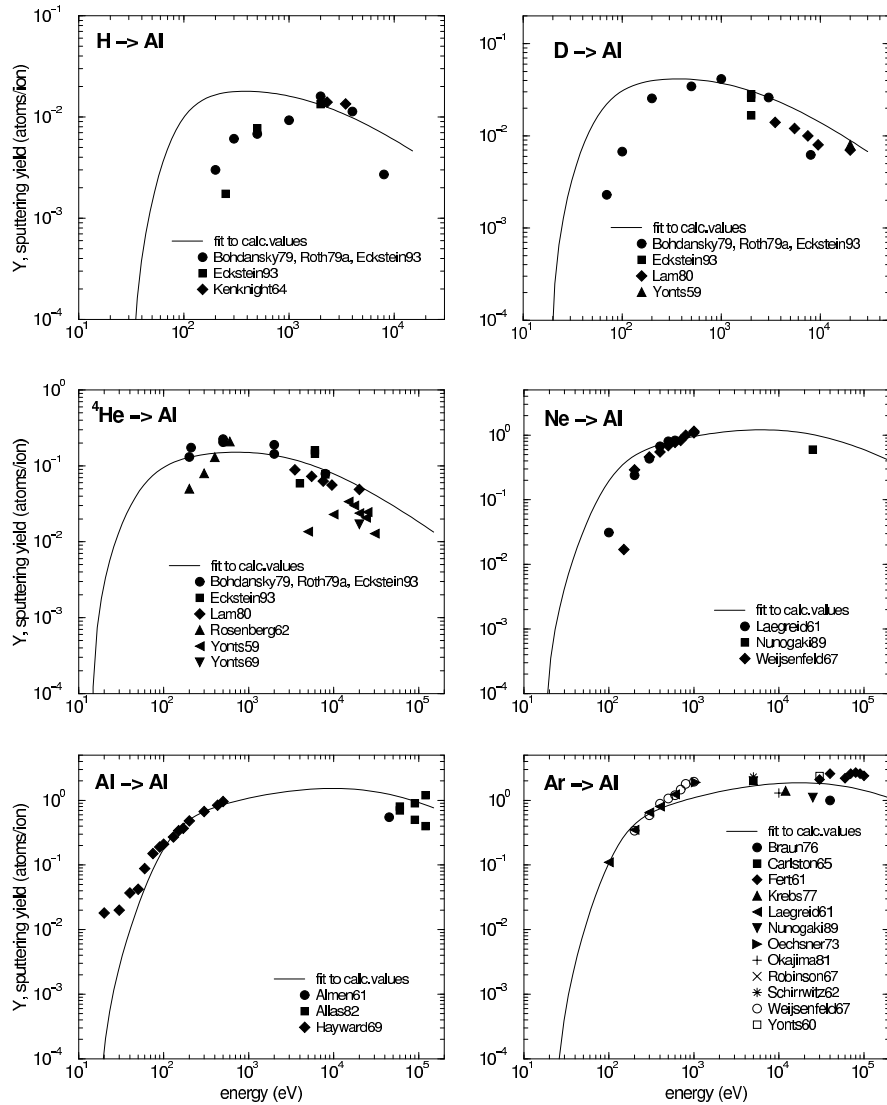


**Fig. 11.** Energy dependence of sputtering yields of Al for bombardment at normal incidence with H [27, 49–51], D [27, 95, 96],  $^{4}\text{He}$  [27, 50, 51, 54, 95–97], Ne [63, 98, 99], Al [79, 100, 101] and Ar [63, 88, 94, 98, 99, 102–108]

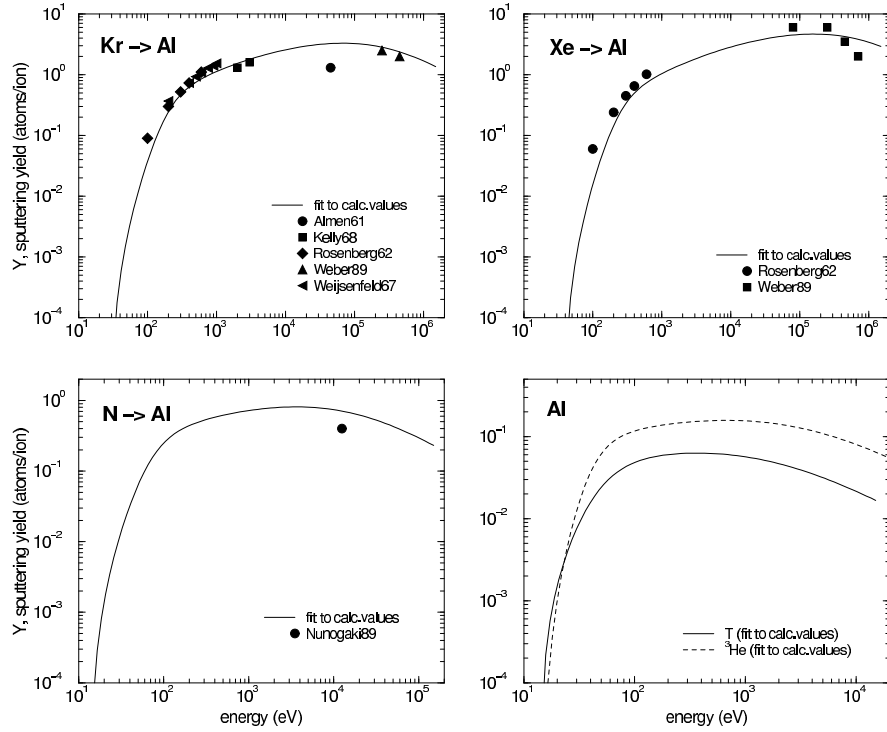


**Fig. 12.** Energy dependence of sputtering yields of Al for bombardment at normal incidence with Kr [54,90,98,109,110], Xe [54,110], N [99] and T,  ${}^3\text{He}$

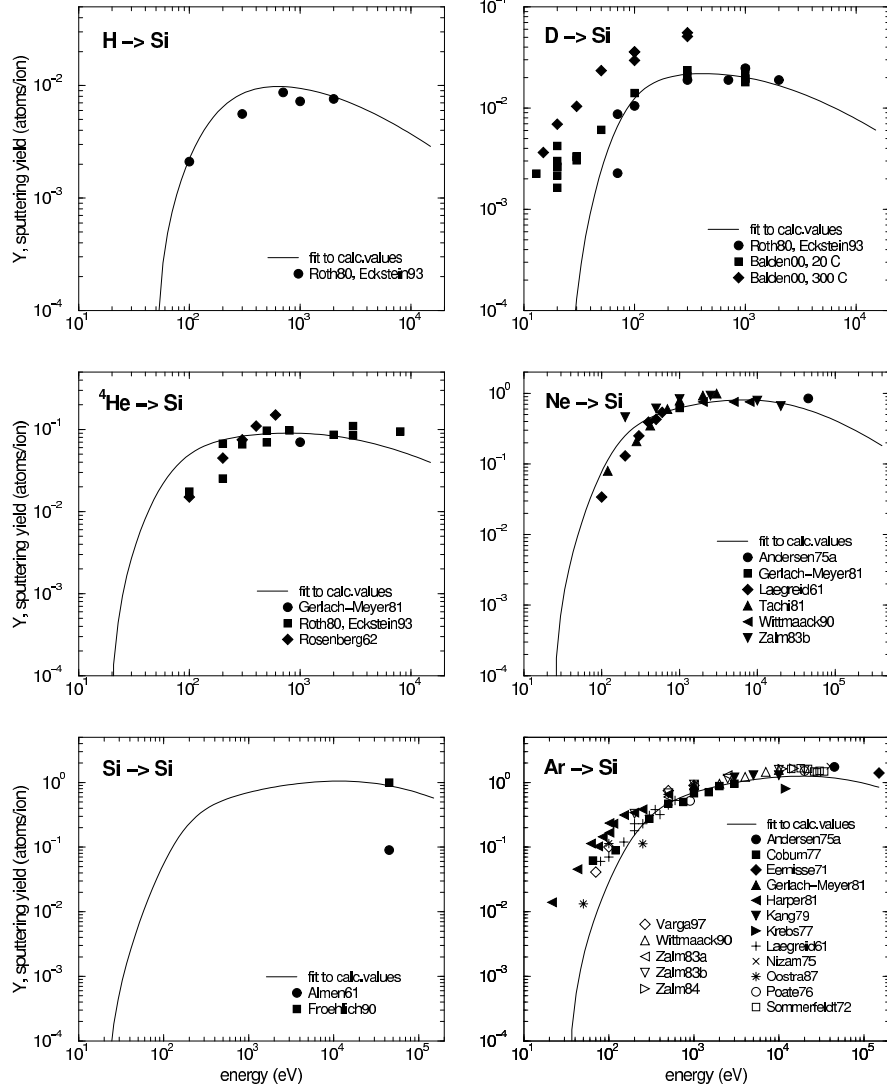


**Fig. 13.** Energy dependence of sputtering yields of Si for bombardment at normal incidence with H [27,111], D [27,111,112],  ${}^4\text{He}$  [27,54,111,113], Ne [63,113–117], Si [79,118] and Ar [63,94,113,114,116,117,119–129]

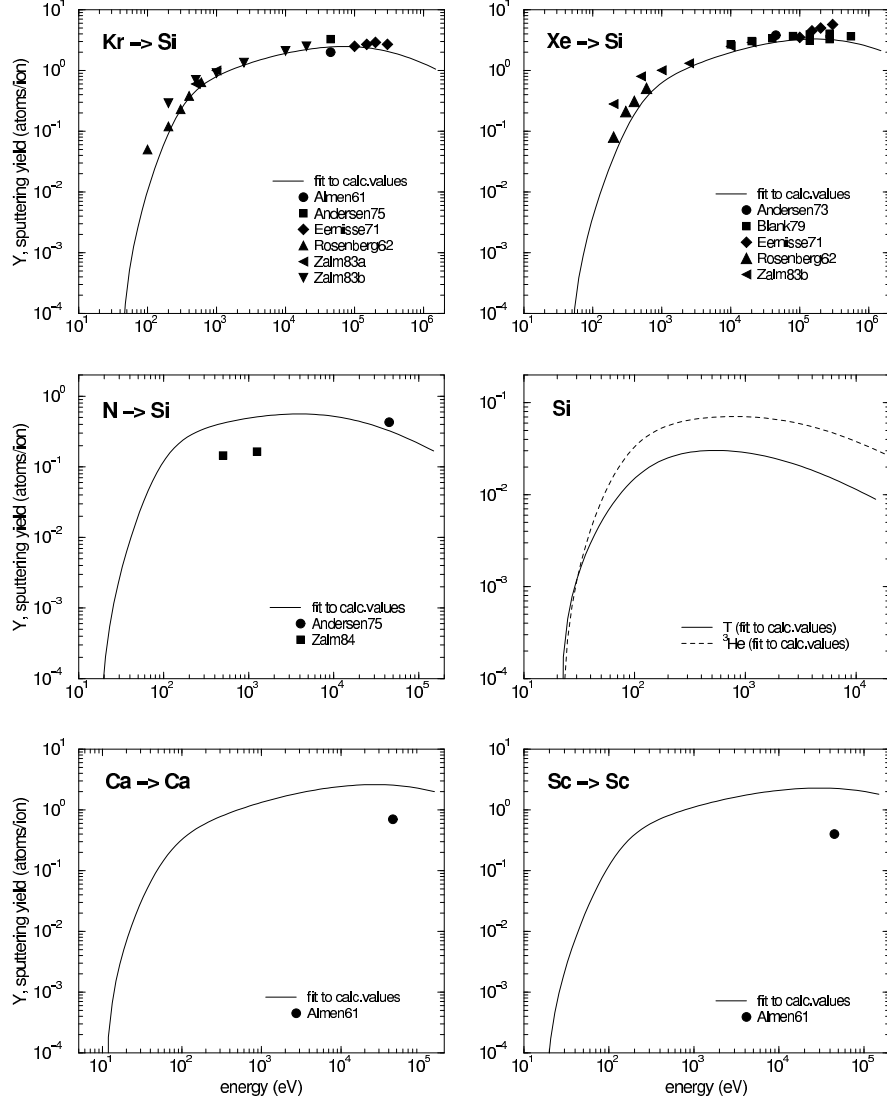


**Fig. 14.** Energy dependence of sputtering yields of Si for bombardment at normal incidence with Kr [54,90,114,116,120,126], Xe [54,114,116,120,130], N [114,127], and T,  ${}^3\text{He}$  and Ca [79] and Sc [79] selfsputtering

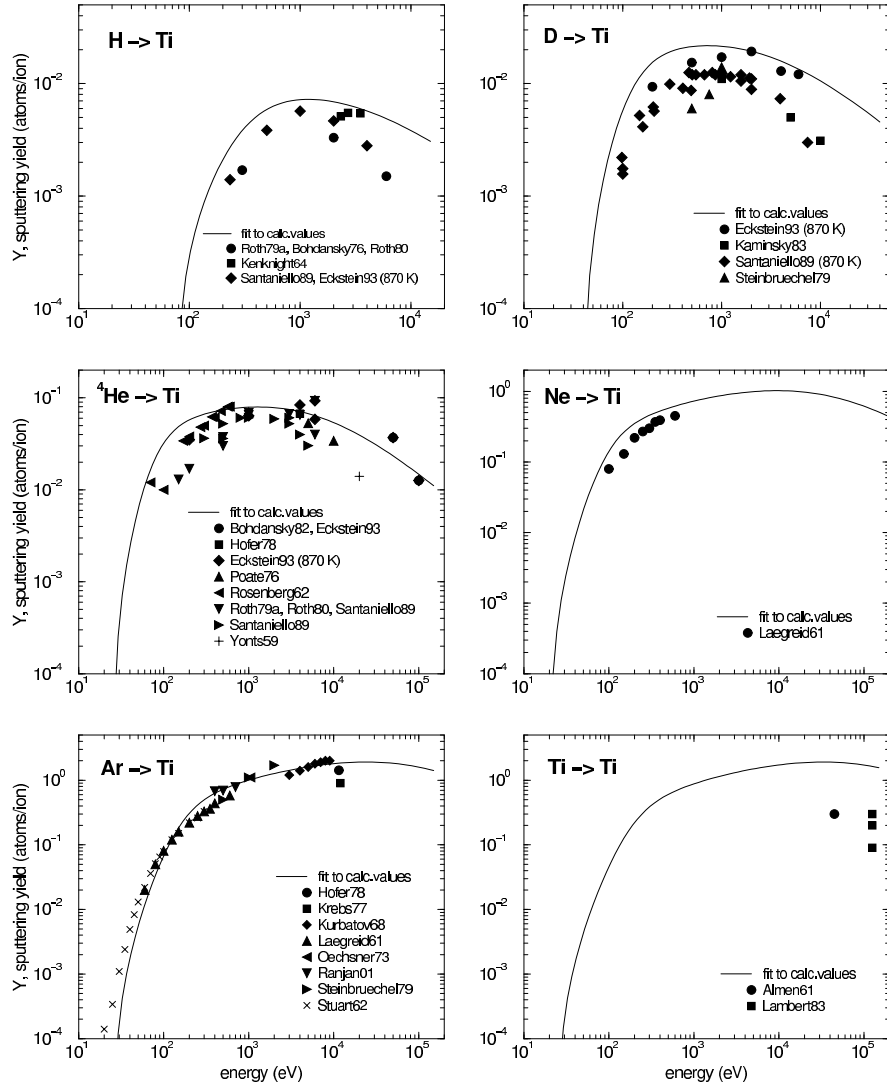


**Fig. 15.** Energy dependence of sputtering yields of Ti for bombardment at normal incidence with H [27,49,51,69,111,132], D [27,131–133],  ${}^4\text{He}$  [27,54,123,132,134,135], Ne [63], Ar [63,94,105,133,134,136–138] and Ti [79,139]

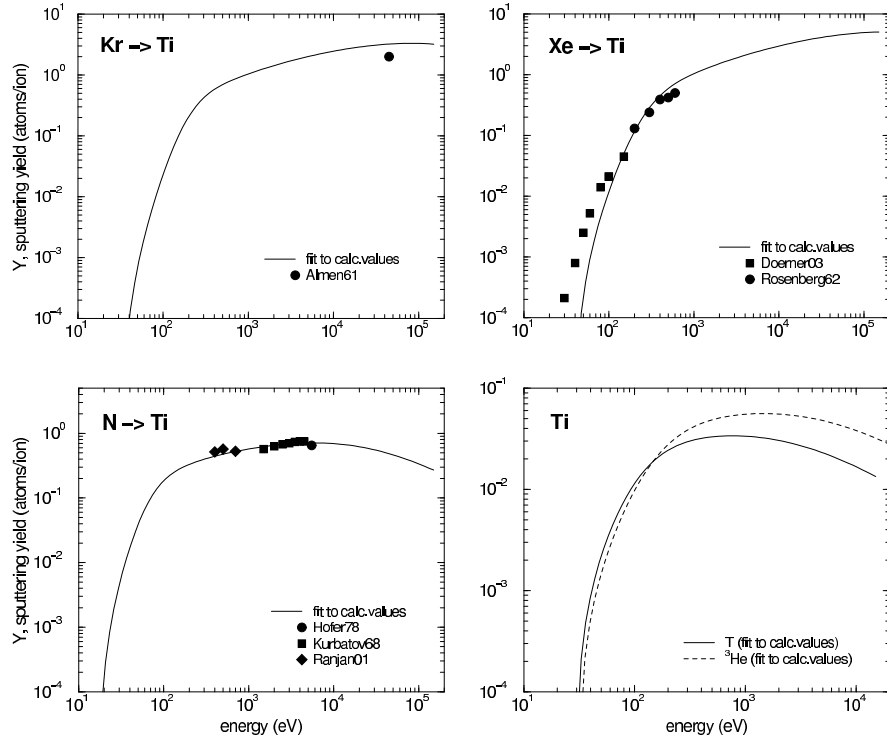


**Fig. 16.** Energy dependence of sputtering yields of Ti for bombardment at normal incidence with Kr [90], Xe [54,18], N [134,137,138] and T,  ${}^3\text{He}$

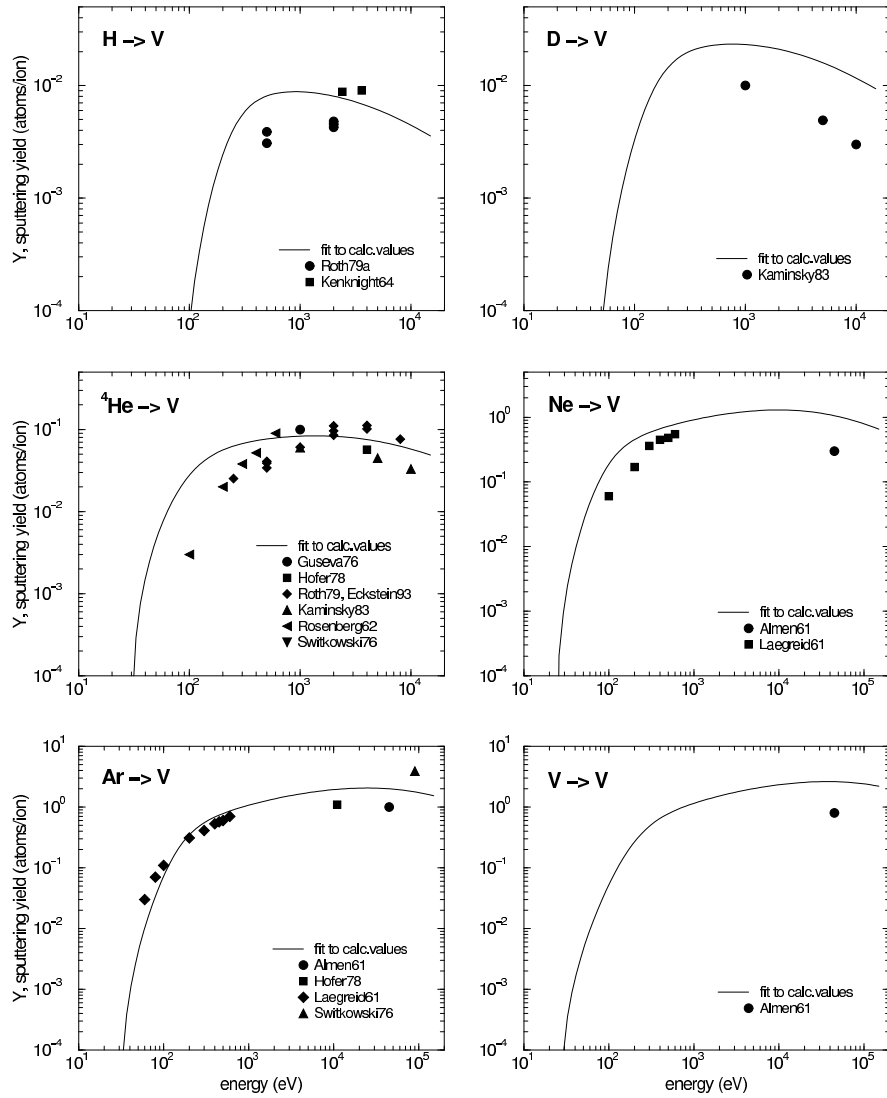


**Fig. 17.** Energy dependence of sputtering yields of V for bombardment at normal incidence with H [49,51], D [131],  ${}^4\text{He}$  [27,54,51,131,134,140,141], Ne [63,90], Ar [63,90,134,141] and V [79]

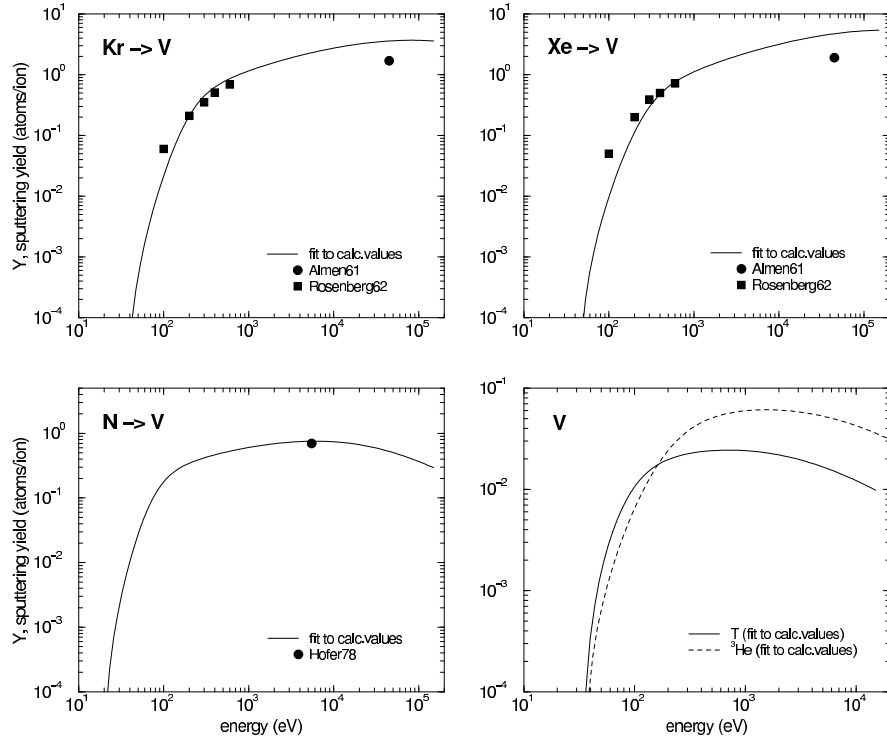


**Fig. 18.** Energy dependence of sputtering yields of V for bombardment at normal incidence with Kr [54,90], Xe [54,90], N [134] and T,  ${}^3\text{He}$

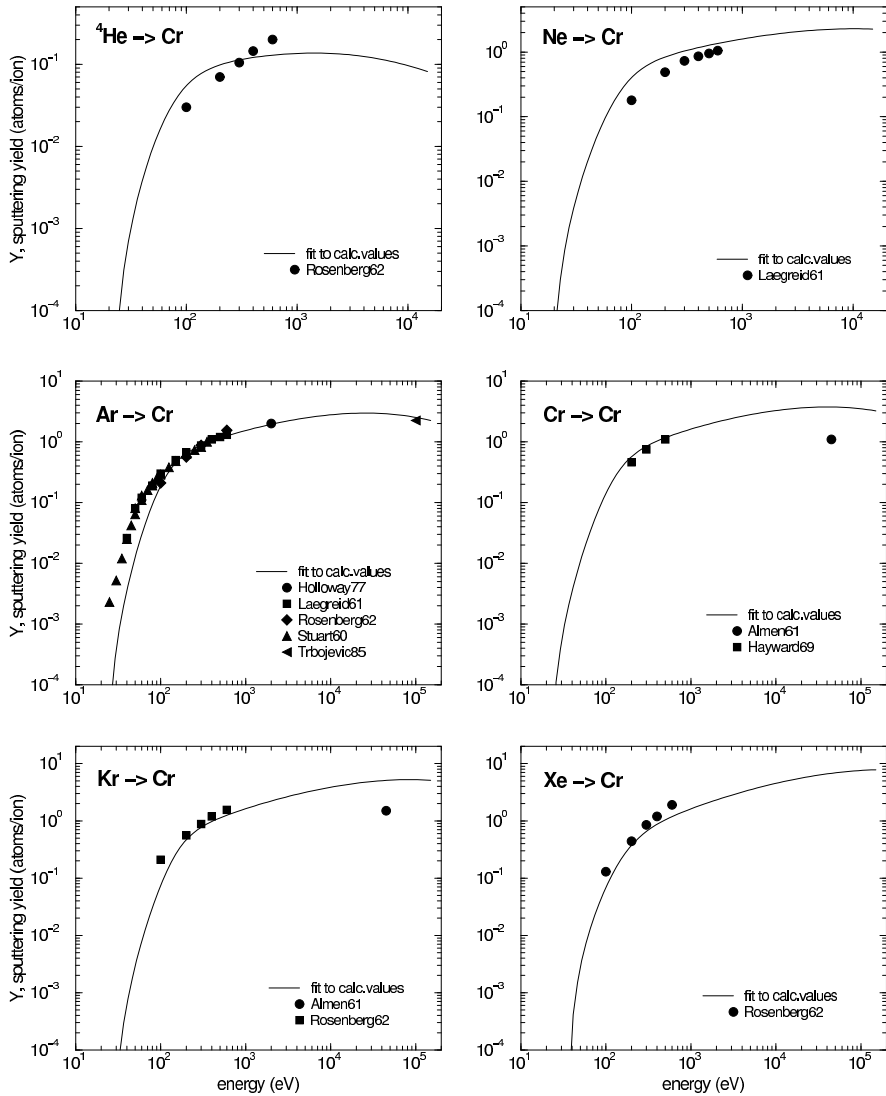


**Fig. 19.** Energy dependence of sputtering yields of Cr for bombardment at normal incidence with  ${}^4\text{He}$  [54], Ne [63], Ar [54,63,142–144], Cr [79,101], Kr [54,90], Xe [54]

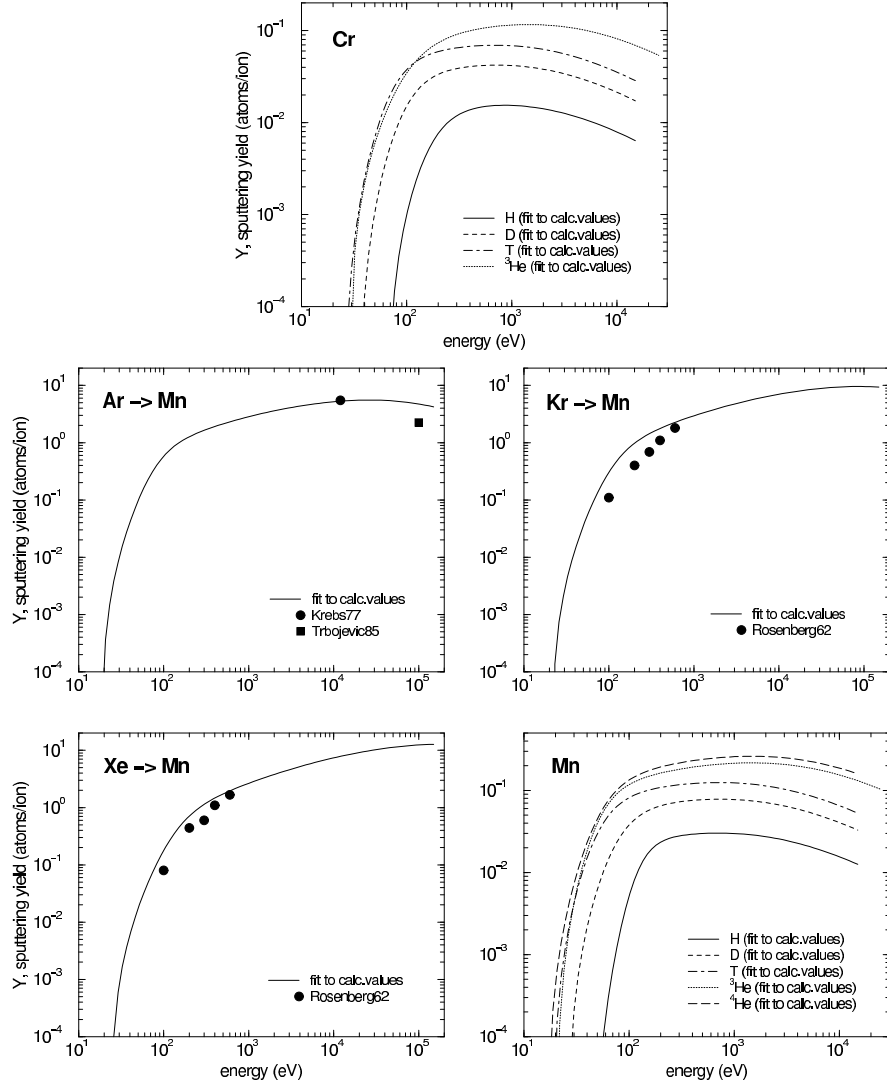


**Fig. 20.** Energy dependence of sputtering yields of Cr for bombardment at normal incidence with H, D, T,  $^3\text{He}$ , and energy dependence of sputtering yields of Mn for bombardment at normal incidence with Ar [94,144], Kr [54], Xe [54], and H, D, T,  $^3\text{He}$ ,  $^4\text{He}$

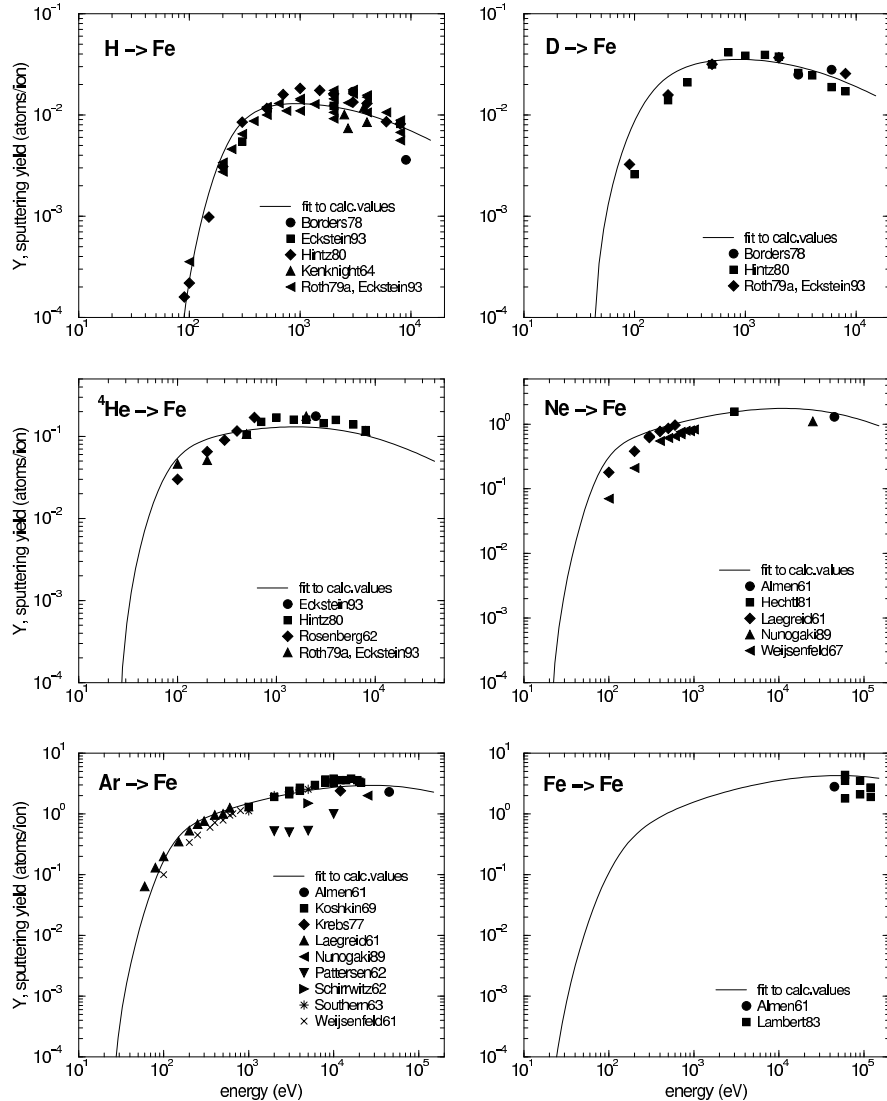


**Fig. 21.** Energy dependence of sputtering yields of Fe for bombardment at normal incidence with H [27,49,51,75,145], D [27,51,75,145],  ${}^4\text{He}$  [27,51,54], Ne [63,90,78,98,99], Ar [15,63,88,90,94,98,99,146,147], Fe [79,139]

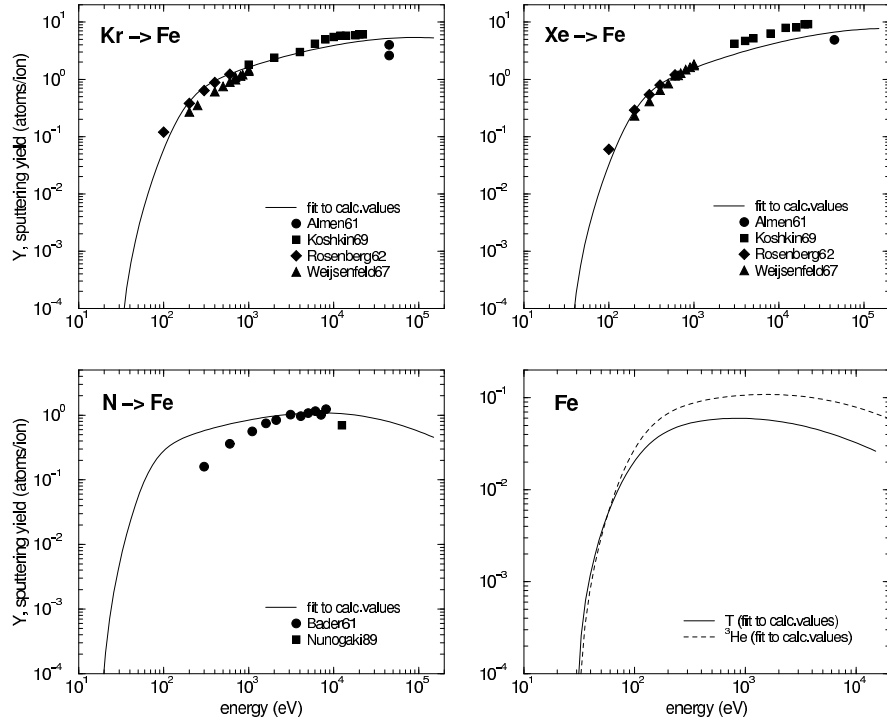


**Fig. 22.** Energy dependence of sputtering yields of Fe for bombardment at normal incidence with Kr [54,90,98,147], Xe [54,90,98,147], N [99,148], and T,  ${}^3\text{He}$

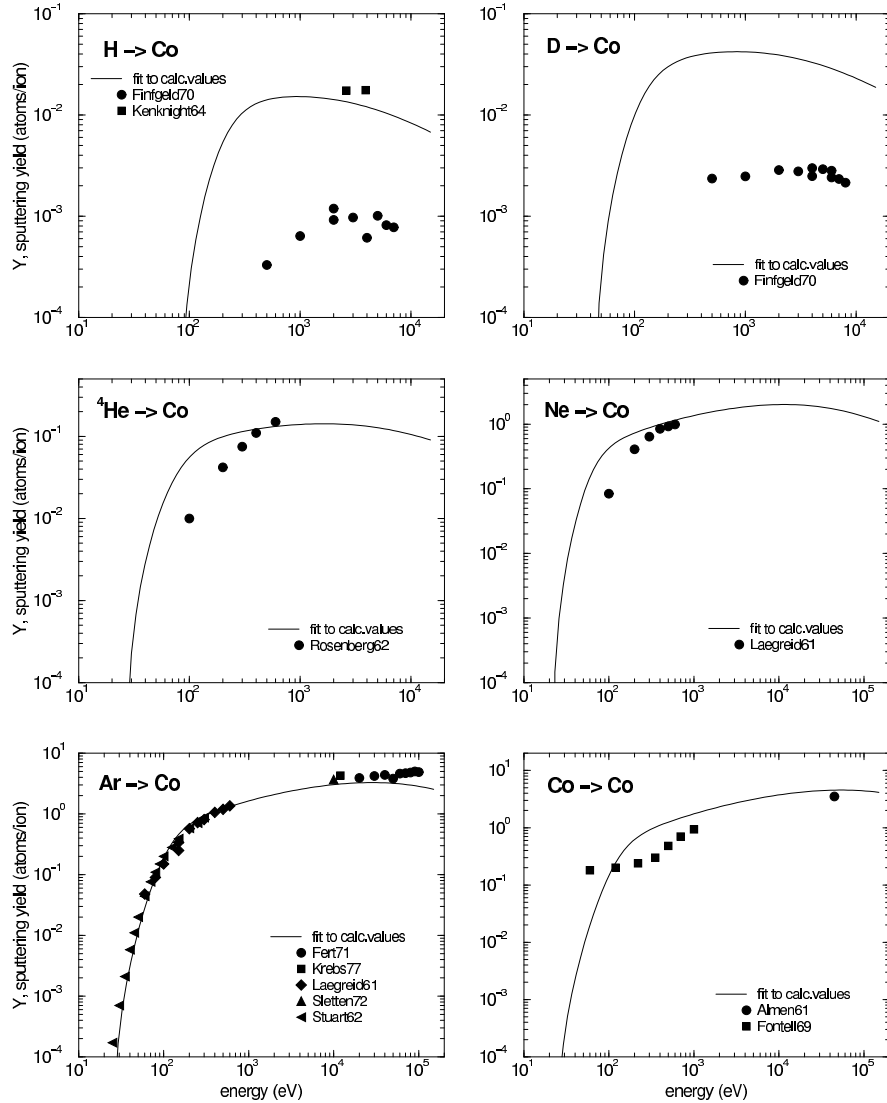


**Fig. 23.** Energy dependence of sputtering yields of Co for bombardment at normal incidence with H [49, 149], D [149],  ${}^4He$  [54], Ne [63], Ar [63, 94, 104, 136, 150] and Co [79, 151]

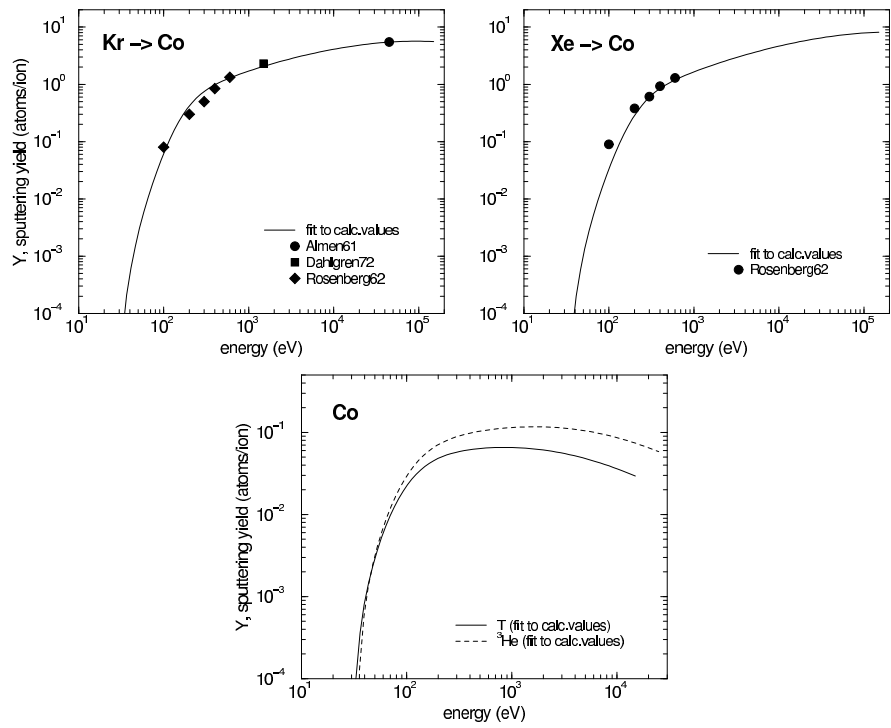


**Fig. 24.** Energy dependence of sputtering yields of Co for bombardment at normal incidence with Kr [54,90,152], Xe [54], and T,  ${}^3\text{He}$

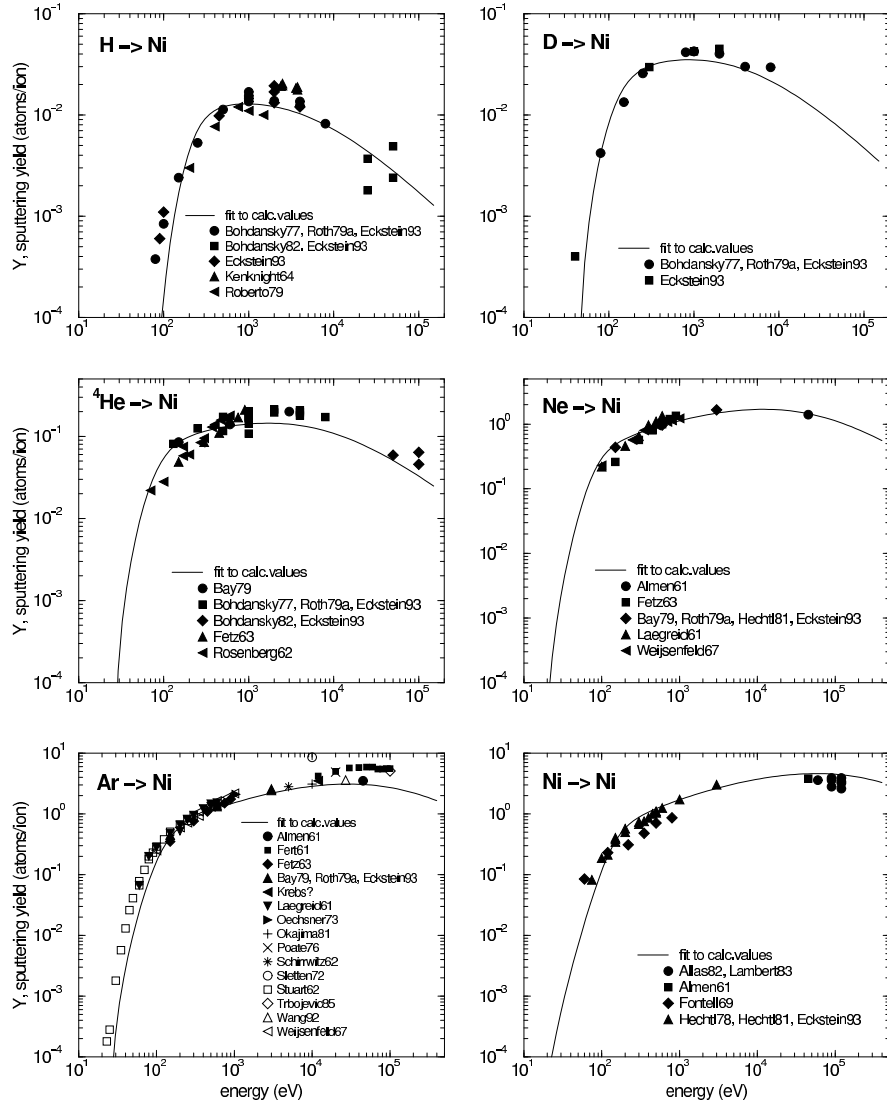


**Fig. 25.** Energy dependence of sputtering yields of Ni for bombardment at normal incidence with H [27, 49, 51, 135, 153, 154], D [27, 153],  $^4\text{He}$  [27, 51, 54, 55, 135, 153, 155], Ne [27, 51, 55, 63, 78, 90, 98, 155], Ar [27, 51, 55, 63, 88, 90, 94, 98, 104–106, 123, 136, 144, 150, 155, 156] and Ni [27, 78, 79, 100, 139, 151, 157]

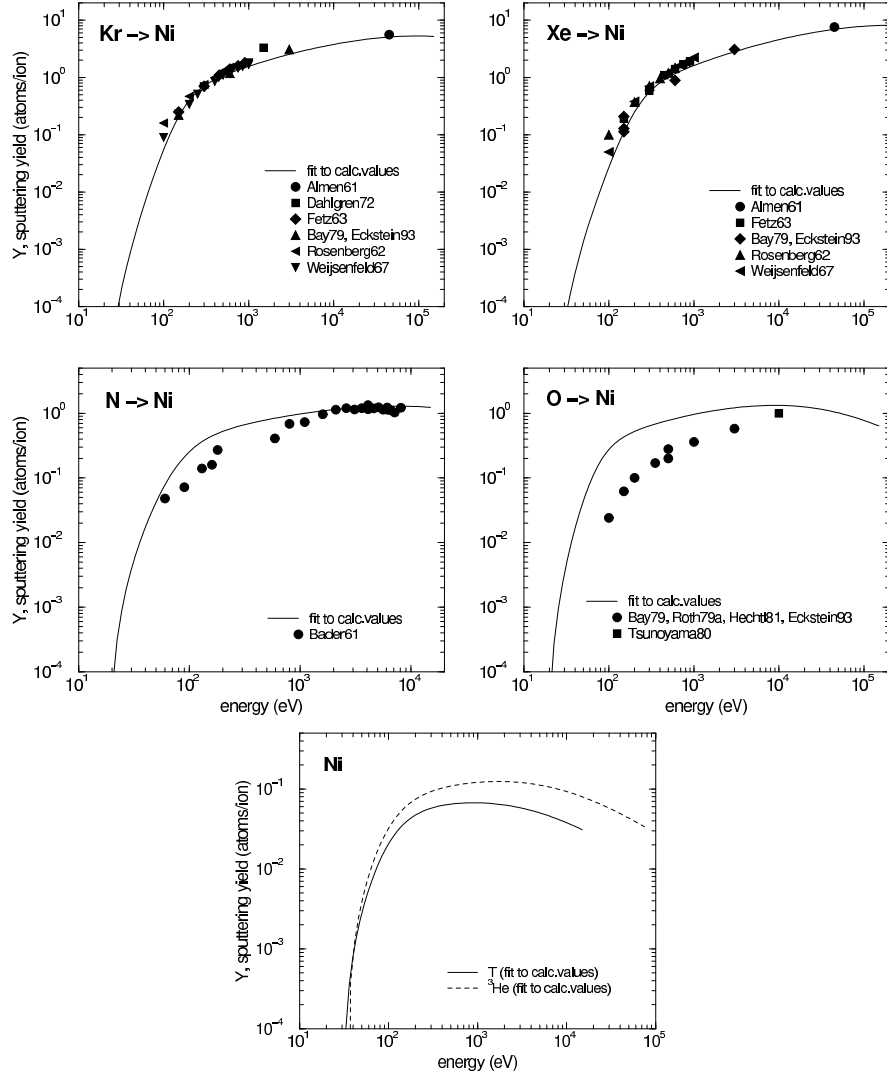


**Fig. 26.** Energy dependence of sputtering yields of Ni for bombardment at normal incidence with Kr [27,54,55,90,98,152,155], Xe [27,54,55,90,98,155], N [148], O [27,51,78,155,158] and T,  ${}^3\text{He}$

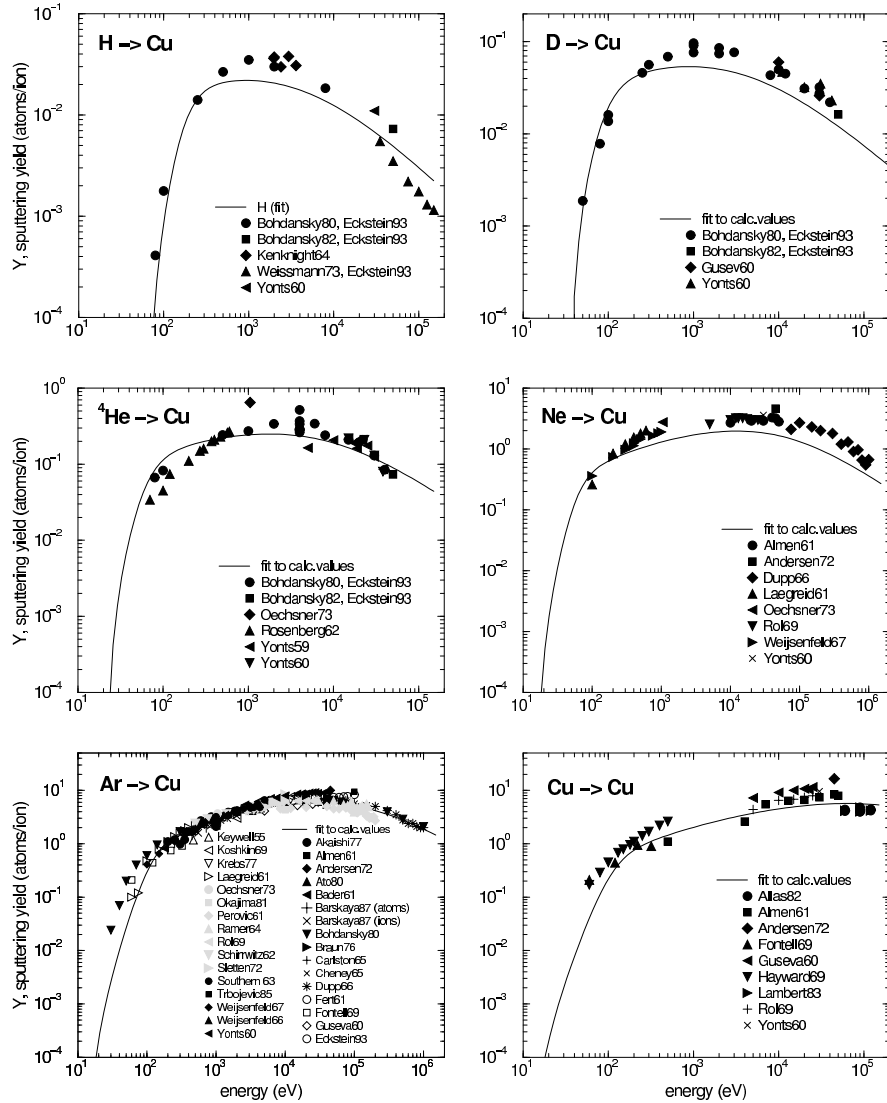


**Fig. 27.** Energy dependence of sputtering yields of Cu for bombardment at normal incidence with H [27, 49, 108, 135, 159, 160], D [27, 108, 135, 159, 161],  $^4\text{He}$  [27, 54, 96, 105, 108, 135, 159], Ne [63, 90, 98, 105, 108, 162–164], Ar [27, 63, 88, 90, 94, 98, 102–106, 108, 144, 146–148, 150, 151, 159, 161–172], Cu [79, 100, 101, 108, 139, 151, 161, 162, 164]

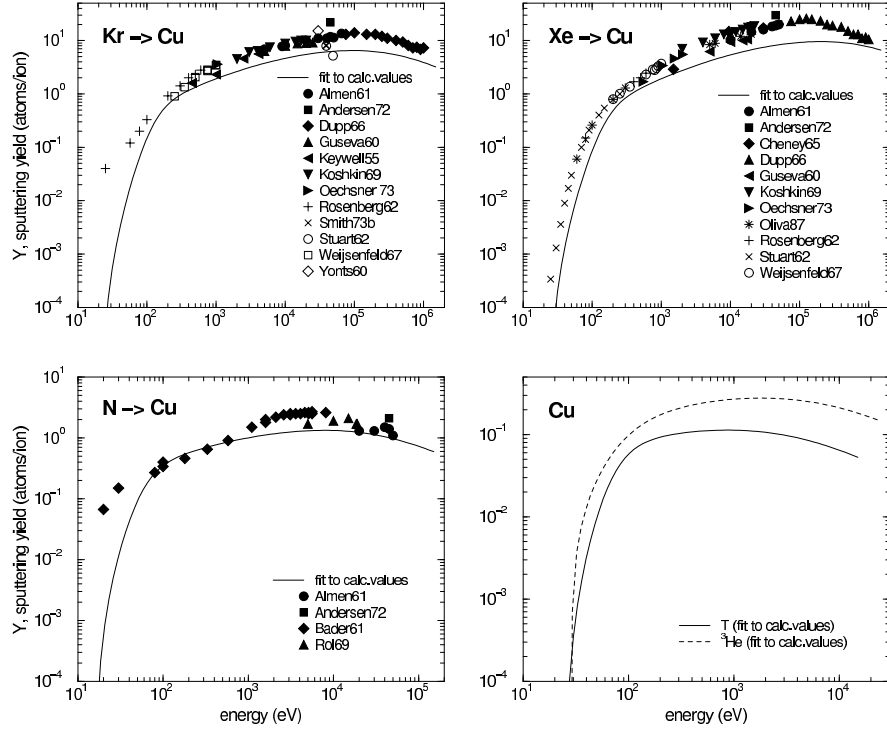


**Fig. 28.** Energy dependence of sputtering yields of Cu for bombardment at normal incidence with Kr [54,90,98,105,108,136,147,161–163,165,173], Xe [54,90,98,105,136,147,161–163,168,174], N [90,148,162,164], and T,  ${}^3\text{He}$

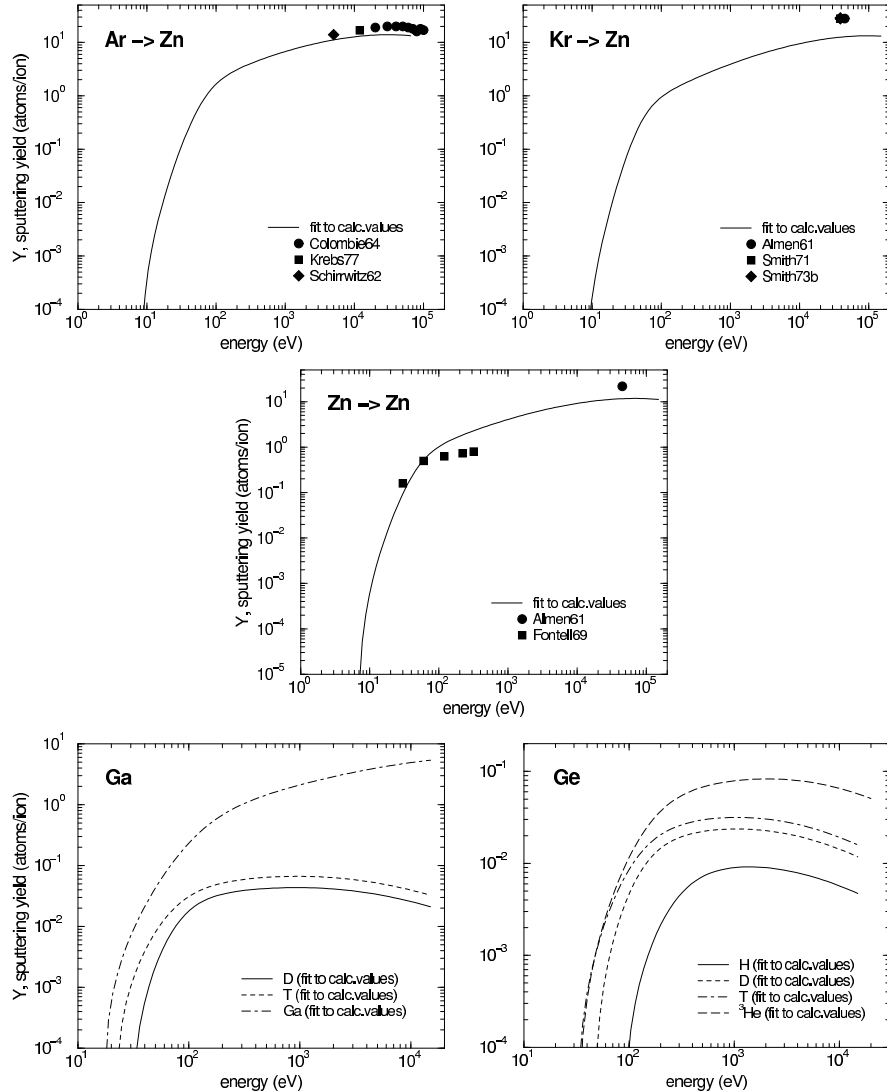


**Fig. 29.** Energy dependence of sputtering yields of Zn for bombardment at normal incidence with Ar [88,94,175], Kr [90,173,176], Zn [79,151], and energy dependence of sputtering yields of Ga for the bombardment at normal incidence with D, T, Ga, and energy dependence of sputtering yields of Ge for the bombardment at normal incidence with H, D, T,  ${}^3\text{He}$

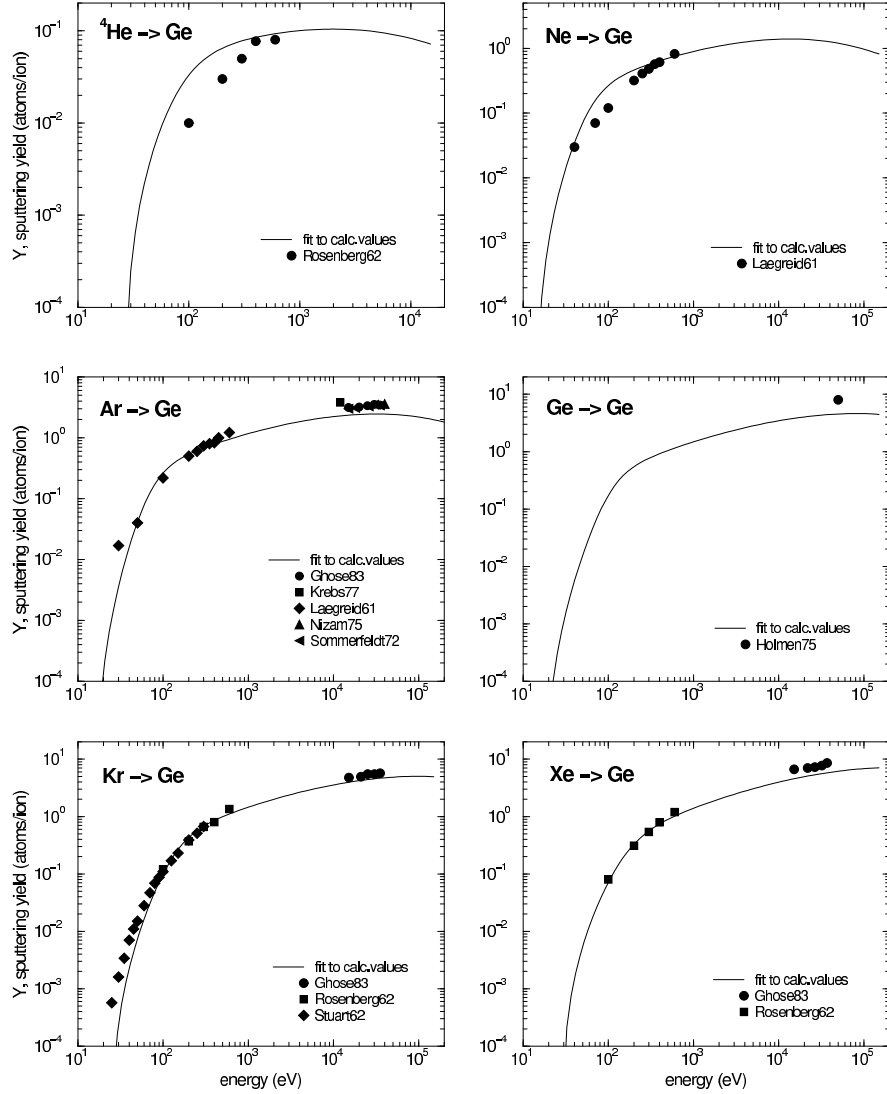


**Fig. 30.** Energy dependence of sputtering yields of Ge for bombardment at normal incidence with  ${}^4\text{He}$  [54], Ne [63], Ar [63,94,121,122,177], Ge [178], Kr [54,136,177], Xe [54,177]

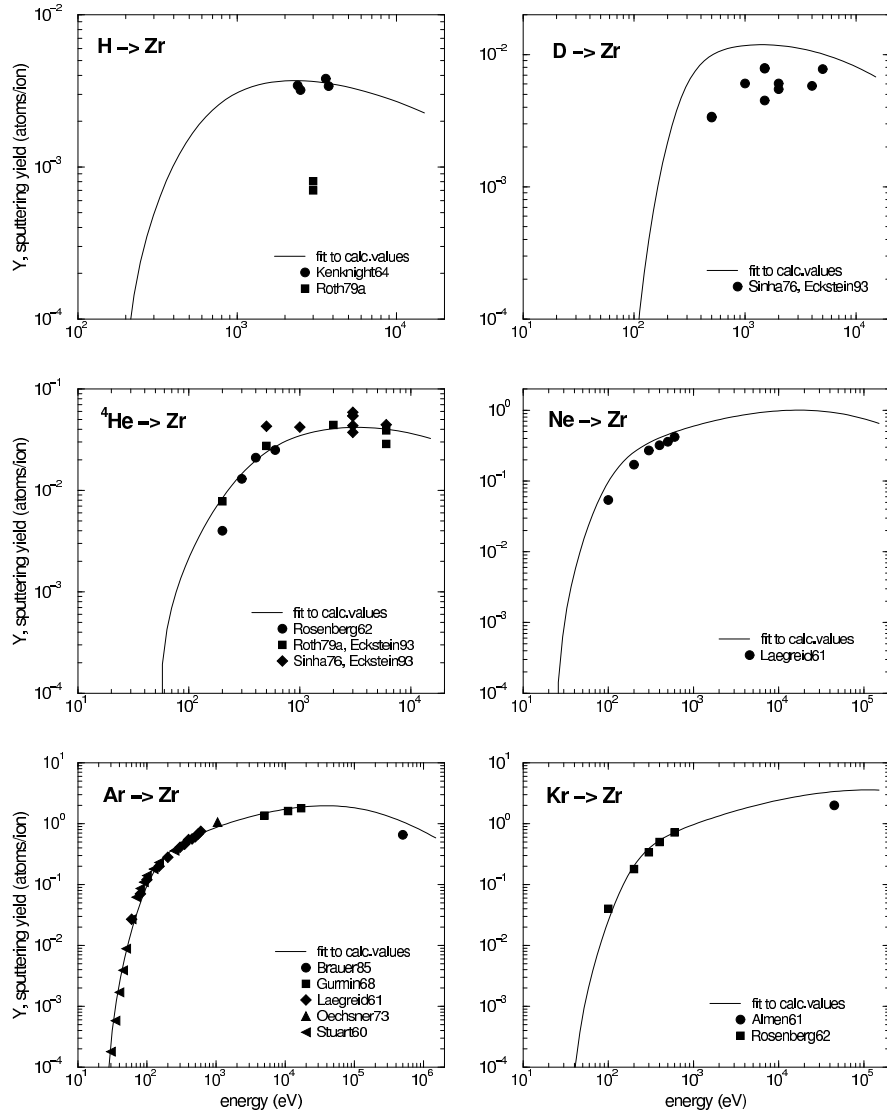


**Fig. 31.** Energy dependence of sputtering yields of Zr for bombardment at normal incidence with H [49,51], D [27,179],  ${}^4He$  [27,54,51,179], Ne [63], Ar [63,105,180–182], Kr [54,90]

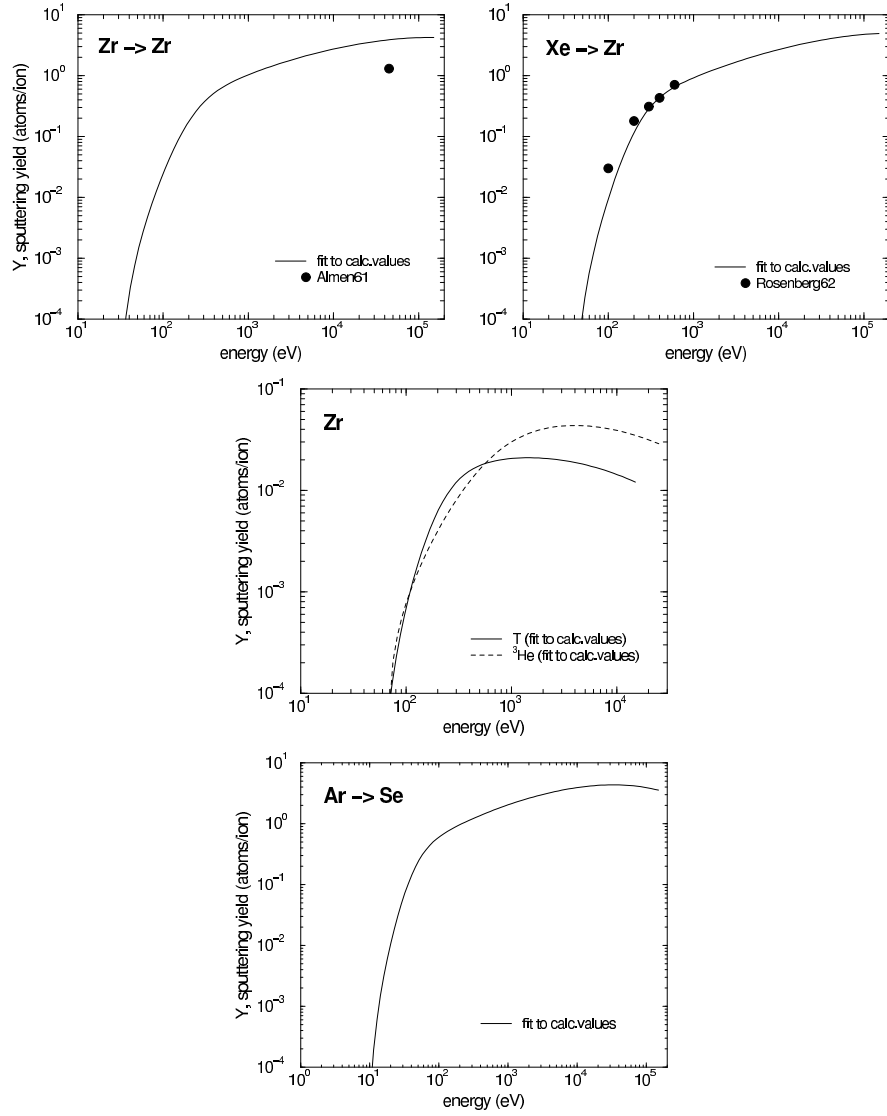


**Fig. 32.** Energy dependence of sputtering yields of Zr for bombardment at normal incidence with Zr [79], Xe [54], and T,  $^3\text{He}$ , and for bombardment at normal incidence of Se with Ar

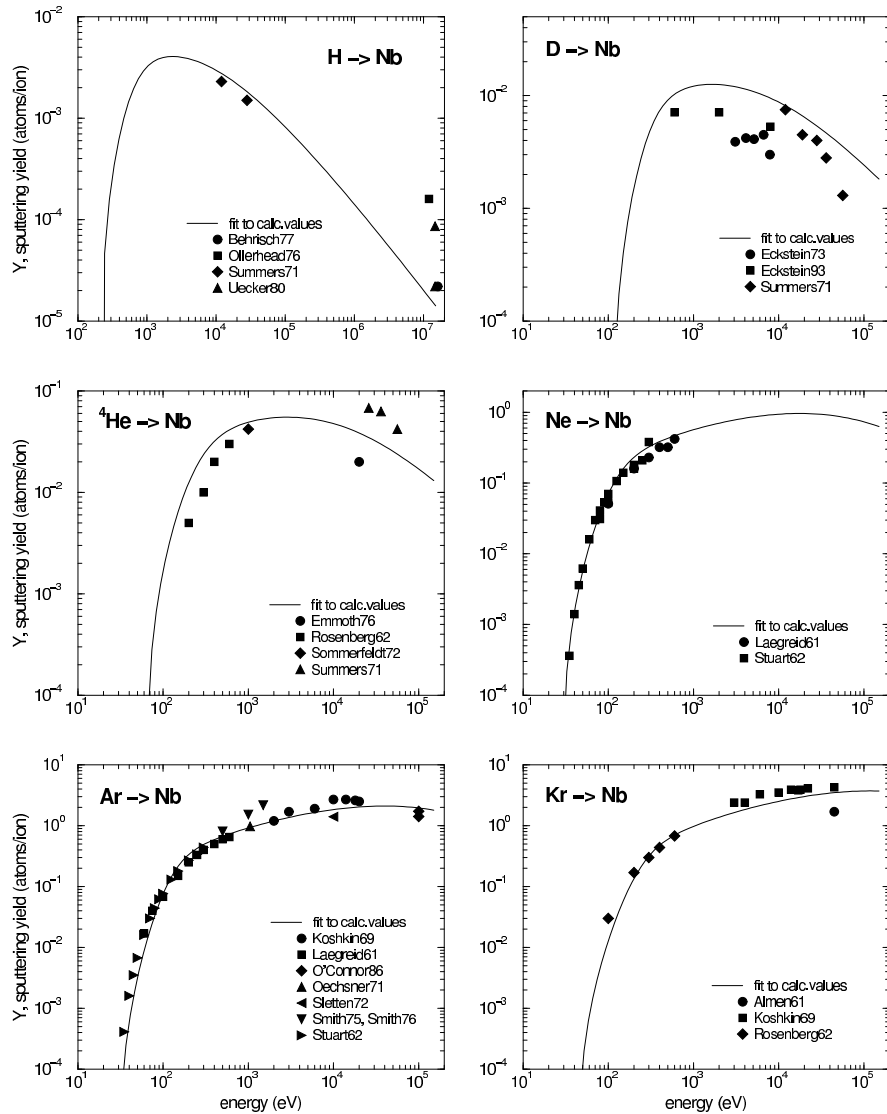


**Fig. 33.** Energy dependence of sputtering yields of Nb for bombardment at normal incidence with H [183–186], D [185, 188, 189],  ${}^4\text{He}$  [54, 121, 185, 190], Ne [63, 136], Ar [63, 70, 136, 147, 150, 191–193], Kr [54, 90, 147]

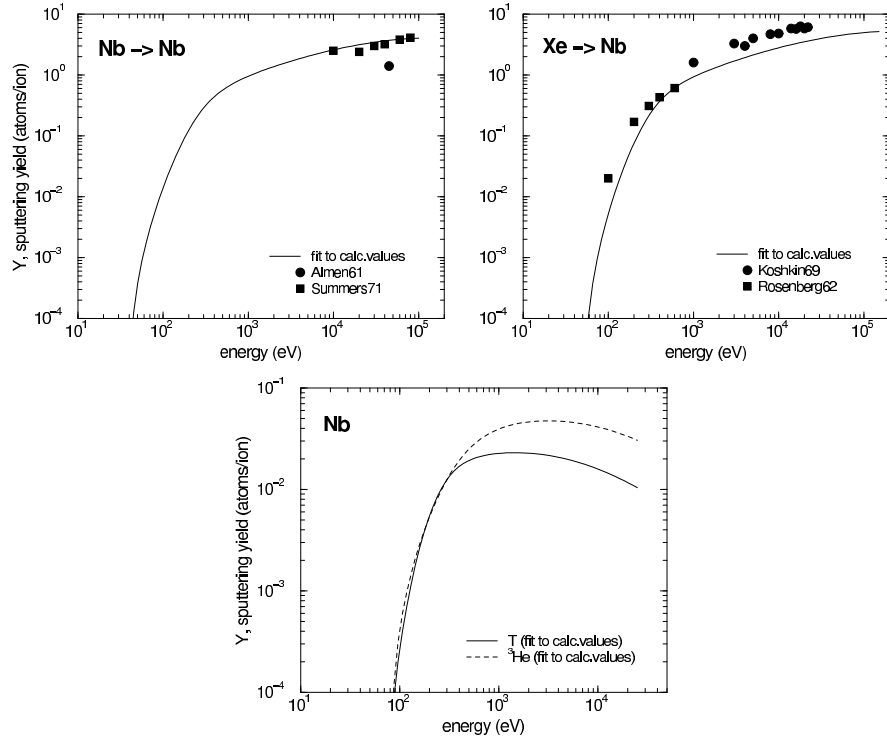


**Fig. 34.** Energy dependence of sputtering yields of Nb for bombardment at normal incidence with Nb [79,185,187], Xe [54,147], and T,  ${}^3\text{He}$

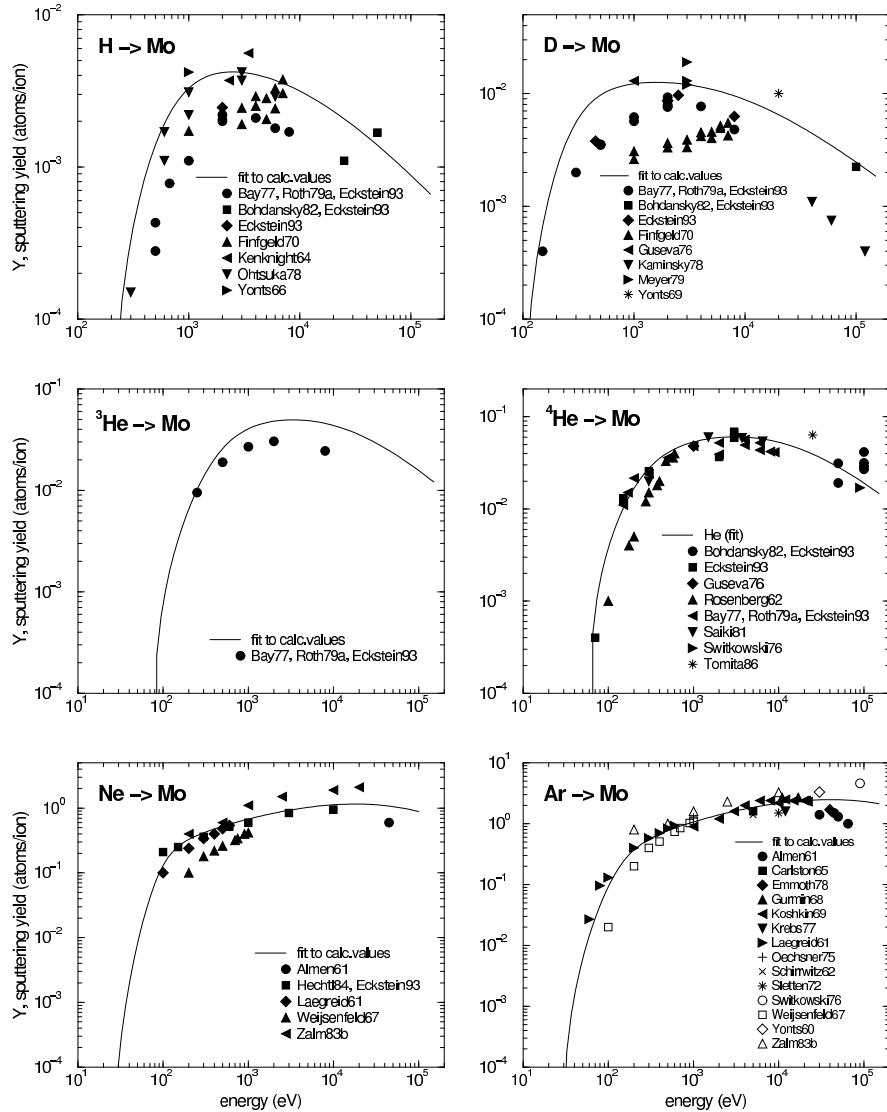


**Fig. 35.** Energy dependence of sputtering yields of Mo for bombardment at normal incidence with H [27,49,51,108,135,149,194,195], D [27,51,97,135,140,149,194,196,197],  $^3\text{He}$  [27,51,194],  $^4\text{He}$  [27,54,51,135,140,141,194,198,199], Ne [27,63,90,98,116], Ar [63,88,90,94,98,103,108,116,141,147,150,181,200,201]

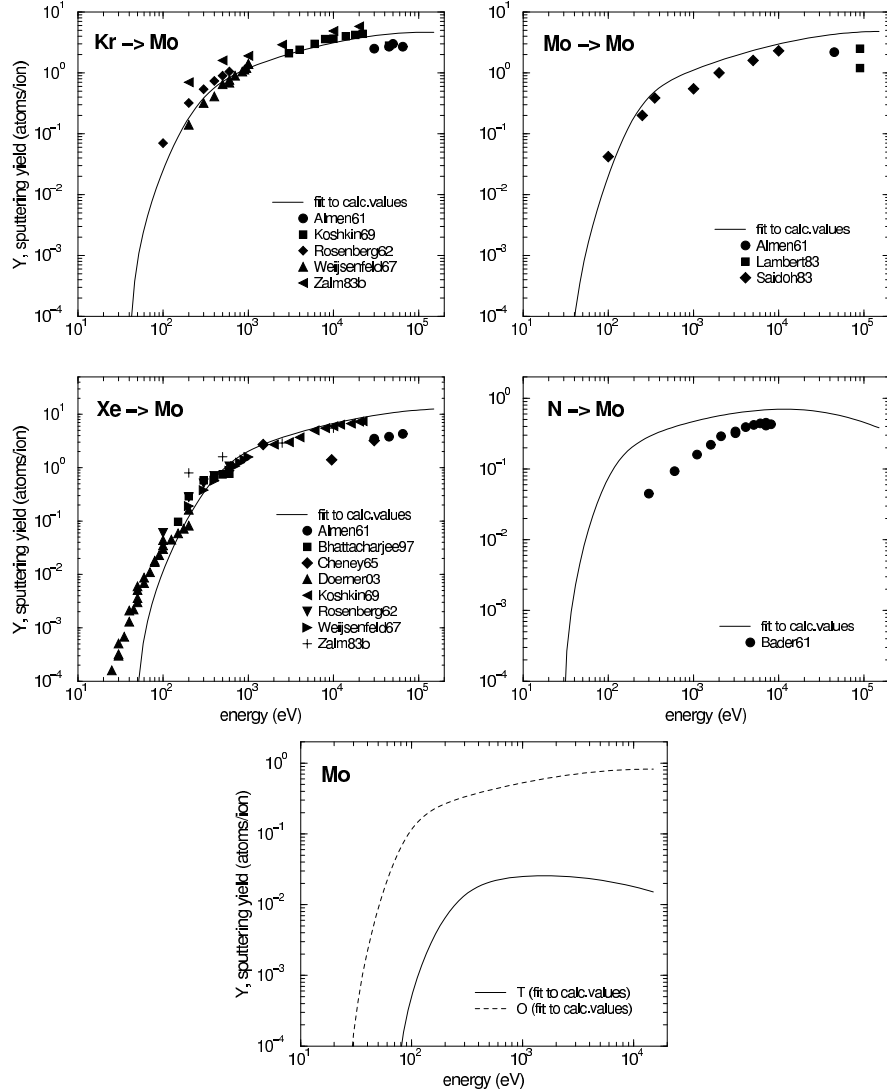


**Fig. 36.** Energy dependence of sputtering yields of Mo for bombardment at normal incidence with Kr [54,90,98,116,147], Mo [79,139,202,203], Xe [18,54,90,98,116,147,168,204], N [148] and T, O

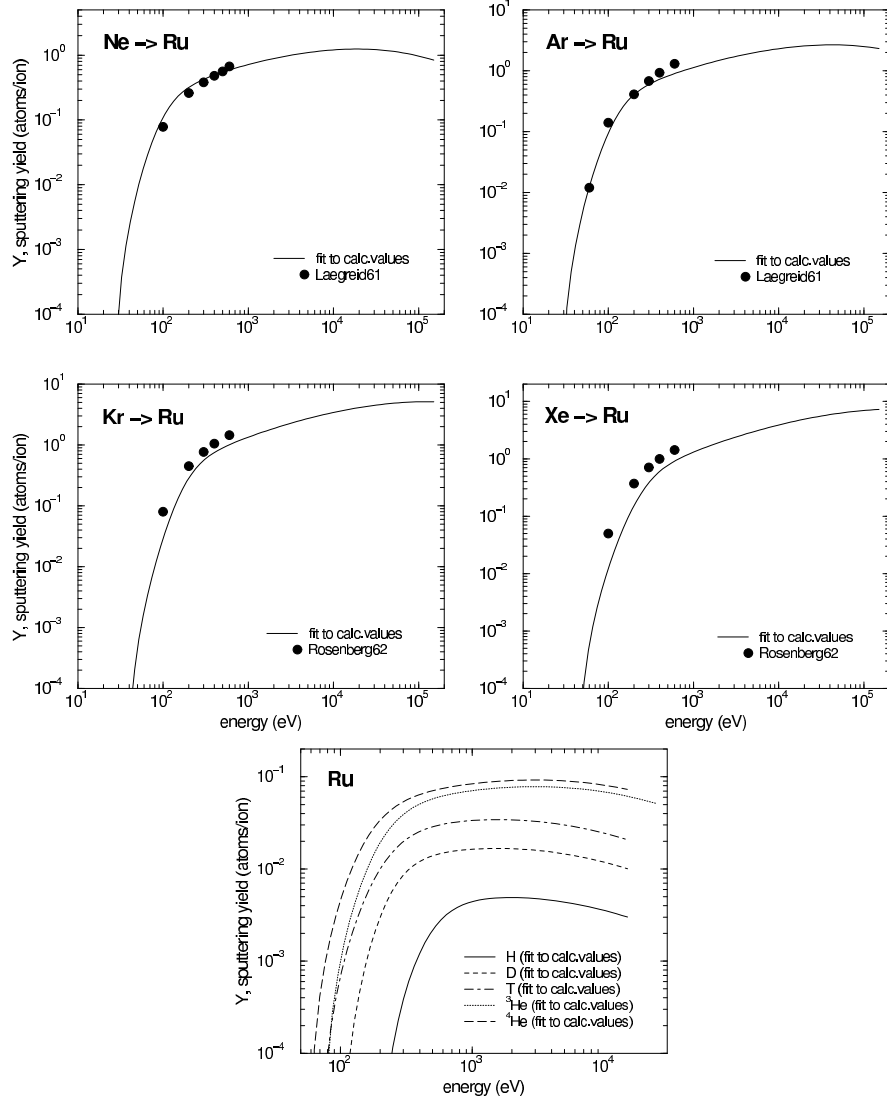


**Fig. 37.** Energy dependence of sputtering yields of Ru for bombardment at normal incidence with Ne [54], Ar [63], Kr [54], Xe [54] and H, D, T,  ${}^3\text{He}$ ,  ${}^4\text{He}$

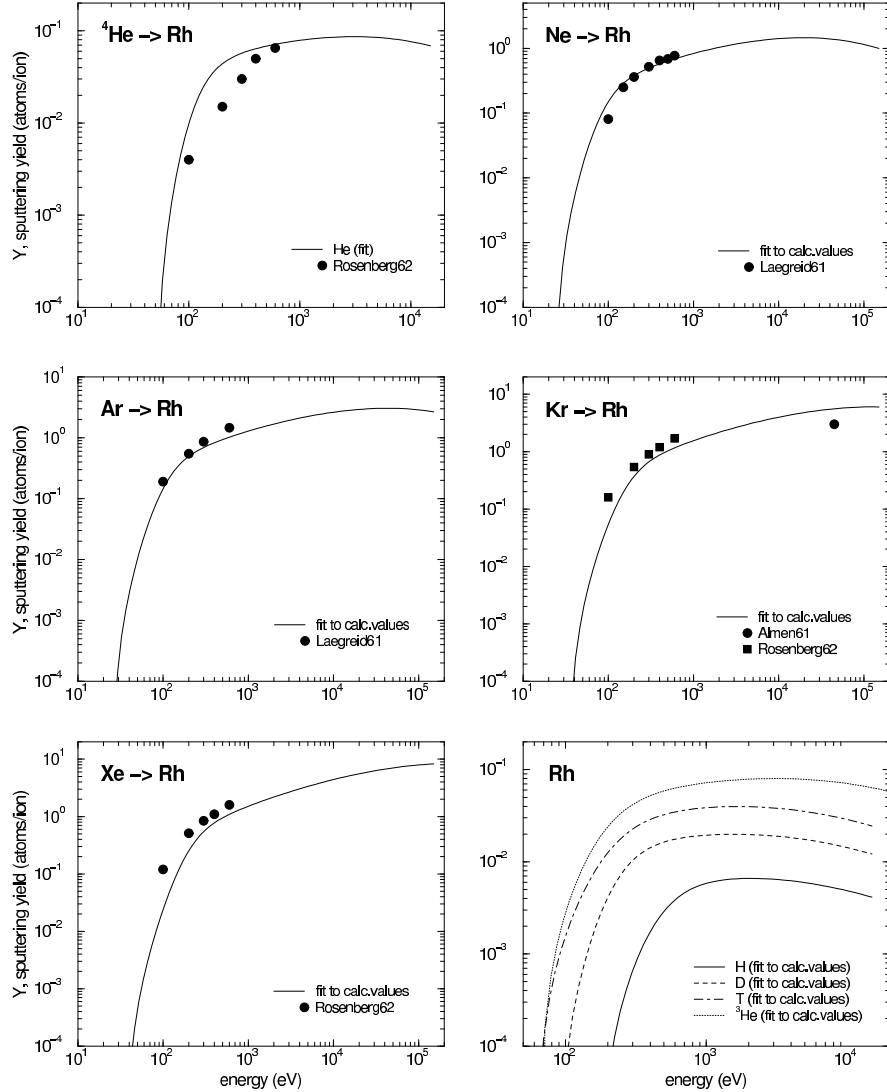


**Fig. 38.** Energy dependence of sputtering yields of Rh for bombardment at normal incidence with  ${}^4\text{He}$  [54], Ne [63], Ar [63], Kr [54,90], Xe [54], and H, D, T,  ${}^3\text{He}$

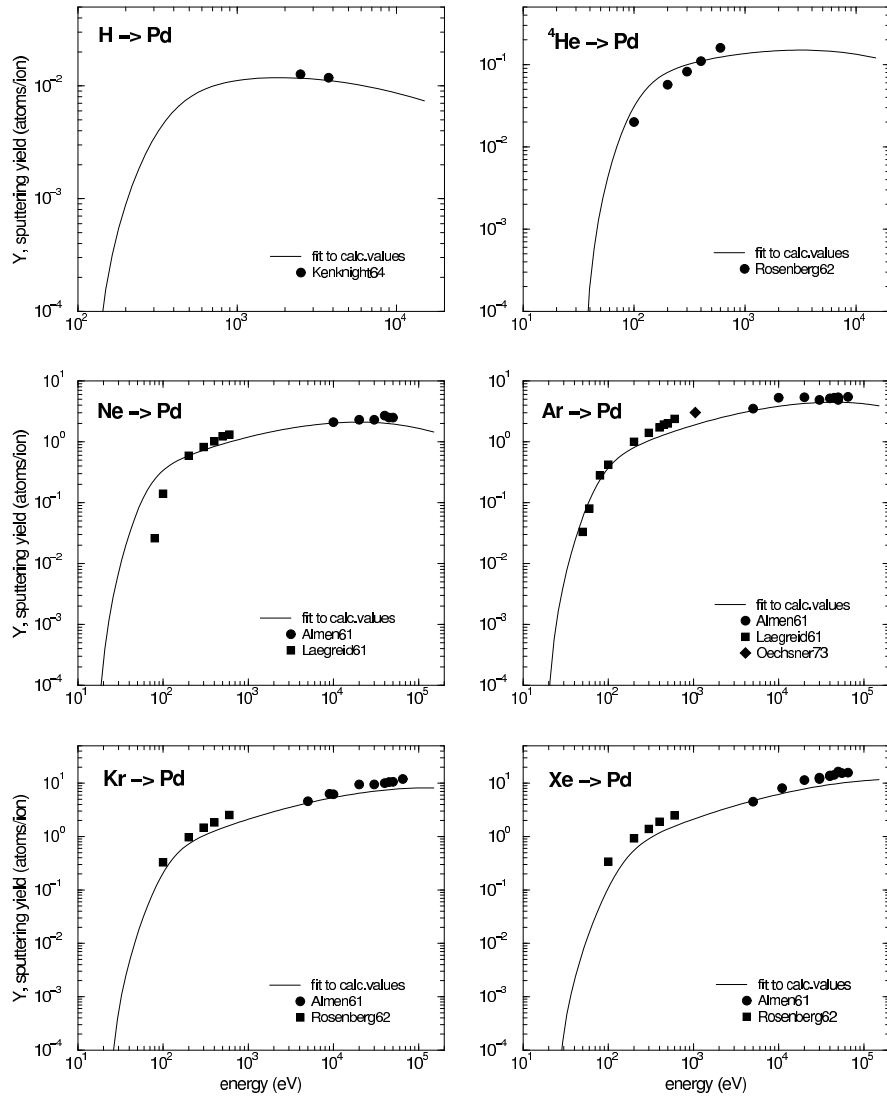


**Fig. 39.** Energy dependence of sputtering yields of Pd for bombardment at normal incidence with H [49],  ${}^4He$  [54], Ne [63,90], Ar [63,90,105], Kr [54,90], Xe [54,90]

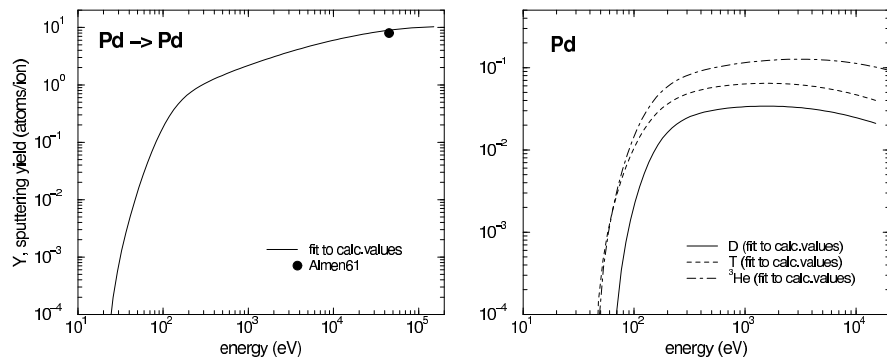


**Fig. 40.** Energy dependence of sputtering yields of Pd for bombardment at normal incidence with Pd [79], and D, T,  ${}^3\text{He}$

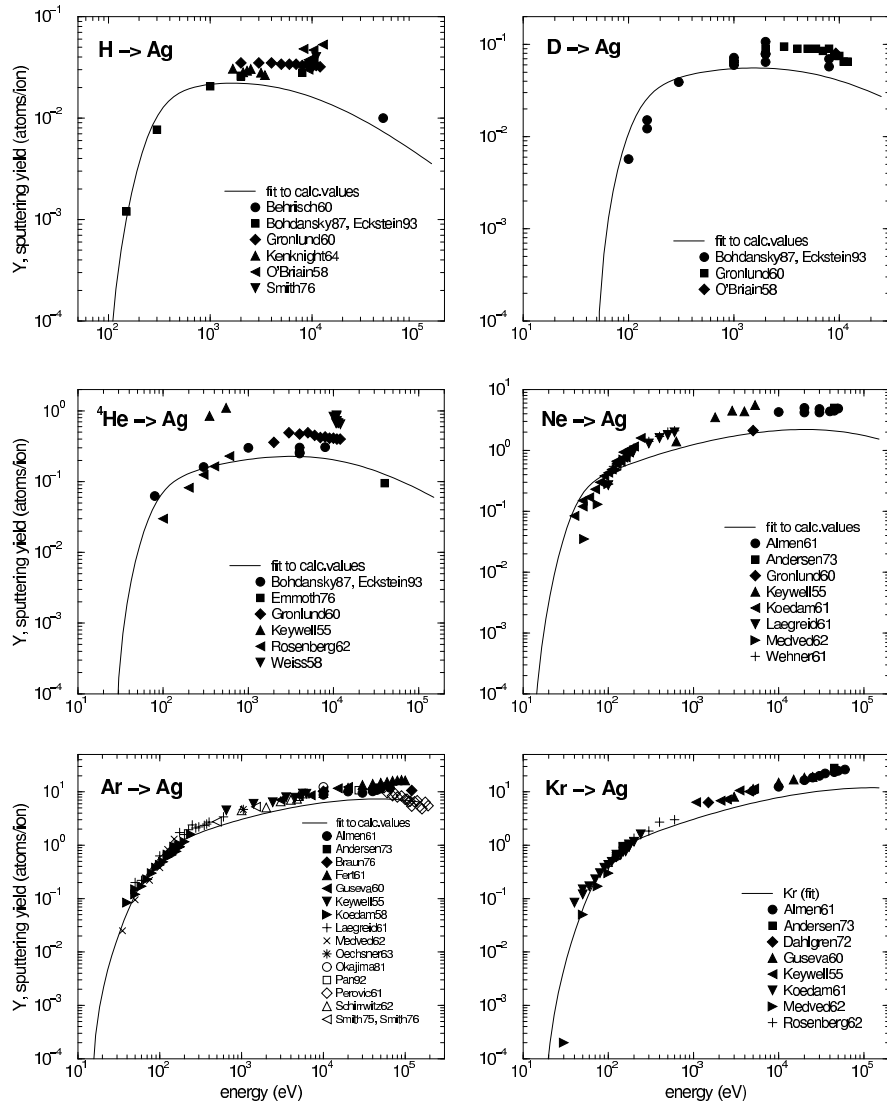


**Fig. 41.** Energy dependence of sputtering yields of Ag for bombardment at normal incidence with H [27,49,70,205–208], D [27,205,206,208],  ${}^4He$  [27,54,165,190,205,208–210], Ne [63,90,165,205,211–214], Ar [63,70,88,90,102,104–106,161,165,166,192,210,212–215], Kr [54,90,152,161,165,212–214]

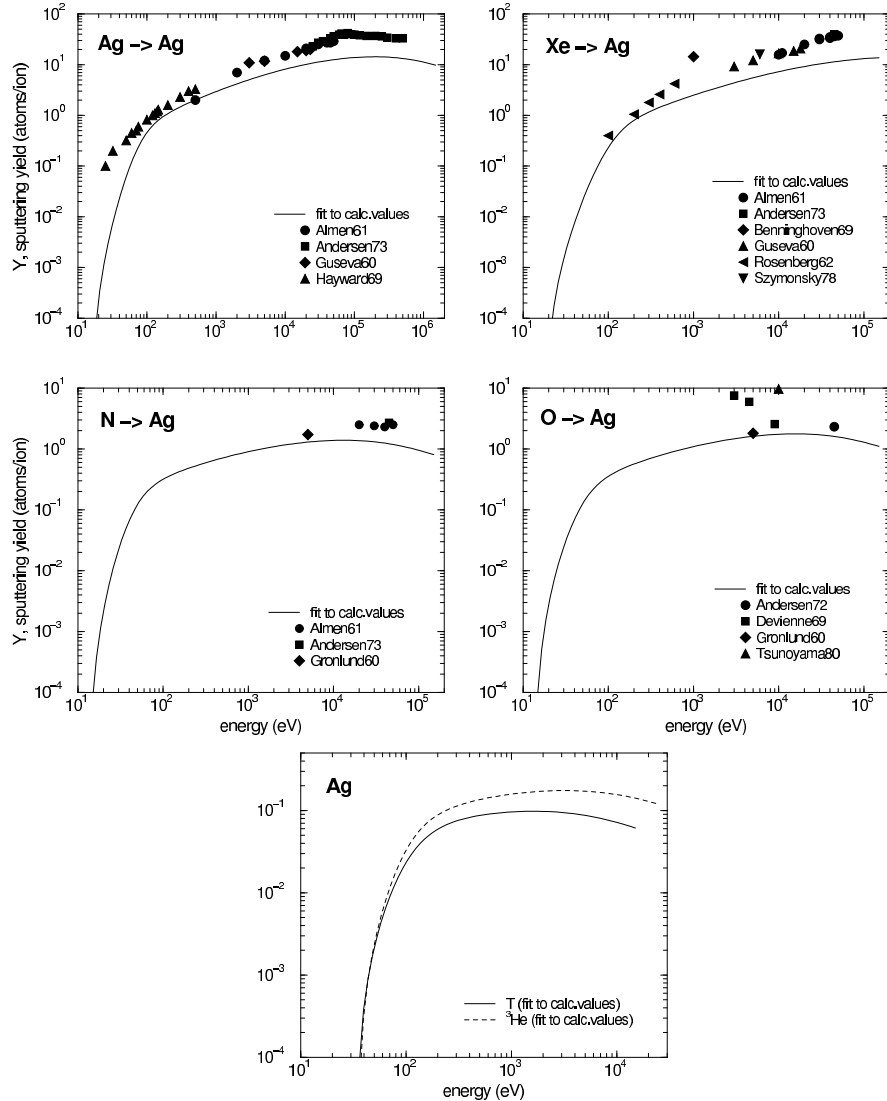


**Fig. 42.** Energy dependence of sputtering yields of Ag for bombardment at normal incidence with Ag [79,101,161,214], Xe [54,90,161,210,214,216], N [90,205,214], O [158,162,205,217] and T,  ${}^3\text{He}$

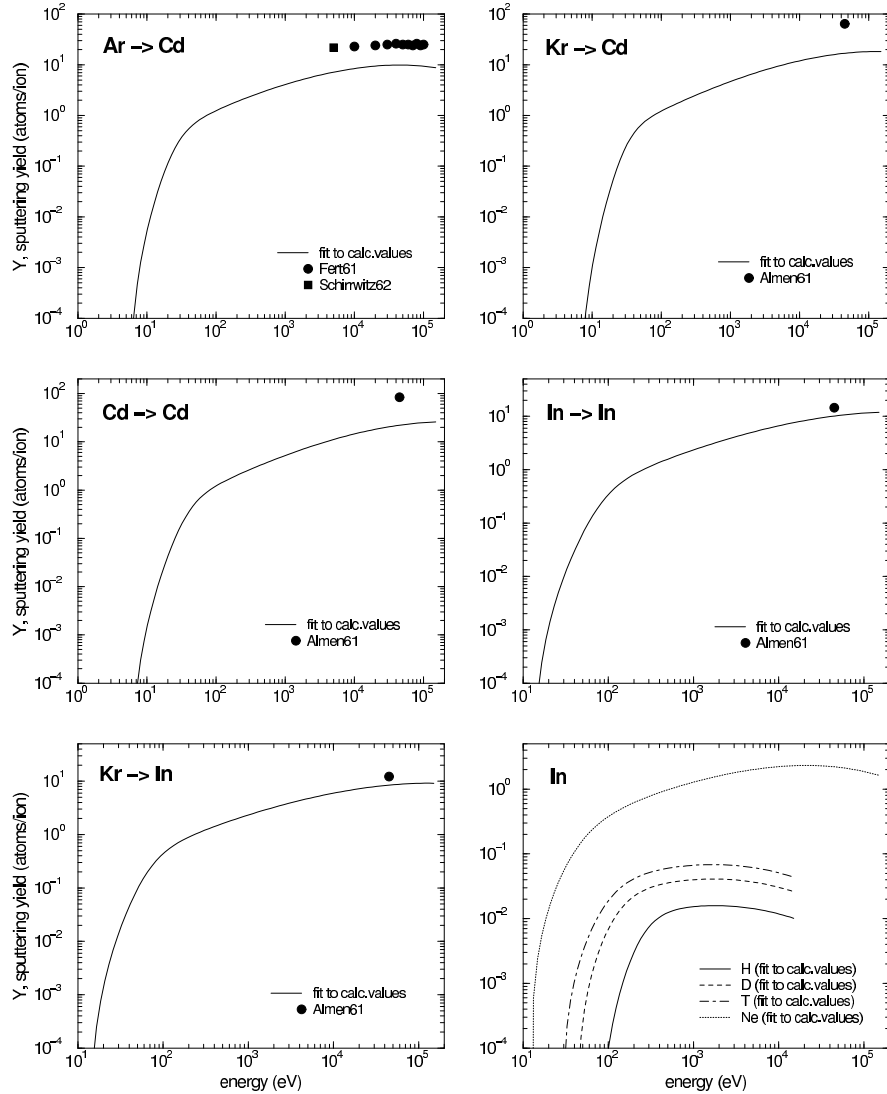


**Fig. 43.** Energy dependence of sputtering yields of Cd for bombardment at normal incidence with Ar [88,104], Kr [90], Cd [79], and for bombardment at normal incidence of In with Kr [90], In [79], and H, D, T, Ne

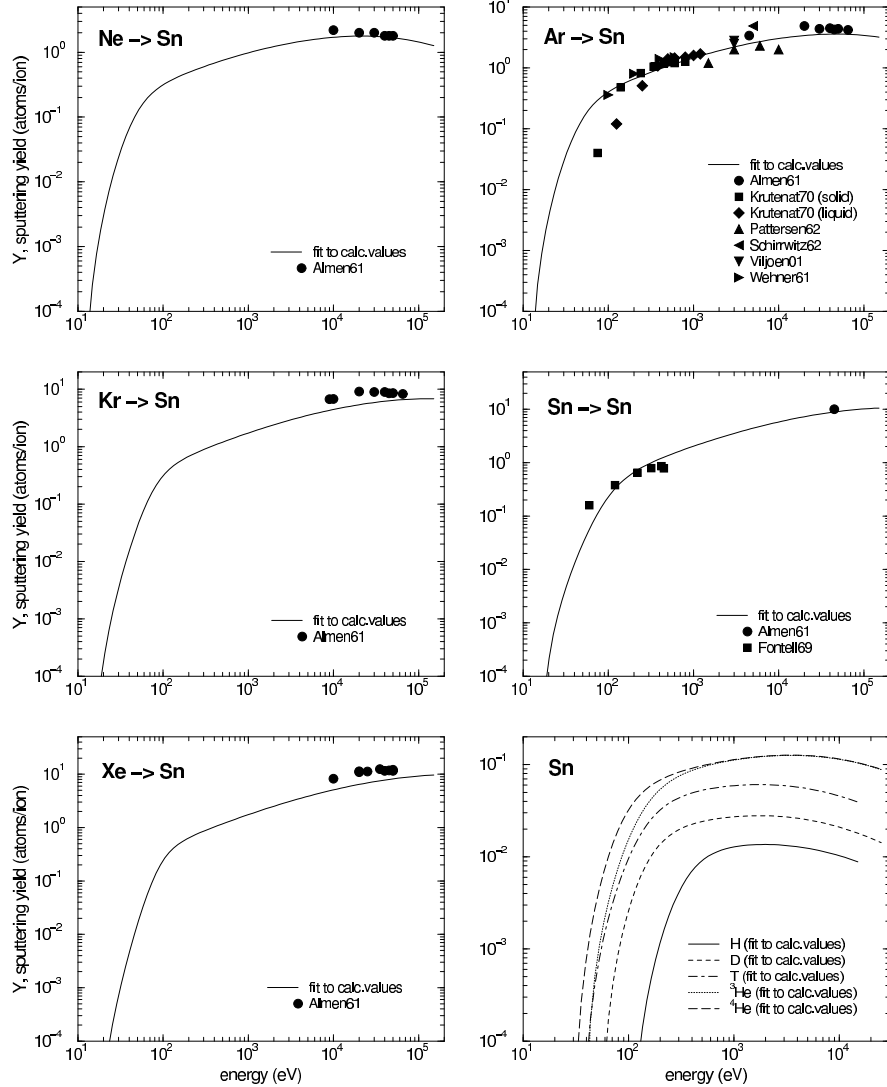


**Fig. 44.** Energy dependence of sputtering yields of Sn for bombardment at normal incidence with Ne [90], Ar [15,88,90,211,218,219], Kr [90], Sn [79,151], Xe [90], and H, D, T,  ${}^3\text{He}$ ,  ${}^4\text{He}$

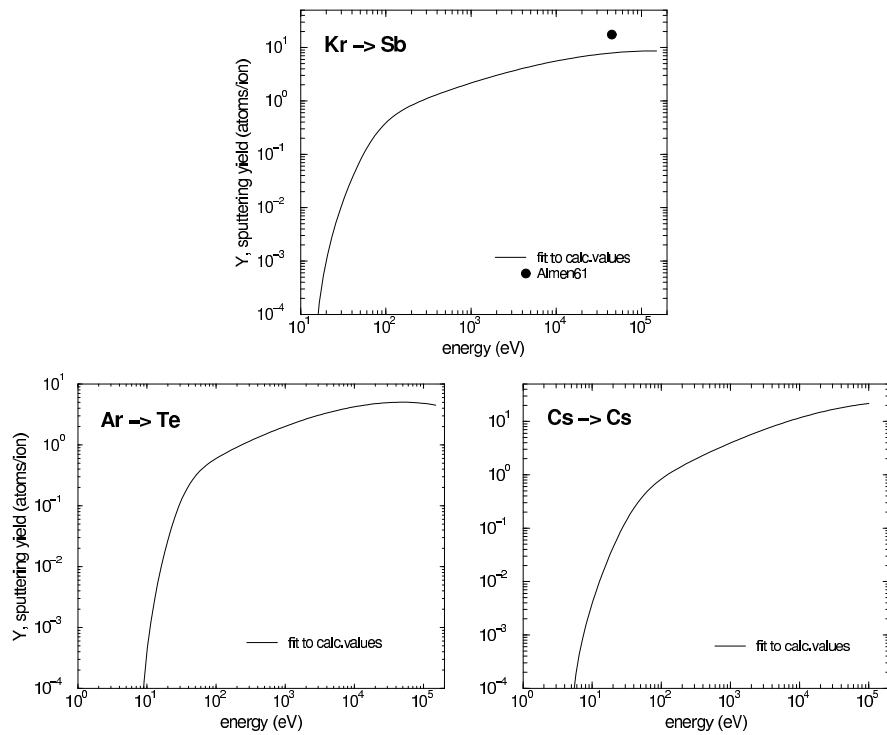


**Fig. 45.** Energy dependence of sputtering yields of Sb for bombardment at normal incidence with Kr [90], and for bombardment at normal incidence of Te with Ar and Cs with Cs

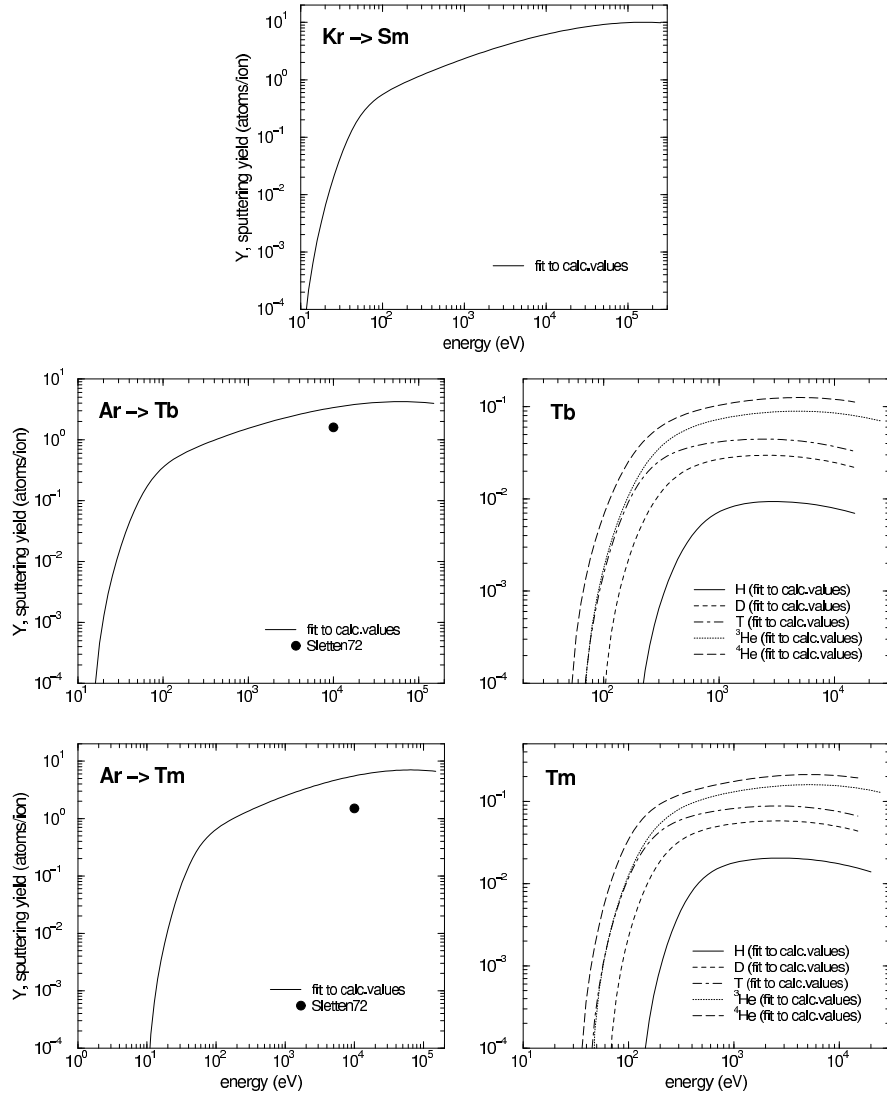


**Fig. 46.** Energy dependence of sputtering yields of Sm for bombardment at normal incidence with Kr, the bombardment at normal incidence of Tb with Ar [150] and H, D, T,  $^3\text{He}$ ,  $^4\text{He}$ , and for bombardment at normal incidence of Tm with Ar [150] and H, D, T,  $^3\text{He}$ ,  $^4\text{He}$

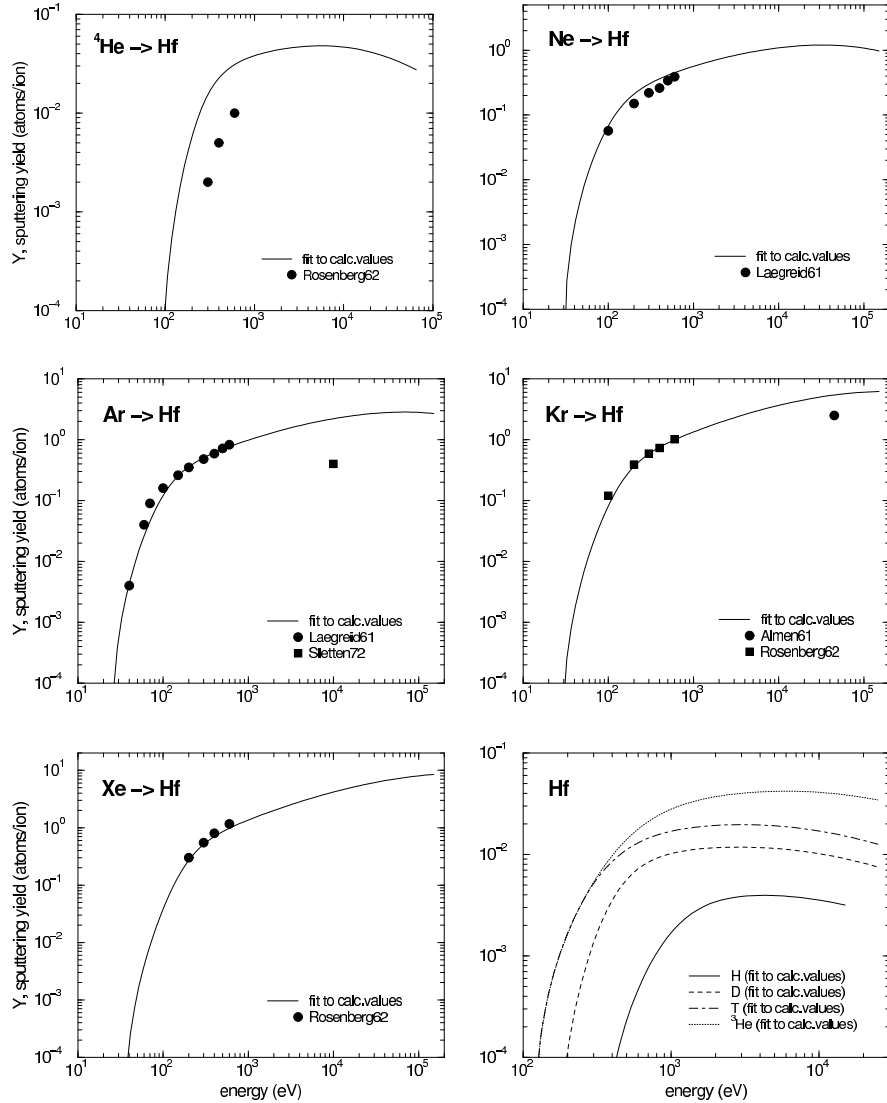


**Fig. 47.** Energy dependence of sputtering yields of Hf for bombardment at normal incidence with  ${}^4\text{He}$  [54], Ne [63], Ar [63,150], Kr [54,90], Xe [54], and H, D, T and  ${}^3\text{He}$

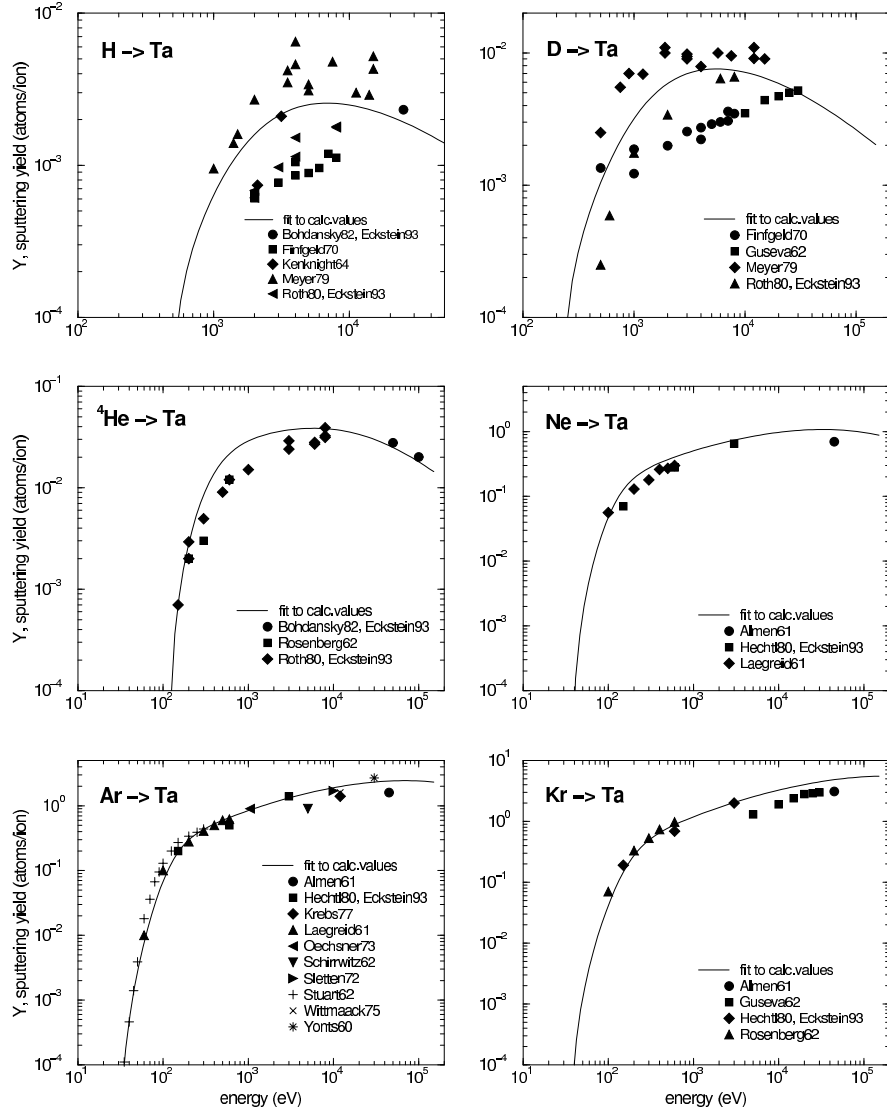


**Fig. 48.** Energy dependence of sputtering yields of Ta for bombardment at normal incidence with H [27,49,111,135,149,197], D [27,111,149,197,220],  ${}^4He$  [27,54,111,135], Ne [27,63,90,221], Ar [27,63,88,90,94,105,108,136,150,221,222], Kr [27,54,90,220,221]

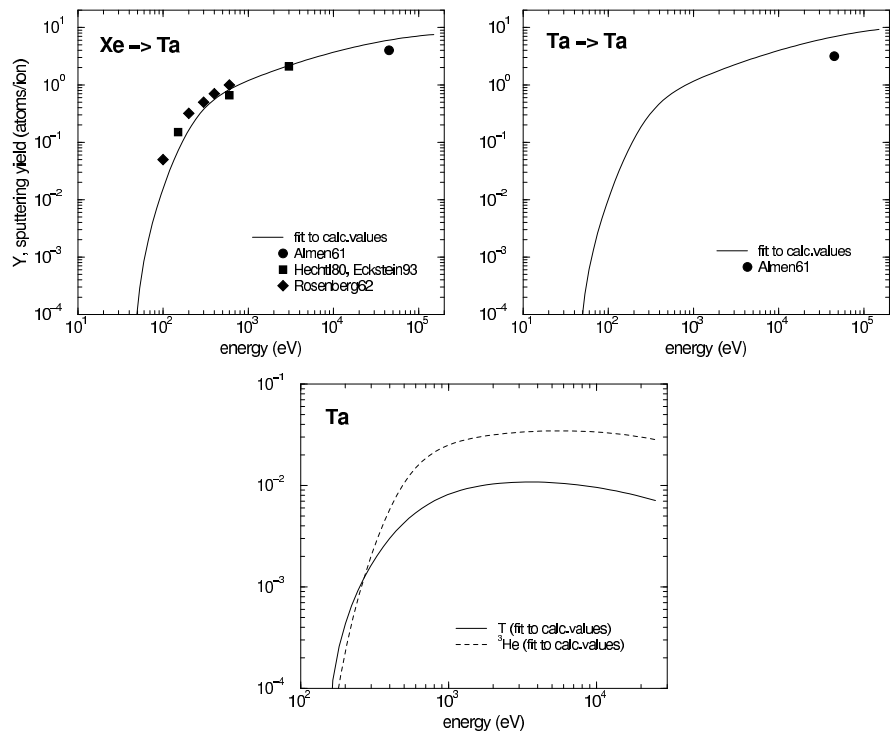


**Fig. 49.** Energy dependence of sputtering yields of Ta for bombardment at normal incidence with Xe [27,54,90,221], Ta [79], and T,  $^3He$

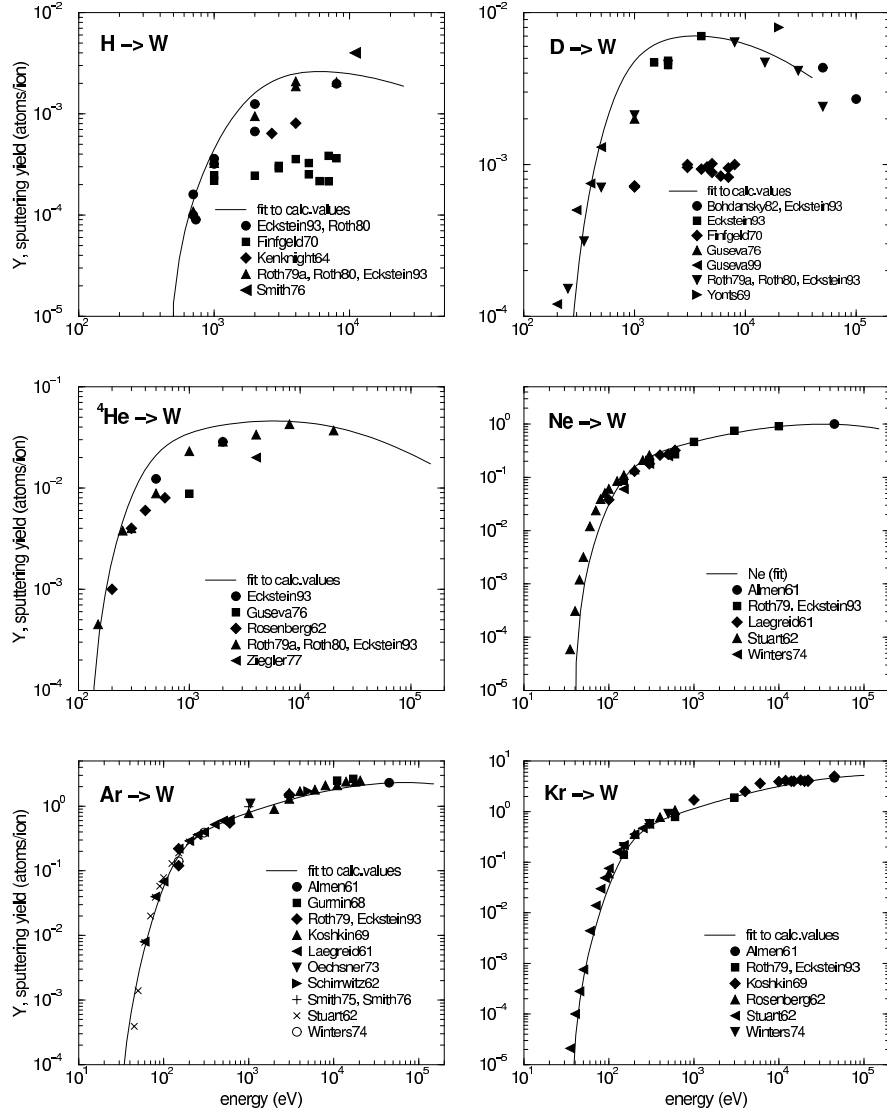


**Fig. 50.** Energy dependence of sputtering yields of W for bombardment at normal incidence with H [27,49,51,70,111,149], D [17,27,51,97,111,135,140,149],  $^4\text{He}$  [27,51,54,111,140,223], Ne [27,50,63,90,136,224], Ar [27,50,63,70,88,90,105,136,147,181,192,224], Kr [27,54,50,90,136,147,224]

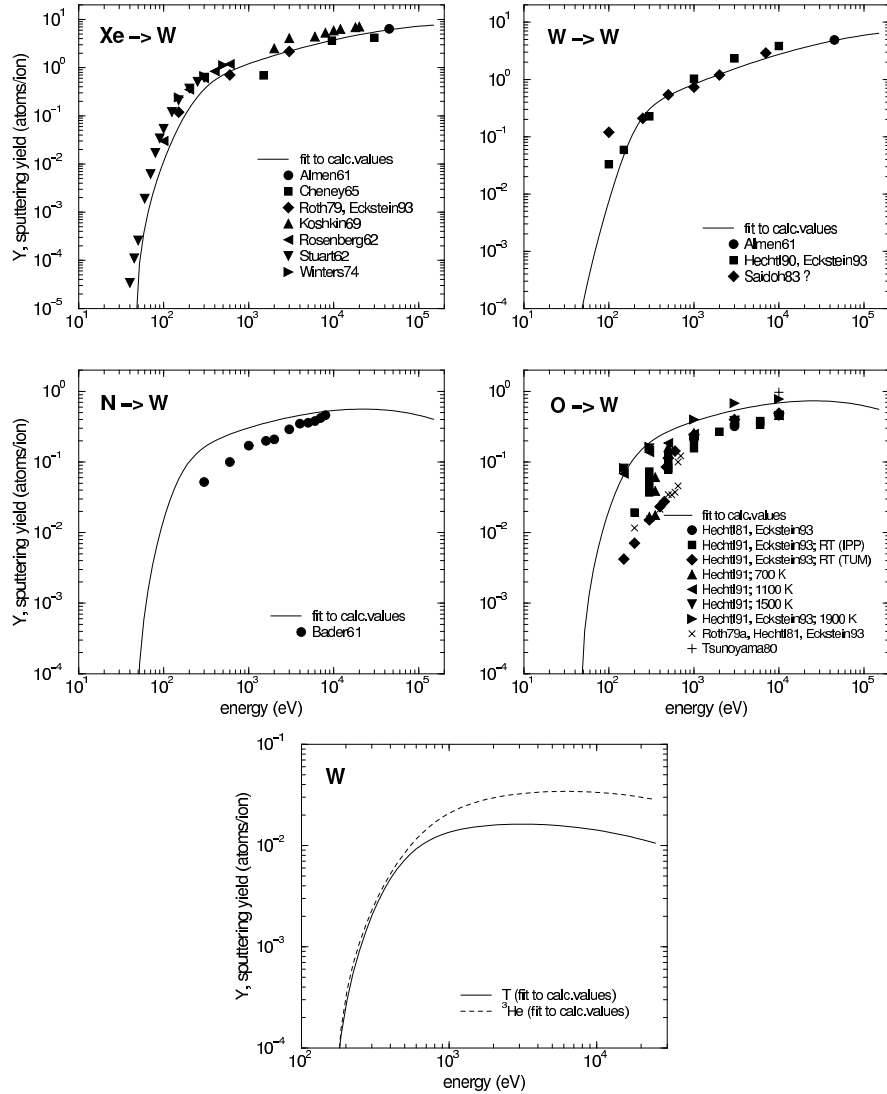


**Fig. 51.** Energy dependence of sputtering yields of W for bombardment at normal incidence with Xe [27,54,50,90,136,147,168,224], W [27,79,202,203,225], N [148], O [27,51,78,158,225] and T,  ${}^3\text{He}$

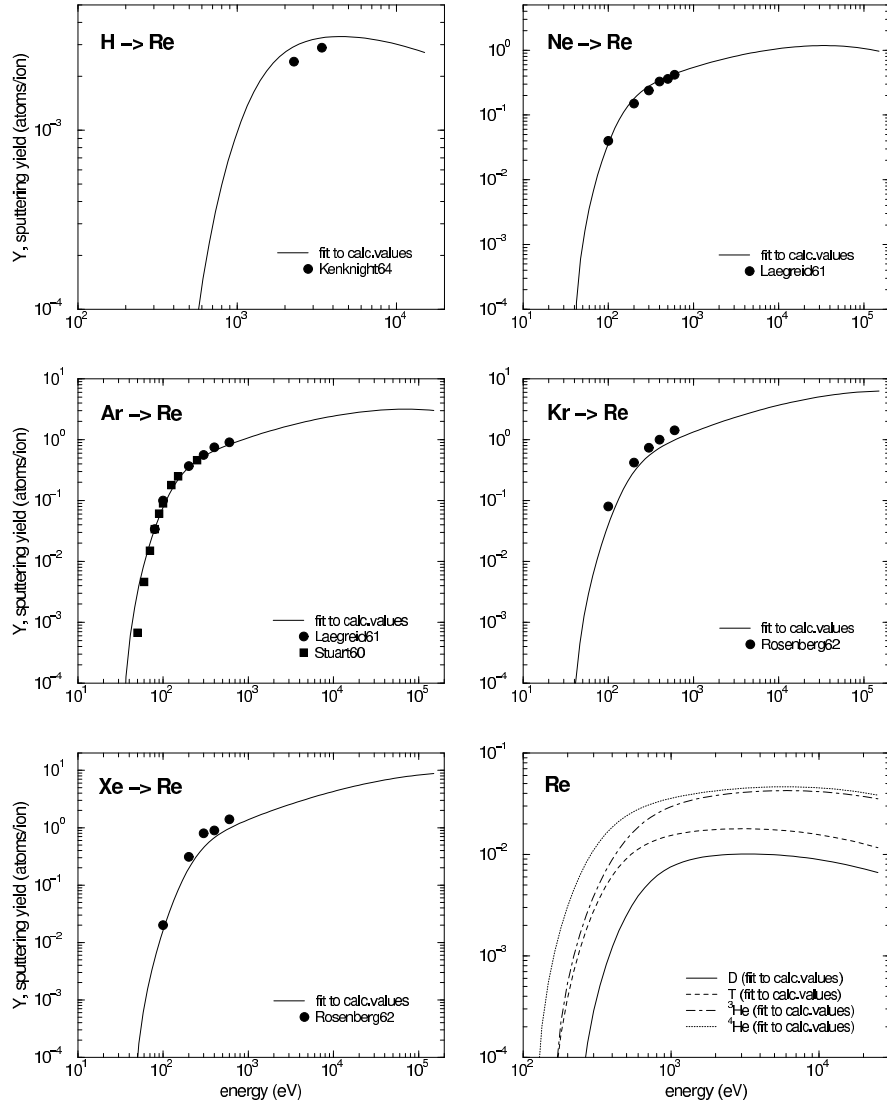


**Fig. 52.** Energy dependence of sputtering yields of Re for bombardment at normal incidence with H [49], Ne [63], Ar [63,182], Kr [54], Xe [54] and D, T,  $^3He$ ,  $^4He$

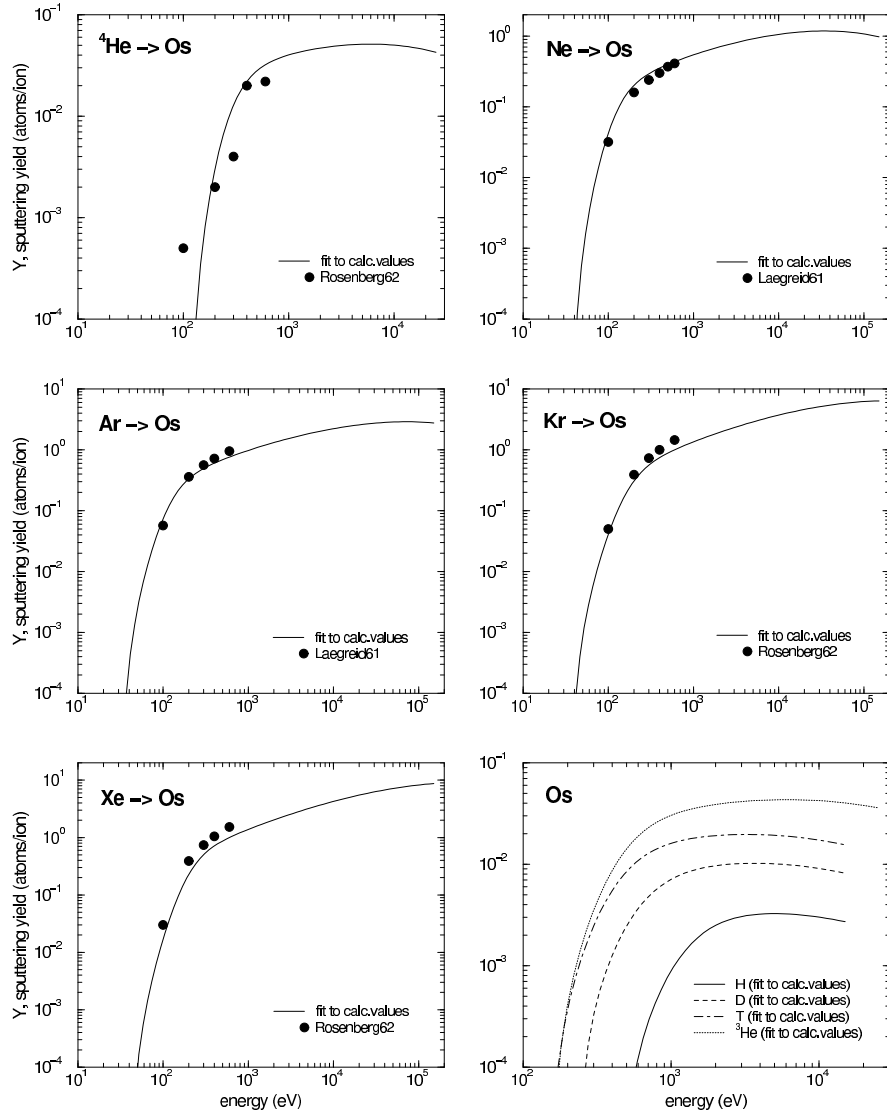


**Fig. 53.** Energy dependence of sputtering yields of Os for bombardment at normal incidence with  ${}^4\text{He}$  [54], Ne [63], Ar [63], Kr [54], Xe [54], and H, D, T,  ${}^3\text{He}$

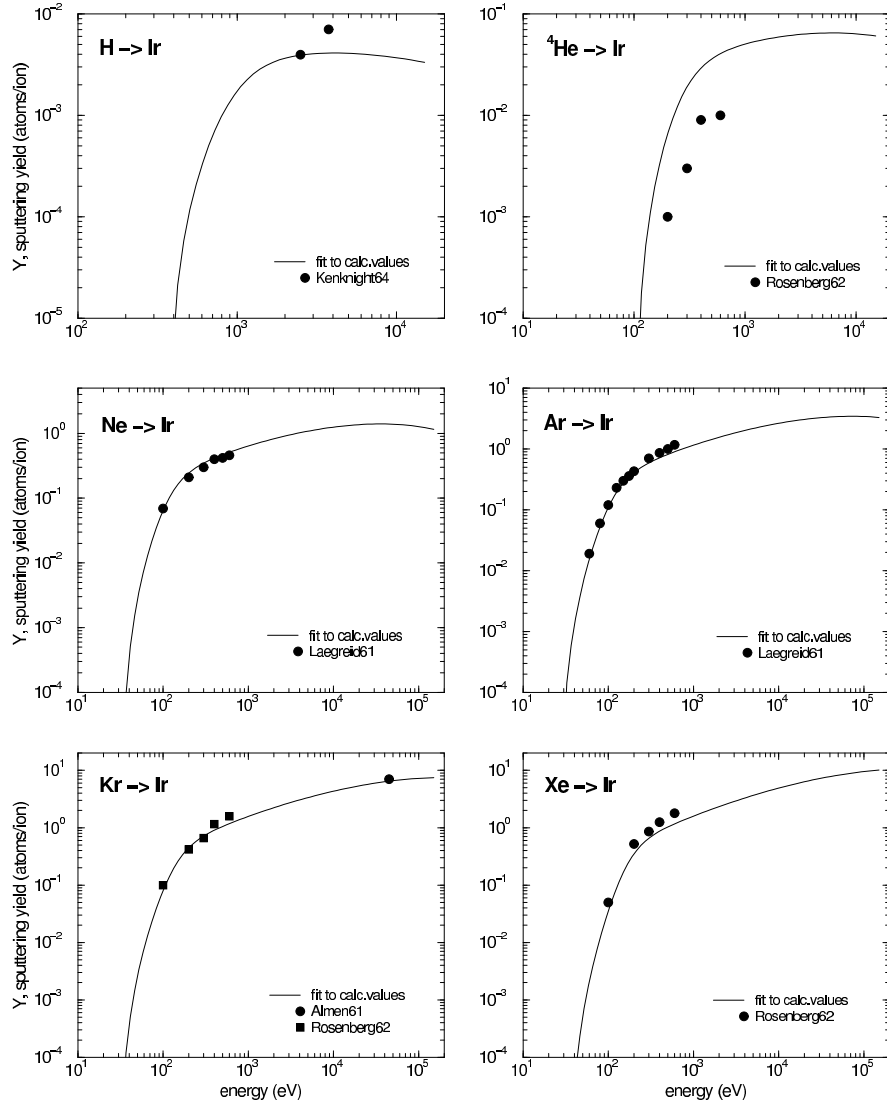


**Fig. 54.** Energy dependence of sputtering yields of Ir for bombardment at normal incidence with H [49],  ${}^4He$  [54], Ne [63], Ar [63], Kr [54,90], Xe [54]

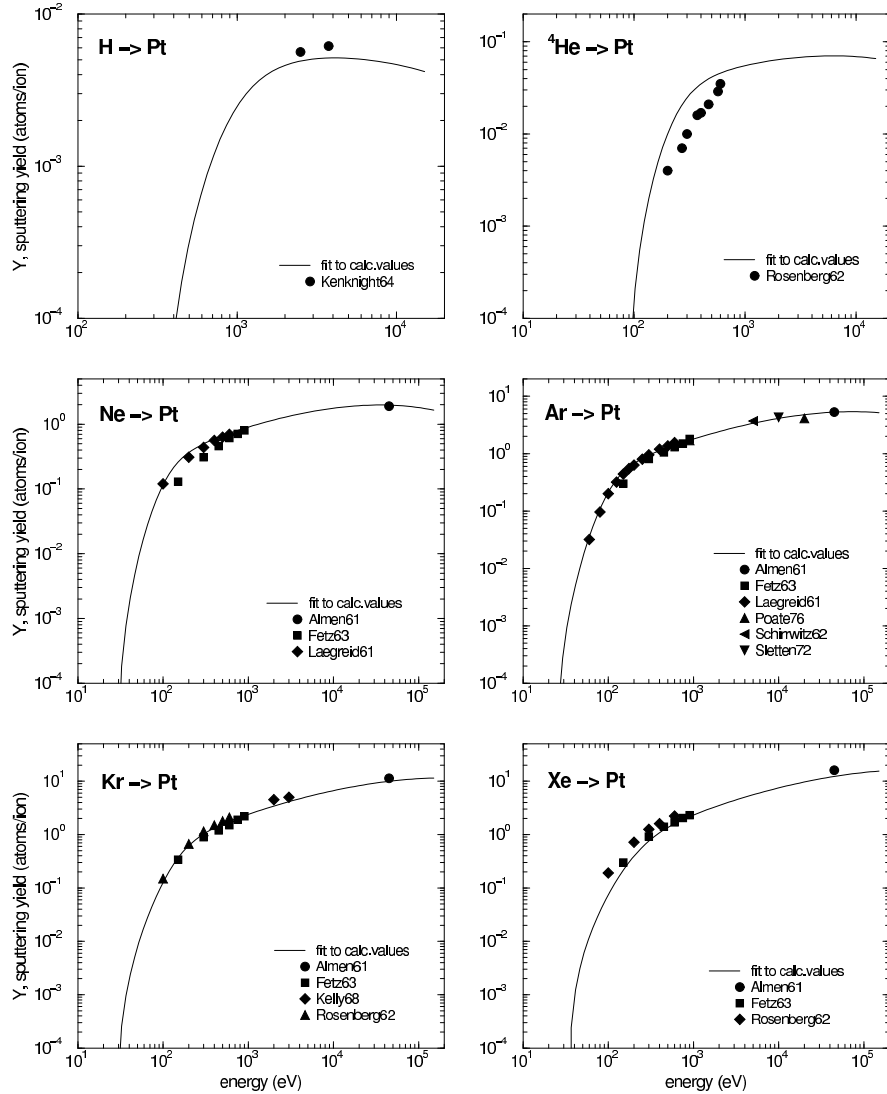


**Fig. 55.** Energy dependence of sputtering yields of Pt for bombardment at normal incidence with H [49],  ${}^4\text{He}$  [54], Ne [55,63,90], Ar [55,63,88,90,123,150], Kr [54,55,90,109], Xe [54,55,90]

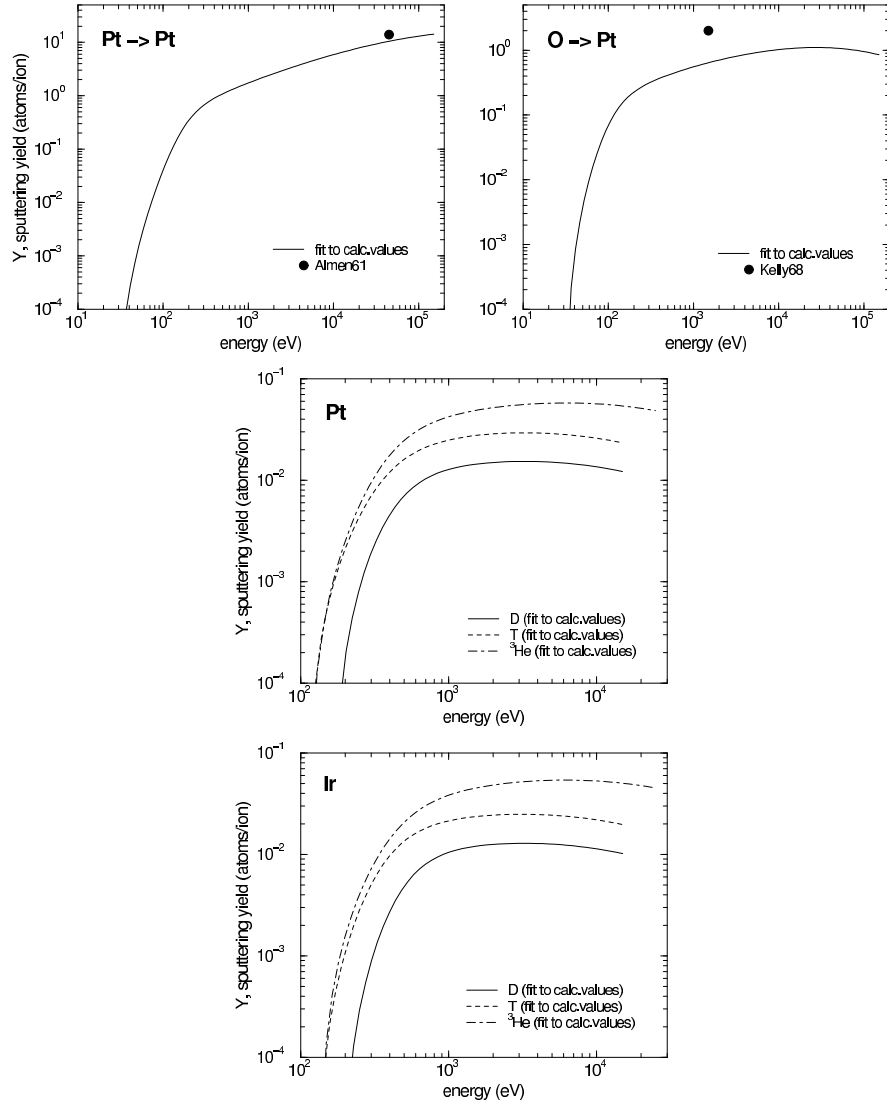


**Fig. 56.** Energy dependence of sputtering yields of Pt for bombardment at normal incidence with Pt [79], O [109] and D, T, and  $^3\text{He}$ , and of Ir for bombardment at normal incidence with D, T, and  $^3\text{He}$

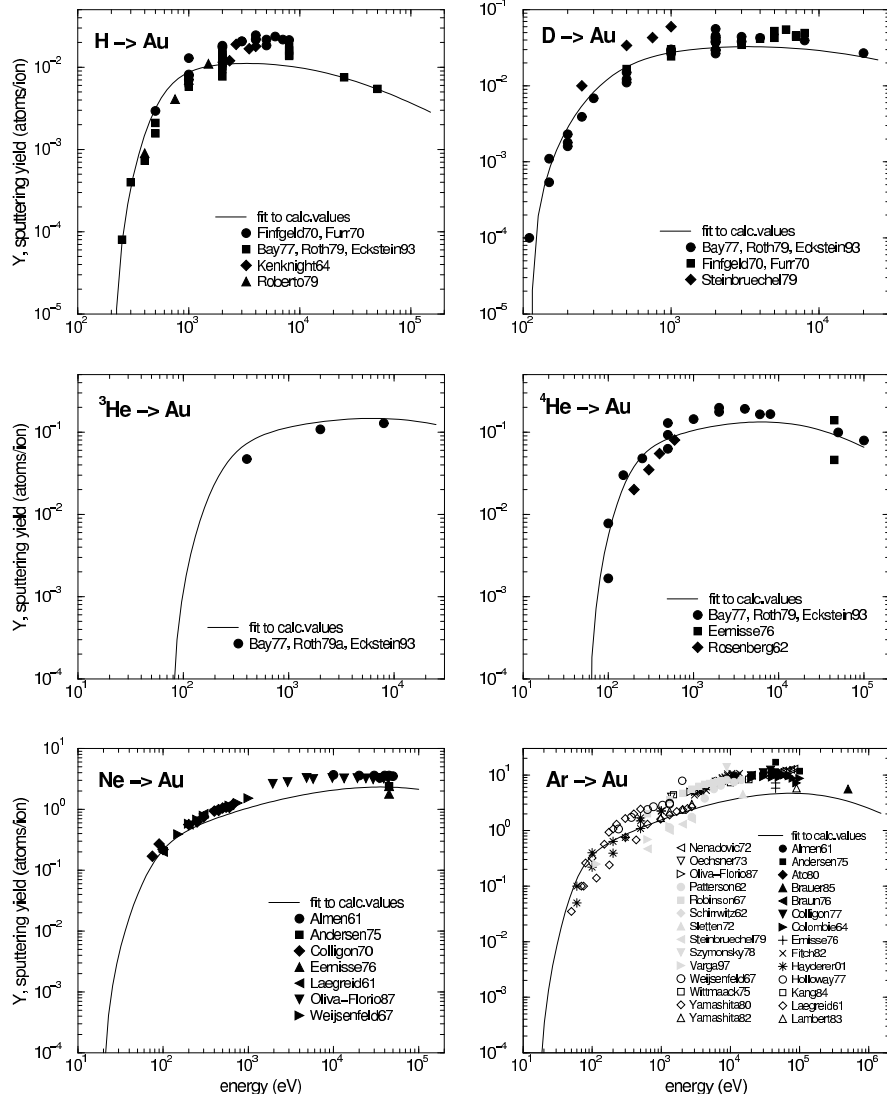


**Fig. 57.** Energy dependence of sputtering yields of Au for bombardment at normal incidence with H [27,49,50,149,154,194,194,226], D [27,50,133,149,194,226],  ${}^3\text{He}$  [27,51,194],  ${}^4\text{He}$  [27,54,50,194,227], Ne [63,90,98,174,227–229], Ar [15,63,77,88,90,98,102,105,107,129,133,139,143,150,171,174,175,180,210,216,222,227,229–234]

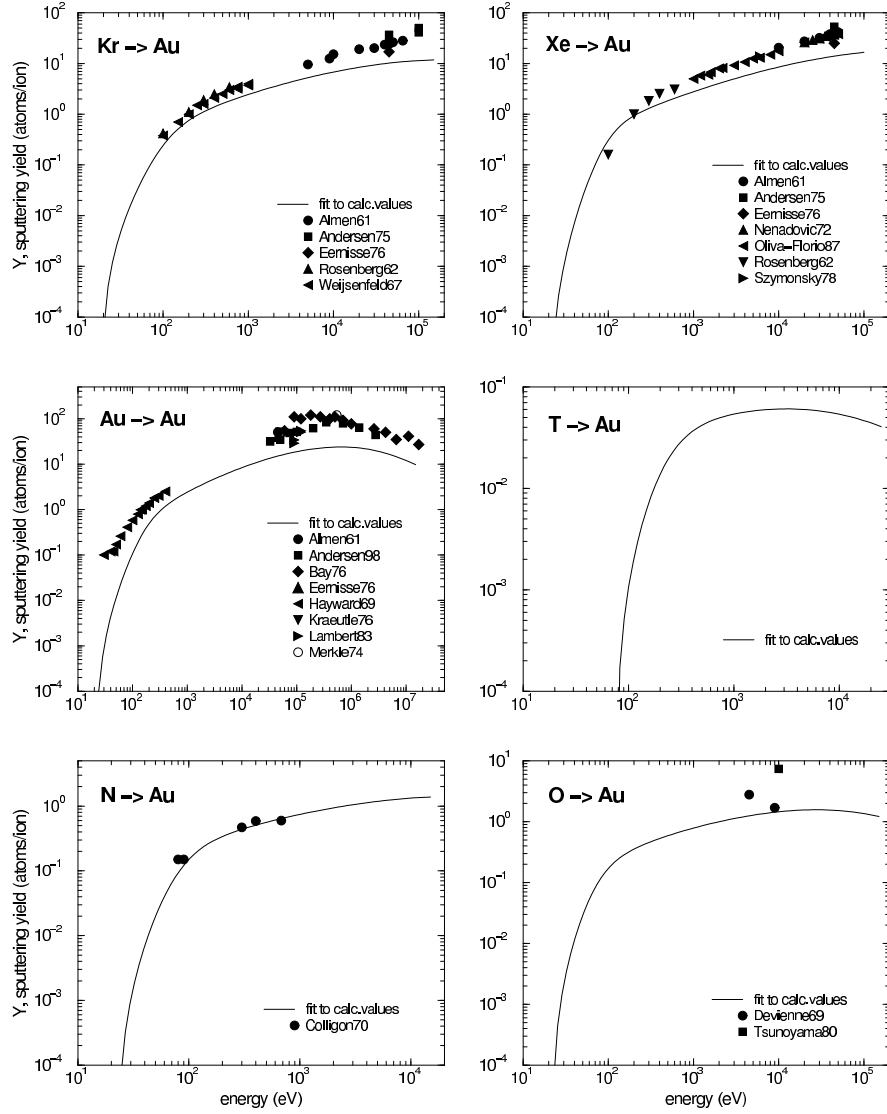


**Fig. 58.** Energy dependence of sputtering yields of Au for bombardment at normal incidence with Kr [54,90,98,227,229], Xe [54,90,174,216,227,229,230], Au [79,101,139,227,235–238], T, N [228], O [158,217]

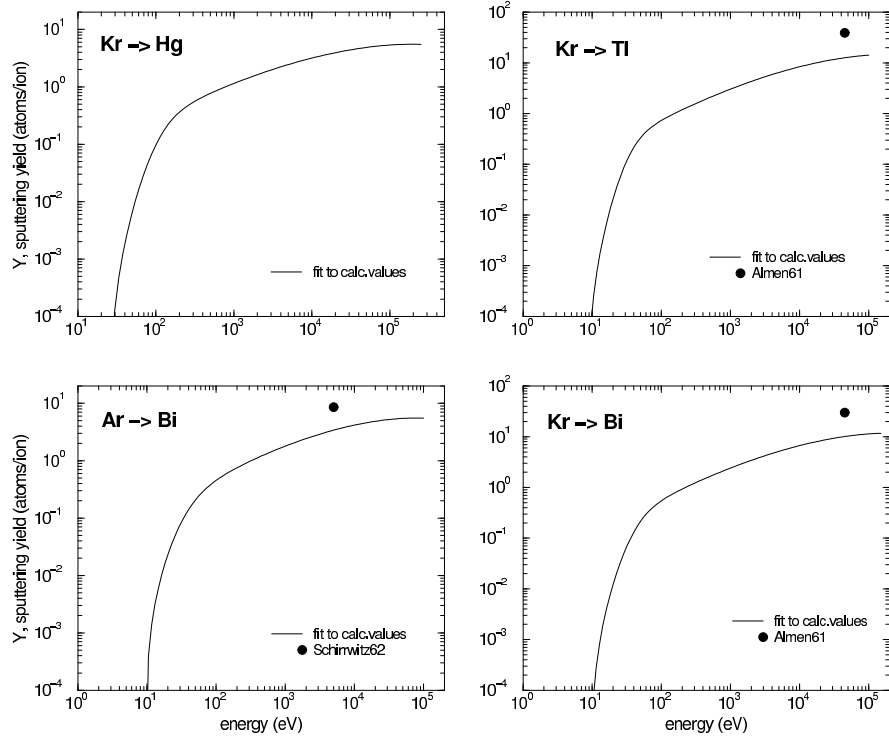


**Fig. 59.** Energy dependence of sputtering yields of Hg and Tl for bombardment at normal incidence with Kr [90] and of Bi bombardment at normal incidence with Ar [88], Kr [90]

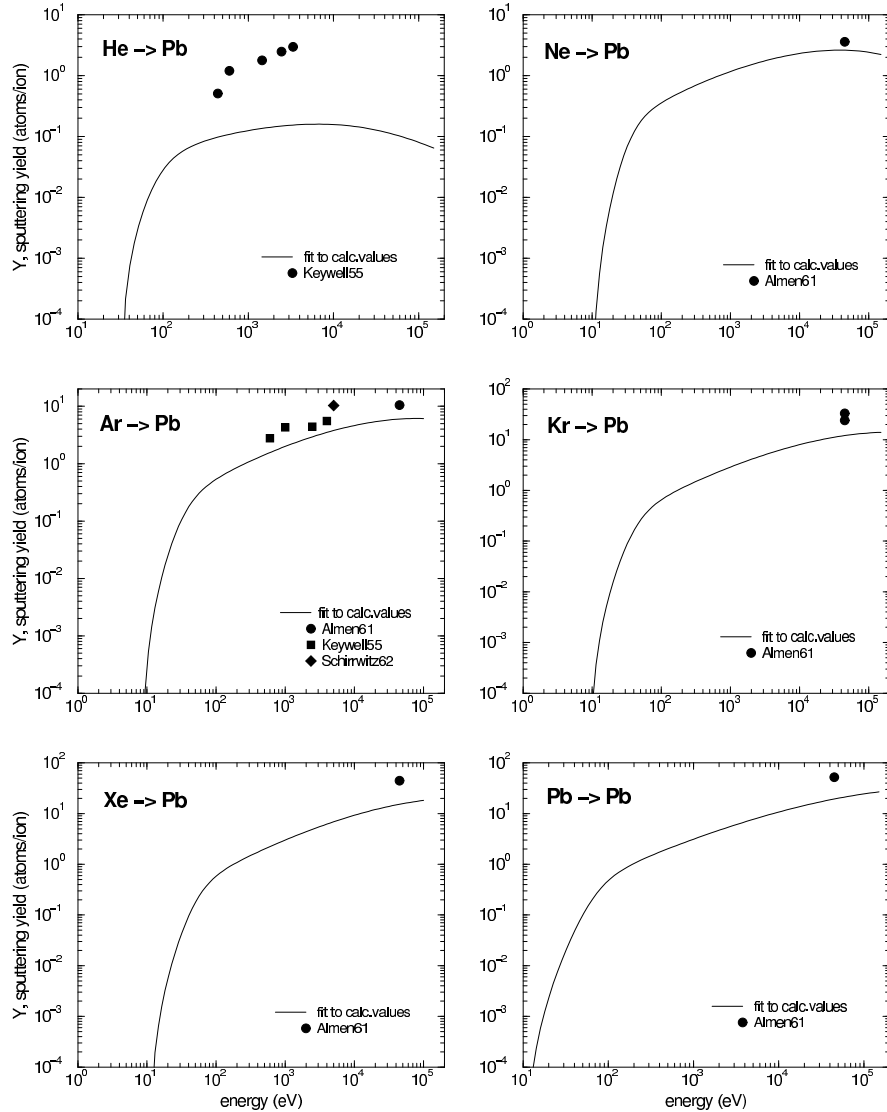


**Fig. 60.** Energy dependence of sputtering yields of Pb for bombardment at normal incidence with He [165], Ne [90], Ar [88,90,165], Kr [90], Xe [90], Pb [79]

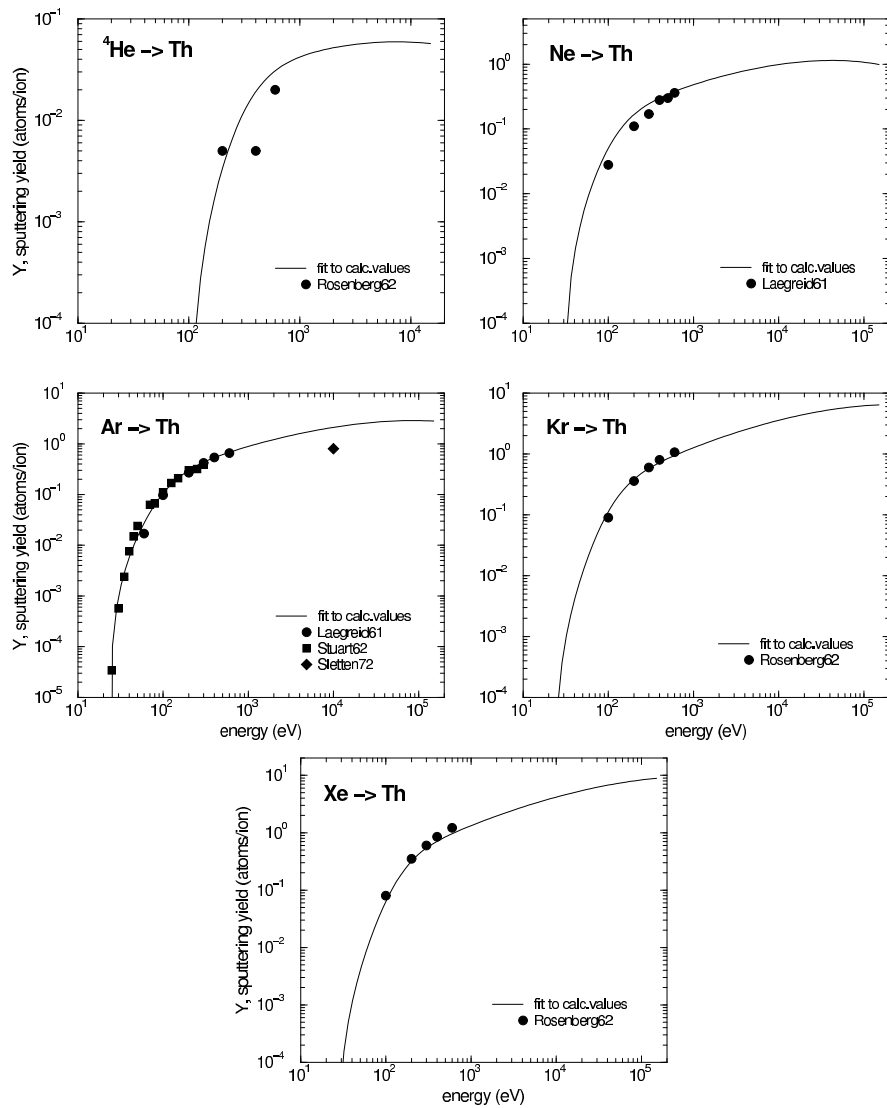


**Fig. 61.** Energy dependence of sputtering yields of Th for bombardment at normal incidence with  ${}^4\text{He}$  [54], Ne [63], Ar [63,136,150], Kr [54], Xe [54]

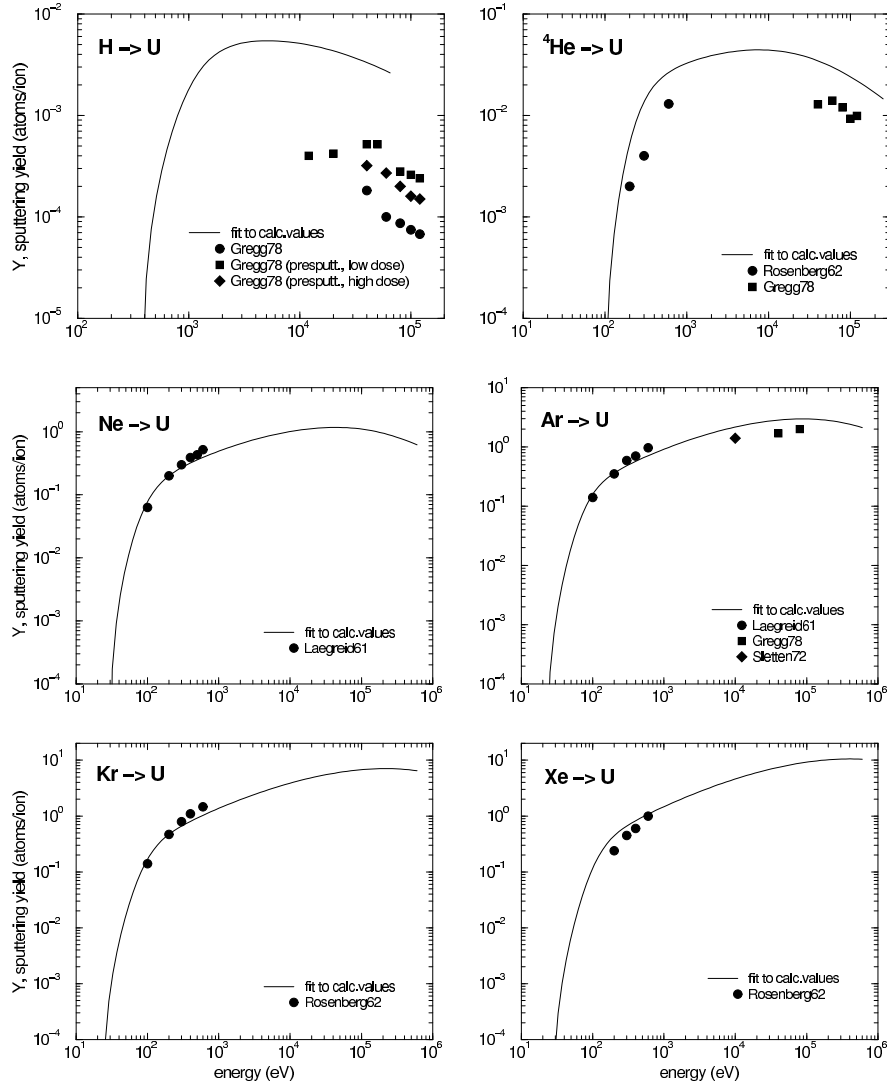


**Fig. 62.** Energy dependence of sputtering yields of U for bombardment at normal incidence with H [239],  $^4He$  [54,239], Ne [63], Ar [63,150,239], Kr [54], Xe [54]

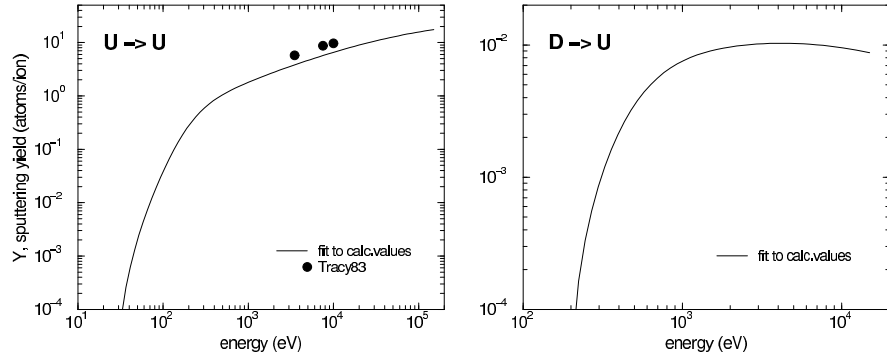


**Fig. 63.** Energy dependence of sputtering yields of U for bombardment at normal incidence with U [240], D

The agreement of the experimentally determined sputtering yields at normal incidence with the fit to the calculated values is generally reasonable. This gives confidence to the calculated and measured values. Deviations of up to a factor of two are likely due to uncertainties in the different experiments. Even for noble gases implanted into targets the measured sputtering yield can change by up to 30% [130].

There are some obvious deviations:

For carbon and silicon bombardment by hydrogen isotopes and oxygen the measured sputtering yields are definitely larger than the calculated curves, especially at low energies, see figures 8 and 13. This is an indication for a different mechanism contributing to sputtering, which is named chemical sputtering (see Chapter by Jacob, Roth). For materials which form oxides with a strong binding the measured sputtering yields are lower as in the case of beryllium, aluminum and tantalum [88]. The influence of an residual oxygen pressure in the vacuum system on the measured yield has been investigated systematically confirming lower yields of oxides on the surface [101,134,241,242]. For some targets, as for example beryllium, the target had to be heated to an elevated temperature so that Be diffuses through the oxide layer resulting in a clean Be surface [48]. Experimental data below 100 eV may be too large due to the energy width and the angular divergence of the incident beam [243], energetic neutrals in the ion beam, surface roughness and adatoms. Also implantation of heavy noble gases in low Z targets can increase the yield and may shift the threshold to lower energies [18]. Experimental data deviating by an order of magnitude from the calculated curves are probably erroneous as in the case of hydrogen isotope bombardment of cobalt, see Fig. 23.

For Cu, Ag, and Au there is a general tendency, that the measured yields are systematically higher at energies above about 1 keV than the calculated curves. The reason could be a problem of the interaction potential, the surface binding energy, or the inelastic energy loss. An experimental reason could be

a large fraction of sputtered molecular species. But the most likely reason for the observed discrepancy is the occurrence of collisional spikes, which give a larger contribution to the yield than for neighbour elements (such as Pt in the case of Au) [244], see also Chapter by Assmann, Toulemonde, Trautmann.

Extraordinarily high sputtering yields of the order of  $10^5$  are reported for the sputtering of sulfur with He ions [245,246]. These results cannot be understood by collisional effects; they are explained by the implantation of charge into the insulating material by the incoming ions and electrostatic repulsion.

In some experiments such as in fusion plasma devices the incident flux (of hydrogen) has a distribution in energy and angle of incidence [247]. Calculated yields for a Maxwellian distribution of hydrogen isotopes on several targets are provided in [36,248].

The dependence of the sputtering yield on the target density has been studied by *Shulga* [249,250] with computer simulation showing a slight increase in the yield with increasing target density.

### 3.4 Angle of Incidence Dependence of the Sputtering Yield

The sputtering yield depends on the angle of incidence of the bombarding particle. Yields have been calculated with TRIM.SP for different angles of incidence at various energies for several ion-target combinations Analogously to the energy dependence of the sputtering yield, the angular dependence of calculated values is fitted with an algebraic formula [44] and subsequently compared to experimental data.

$$\frac{Y(E_0, \theta_0)}{Y(E_0, 0)} = \left\{ \cos \left[ \left( \frac{\theta_0}{\theta_0^*} \frac{\pi}{2} \right)^c \right] \right\}^{-f} \exp \left\{ b \left( 1 - 1 / \cos \left[ \left( \frac{\theta_0}{\theta_0^*} \frac{\pi}{2} \right)^c \right] \right) \right\} \quad (6)$$

$$\theta_0^* = \pi - \arccos \sqrt{\frac{1}{1 + E_0/E_{sp}}} \geq \frac{\pi}{2} \quad (7)$$

$\theta_0^*$  takes care of the effect, that an angle of incidence of  $90^\circ$  cannot be reached, if the projectile experience a binding energy  $E_{sp}$  (to simulate a chemical binding).  $E_{sp} = E_{sb}$  for selfbombardment with  $E_{sb}$  being the surface binding energy (heat of sublimation),  $E_{sp} = 1$  eV is assumed for hydrogen isotopes and nitrogen,  $E_{sp} = 0$  for nobel gases. This projectile binding effect is only important at low energies and especially for selfbombardment. If  $E_{sp} = 0$ ,  $\theta_0^*$  becomes  $\pi/2$  and formula (6) is close to the Yamamura formula [251] besides the parameter  $c$ . If  $E_{sp} > 0$  the projectile experiences an acceleration and a refraction (decrease of the angle of incidence). The angle  $\theta_{0m}$ , at which the angular dependence reaches its maximum, is determined by

$$\theta_{0m} = \frac{2}{\pi} \theta_0^* (\arccos(b/f))^{1/c} \quad (8)$$

The values of the parameters  $f, c, b$  obtained by fitting the calculated yields (with TRIM.SP) with Bayesian statistics are provided in Tables 10 to 24 together with values  $Y(E_0, 0), E_{sp}, \theta_0^*, \theta_{0m}$ . Figures are only given, if experimental data for more than three angles of incidence are available.

The general behaviour of the angular dependence of the calculated sputtering yields is shown in Fig. 64. As an example for noble gas ions Fig. 64a shows for  ${}^4\text{He}$  on nickel, that the maximum of the angular dependence shifts to larger angles of incidence with increasing projectile energy, and that the ratio of maximum yield to the yield at normal incidence increases also with the incident energy. Close to threshold of sputtering the maximum of the dependence moves towards normal incidence. The situation is different for a case, where the binding of the projectile to the target becomes important such as for selfsputtering. Fig. 64b shows the angular dependence for copper selfbombardment. Close to the threshold energy of sputtering the maximum occurs at large angles of incidence, moves then to smaller angles of incidence with increasing projectile energy. It shows the same behaviour as for noble gas ions at higher energies, where the influence of the projectile binding energy,  $E_{sp}$ , becomes negligible.

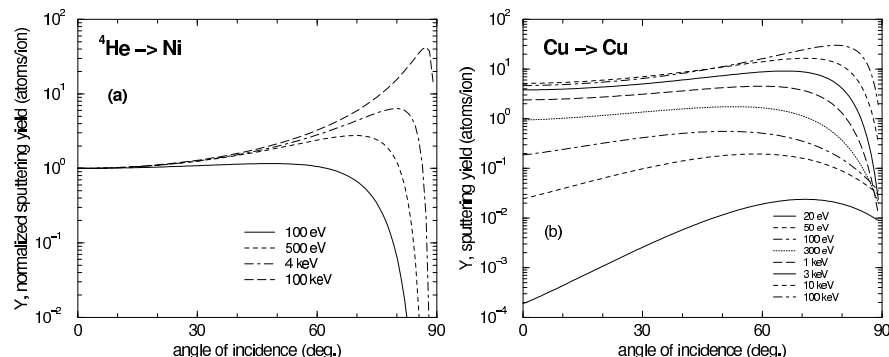


**Fig. 64.** Fit curves to the calculated angular dependence of sputtering yields at different incident energies for bombardment of nickel with helium (normalized at normal incidence)(a) and for selfsputtering of copper (b)

Plots of the angular dependence of the fits to the calculated sputtering yields are given in Figs. 65 - 86. In these plots the yields measured by many authors are introduced. In some figures the yield is normalized to the yield at normal incidence, because the experimental data were available in this form.

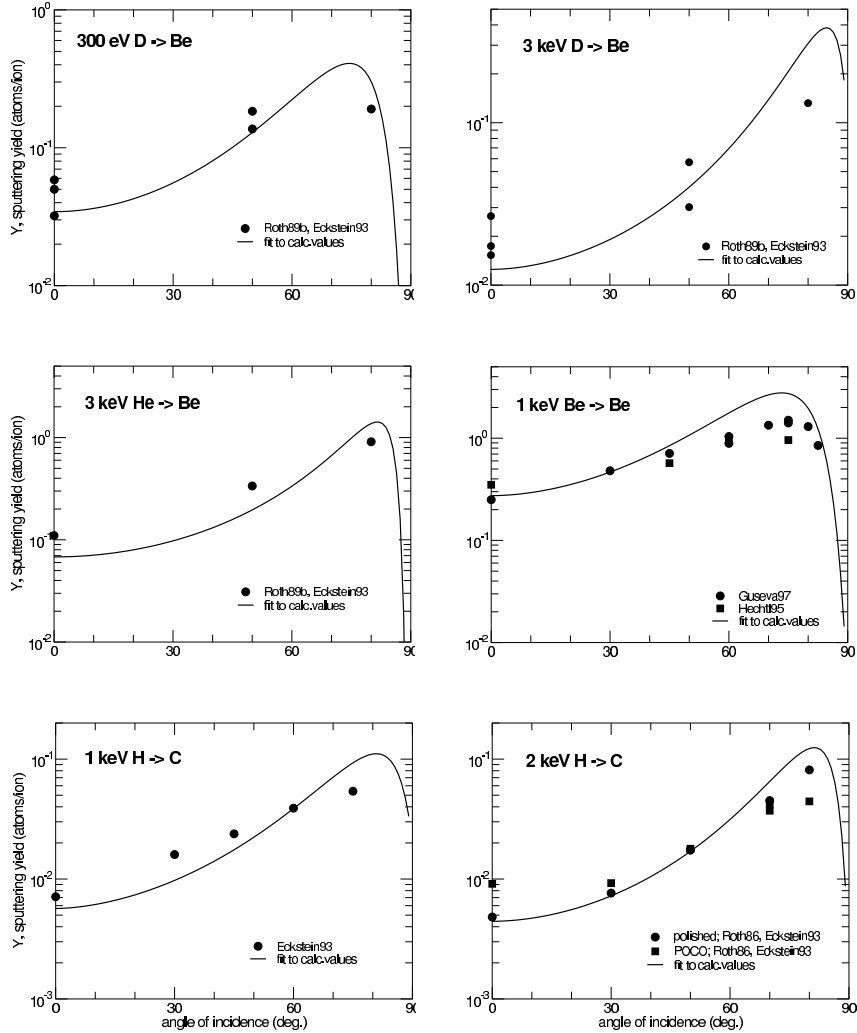


**Fig. 65.** Comparison of measured and calculated angular dependence of sputtering yields at different energies for different ion-target combinations: 0.3 keV D on Be [27,252], 3 keV D on Be [27,252], 3 keV  ${}^4\text{He}$  on Be [27,252], 1 keV Be on Be [60,61], 1 keV H on C [27], 2 keV H on C [27,253]

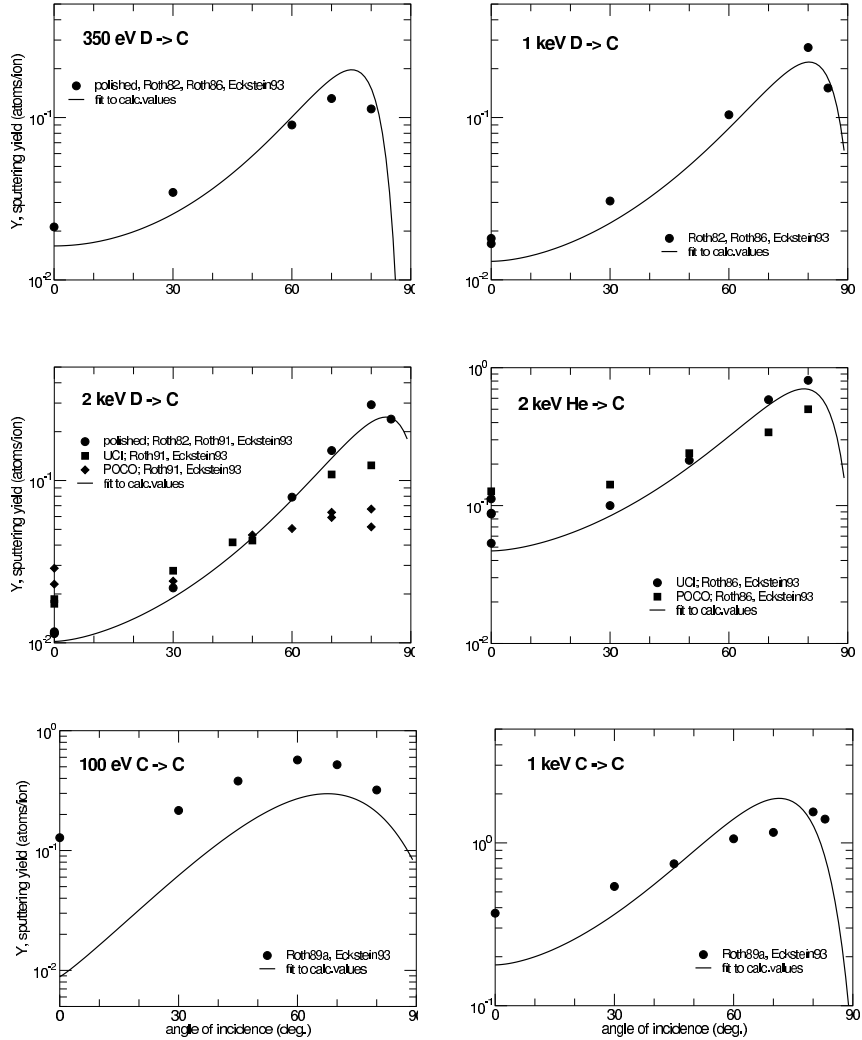


**Fig. 66.** Comparison of measured and calculated angular dependence of sputtering yields at different energies for different ion-target combinations: 0.35 keV D on C [27,253,254], 1 keV D on C [27,253,254], 2 keV D on C [27,269,254], 2 keV  ${}^4\text{He}$  on C [27,253], 100 eV C on C [27,83], 1 keV C on C [27,83]

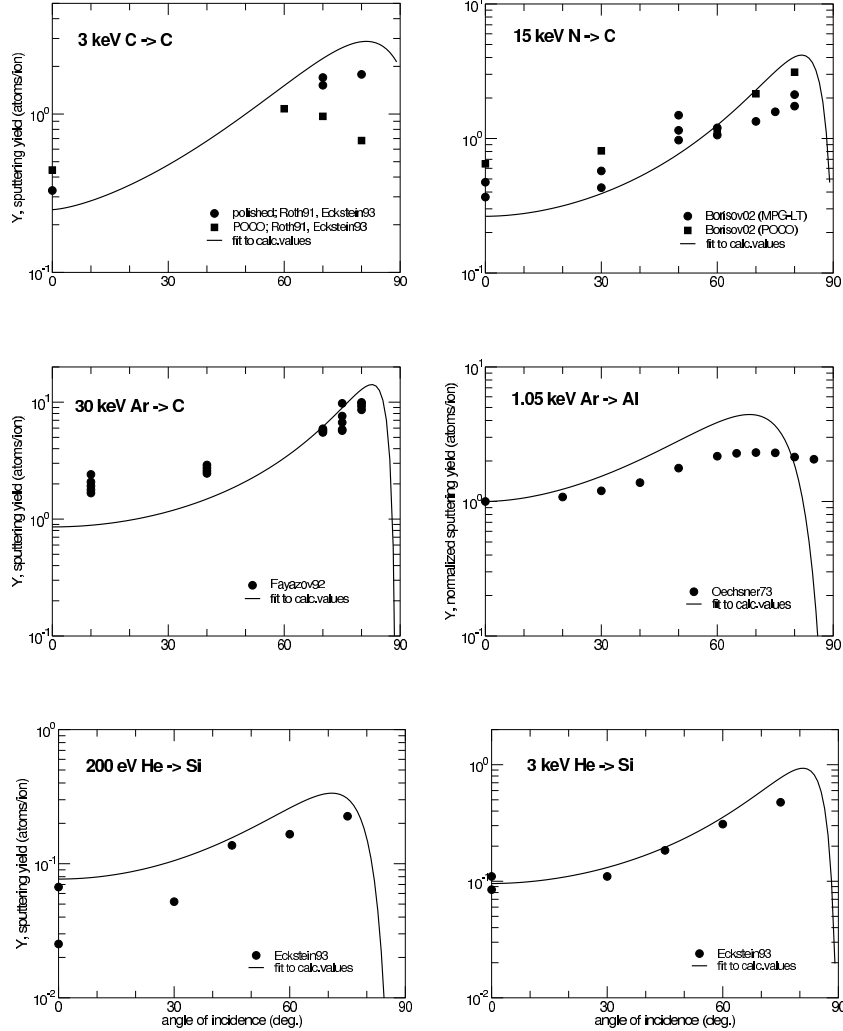


**Fig. 67.** Comparison of measured and calculated angular dependence of sputtering yields at different energies for different ion-target combinations: 3 keV C on C [27,269], 15 keV N on C [93], 30 keV Ar on C [255], 1.05 keV Ar on Al [105], 0.2 keV  ${}^4\text{He}$  on Si [27], 3 keV  ${}^4\text{He}$  on Si [27]

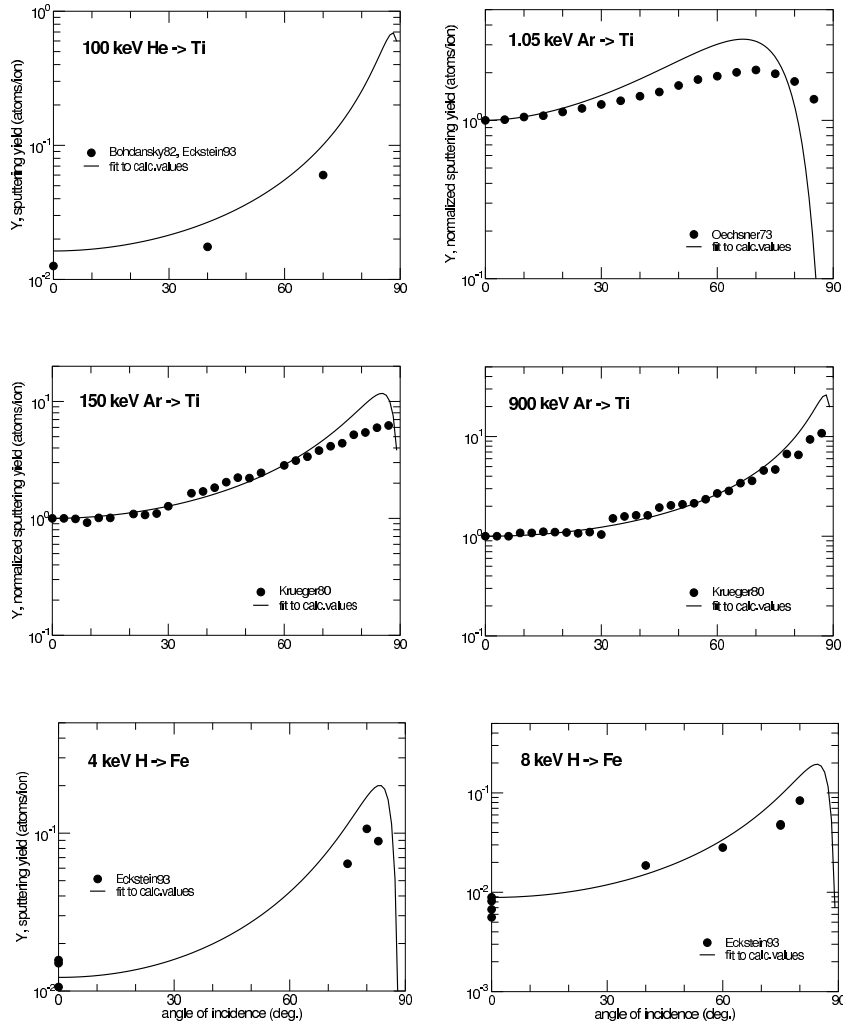


**Fig. 68.** Comparison of measured and calculated angular dependence of sputtering yields at different energies for different ion-target combinations: 100 keV  ${}^4\text{He}$  on Ti [27,135], 1.05 keV Ar on Ti [105], 150 keV Ar on Ti [256], 900 keV Ar on Ti [256], 4 keV H on Fe [27], 8 keV H on Fe [27]

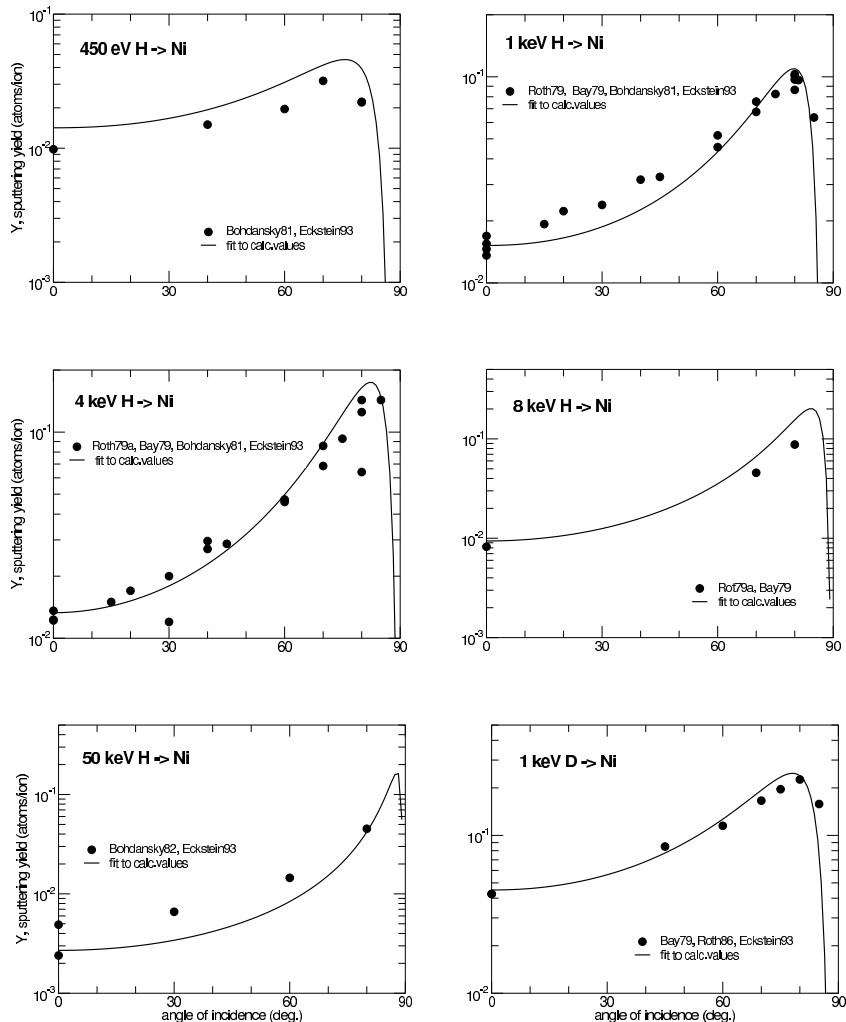


**Fig. 69.** Comparison of measured and calculated angular dependence of sputtering yields at different energies for different ion-target combinations: 0.45 keV H on Ni [27,257], 1 keV H on Ni [27,51,257,258], 4 keV H on Ni [27,51,257,258], 8 keV H on Ni [51,258], 50 keV H on Ni [27,135], 1 keV D on Ni [27,253,258]

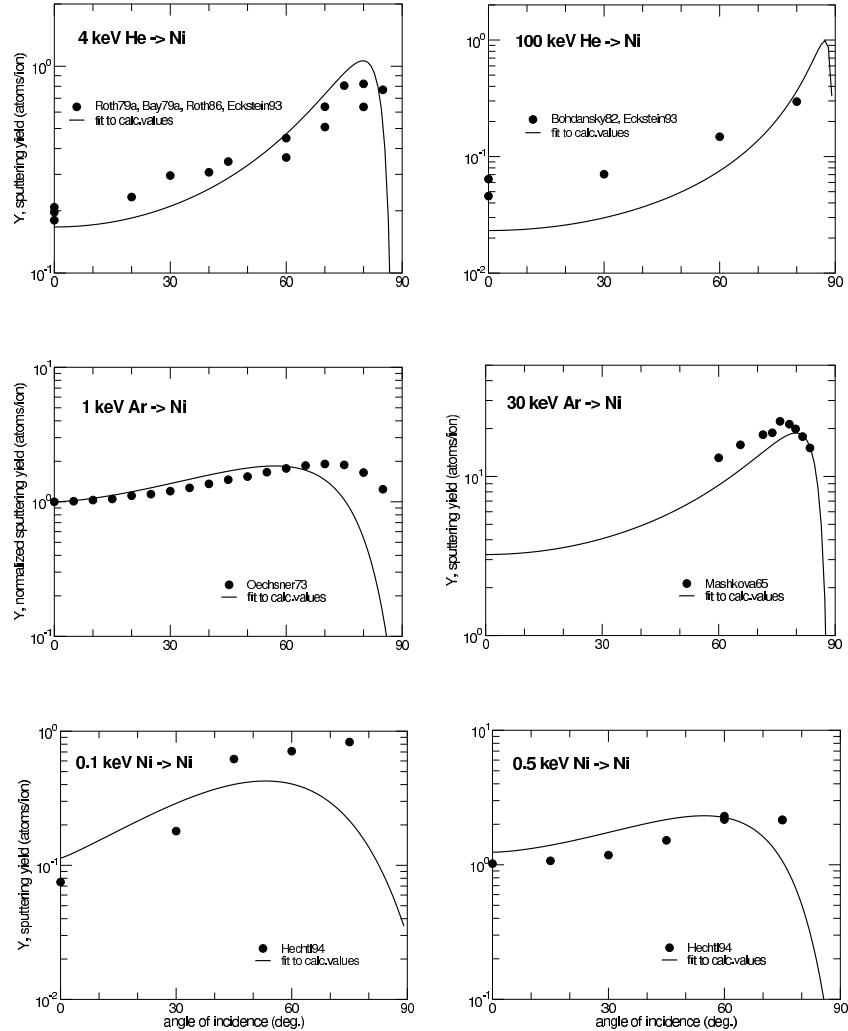


**Fig. 70.** Comparison of measured and calculated angular dependence of sputtering yields at different energies for different ion-target combinations: 4 keV He on Ni [27,51,253,258], 100 keV He on Ni [27,135], 1.05 keV Ar on Ni [105], 30 keV Ar on Ni [259], 0.1 keV Ni on Ni [260], 0.5 keV Ni on Ni [260]

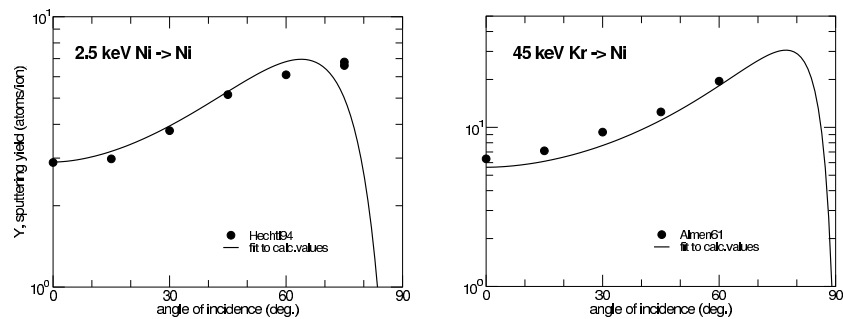


**Fig. 71.** Comparison of measured and calculated angular dependence of sputtering yields at different energies for different ion-target combinations: 2.5 keV Ni on Ni [260], 45 keV Kr on Ni [90]

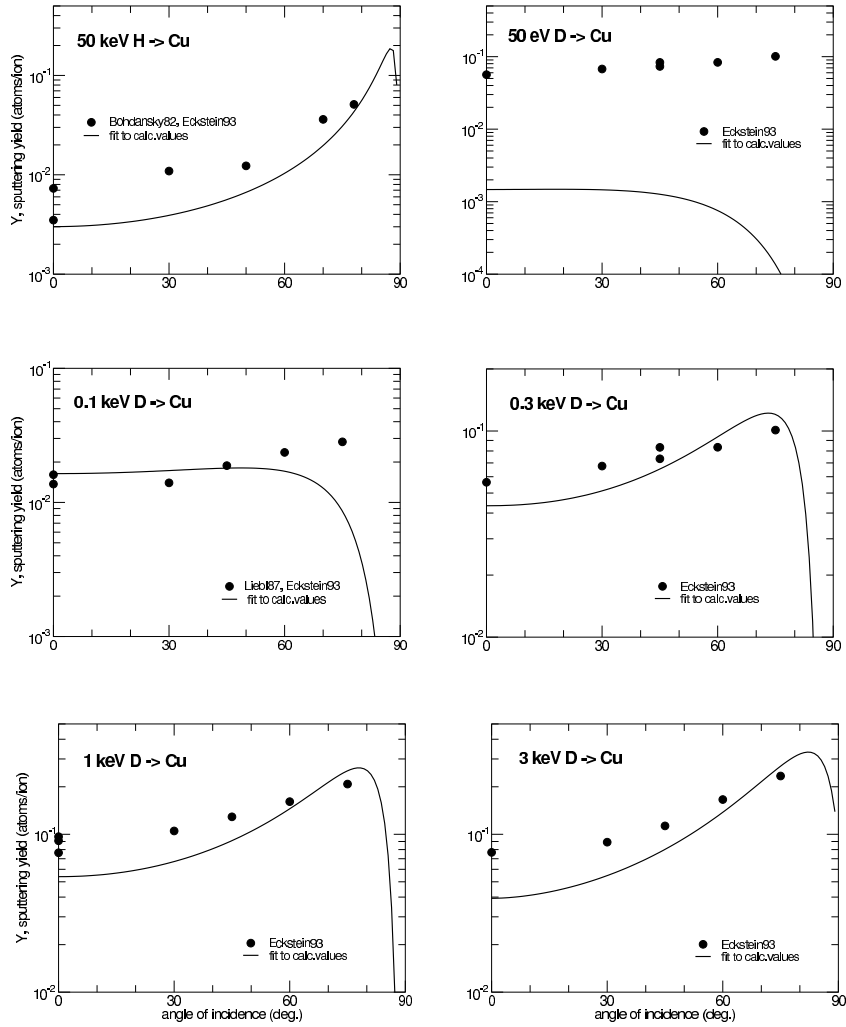


**Fig. 72.** Comparison of measured and calculated angular dependence of sputtering yields at different energies for different ion-target combinations: 50 keV H on Cu [27,135], 0.05 keV D on Cu [27], 0.1 keV D on Cu [27,261], 0.3 keV D on Cu [27], 1 keV D on Cu [27], 3 keV D on Cu [27]

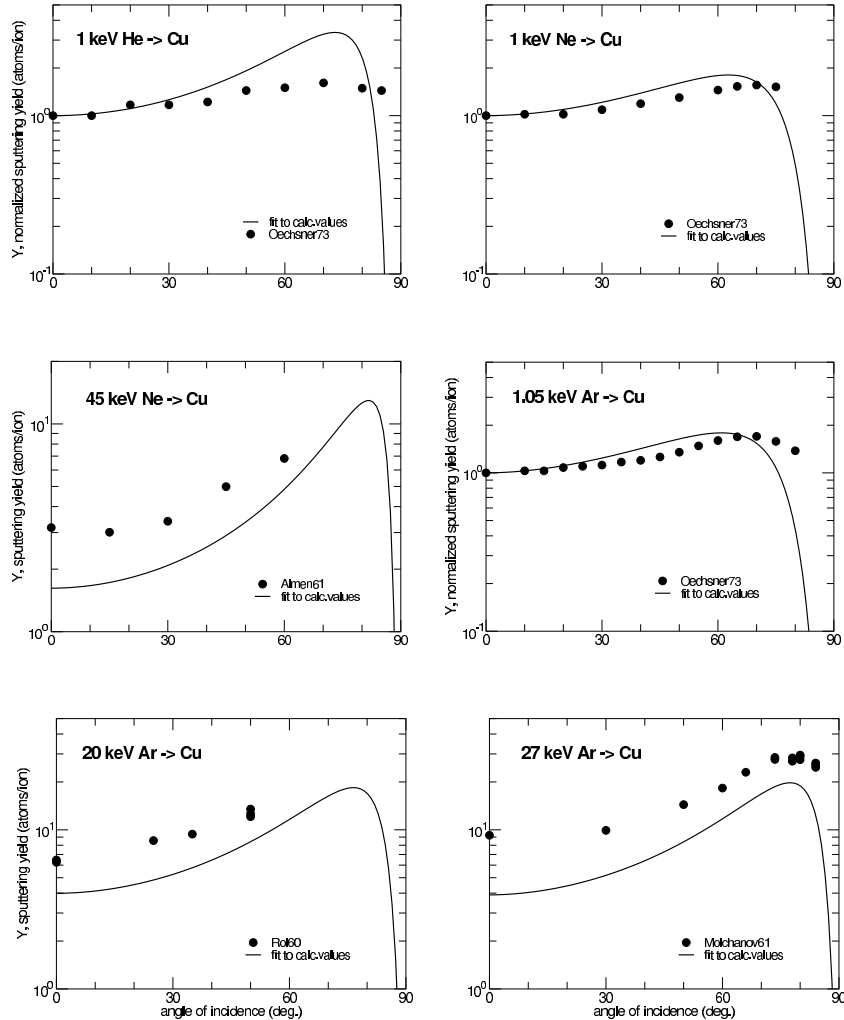


**Fig. 73.** Comparison of measured and calculated angular dependence of sputtering yields at different energies for different ion-target combinations: 1 keV He on Cu [105], 1 keV Ne on Cu [105], 45 keV Ne on Cu [90], 1.05 keV Ar on Cu [105], 20 keV Ar on Cu [262], 27 keV Ar on Cu [263]

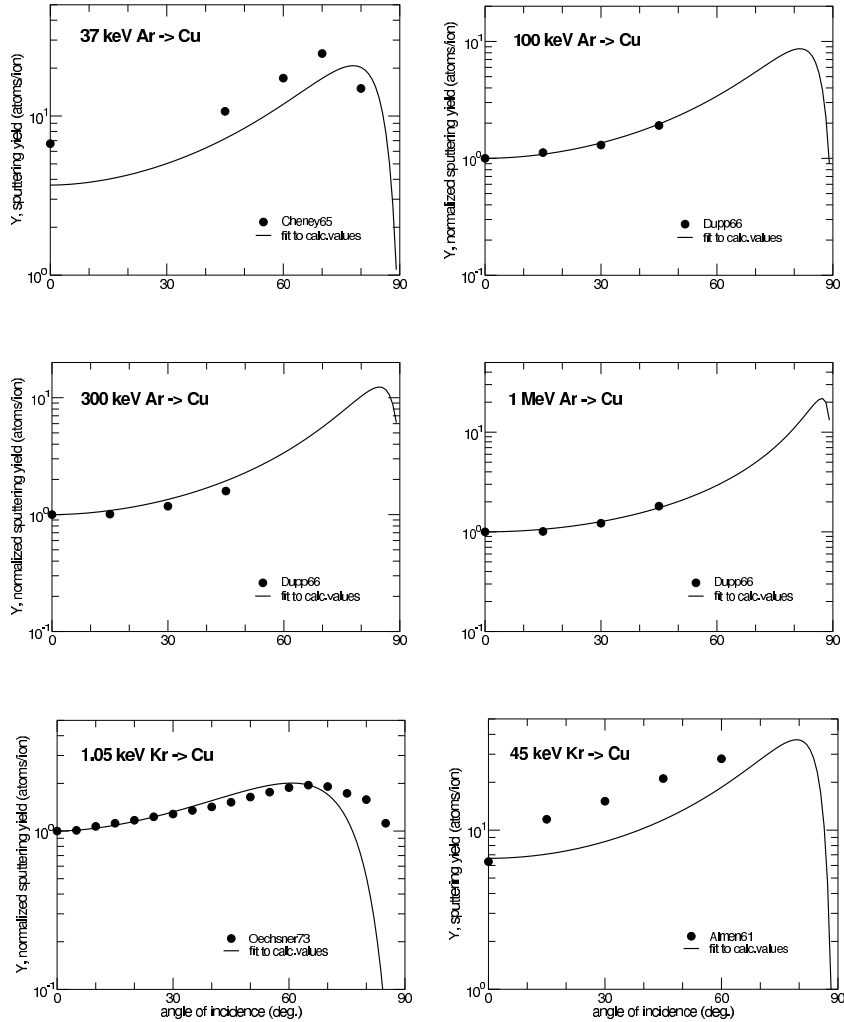


**Fig. 74.** Comparison of measured and calculated angular dependence of sputtering yields at different energies for different ion-target combinations: 37 keV Ar on Cu [168], 100 keV Ar on Cu [163], 300 keV Ar on Cu [163], 1 MeV Ar on Cu [163], 1.05 keV Kr on Cu [105], 45 keV Kr on Cu [90]

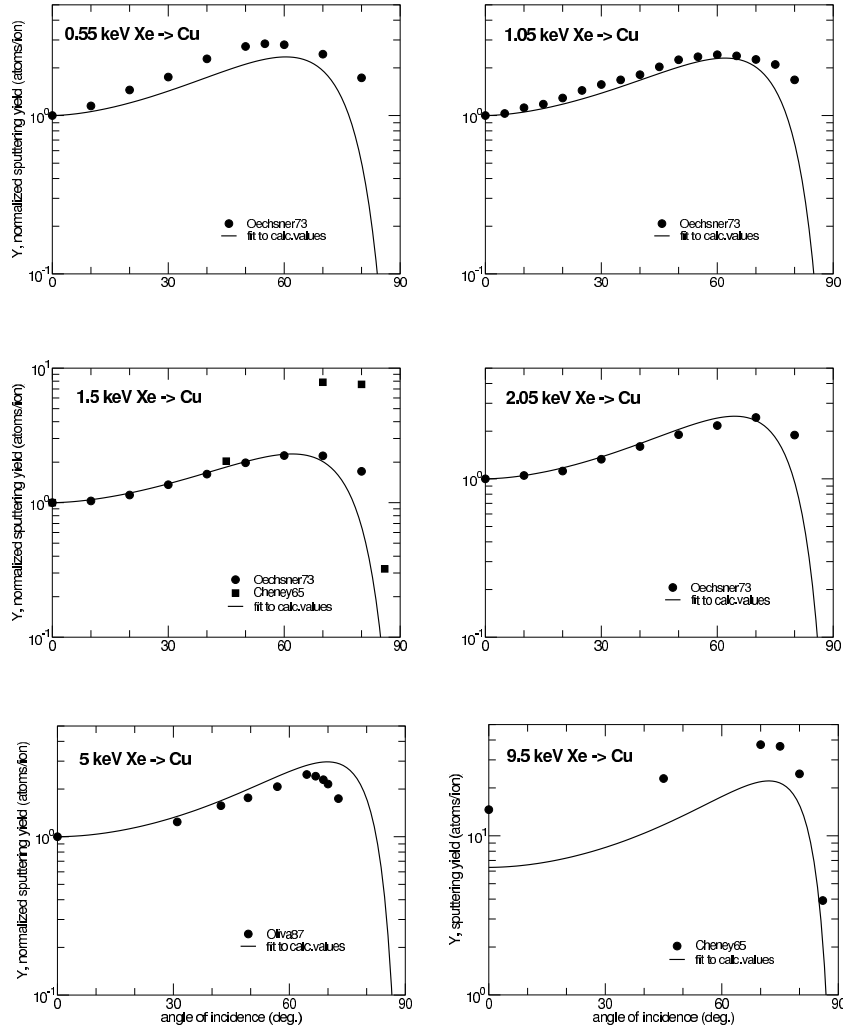


**Fig. 75.** Comparison of measured and calculated angular dependence of sputtering yields at different energies for different ion-target combinations: 0.55 keV Xe on Cu [105], 1.05 keV Xe on Cu [105], 1.5 keV Xe on Cu [105,168], 2.05 keV Xe on Cu [105], 5 keV Xe on Cu [174], 9.5 keV Xe on Cu [168]

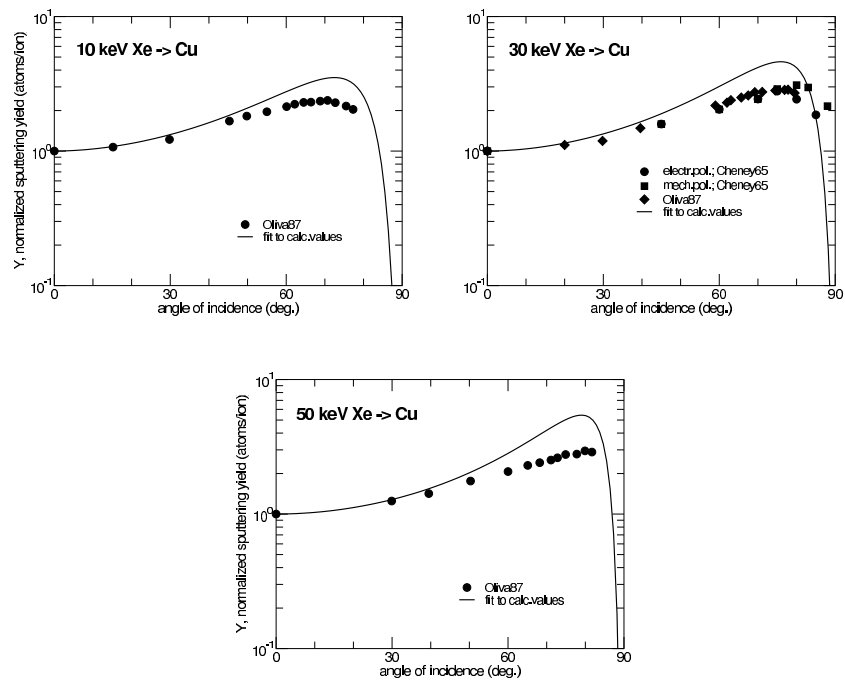


**Fig. 76.** Comparison of measured and calculated angular dependence of sputtering yields at different energies for different ion-target combinations: 10 keV Xe on Cu [174], 30 keV Xe on Cu [168,174], 50 keV Xe on Cu [174]

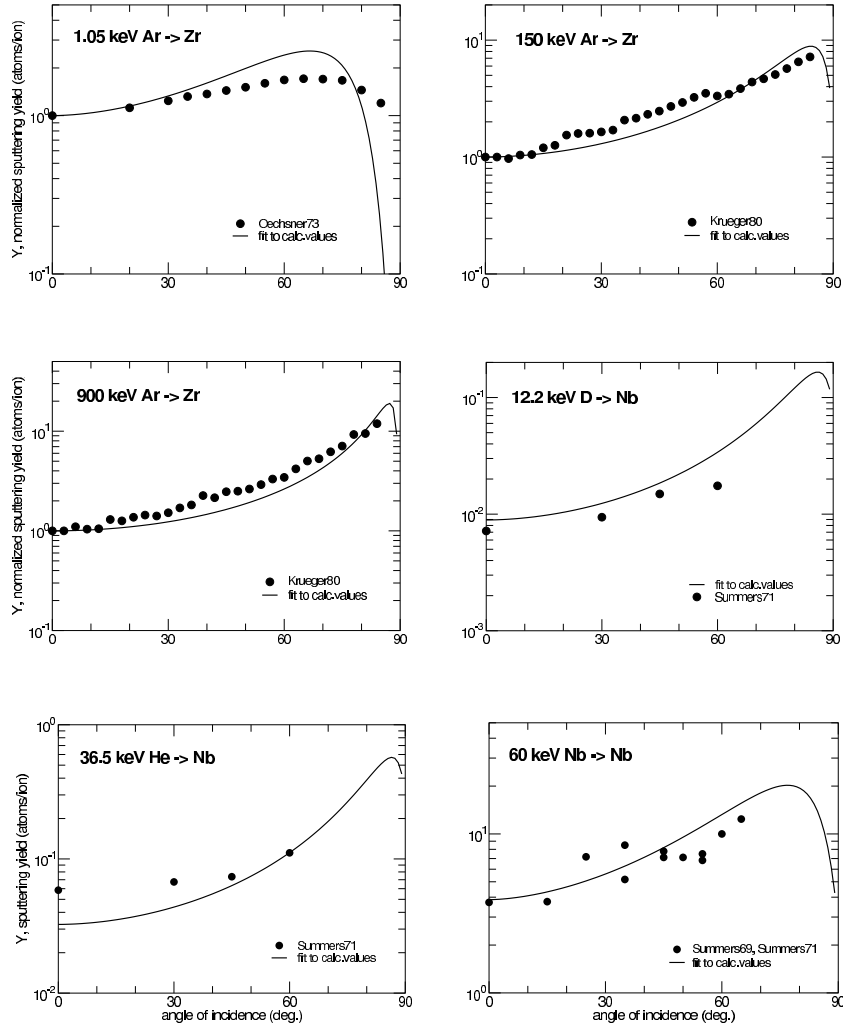


**Fig. 77.** Comparison of measured and calculated angular dependence of sputtering yields at different energies for different ion-target combinations: 1.05 keV Ar on Zr [105], 150 keV Ar on Zr [256], 900 keV Ar on Zr [256], 12.2 keV D on Nb [185], 36.5 keV He on Nb [185], 60 keV Nb on Nb [185,187]

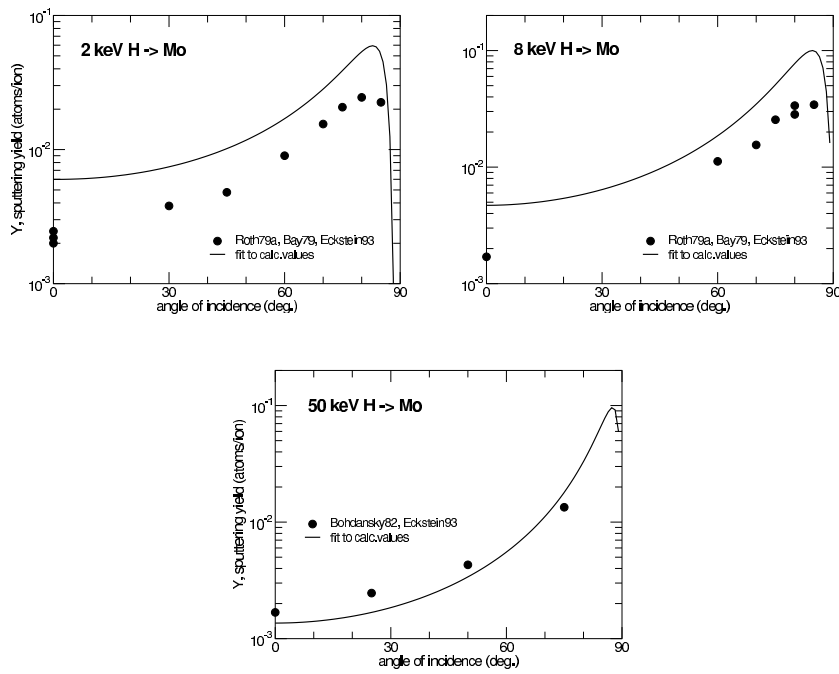


**Fig. 78.** Comparison of measured and calculated angular dependence of sputtering yields at different energies for different ion-target combinations: 2 keV H on Mo [27,51,258], 8 keV H on Mo [27,51,258], 50 keV H on Mo [27,135]

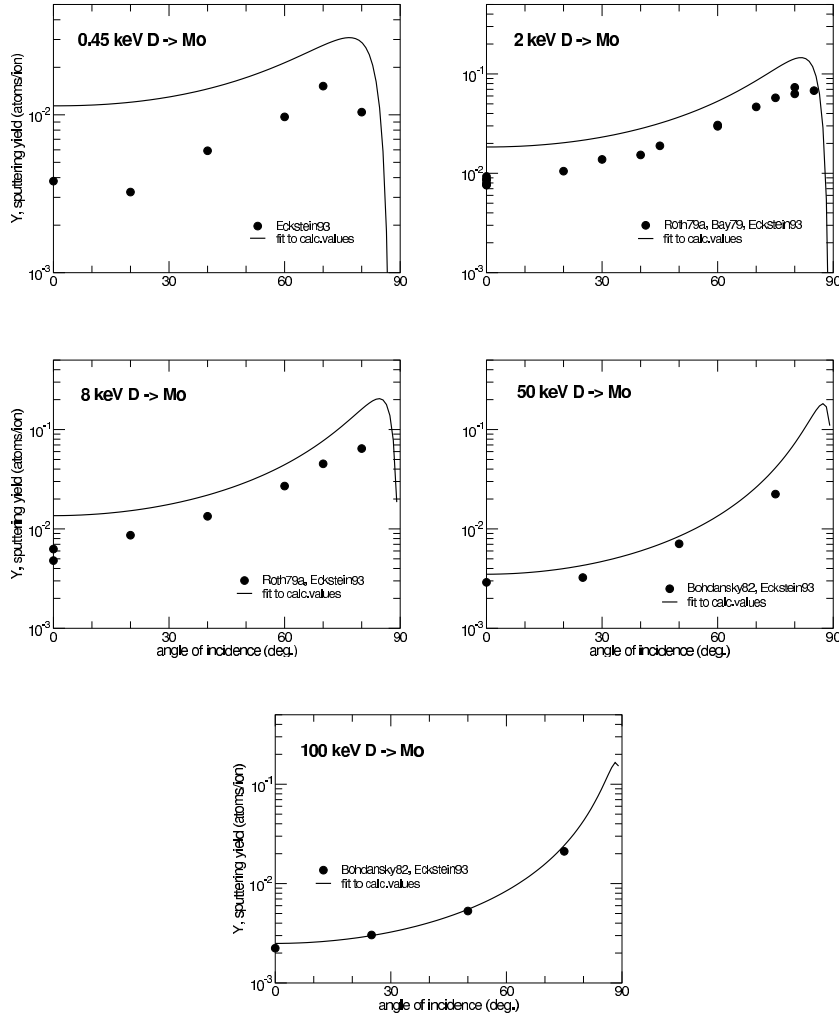


**Fig. 79.** Comparison of measured and calculated angular dependence of sputtering yields at different energies for different ion-target combinations: 0.45 keV D on Mo [27], 2 keV D on Mo [27,51,258], 8 keV D on Mo [27,51], 50 keV D on Mo [27,135], 100 keV D on Mo [27,135]

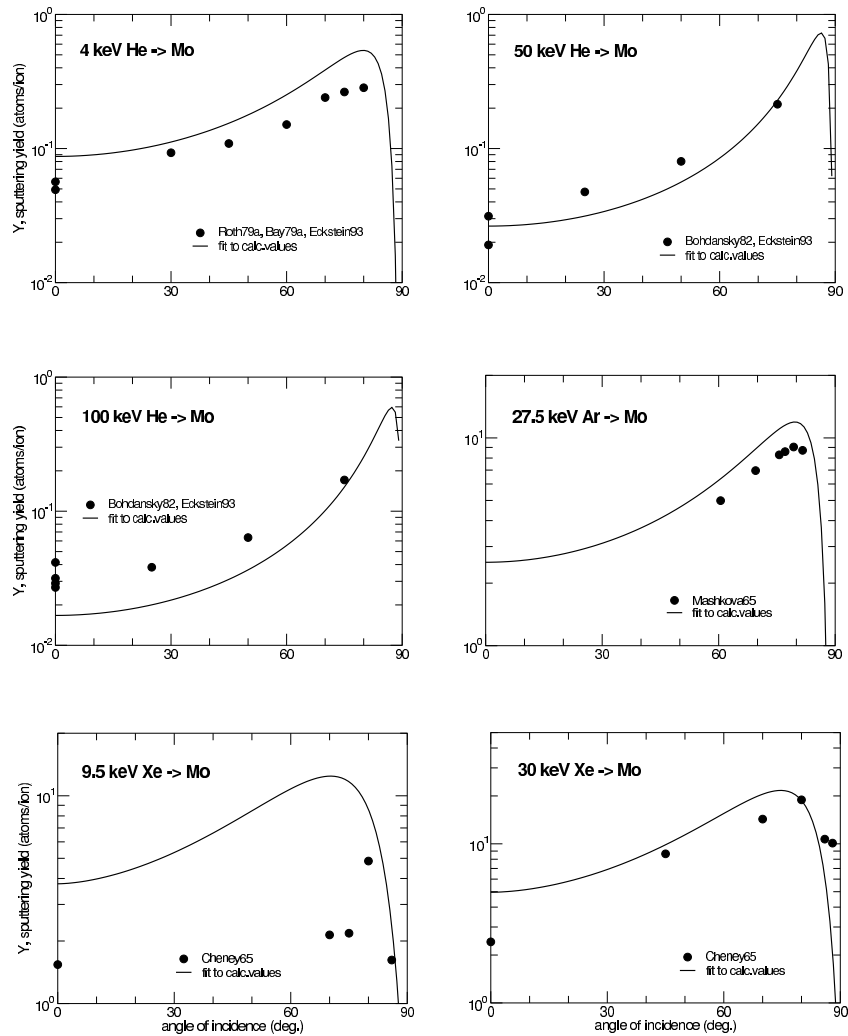


**Fig. 80.** Comparison of measured and calculated angular dependence of sputtering yields at different energies for different ion-target combinations: 4 keV He on Mo [27,51,258], 50 keV He on Mo [27,135], 100 keV He on Mo [27,135], 27.5 keV Ar on Mo [259], 9.5 keV Xe on Mo [168], 30 keV Xe on Mo [168]

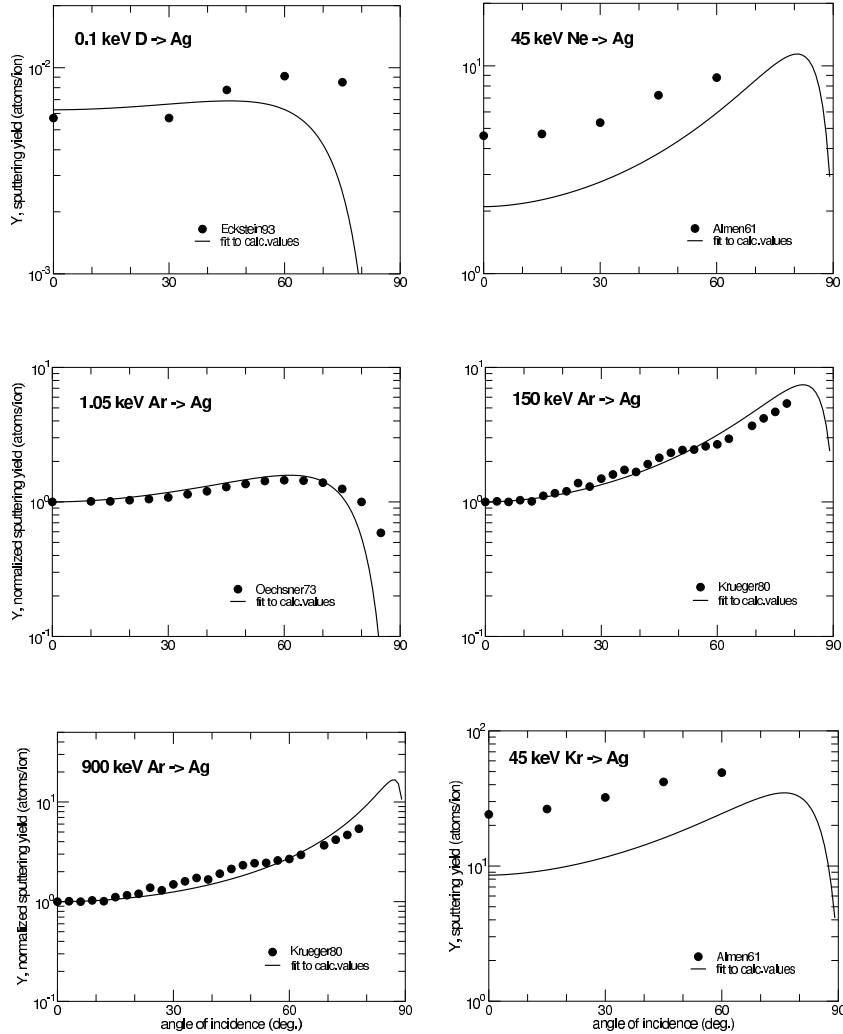


**Fig. 81.** Comparison of measured and calculated angular dependence of sputtering yields at different energies for different ion-target combinations: 0.1 keV D on Ag [27], 45 keV Ne on Ag [90], 1.5 keV Ar on Ag [105], 150 keV Ar on Ag [256], 900 keV Ar on Ag [256], 45 keV Kr on Ag [90]

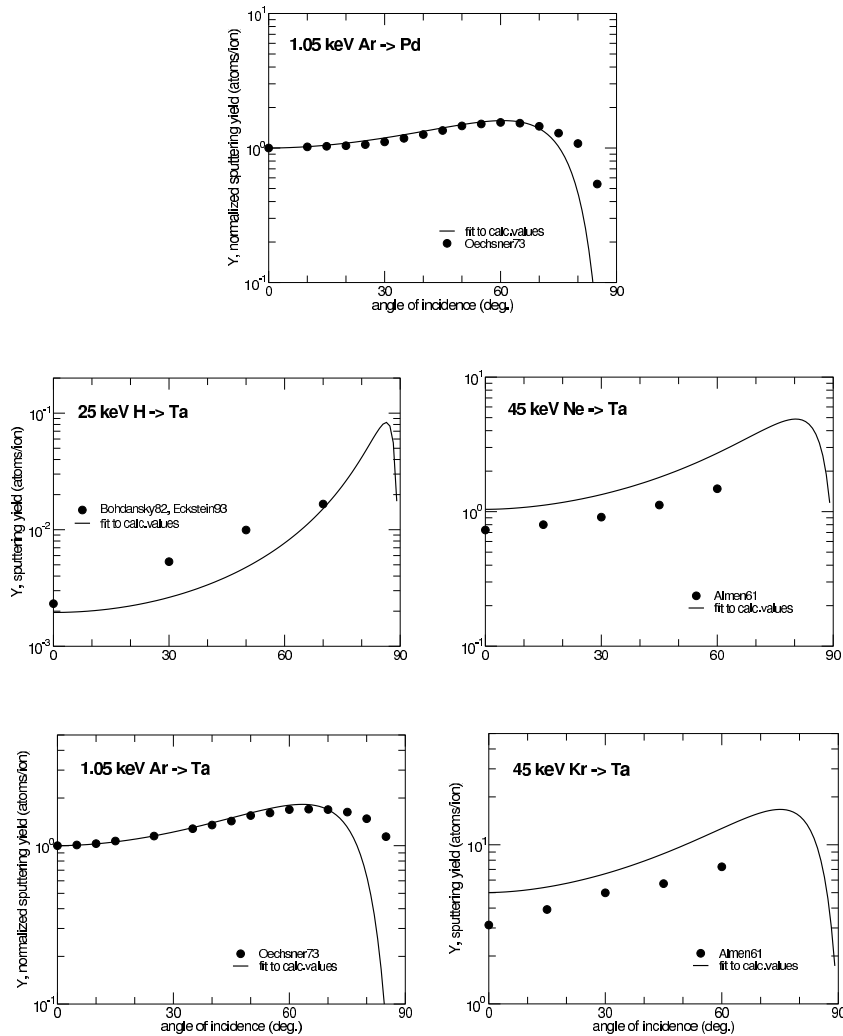


**Fig. 82.** Comparison of measured and calculated angular dependence of sputtering yields at different energies for different ion-target combinations: 1.05 keV Ar on Pd [105], 25 keV H on Ta [27,135], 45 keV Ne on Ta [90], 1.5 keV Ar on Ta [105], 45 keV Kr on Ta [90]

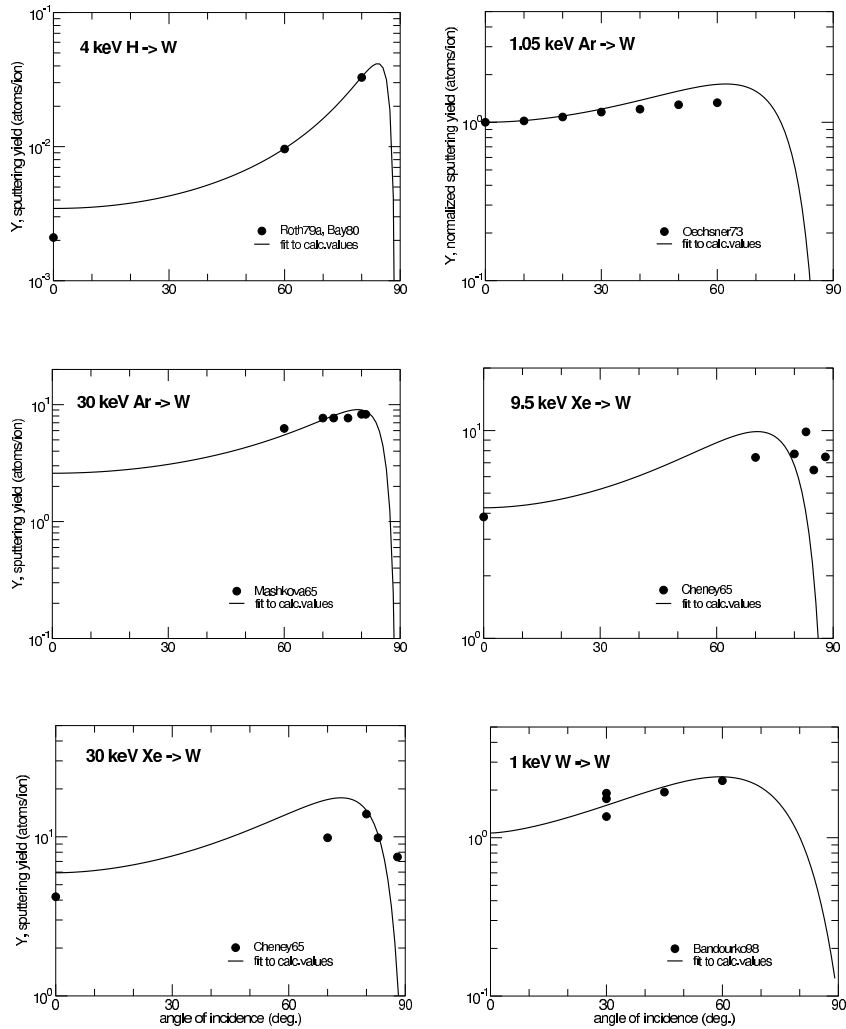


**Fig. 83.** Comparison of measured and calculated angular dependence of sputtering yields at different energies for different ion-target combinations: 4 keV H on W [51,264], 1.05 keV Ar on W [105], 30 keV Ar on W [259] 9.5 keV Xe on W [168], 30 keV Xe on W [168], 1 keV W on W [265]

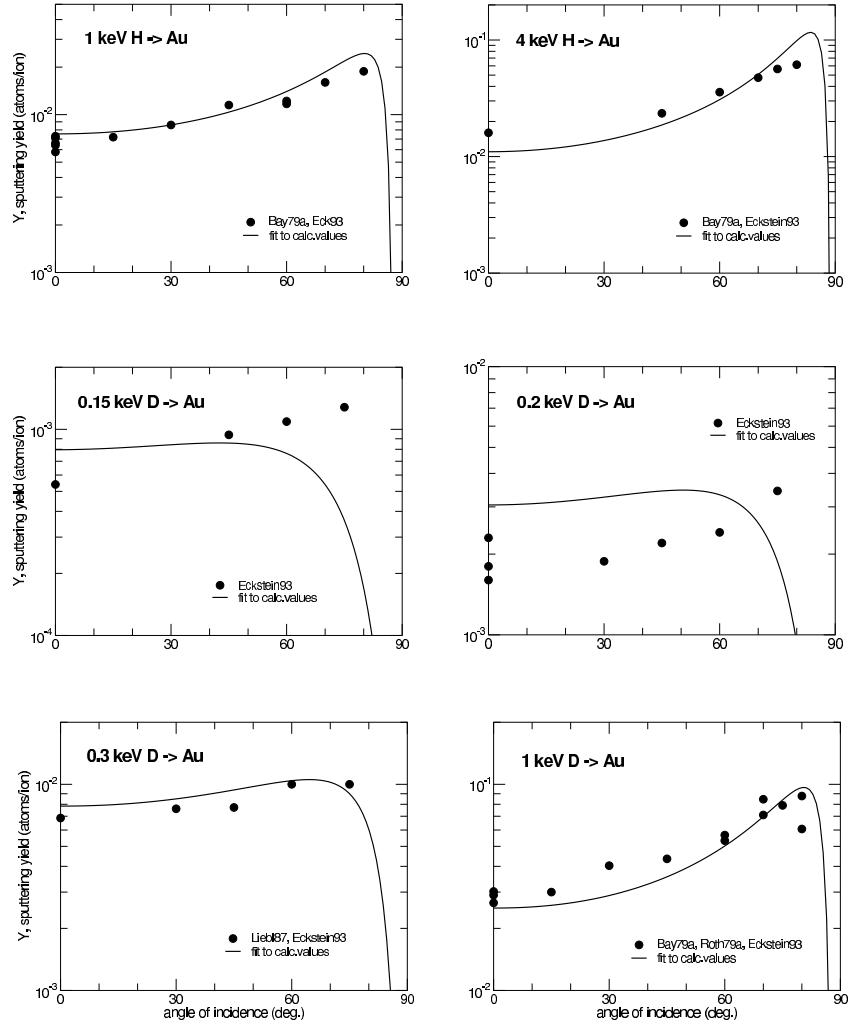


**Fig. 84.** Comparison of measured and calculated angular dependence of sputtering yields at different energies for different ion-target combinations: 1 keV H on Au [27,258], 4 keV H on Au [27,258], 0.15 keV D on Au [27], 0.2 keV D on Au [27], 0.3 keV D on Au [27,261], 1 keV D on Au [27,51,258]

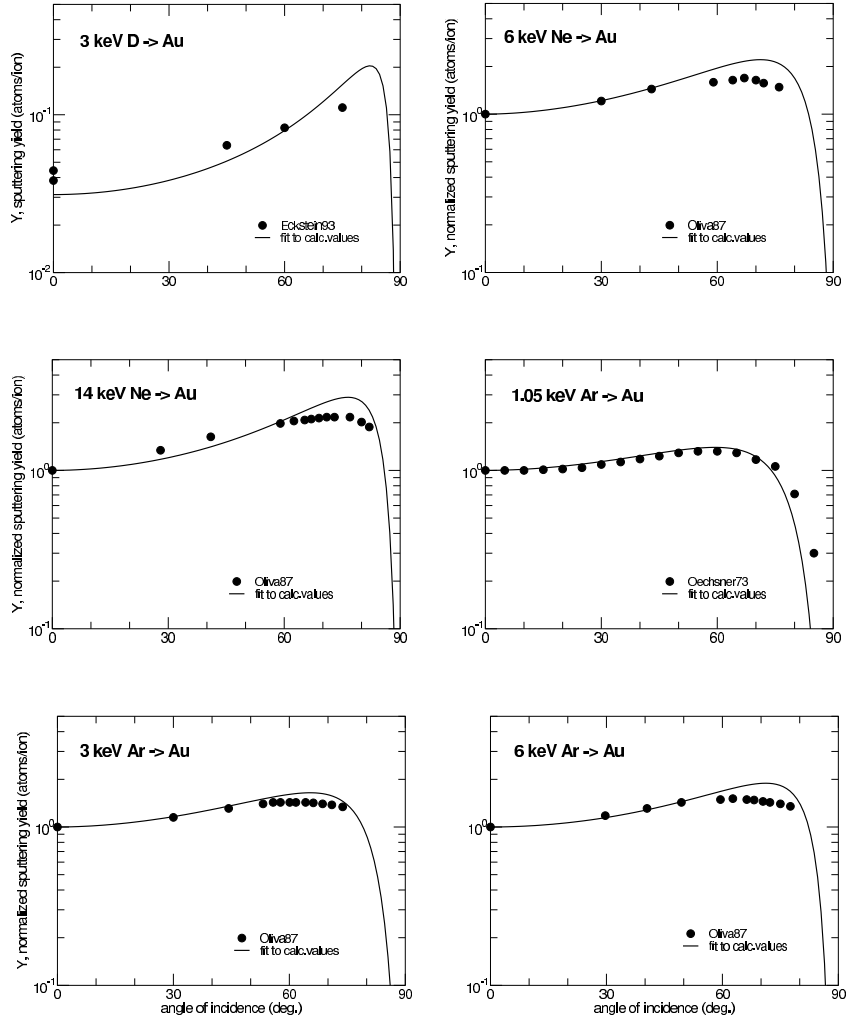


**Fig. 85.** Comparison of measured and calculated angular dependence of sputtering yields at different energies for different ion-target combinations: 3 keV D on Au [27], 6 keV Ne on Au [174], 14 keV Ne on Au [174], 1.05 keV Ar on Au [105], 3 keV Ar on Au [174], 6 keV Ar on Au [174]

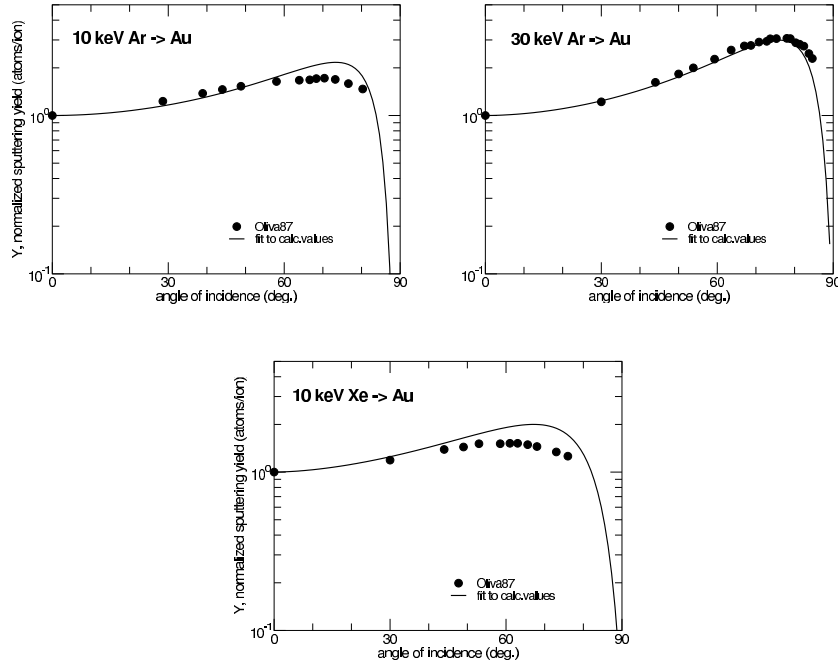


**Fig. 86.** Comparison of measured and calculated angular dependence of sputtering yields at different energies for different ion-target combinations: 10 keV Ar on Au [174], 30 keV Ar on Au [174], 10 keV Xe on Au [174]

The reasonable agreement of the experimental and calculated yields give again confidence to the calculated values. The angular dependence of the measured sputtering yield is dependent on the roughness of the target. There is a general tendency, that the yield at normal incidence is somewhat higher for rough surfaces than for flat ones and the opposite is true for large angles of incidence. At about 45° the values for flat and rough surfaces are approximately the same. Küstner et al. [266,267] determined the surface roughness with a tunneling microscope and produced from that a distribution of angles of incidence. Using this distribution as input to a Monte Carlo calculation provided a much better agreement of the calculated values with the experimental data. Also the assumption of simple geometrical surface structures in simulation codes gives better agreement with experimental data [268]. For very rough surfaces the experimental yield at the maximum of the angular dependence can be a factor of five lower compared to a polished surface [269].

Citations of experimental data and static calculations of sputtering yields at normal and oblique incidence for elemental targets not included in fits and figures due to limited values. They are summarized in Tables 25 - 28.

### 3.5 Threshold Energy of Sputtering

The threshold energy,  $E_{th}$ , must meet the condition, that the maximum transferable energy in a collision is larger than the surface binding energy. This means, that  $E_{th} + E_{sp} > E_{sb}/\gamma$ , where  $E_{sp}$  is the binding energy of a projectile to the target surface ( $E_{sp} = 0$  for noble gas ions),  $E_{sb}$  is the surface binding energy (heat of sublimation), and  $\gamma = 4M_1M_2/(M_1 + M_2)^2$  is the energy transfer factor in a binary collision.  $M_1$  and  $M_2$  are the masses of the projectile and target atom, respectively. This minimum energy is only an energy consideration, but does not take into account the necessary change in momentum.

The threshold energy cannot be determined directly. It can be obtained by extrapolating the sputtering yields to low energies [189,52] using a formula such as (2). The threshold energies determined from the calculated sputtering yields by this fitting are shown in Tables 1 to 9. The resulting threshold energies obtained from the data fitting are presented in Fig. 87 in the form of  $\gamma(E_{th} + E_{sp})/E_{sb} = E_{th}^{red}$  versus the mass ratio  $M_2/M_1$ , because then  $E_{th}^{red}$  should approach unity for large mass ratios. At low mass ratios the uncertainty in the threshold energy becomes rather large. Besides the above mentioned energy consideration the momentum reversal for an incident projectile is important. For a light projectile the momentum reversal occurs mainly in one collision of an incident light ion with a heavy target atom [270]. For smaller mass ratios several collisions are necessary for the momentum reversal thus increasing  $E_{th}^{red}$  [271]. The scatter of the values shows, that the threshold energies at low mass ratios are not well defined.

The threshold energy depends also on the angle of incidence. It has been shown by simulations, that this dependence is stronger for heavy projectiles than for light incident ions [272].

## 4 Single Crystalline Materials

The sputtering yields are largely influenced by the crystallinity and the orientation of the crystal relative to the incident ion beam. For incidence parallel to crystal planes and/or low index crystal axes the sputtering yields show pronounced minima [90,273–276]. In these directions the crystal looks more transparent and the sputtering is reduced. The probability of energy transfer from the incident atoms to lattice atoms in these open directions is reduced. The angular distributions of sputtered atoms are highly anisotropic and the atoms are emitted in closely packed directions. This was first observed experimentally by Wehner (Wehner spots) [277] and also established in computer

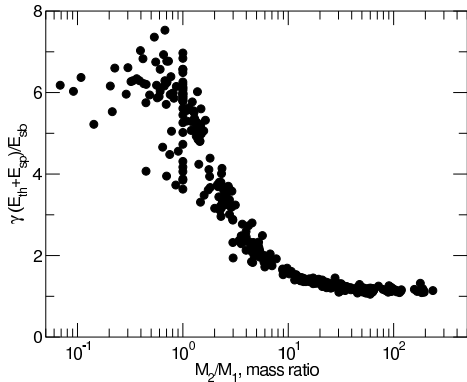


**Fig. 87.** Threshold energy,  $E_{th}$ , of the sputtering yield at normal incidence determined by the fitting procedure in the form of  $\gamma(E_{th} + E_{sp})/E_{sb}$  versus the mass ratio of target mass divided by ion mass.  $E_{sb}$  is the surface binding energy,  $E_{sp}$  the binding energy of a projectile to the target surface

simulations [278]. Surveys of these investigations are given in [1,276] and in Tables 32 and 33. An example is shown in Fig. 88, where the sputtering yield is presented for the bombardment of Cu(001) with argon for two incident energies and two incident azimuthal angles [279]. At 5 keV incidence the yield shows clear evidence of the open directions, in which the incident ions have a larger penetration depth and show a lower sputtering yield. The experimental data [280] agree nicely with the curves calculated with MARLOWE, although the surface region is damaged in the experiment by the incident beam. Some crystallinity must, therefore, remain after bombardment, at least for metals. It is interesting to note, that at lower energies (0.5 keV) the crystalline behaviour in the sputtering yield has disappeared in the results of the MARLOWE calculations.

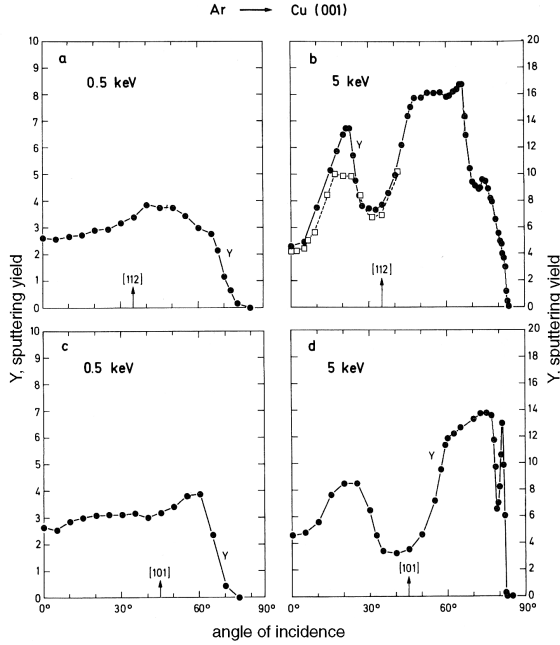


**Fig. 88.** Dependence of the sputtering yield,  $Y$ , on the angle of incidence for the bombardment of a Cu single crystal with a (001) surface. a,b: the plane of incidence is parallel to the [110] surface direction. c,d: the plane of incidence is parallel to the [100] surface direction (from [279]). Open squares in b are experimental data [280], all other points values calculated with MARLOWE

## 5 Multicomponent Targets

Sputtering becomes more complex, if the target consists of two or more different atomic species [281]. This is generally the case, because some of the projectiles are implanted and trapped even in a mono-atomic target (species which form solids as metals, for example). The topic of preferential sputtering belongs to this section. The complication arises, because the energy transfer from the projectile to the various target species is different and lighter elements have longer ranges. This leads to a target composition change with depth, and consequently to a change of the particle reflection coefficient and the partial sputtering yields,  $Y_i$ . In a multicomponent target  $Y_i$  is defined in the usual way as the ratio of the sputtered atoms of species (component)  $i$  per projectile. The composition changes proceed with bombardment until at some incident fluence a steady state or equilibrium is reached. The situation may become even more complex by compound formation (for example oxides, carbides, etc.), possible diffusion and segregation effects; surface roughness

may also change with fluence. Diffusion may be suppressed if the target temperature is low enough.

### 5.1 Fluence Dependence

It is known for a long time, that sputtering depends on fluence, especially for systems such as O bombardment of Al or Si [282] because of a compound formation (oxide). Computer simulations have been performed for a better understanding of these processes. Considering only collisional effects, a distinction can be made between a deposition and an erosion regime in the case of a bombardment with nonvolatile projectiles. If more atoms are implanted than atoms are sputtered, deposition dominates and the situation is that of a deposition regime. The border between the two regimes is given by [283]

$$1 - R_N = \sum Y_i = Y_{tot} \quad \text{or} \quad R_N + \sum Y_i = 1 \quad (9)$$

where  $R_N$  is the particle reflection coefficient and  $Y_i$  are the partial sputtering yields forming the total sputtering yield,  $Y_{tot}$ . Because  $R_N$  and  $Y_i$  depend on the angle of incidence, the border between the two regimes shift with the incident angle. In both regimes steady state is reached, if the partial yields become constant with increasing fluence. In the deposition regime this will happen, if a layer of the projectile species on top of the original target reaches some thickness, so that backscattered particles and sputtered atoms must come from this layer. The thickness of this layer will still increase with further bombardment, but no other changes will occur due to the selfbombardment. In the erosion case, a final depth distribution of the different species will form at steady state at a sufficiently high fluence. This depth profile will not change anymore with increasing fluence although the target thickness will decrease. Steady state is generally reached for an incident particle fluence,  $f_{eq}$ , at which a layer corresponding to the range  $R$  of the implanted ions is removed by sputtering. i.e.  $f_{eq}Y_{tot} = \rho R$ , where  $\rho$  is the atomic density of the sputtered layer. This gives for the fluence,  $f_{eq}$ , to reach steady state or equilibrium [284,285]

$$f_{eq} = \rho R / Y_{tot} \quad (10)$$

The values,  $R$  and  $Y_{tot}$ , depend on the projectile energy and the angle of incidence.  $R$  increases monotonically with energy, whereas  $Y_{tot}$  has a maximum at some energy. This means, that  $f_{eq}$  has a minimum close to the energy, where the yield has its maximum. For heavy ions,  $f_{eq}$  is of the order of  $10^{17}$  atoms/cm<sup>2</sup>, whereas for light ions the equilibrium fluence can be much higher. Analogously,  $f_{eq}$  decreases with an increasing angle of incidence until  $Y_{tot}$  reaches a maximum.

Impurities of heavy mass atoms or implantation of heavy ions in a target of light elements will increase the sputtering yield due to the larger scattering and larger scattering cross-section. The opposite effect will occur by light

atom impurities in a matrix of heavy mass atoms. The first effect has been demonstrated experimentally by the implantation of Xe into Si [130]. Also TRIDYN computer simulation can reproduce this effect in good agreement with the experimental data [286]. This sputtering yield amplification is also called the SYA effect; it has been demonstrated for example by computer calculations with the program T-DYN [287] for the bombardment of thin layers of Al on several metallic substrates with noble gas ions [288].

## 5.2 Oscillations in the Partial Sputtering Yields

At bombardment of a polycrystalline target consisting of low Z atoms with heavy projectiles in the erosion regime oscillations in the partial sputtering yields have been found [289], see Fig. 89. At the beginning of the bombardment the implanted projectiles built up a profile at a depth corresponding to the mean range,  $R$ . Further bombardment broadens and increases the implanted profile. Due to the simultaneous erosion of the surface, the profile moves toward the surface. When the profile reaches the surface, the implanted atoms are removed effectively by selfsputtering. After removal of the implanted layer the partial sputtering yield of implanted atoms is reduced. Further bombardment builds up a new profile of implanted atoms, which is broader and less pronounced than the first one. This process may repeat a few times until a steady state profile is reached and oscillations die out. The partial sputtering yield of the heavy atoms reach a maximum, when the maximum of the depth profile appears at the surface. The minimum of the profile occurs, when the atomic fraction of the heavy atoms at the surface is lowest. These oscillations have been predicted with TRIDYN computer simulations [289] and have been confirmed by experiment [290]. The oscillatory behaviour will show up only for large mass ratios ( $M_2/M_1 > 5$ ) and not too oblique angles of incidence, and if diffusion and/or segregation can be neglected. A similar example of In implantation into Si [291] can be explained in the same way by collisional effects, although the fluence in this experiment was not large enough to measure oscillations but only the first maximum. In such cases eq. (10) does not apply. Calculated dynamic behaviour of Be and C targets by Cs bombardment has been reported by *Sielanko* and coworkers [292].

## 5.3 Sputtering of Compounds

Sputtering of compound targets by noble gas ions is always in the erosion regime, if retention of noble gases in the target is neglected. Due to the different energy transfer of the ion to the components of the compound target preferential sputtering will occur, causing different partial yields. The original stoichiometry will be modified in the projectile range. Usually one species is depleted in the target with increasing fluence until some steady state condition is established and the target is sputtered stoichiometrically. In these

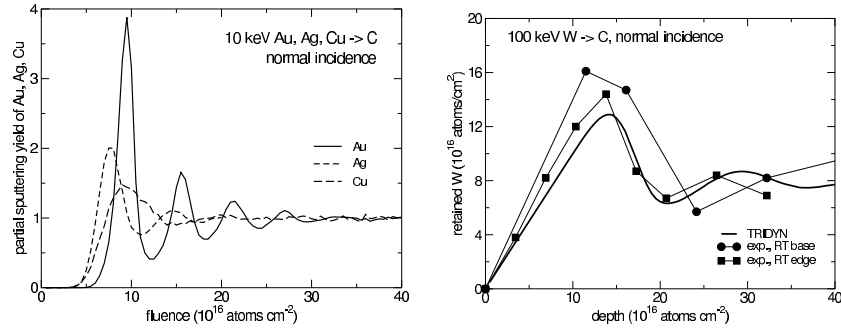


**Fig. 89.** Fluence dependence of partial sputtering yields for normal incidence bombardment. Left: Calculated partial yields due to the bombardment of C with 10 keV Au, Ag, Cu atoms [289]. Right: Comparison of measured and calculated retained W in C due to the bombardment od C with 100 keV W atoms [290]

cases the fluence at which the yields have been measured should be always given. In many experimental results steady state conditions prevail due to the large fluences needed for example in weight change measurements. In Fig. 90 the partial yields of C and Ta due to the bombardment of TaC with 1 keV He at normal incidence are shown versus the incident He fluence. The fluence at which steady state conditions are reached is about  $3 \cdot 10^{18}$  atoms/ $\text{cm}^2$ . For hydrogen bombardment this steady state fluence will be even higher, for heavier noble gases it will be lower. The target composition close to the surface resembles more a Ta target than a TaC target as can be seen in Fig. 90 from the C atomic fraction versus depth. The C depletion will be larger for hydrogen bombardment, but smaller for heavy atom incidence. For the bombardment of TiC the preferential sputtering effect is smaller due to the lower mass of Ti compared to Ta and due to the lower surface binding energy of Ti compared to Ta. The experimental equilibrium surface concentrations are close to those calculated [293,294]. The following compound targets which have been investigated experimentally and by calculations (static calculations which means low fluence) are summarized in Tables 34 to 36.

Another topic in this field is the simultaneous bombardment with two or more species. This occurs for example in fusion plasmas, where the dominant wall bombarding species is hydrogen but with impurities of helium, carbon, oxygen, and heavier ions. All the incident particles have an energy and angular distribution, and due to a sheath potential in front of the vessel wall ions in different charge states are accelerated towards the vessel wall. Such kind of problems have been discussed in [295,296] for a D influx with C impurity on Be, Si, C, Mo, and W, and in [297] for D and  ${}^4\text{He}$  bombardment of carbon material.

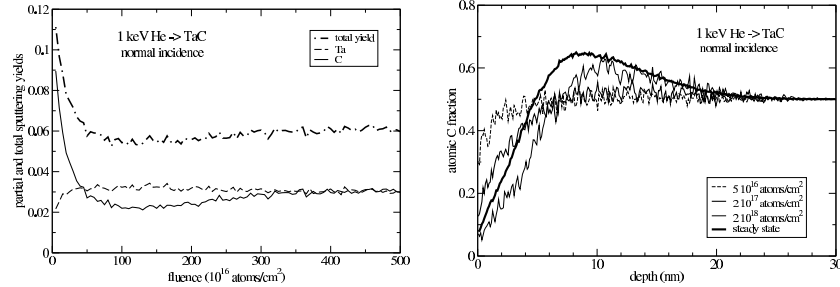


**Fig. 90.** Calculation of the bombardment of TaC with 1 keV He at normal incidence. Left: fluence dependence of partial sputtering yields of C and Ta. Right: depth distribution of the C atomic fraction for several fluences and steady state

#### 5.4 Isotope Sputtering

The sputtering of isotope mixtures is also nonstoichiometric at low fluence. In most cases the lighter isotope is sputtered preferentially. This is usually described by the value of fractionation, which is defined as

$$\delta = \frac{Y(M_i)}{Y(M_j)} \frac{N_j}{N_i} - 1 \quad (11)$$

where  $Y(M_i)$  and  $Y(M_j)$  are the partial sputtering yields of mass  $M_i$  and  $M_j$ , respectively, and  $N_i$  and  $N_j$  are the normalized abundances ( $\sum N_k = 1$ ) of species i and j, respectively. The first theoretical prediction for the partial sputtering yield ratio has been given by analytic theory [298] and has been reviewed in [299]

$$\frac{Y(M_i)}{Y(M_j)} = \frac{N_i}{N_j} \left( \frac{M_j}{M_i} \right)^{2m} \quad (12)$$

This gives a value for the fractionation, which is only dependent on the mass ratio:

$$\delta = \left( \frac{M_j}{M_i} \right)^{2m} - 1 \quad (13)$$

The value  $m$  is the parameter in the power potential. It should be smaller than unity and has been chosen between 0.05 and 0.3. BCA computer simulations found a value of about 1/6 from the high energy slope of energy distributions of sputtered atoms [28,300]. Because of the similar masses and the small value of  $m$ , the value of  $\delta$  is of the order of a few percent. Measurements and computer simulations have shown, that isotope sputtering is

more complex than predicted by the analytic theory. Measurements found, that the fractionation depends on the polar emission angle of sputtered atoms [301]. This was also found by molecular dynamics [302] and by Monte Carlo calculations [272]. The main result of these newer investigations are, that the fractionation is generally larger than expected from formula (13), see also [303–305]. Further computer simulation studies have shown, that the fractionation shows an energy and a weak incident angular dependence [285]. The main reason for the discrepancy between the theoretical result and the computed finding is the neglect of PKA in the theoretical approach. The simulations show clearly, that the energy and angular dependence originate predominantly from PKAs. Their contribution becomes dominant at low energies, especially near the threshold. The SKAs, which are only regarded in the analytic theory, show also in the simulations nearly no energy or angular dependence. Isotope sputtering is an important subject in planetary science [306].

## 6 Temperature Dependence of the Sputtering Yield

The collisional sputtering should not depend on temperature, at least for randomized target structures as long as the surface binding energy is constant. However, the surface binding energy (heat of sublimation) shows a small step at the solid-liquid transition. This step is of the order of 0.1 eV and the effect on the sputtering yield is very small and in experiments it is obscured by the onset of vaporization [307]. For single crystals lattice vibrations and annealing of lattice damage influence the Wehner spots or channeling dips in the sputtering yield [276]. In the case of multicomponent targets diffusion and segregation can change the collisional results largely as found experimentally [308,309] and modelled by simulations. For temperatures close to the melting point an exponential increase of the erosion yield is found experimentally. This can be attributed to evaporation [310,208].

The influence of the magnetic state has been investigated for Fe and Ni single crystals by [311,312] with MD; the effect is a consequence of slight changes in the interaction potential for the paramagnetic and the ferromagnetic state.

New experiments found subthreshold sputtering at high temperatures in the case of sputtering of tungsten at 1470 K [313] and at higher temperatures (2500 to 3400 K) [314]. The measured yield is reported to be about  $10^{-4}$  for 5 eV D bombardment. The effect is explained by sputtering of weakly bound adsorbed W atoms at the surface due to damage and the near surface implantation of gaseous atoms below the surface. Similar effects have been reported for Li [315] and Sn [316].

## 7 Yield Fluctuations

The sputtering yield shows fluctuations, i.e. a different yield for every incident ion, due to the stochastic slowing down process of projectiles and recoils in the target. These fluctuations are not accessible experimentally but theoretically and by computer simulation. *Harrison* [22] called them ASI distributions (for 'atoms per single ion'). A theoretical approach [317] did not give any distributions but predicted large fluctuations. In a more detailed investigation [318,319] the probability distributions of the sputtering yield were calculated by Monte Carlo simulations for Nickel bombarded with several ions at different incident energies and angles of incidence. The distributions were fitted with the two-parametric negative binomial distribution,

$$L_{\zeta\eta} = \frac{\Gamma(n + \zeta\eta)\phi^{\zeta\eta}}{n!\Gamma(\zeta\eta)(1 + \eta)^{n+\zeta\eta}} \quad (14)$$

where  $n$  is an integer and  $\zeta, \eta$  are parameters. The negative binomial distribution is broader than a Poisson distribution with the same yield (mean value of the distribution). Only at low energies and normal incidence the distributions were close to a Poisson distribution. At higher energies and oblique angles of incidence up to 100 atoms per single ion can be sputtered, see Fig. 91. This may explain the surface roughening by ion bombardment.

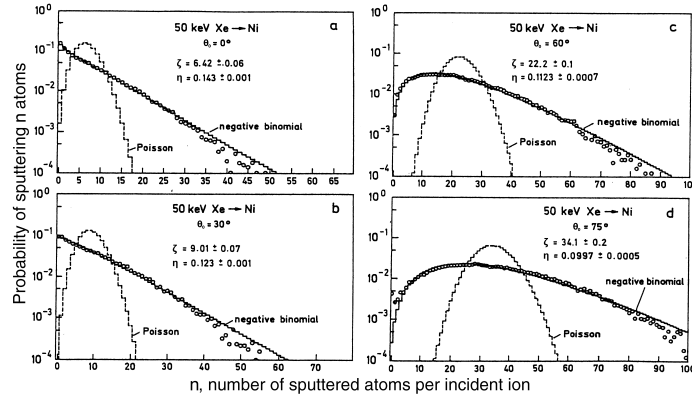


**Fig. 91.** Probability of sputtering  $n$  atoms versus the number,  $n$ , of sputtered atoms per single projectile. Ni is bombarded with 50 keV Xe at four angles of incidence,  $\theta_0$ . The open circles show the distributions calculated with TRIM.SP [318]. The values  $\zeta$  and  $\eta$  are the parameters of the negative binomial distribution, where  $\zeta = Y$  and  $\eta$  is a measure of the width of the distribution. The corresponding Poisson distribution is given for comparison

In another investigation the  $r^{-m}$  power potential was used in a Monte Carlo program [320]. The calculated distributions could not be fitted by a negative binomial distribution.

## 8 Time Evolution of the Sputtering Yield

The sputtered atoms need time to leave the target from their original site. According to their depth of origin, their path to the surface and their energy, a distribution of escape times will develop. Whereas time is naturally included in MD programs, it is not necessary in BCA programs. But time has been incorporated, in MARLOWE [321], ACAT [322] and in TRIM [323–325]. Simulations have shown [22,325–327], that the escape times of sputtered atoms are typically less than one ps. Light sputtered atoms show a shorter escape time than heavy atoms as demonstrated in Fig. 92.

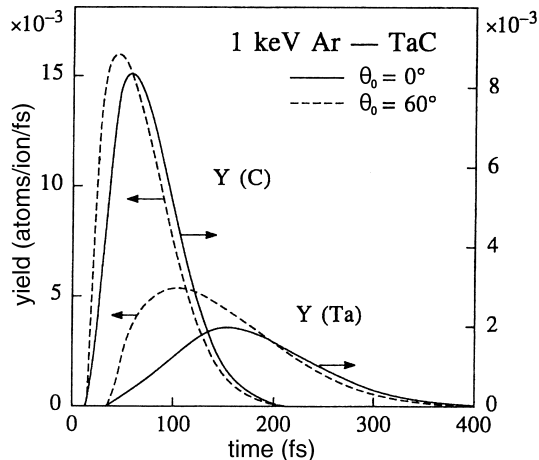


**Fig. 92.** Sputtering yield versus time for the bombardment of TaC with 1 keV Ar at two angles of incidence,  $\theta_0$ , Fig.1b of [325]

The maximum of the escape time dependence of the yield exhibit a shorter time for oblique incidence than for normal incidence. Also the energy and angular distributions of sputtered atoms show a time dependence [325,327].

## 9 Conclusions

The sputtering process of ion bombardment with energies from the threshold to the MeV range can be well described by BCA computer programs. The sputtering yields for many ion-target combinations agree in most cases very

well with experimental yields. For practical use the constants in the algebraic formulae for the energy and angular dependence of the sputtering yield for mono-atomic targets have been determined and summarized in tables.

## References

1. R. Behrisch: Ergeb. Exakt. Naturw. **35**, 295 (1964)
2. H. H. Andersen, H. L. Bay: In *Sputtering by Particle Bombardment I*, ed. by R. Behrisch, Top. Appl. Phys. **47**, 145 (1981), Russ. translation: (MIR, Moscow 1984)
3. G. Carter: In *Sputtering by Particle Bombardment II*, ed. by R. Behrisch, Top. Appl. Phys. **52**, 213 (1983), Russ. translation: (MIR, Moscow 1986)
4. B. M. U. Scherzer: In *Sputtering by Particle Bombardment II*, ed. by R. Behrisch, Top. Appl. Phys. **52**, 271 (1983), Russ. translation: (MIR, Moscow 1986)
5. G. M. McCracken: Rep. Prog. Phys. **38**, 241 (1975)
6. G. Sauerbrey: Z. Phys. **155**, 206 (1959)
7. D. McCown: Rev. Sci. Instrum. **32**, 133 (1961)
8. E. P. Eernisse: J. Vac. Sci. Technol. **12**, 564 (1975)
9. R. Weissmann, R. Behrisch: Radiat. Eff. **18**, 55 (1973)
10. H. von Seefeld, R. Behrisch, B. M. U. Scherzer, Ph. Staib, H. Schmidl: Proc. 7th Intern. Conf. Atomic Collisions in Solids, Vol. II, (Moscow State Univ. Publ. House, Moscow 1980) pp. 327
11. H. Fetz: Z. Phys. **119**, 590 (1942)
12. H. G. Scott: J. Appl. Phys. **33**, 2011 (1962)
13. G. K. Wehner, D. Rosenberg: J. Appl. Phys. **32**, 887 (1960)
14. R. S. Nelson, B. W. Farmery, M. W. Thompson: Proc. R. Soc. **259**, 458 (1961)
15. H. Pattersen, D. H. Tomlin: Proc. R. Soc. London A **265**, 474 (1962)
16. M. I. Guseva, A. L. Suvorov, S. N. Korshunov, N. E. Lazarev: J. Nucl. Mater. **266-269**, 222 (1999)
17. M. I. Guseva, A. L. Suvorov, S. N. Korshunov, N. E. Lazarev: J. Techn. Phys. **69**, 69 (1999)
18. R. P. Doerner, D.G. Whyte, D. M. Goebel: J. Appl. Phys. **93**, 5816 (2003)
19. H. P. Summers: *Atomic Data and Analysis Structure - User Manual*, Rep. JET-IR(94) (JET Joint Undertaking, Abingdon 1994)
20. P. Sigmund: Phys. Rev. **184**, 383 (1969);
21. P. Sigmund: Phys. Rev. **187**, 768 (1969)
22. D. E. Harrison, Jr.: CRC Critical Reviews in Solid State and Material Sciences, Vol.14, Supplement 1, CRC Press 1988
23. M. T. Robinson: In *Fundamental Processes in Sputtering of Atoms and Molecules (SPUT92)*, K. Dan. Videns. Selsk. Mat. Fys. Medd. **33**, 27 (1993)
24. Y. Yamamura and H. Tawara: NIFS-DATA-23, NIFS, Nagoya (1995)
25. Y. Yamamura and H. Tawara: Atomic Data and Nucl. Data Tables **62**, 149-253 (1996)
26. W. Takeuchi, Y. Yamamura: Radiat. Eff. **71**, 53 (1983)
27. W. Eckstein, C. García-Rosales, J. Roth, W. Ottenberger: Sputtering Data, Report IPP 9/82, Garching, (1993)
28. J. P. Biersack, W. Eckstein: Appl. Phys. **34**, 73 (1984)
29. W. Eckstein: *Computer Simulation of Ion-Solid Interactions*, Springer Series in Material Science, Vol.10, (Springer, Berlin, Heidelberg 1991), Russ. translation: (MIR, Moscow 1995)
30. S. T. Nakagawa, Y. Yamamura: Radiat. Eff. **105**, 239 (1988)
31. W. D. Wilson, L. G. Haggmark, J. P. Biersack: Phys. Rev. B **15**, 2458 (1977)

32. W. Eckstein: unpublished results, can be retrieved from <ftp://ftp.rzg.mpg.de/ftp/pub/ipp/eckstein/rep05>
33. Y. Yamamura, W. Takeuchi and T. Kawamura: NIFS-DATA-45, Nagoya (1998)
34. W. Möller, W. Eckstein: Nucl. Instrum. Methodsds B **2**, 814 (1984)
35. W. Möller, W. Eckstein, J. P. Biersack: Comput. Phys. Commun. **51**, 355 (1988)
36. W. Eckstein: Report IPP 9/132, Garching (2002)
37. W. Eckstein, J. Bohdansky, J. Roth: *Physical Sputtering*, Nucl. Fusion, Vol.1 (Supplement), (IAEA, Vienna 1991), pp. 51
38. W. Eckstein, E. S. Mashkova, V. A. Molchanov, A. I. Tolmachev: Nucl. Instrum. Methods B **115**, 482 (1996)
39. W. Eckstein: J. Nucl. Mater. **248**, 1 (1997)
40. W. Eckstein: Sputtering, Reflection and Range Values for Plasma Edge Codes, Report IPP 9/117, Garching, (1998)
41. W. Eckstein, J. A. Stephens, R. E. H. Clark, J. W. Davis, A. A. Haasz, E. Vietzke, Y. Hirooka: *Particle Induced Erosion of Be, C and W in Fusion Plasmas, Part B: Physical Sputtering and Radiation-Enhanced Sublimation*, Atomic and Plasma-Material Interaction Data for Fusion, (IAEA, Vienna 2001)
42. R. K. Janev, Yu. V. Ralchenko, T. Kenmotsu, K. Hosaka: J. Nucl. Mater. **290** - **293**, 104 (2001)
43. C. García-Rosales, W. Eckstein, J. Roth: J. Nucl. Mater. **218**, 8 (1994)
44. W. Eckstein, R. Preuss: J. Nucl. Mater. **320**, 209 (2003)
45. J. Lindhard, V. Nielsen, M. Scharff: K. Dan. Vidensk. Selsk. Mat. Fys. Medd. **36**, No.10 (1968)
46. J. P. Allain, D. N. Ruzic, M. R. Hendricks: J. Nucl. Mater. **290-293**, 180 (2001)
47. J. Roth, W. Eckstein, M. Guseva: Fusion Engineering Design **37**, 465 (1997)
48. J. Bohdansky, J. Roth, W. Ottenberger: IPP-JET Report 31, Garching (1985)
49. C. E. Kenknight, G. K. Wehner: J. Appl. Phys. **35**, 322 (1964)
50. J. Roth, J. Bohdansky, R. S. Blewer, W. Ottenberger: J. Nucl. Mater. **85&86**, 1077 (1979)
51. J. Roth, J. Bohdansky, W. Ottenberger: Report IPP 9/26, Garching (1979)
52. J. Bohdansky, J. Roth: J. Nucl. Mater. **122 & 123**, 1417 (1984)
53. J. Roth: J. Nucl. Mater. **145-147**, 87 (1987)
54. D. Rosenberg, G. K. Wehner: J. Appl. Phys. **33**, 1842 (1962)
55. H. Fetz, H. Oechsner: In *Proc. 6ieme Int. Conf. Phénomène dans les Gaz*, Paris (1963) p. 39
56. Y. Hirooka, J. Won, R. Boivin, D. Sze, V. Neumoin: J. Nucl. Mater. **228**, 148 (1996)
57. Y. Hirooka, J. Won, R. Boivin, D. Sze, V. Neumoin: J. Nucl. Mater. **230**, 173 (1996)
58. M. I. Guseva, V. M. Gureev, S. N. Korshunov, V. E. Neumoin, Yu. A. Sokolov, V. G. Stolyarova, V. I. Vasiliev, S. V. Rylov, V. M. Strunnikov: J. Nucl. Mater. **220-222**, 957 (1995)
59. M. I. Guseva, A. Yu. Birukov, V. M. Gureev, L. S. Daneljan, S. N. Korshunov, Yu. V. Martynenko, P.S. Moskovkin, Yu. A. Sokolov, V. G. Stolyarova, V. S. Kulikauskas, V. V. Zatekin: J. Nucl. Mater. **233-237**, 681 (1996)
60. E. Hecht, J. Roth, W. Eckstein, C. H. Wu: J. Nucl. Mater. **220-222**, 883 (1995)

61. M. I. Guseva, S. N. Korshunov, V. M. Gureev, Yu. V. Martynenko, V. E. Neumoin, V. G. Stolyarova: J. Nucl. Mater. **241-243**, 1117 (1997)
62. S. N. Korshunov, M. I. Guseva, V. M. Gureev, V. E. Neumoin, V. G. Stolyarova: In *Proc. 3rd Int. Workshop on Be Technology for Fusion*, ed. H. Kawamura, M. Okamoto, JAERI-Conf. 98-001, Mito (1997) p. 216
63. N. Laegreid, G. K. Wehner: J. Appl. Phys. **32**, 365 (1961)
64. C. H. Wu, E. Hechtl, H. R. Yang, W. Eckstein: J. Nucl. Mater. **176-177**, 845 (1990)
65. S. Miyagawa, Y. Ato, Y. Moriya: J. Appl. Phys. **49**, 6194 (1978)
66. E. Hechtl, A. Mazanec, W. Eckstein, J. Roth, C. García-Rosales: J. Nucl. Mater. **196-198**, 713 (1992)
67. Y. Ito, S. Kuriki, M. Saidoh, M. Nishikawa: Jpn. J. Appl. Phys. **33**, 5959 (1994)
68. R. Behrisch, J. Bohdansky, G. H. Oetjen, J. Roth, G. Schilling, H. Verbeek: J. Nucl. Mater. **60**, 321 (1976)
69. J. Bohdansky, J. Roth, M. K. Sinha: In *Proc. 9th Symp. on Fusion Technology*, (Pergamon, London 1976) pp. 541
70. J. N. Smith, Jr., C. H. Meyer, Jr., J. K. Layton: Nucl. Technol. **29**, 318 (1976)
71. J. N. Smith, Jr., C. H. Meyer, Jr., J. K. Layton: J. Nucl. Mater. **67**, 234 (1977)
72. J. Bohdansky, H. L. Bay, W. Ottenberger: J. Nucl. Mater. **76& 77**, 163 (1978)
73. A. A. Haasz, J. W. Davis, C. H. Wu: J. Nucl. Mater. **162-164**, 915 (1989)
74. M. Balden, J. Roth: J. Nucl. Mater. **280**, 39 (2000)
75. J. A. Borders, R. A. Langley, K. L. Wilson: J. Nucl. Mater. **76**, 168 (1978)
76. C. García-Rosales, J. Roth: J. Nucl. Mater. **196 - 198**, 573 (1992)
77. M. Yamashita, In *Proc. 4th Symp. on Ion Sources and Appl. Technology*, (Tokyo 1980) pp. 311
78. E. Hechtl, J. Bohdansky, J. Roth: J. Nucl. Mater. **103 & 104**, 333 (1981)
79. O. Almén, G. Bruce: Nucl. Instrum. Methods **11**, 279 (1961)
80. R. A. Langley, J. Bohdansky, W. Eckstein, P. Mioduszewski, J. Roth, E. Taglauer, E. W. Thomas, H. Verbeek, K. L. Wilson: Nuclear Fusion, Special Issue 1984, (IAEA, Vienna 1984), pp. 72
81. U. Mayerhofer: Diploma thesis, Technical University of Munich, 1986
82. H. Bergsaker, S. Nagata, B. Emmoth: J. Nucl. Mater. **145-147**, 364 (1987)
83. J. Roth, J. Bohdansky, W. Ottenberger: J. Nucl. Mater. **165**, 193 (1989)
84. G. K. Wehner: General Mills Report 2309 (1962)
85. E. Hechtl, J. Bohdansky: J. Nucl. Mater. **122& 123**, 1431 (1984)
86. E. Hechtl, J. Bohdansky: J. Nucl. Mater. **141 - 143**, 139 (1986)
87. S. Nagata, H. Bergsaker, B. Emmoth, L. Ilyinsky: Nucl. Instrum. Methods B **18**, 515 (1987)
88. H. Schirrweitz: Beitr. Plasmaphys. **2**, 188 (1962)
89. G. Betz, R. Dobrozemsky, F. P. Viehböck, H. Wottke: In *Proc. 9th Int. Conf. Phenomenon Ionized. Gases*, (Bucharest 1969) p. 91
90. O. Almén, G. Bruce: Nucl. Instrum. Methods **11**, 257 (1961)
91. S. Grigull, W. Jacob, D. Henke, C. Spaeth, L. Sümmchen, W. Sigle: J. Appl. Phys. **83**, 5185 (1998)
92. S. Grigull, R. Behrisch, S. Parascandola: J. Nucl. Mater. **275**, 158 (1999)
93. A. M. Borisov, W. Eckstein, E. S. Mashkova: J. Nucl. Mater. **304**, 15 (2002)
94. K. H. Krebs: In *Atomic and Molecular Data for Fusion* (IAEA, Vienna 1977) pp. 185
95. S. K. Lam, M. Kaminsky: J. Nucl. Mater. **89**, 205 (1980)

96. O. C. Yonts, D. E. Robinson: ORNL 2802 (1959)
97. O. C. Yonts: In *BNS Nucl. Fusion Reactor Conf.*, (Culham 1969) p. 424
98. C. H. Weissenfeld: Philips Research Reports Supplements No.2 (1967), see also Thesis (1966)
99. M. Nunogaki, M. Uchida, Y. Kuratomi, K. Miyazaki: Nucl. Instrum. Methods B **37/38**, 325 (1989)
100. R. G. Allas, A. R. Knudson, J. M. Lambert, P. A. Treado, G. W. Reynolds: Nucl. Instrum. Methods **194**, 615 (1982)
101. W. H. Hayward, A. R. Wolter: J. Appl. Phys. **40**, 2911 (1969)
102. M. Braun, B. Emmoth, R. Buchta: Radiat. Eff. **28**, 77 (1976)
103. C. E. Carlston, C. D. Magnuson, A. Comeaux, P. Mahavedan: Phys. Rev. **138**, A759 (1965)
104. C. Fert, N. Colombie, B. Fagot, Pham van Chuong: In *Le Bombardment Ionique*, (Paris 1961) p. 67
105. H. Oechsner: Z. Phys. **261**, 37 (1973)
106. Y. Okajima: Jpn. J. Appl. Phys. **20**, 2313 (1981)
107. M. T. Robinson, A. L. Southern: J. Appl. Phys. **38**, 2969 (1967)
108. O. C. Yonts, C. E. Normand, D. E. Harrison: J. Appl. Phys. **31**, 447 (1960)
109. R. Kelly: J. Appl. Phys. **39**, 5298 (1968)
110. T. Weber, K.-P. Lieb: Nucl. Instrum. Methods B **44**, 54 (1989)
111. J. Roth, J. Bohdansky, A. P. Martinelli: Radiat. Eff. **48**, 213 (1980)
112. M. Balden, J. Roth: J. Nucl. Mater. **279**, 351 (2000)
113. U. Gerlach-Meyer, J. W. Coburn, E. Kay: Surf. Sci. **103**, 177 (1981)
114. H. H. Andersen, H. L. Bay: J. Appl. Phys. **46**, 1919 (1975)
115. S. Tachi, K. Miyake, T. Tokuyama: Jpn. J. Appl. Phys. **20**, L411 (1981)
116. P. C. Zalm: J. Appl. Phys. **54**, 2660 (1983)
117. K. Wittmaack, D. B. Poker: Nucl. Instrum. Methods B **47**, 224 (1990)
118. O. Frölich, H. Baumann, K. Bethge: Nucl. Instrum. Methods B **50**, 436 (1990)
119. J. W. Coburn, H. F. Winters, T. J. Chuang: J. Appl. Phys. **48**, 3532 (1977)
120. E. P. Eernisse: J. Appl. Phys. **42**, 4774 (1971)
121. H. Sommerfeldt, E. S. Mashkova, V. A. Molchanov: Phys. Lett. A **38**, 237 (1972)
122. J. Nizam, N. Benazeth-Colombie: Revue de Physique Appl. **10**, 183 (1975)
123. J. M. Poate, W. L. Brown, R. Homer, W. M. Augustyniak, J. W. Mayer, K. N. Tu, W. F. van der Weg: Nucl. Instrum. Methods **132**, 345 (1976)
124. S. T. Kang, R. Shimizu, T. Okutani: Jpn. J. Appl. Phys. **18**, 1717 (1979)
125. J. M. E. Harper, J. J. Cuomo, P. A. Leary, G. M. Summa, H. R. Kaufman, F. J. Bresnock: J. Electrochem. Soc.: Solid-State Sci. Technol. **128**, 1077 (1981)
126. P. C. Zalm, L. J. Beckers, F. H. M. Sanders: Nucl. Instrum. Methods **209-210**, 561 (1983)
127. P. C. Zalm, L. J. Beckers: J. Appl. Phys. **56**, 220 (1984)
128. D. J. Oostra, R. P. van Ingen, A. E. de Vries, G. N. A. van Veen: Appl. Phys. Lett. **50**, 1506 (1987)
129. P. Varga, T. Neidhart, M. Sporn, G. Libiseller, M. Schmid, F. Aumayr, H. P. Winter: Physica Scripta T **73**, 307 (1997)
130. P. Blank, K. Wittmaack: J. Appl. Phys. **50**, 1519 (1979)
131. M. Kaminsky: Private communication
132. A. Santaniello, J. Appelt, J. Bohdansky, J. Roth: J. Nucl. Mater. **162-164**, 951 (1989)

133. Ch. Steinbrüchel, D. M. Gruen, J. Dawson: *J. Vac. Sci. Technol.* **16**, 251 (1979)
134. W. O. Hofer, H. L. Bay, P. J. Martin: *J. Nucl. Mater.* **76& 77**, 156 (1978)
135. J. Bohdansky, G. L. Chen, W. Eckstein, J. Roth, B. M. U. Scherzer, R. Behrisch: *J. Nucl. Mater.* **111& 112**, 717 (1982)
136. R. V. Stuart, G. K. Wehner: *J. Appl. Phys.* **33**, 2345 (1962)
137. O. V. Kurbatov: *Sov. Phys. Techn. Phys.* **12**, 1328 (1968)
138. R. Ranjan, J. P. Allain, M. R. Hendricks, D. N. Ruzic: *J. Vac. Sci. Technol. A* **19**, 1004 (2001)
139. J. M. Lambert, P. A. Treado, D. Trbojevic, R. G. Allas, A. R. Knudson, G. W. Reynolds, F. R. Vozzo: *IEEE Trans. Nucl. Sci.* **NS-30**, 1285 (1983)
140. M. I. Guseva, Yu. V. Martynenko: *Fiz. Plas. (USSR)* **2**, 593 (1976)
141. Z. E. Switkowski, F. M. Mann, D. W. Kneff, R. W. Ollerhead, T. A. Tombrello: *Radiat. Eff.* **29**, 65 (1976)
142. R. V. Stuart, G. K. Wehner: *Phys. Rev. Lett.* **4**, 409 (1960)
143. P. H. Holloway: *Surf. Sci.* **66**, 479 (1977)
144. D. Trbojevic, P. A. Treado, G. S. Daniel: *Nucl. Instrum. Methods B* **10-11**, 743 (1985)
145. E. Hintz, D. Rusbüldt, B. Schweer, J. Bohdansky, J. Roth, A. P. Martinelli: *J. Nucl. Mater.* **93 & 94**, 656 (1980))
146. A. L. Southern, W. R. Willis, M. T. Robinson: *J. Appl. Phys.* **34**, 153 (1963)
147. V. K. Koshkin: In *Phenom. Ioniz. Gases*, (Bucharest 1969) pp. 92
148. M. Bader, F. C. Witteborn, T. W. Snouse: *NASA Techn. Report R-105* (1961)
149. C. R. Finfgeld: Report ORO-3557-15, Salem (1970)
150. G. Sletten, P. Knudsen: *Nucl. Instrum. Methods* **102**, 459 (1972)
151. A. Fontell, E. Arminen: *Can. J. Phys.* **47**, 2405 (1969)
152. S. D. Dahlgren, E. D. McClanahan: *J. Appl. Phys.* **43**, 1514 (1972)
153. J. Bohdansky, H. L. Bay, J. Roth: In *Prog. 7th Int. Vac. Congr. and 3<sup>rd</sup> Int. Conf. on Solid Surfaces*, ed. by R. Dobrozemsky, F. Rüdenauer, F. P. Viehböck, A. Breth, (Techn. Univ., Wien 1977) pp. 1509
154. J. B. Roberto, R. A. Zuhr, J. L. Moore, G. D. Alton: *J. Nucl. Mater.* **85& 86**, 1073 (1979)
155. H. L. Bay, J. Bohdansky, E. Hecht: *Radiat. Eff.* **41**, 77 (1979)
156. Zh. Wang, J. Zhang, J. Pan, Zh. Tao: *Phys. Lett. A* **164**, 227 (1992)
157. E. Hecht, H. L. Bay, J. Bohdansky: *Appl. Phys.* **16**, 147 (1978)
158. K. Tsunoyama, T. Suzuki, Y. Ohashi, H. Kishidaka: *Surf. Interf. Anal.* **2**, 212 (1980)
159. J. Bohdansky: *J. Nucl. Mater.* **93& 94**, 44 (1980)
160. R. Weissmann, R. Behrisch: *Radiat. Eff.* **19**, 69 (1973)
161. M. I. Guseva: *Fiz. Tverd. Tela* **1**, 1540 (1959); Engl. transl. : *Sov. Phys. Solid State* **1**, 1410 (1960)
162. H. H. Andersen, H. L. Bay: *Radiat. Eff.* **13**, 67 (1972)
163. G. Dupp, A. Scharmann: *Z. Phys.* **192**, 284 (1966)
164. P. K. Rol: *Physica* **26**, 1000 (1969)
165. F. Keywell: *Phys. Rev.* **97**, 1611 (1955)
166. B. Perovic, B. Cobic: In *Ioniz. Phenom. Gases*, (Munich 1961) p.1165
167. C. E. Ramer, N. A. Narasimham, H. K. Reynolds, J. C. Alldred: *J. Appl. Phys.* **35**, 1673 (1964)
168. K. B. Cheney, E. T. Pitkin: *J. Appl. Phys.* **36**, 3542 (1965)
169. K. Akaishi, A. Kiyahara, Z. Kabeya, M. Komizo, T. Gotoh: *J. Vac. Soc. Japan* **20**, 161 (1977)

170. K. Akaishi, A. Kiyahara, Z. Kabeya, M. Komizo, T. Gotoh: In *Prog. 7th Int. Vac. Congr. and 3<sup>rd</sup> Int. Conf. on Solid Surfaces*, ed. by R. Dobrozemsky, F. Rüdenauer, F. P. Viehböck, A. Breth, (Techn. Univ., Wien 1977) pp. 1477
171. Y. Ato: J. Vac. Soc. Japan **23**, 339 (1980)
172. A. Ya. Barskaya, S. P. Varshavskii, O. Ryazantseva, L. A. Sena: Zh. Tekh. Fiz. **57**, 1223 (1987)
173. H. J. Smith: Radiat. Eff. **18**, 73 (1973)
174. A. Oliva-Florio, R. A. Baragiola, M. M. Jakas, E. V. Alonso, J. Ferrón: Phys. Rev. B **35**, 2198 (1987)
175. N. Colombie: Thesis, Univ. Toulouse (1964)
176. H. J. Smith: Phys. Lett. **37A**, 289 (1971)
177. D. Ghose, D. Basu, S. B. Karmohapatro: phys. stat. solidi A **77**, 121 (1983)
178. G. Holmen: Radiat. Eff. **24**, 7 (1975)
179. M. K. Sinha, J. Roth, J. Bohdansky: In *Proc. 9th Symp. Fusion Technol.*, (Pergamon, New York 1976) pp. 41
180. G. Bräuer, D. Hasselkamp, W. Krüger, A. Schramann: Nucl. Instrum. Methods B **12**, 458 (1985)
181. B. M. Gurmin: Sov. Phys. Solid State **10**, 324 (1968)
182. R. V. Stuart, G. K. Wehner: In *Trans. 7th Natl. Vac. Symp.*, (Pergamon, New York 1960) pp. 290
183. R. Behrisch, O. K. Harling, M. T. Thomas, R. L. Brodzinski, L. H. Jenkins, G. J. Smith, J. F. Wedelking, M. J. Saltmarsh, M. Kaminsky, S. K. Das, C. M. Logan, R. Meisenheimer, J. E. Robinson, M. Shimotomai, D. A. Thompson: J. Appl. Phys. **48**, 3914 (1977)
184. R. W. Ollerhead, F. M. Mann, D. W. Kuff, Z. E. Switkowski, T. A. Tombrello: Phys. Rev. Lett. **36**, 439 (1976)
185. A. J. Summers, N. J. Freeman, N. R. Daly: J. Appl. Phys. **42**, 4774 (1971)
186. H. Uecker, A. Riccato, G. R. Thacker, J. Ney, J. P. Biersack: J. Nucl. Mater. **93 & 94**, 670 (1980)
187. A. J. Summers, N. J. Freeman, N. R. Daly: Proc. Brit. Nucl. Soc. 1969, p. 347
188. W. Eckstein, B. M. U. Scherzer, H. Verbeek: Radiat. Eff. **18**, 135 (1973)
189. W. Eckstein: Nucl. Instrum. Methods B **83**, 329 (1993)
190. B. Emmoth, M. Braun, H. P. Palenius: J. Nucl. Mater. **63**, 482 (1976)
191. H. Oechsner: Habil. Schrift, Würzburg (1971)
192. J. N. Smith, Jr., Trans. Am. Nucl. Soc. **22**, 29 (1975)
193. J. P. O'Connor, L. M. Baumel, P. G. Blauner, K. M. Hubbard, M. R. Weller, R. A. Weller: Nucl. Instrum. Methods B **13**, 365 (1986)
194. H. L. Bay, J. Roth, J. Bohdansky: J. Appl. Phys. **48**, 4722 (1977)
195. H. Ohtsuka, R. Yamada, K. Sone, M. Saidoh, T. Abe: J. Nucl. Mater. **76 & 77**, 188 (1978)
196. M. Kaminsky, S. K. Das, P. Busza, J. Cecchi: In *Int. Symp. Fusion Technology*, (Euratom, Padova 1978) pp. 112
197. C. H. Meyer, Jr., J. N. Smith, Jr.: J. Vac. Sci. Technol. **16**, 248 (1979)
198. K. Saiki, H. Tanaka, S. Tanaka, A. Koma: J. Nucl. Mater. **97**, 173 (1981)
199. M. Tomita, T. Nate, S. Miyagi, M. Sakisaka: J. Nucl. Mater. **138**, 248 (1986)
200. H. Oechsner: Appl. Phys. **8**, 185 (1975)
201. B. Emmoth, Th. Fried, M. Braun: J. Nucl. Mater. **76 & 77**, 129 (1978)
202. M. Saidoh, K. Sone: Jpn. J. Appl. Phys. **22**, 1361 (1983);
203. M. Saidoh, K. Sone: JAERI-M 58 (1983)

204. S. Bhattacharjee, J. Zhang, V. Shutthanandan, P. K. Ray, N. R. Shivaparan, R. J. Smith: Nucl. Instrum. Methods B **129**, 123 (1997)
205. F. Grønlund, W. J. Moore: J. Chem. Phys. **32**, 1540 (1960)
206. C. D. O'Briain, A. Lindner, W. J. Moore: J. Chem. Phys. **29**, 3 (1958)
207. R. Behrisch: Diploma thesis, University of Munich (1960)
208. J. Bohdansky, H. Lindner, E. Hecht, A. P. Martinelli, J. Roth: Nucl. Instrum. Methods B **18**, 509 (1987)
209. A. Weiss, L. Heldt, W. J. Moore: J. Chem. Phys. **29**, 7 (1958)
210. A. Benninghoven: Z. Angew. Phys. **27**, 51 (1969)
211. G. K. Wehner, General Mills Report No. 2243 (1961)
212. M. Koedam: Physica **24**, 692 (1962) and Thesis, Univ. Utrecht (1961)
213. D. B. Medved, H. Poppe: J. Appl. Phys. **33**, 1759 (1962)
214. H. H. Andersen, H. L. Bay: Radiat. Eff. **19**, 139 (1973)
215. J. Pan, Zh. Wang, Zh. Tao, J. Zhang: Nucl. Instrum. Methods B **67**, 514 (1992)
216. M. Szymonski, R. S. Bhattacharya, H. Overeijnder, A. E. de Vries: J. Phys. D **11**, 751 (1978)
217. F. - M. Devienne, A. Roustan: C. R. Acad. Sc. Paris **268**, 1362 (1969)
218. R. C. Krutenat, C. Panzera: J. Appl. Phys. **41**, 4953 (1970)
219. E. C. Viljoen, E. Taglauer, J. du Plessis: Nucl. Instrum. Methods B **179**, 515 (2001)
220. M. I. Guseva: Radiotekh. Elektron. **7**, 1680 (1962); Engl. translation: Radio Eng. Electron Phys. USSR **7**, 1563 (1962)
221. E. Hecht: In *Proc. Symp. on Sputtering*, (Techn. Univ., Vienna 1980) pp. 834
222. K. Wittmaack: Surf. Sci. **51**, 626 (1975)
223. J. F. Ziegler, J. J. Cuomo, J. Roth: Appl. Phys. Lett. **30**, 328 (1977)
224. H. F. Winters, D. Horne: Phys. Rev. B **10**, 55 (1974)
225. E. Hecht, H. R. Yang, C. H. Wu, W. Eckstein: J. Nucl. Mater. **176-177**, 874 (1990)
226. A. K. Furr, C. R. Finfgeld: J. Appl. Phys. **41**, 1739 (1970)
227. E. P. Eernisse: Appl. Phys. Lett. **29**, 14 (1976)
228. J. S. Colligon, R. W. Bramham: In *Proc. Atomic Coll. in Solids*, (Brighton 1970) pp. 258
229. H. H. Andersen, H. L. Bay: J. Appl. Phys. **46**, 2416 (1975)
230. T. M. Nenadovic, Z. B. Fotric, D. S. Dimitrijevic: Surf. Sci. **33**, 607 (1972)
231. J. S. Colligon, M. H. Patel: Radiat. Eff. **32**, 193 (1977)
232. R. K. Fitch, E. A. Mahmoud: Thin Solid Films **87**, 379 (1982)
233. M. Yamashita, S. Baba, A. Kinbara: J. Vac. Soc. Japan **25**, 249 (1982)
234. H. J. Kang, E. Kawatoh, R. Shimizu: Surf. Sci. **144**, 541 (1984)
235. K. L. Merkle, P. P. Pronko: J. Nucl. Mater. **53**, 231 (1974)
236. H. L. Bay, H. H. Andersen, W. O. Hofer, O. Nielsen: Nucl. Instrum. Methods **132**, 301 (1976)
237. H. Kräutle: Nucl. Instrum. Methods **137**, 553 (1976)
238. H. H. Andersen, A. Brunelle, S. Della-Negra, J. Depauw, D. Jacquet, and Y. Le Beyec: Phys. Rev. Lett. **80**, 5433 (1998)
239. R. Gregg, T. A. Tombrello: Radiat. Eff. **35**, 243 (1978)
240. J. G. Tracy: ORNL
241. R. Behrisch, J. Roth, J. Bohdansky, A. P. Martinelli, B. Schweer, D. Rusbüldt, E. Hintz: J. Nucl. Mater. **93 & 94**, 645 (1980)

242. A. E. Morgan, H. A. M. de Grefte, N. Warmoltz, H. A. Werner: *Appl. Surf. Sci.* **7**, 372 (1981)
243. P. C. Zalm: *Radiat. Eff. Lett.* **86**, 29 (1983)
244. M. Toulemonde: Private communication
245. D. Fink, J. P. Biersack: *Radiat. Eff.* **64**, 89 (1982)
246. D. Fink, J. P. Biersack, M. Städele, K. Tjan, R. A. Haring, A. E. De Vries: *Nucl. Instrum. Methods B* **1**, 275 (1984)
247. R. Behrisch, G. Federici, A. Kukushkin, D. Reiter: *J. Nucl. Mater.* **313 - 316**, 388 (2003)
248. T. Kawamura, T. Ono, Y. Yamamura: *J. Nucl. Mater.* **220 - 222**, 1010 (1995)
249. V. I. Shulga: *Nucl. Instrum. Methods B* **174**, 77 (2001)
250. V. I. Shulga: *Nucl. Instrum. Methods B* **187**, 178 (2002)
251. Y. Yamamura, Y. Itikawa, N. Itoh: IPPJ-AM-26, Nagoya (1993)
252. J. Roth, W. Eckstein, J. Bohdansky: *J. Nucl. Mater.* **165**, 199 (1989)
253. J. Roth: In *Physics of Plasma-Wall Interactions in Controlled Fusion*, ed. by D. E. Post, R. Behrisch, (Plenum, New York, London 1986) pp. 351
254. J. Roth, J. Bohdansky, K. L. Wilson: *J. Nucl. Mater.* **111 & 112**, 775 (1982)
255. I. M. Fayazov, E. S. Mashkova, V. A. Molchanov, A. V. Siderov, A. I. Tolmachev, W. Eckstein: *Nucl. Instrum. Methods B* **67**, 523 (1992)
256. W. Krüger, A. Scharmann, H. Afzidi, G. Bräuer: SOS, Vienna, 1980 p.125
257. J. Bohdansky, G. L. Chen, W. Eckstein, J. Roth: *J. Nucl. Mater.* **103 & 104**, 339 (1981)
258. H. L. Bay, J. Bohdansky: *Appl. Phys.* **19**, 421 (1979)
259. E. S. Mashkova, V. A. Molchanov: *Sov. Phys. - Techn. Phys.* **9**, 1601 (1965)
260. E. Hecht, A. Mazanec, W. Eckstein, J. Roth: *Nucl. Instrum. Methods B* **90**, 505 (1994)
261. H. Liebl, J. Bohdansky, J. Roth, V. Dose: *Rev. Sci. Instrum.* **58**, 1830 (1987)
262. P. K. Rol, J. M. Fluit, J. Kistemaker: *Physica* **26**, 1000 (1960)
263. V. A. Molchanov, V. G. Tel'kovskii: *Dokl. Akad. Nauk SSSR* **136**, 801 (1961); Engl. transl.: *Sov. Phys. - Doklady* **6**, 137 (1961)
264. H. L. Bay, J. Bohdansky, W. O. Hofer, J. Roth: *Appl. Phys.* **21**, 327 (1980)
265. V. Bandourko, R. Jimbou, K. Nakamura, M. Akiba: *J. Nucl. Mater.* **258-263**, 917 (1998)
266. M. Küstner, W. Eckstein, V. Dose, J. Roth: *Nucl. Instrum. Methods B* **145**, 320 (1998)
267. M. Küstner, W. Eckstein, E. Hecht, J. Roth: *J. Nucl. Mater.* **265**, 22 (1999)
268. Yu. N. Zhukova, E. S. Mashkova, V. A. Molchanov, V. M. Sotnikov, W. Eckstein: *Povern. Phys. Chem. Mek.* **8-9**, 107 (1994)
269. J. Roth, W. Eckstein, E. Gauthier, J. László: *J. Nucl. Mater.* **179 - 181**, 34 (1991)
270. R. Behrisch, G. Maderlechner, B. M. U. Scherzer, M. T. Robinson: *Appl. Phys.* **18**, 391 (1979)
271. W. Eckstein, J. Roth, W. Nagel, R. Dohmen: *J. Nucl. Mater.* **328**, 55 (2004)
272. W. Eckstein, C. García-Rosales, J. Roth: *Nucl. Instrum. Methods B* **83**, 95 (1993)
273. G. J. Ogilvie, M. J. Ridge: *J. Phys. Chem. Sol.* **10**, 217 (1959)
274. P. K. Rol, J. M. Fluit, F. P. Viehböck, M. de Jong: In *Proc. 4th Int. Conf. Phen. Ion. Gases*, Uppsala, ed. by N. R. Nilsson (North-Holland, Amsterdam 1959) pp. 257

275. V. A. Molchanov, V. G. Tel'kovskii, V. M. Chicherov: Sov. Phys. - Doklady **6**, 222 (1961)
276. H. E. Roosendaal: In *Sputtering by Particle Bombardment I*, ed. by R. Behrisch, Top. Appl. Phys. **47**, 219 (1981), Russ. translation: (MIR, Moscow 1984)
277. G. K. Wehner: Phys. Rev. **102**, 690 (1956)
278. Y. Yamamura, W. Takeuchi: Nucl. Instrum. Methods B **29**, 461 (1987)
279. M. Hou, W. Eckstein: Nucl. Instrum. Methods B **13**, 324 (1986)
280. D. Onderdelinden: Can. J. Phys. **46**, 739 (1968)
281. G. Betz, G. K. Wehner: In *Sputtering by Particle Bombardment II*, ed. by R. Behrisch, Top. Appl. Phys. **52**, 11 (1983), Russ. translation: (MIR, Moscow 1986)
282. K. Wittmaack, W. Wach: Nucl. Instrum. Methods **191**, 327 (1981)
283. W. Eckstein: J. Nucl. Mater. **281**, 195 (2000)
284. W. Eckstein, M. Hou, V. I. Shulga: Nucl. Instrum. Methods B **119**, 477 (1996)
285. W. Eckstein, R. Dohmen: Nucl. Instrum. Methods B **129**, 327 (1997)
286. W. Eckstein: unpublished results
287. J. P. Biersack, S. Berg, C. Nender: Nucl. Instrum. Methods B **59/60**, 21 (1991)
288. S. Berg, I. V. Katardjiev: J. Vac. Sci. Technol. A **17**, 1916 (1999)
289. W. Eckstein: Nucl. Instrum. Methods B **171**, 435 (2000)
290. R. A. Zuh, J. Roth, W. Eckstein, U. von Toussaint, J. Luthin: J. Nucl. Mater. **290-293**, 162 (2001)
291. V. S. Touboltsev, G. Dybkjaer, A. Johansen, E. Johnson, L. Sarholt, H. H. Andersen, M. Olsen: Phil. Mag. A **77**, 341 (1998)
292. J. Sielanko, J. Filiks, J. Hereć: Vacuum **70**, 381 (2003)
293. W. Eckstein, J. P. Biersack: Appl. Phys. A **37**, 95 (1985)
294. W. Eckstein, W. Möller: Nucl. Instrum. Methods B **7/8**, 727 (1985))
295. D. Naujoks, W. Eckstein: J. Nucl. Mater. **220 - 222**, 993 (1995)
296. D. Naujoks, W. Eckstein: J. Nucl. Mater. **220**, 93 (1996)
297. V. Bandourko, R. Jimbou, K. Nakamura, M. Akiba, Y. Okumura: J. Nucl. Mater. **313-316**, 413 (2003)
298. N. Andersen, P. Sigmund: K. Dan. Vidensk. Selsk. Mat. Fys. Medd. **39** No.3, 1 (1974)
299. P. Sigmund: K. Dan. Vidensk. Selsk. Mat. Fys. Medd. **93**, 255 (1993)
300. M. T. Robinson: J. Appl. Phys. **54**, 2650 (1983)
301. D. L. Weathers, S. J. Spicklemire, T. A. Tombrello, I. D. Hutcheon, H. Gnaser: Nucl. Instrum. Methods B **73**, 135 (1993)
302. D. Y. Lo, T. A. Tombrello, M. H. Shapiro: Nucl. Instrum. Methods B **40/41**, 270 (1989)
303. H. M. Urbassek, U. Conrad: Nucl. Instrum. Methods B **73**, 151 (1993)
304. V. I. Shulga, P. Sigmund: Nucl. Instrum. Methods B **103**, 383 (1995)
305. V. I. Shulga, P. Sigmund: Nucl. Instrum. Methods B **119**, 359 (1996)
306. T. A. Tombrello: K. Dan. Vidensk. Selsk. Mat. Fys. Medd. **93**, 659 (1993)
307. R. Behrisch, W. Eckstein: Nucl. Instrum. Methods B **82**, 255 (1993)
308. W. Eckstein, V. I. Shulga, J. Roth: Nucl. Instrum. Methods B **153**, 415 (1999)
309. K. Schmid, J. Roth: J. Nucl. Mater. **313-316**, 302 (2003)
310. R. S. Nelson: Phil. Mag. **11**, 219 (1965)
311. V. E. Yurasova, A. S. Mosunov, A. A. Promokhov: Bull. Russian Acad. Sci. **62**, 1164 (1998)

312. D. A. Konov, A. S. Mosunov, G. V. Adamov, L. B. Shelyakin, V. E. Yurasova: Vacuum **64**, 47 (2002)
313. M. I. Guseva, V. M. Gureev, B. N. Kolbasov, S. N. Korshunov, Yu. V. Martynenko, V. B. Petrov, B. I. Khrripunov: JETP Letters **77**, 430 (2003)
314. K. Schmid, J. Roth: Internal report, to be published in J. Nucl. Mater.
315. R. P. Doerner, M. J. Baldwin, R. W. Conn, A. A. Grossman, S. C. Luckhardt, R. Seraydarian, G. R. Tynan, D. G. Whyte: J. Nucl. Mater. **290 - 293**, 166 (2001)
316. M. D. Coventry, J. P. Allain, D. N. Ruzic: J. Nucl. Mater. **335**, 115 (2004)
317. J. E. Westmoreland, P. Sigmund: Radiat. Eff. **6**, 187 (1970)
318. W. Eckstein: Nucl. Instrum. Methods B **33**, 489 (1988)
319. W. Eckstein: Radiat. Eff. Defects Solids **130-131**, 239 (1994)
320. U. Conrad, H. M. Urbassek: Nucl. Instrum. Methods B **48**, 399 (1990)
321. M. T. Robinson: Phys. Rev. B **40**, 10717 (1989)
322. Y. Yamamura: Nucl. Instrum. Methods B **45**, 582 (1990)
323. S. S. Todorov, I. R. Chakarov, D. S. Karpuzov: Vacuum **43**, 543 (1992)
324. R. G. Vichev, D. S. Karpuzov: Nucl. Instrum. Methods B **83**, 345 (1993)
325. R. G. Vichev, W. Eckstein: Nucl. Instrum. Methods B **102**, 272 (1995)
326. M. Hou, W. Eckstein, M. T. Robinson: Nucl. Instrum. Methods B **82**, 234 (1993)
327. R. G. Vichev, W. Eckstein: Nucl. Instrum. Methods B **122**, 215 (1997)
328. A. Grossman, R. P. Doerner, S. Luckhardt: J. Nucl. Mater. **290-293**, 80 (2001)
329. J. László, W. Eckstein: J. Nucl. Mater. **184**, 22 (1991)
330. J. P. Allain, M. D. Coventry, D. N. Ruzic: J. Nucl. Mater. **313 - 316**, 641 (2003)
331. W. Eckstein, A. Sagara, K. Kamada: J. Nucl. Mater. **150**, 266 (1987)
332. W. Eckstein, J. P. Biersack: Z. Phys. B **63**, 109 (1986)
333. P. C. Smith, D. N. Ruzic: Nucl. Fusion **38**, 673 (1998)
334. W. Eckstein, J. Roth, E. Gauthier, J. László: Fusion Technology **19**, 2076 (1991)
335. D. N. Ruzic: Nucl. Instrum. Methods B **47**, 118 (1990)
336. L. G. Haggmark, W. D. Wilson: J. Nucl. Mater. **76 & 77**, 149 (1978)
337. P. S. Chou, N. M. Ghoniem: Nucl. Instrum. Methods B **28**, 175 (1987)
338. W. Eckstein: IPP report 9/54, Garching 1985
339. G. Betz, R. Dobrozemsky, F. P. Viehböck: Int. J. Mass. Spectrom. Ion Phys. **6**, 671 (1971)
340. A. Barna, M. Menyhard, L. Kotis, Gy. J. Kovacs, G. Radnoci, A. Zalar, P. Panjan: J. Appl. Phys. **98**, 024901 (2005)
341. Y. Yamamura: Nucl. Instrum. Methods B **33**, 493 (1988)
342. S. Berg, I. V. Katardjiev: J. Vac. Sci. Technol. A **13**, 831 (1995)
343. A. E. Morgan, H. A. M. de Grefte, H. J. Tolle: J. Vac. Sci. Technol. **18**, 164 (1981)
344. K. Ohya: Nucl. Instrum. Methods B **195**, 281 (2002)
345. D. E. Hanson, B. C. Stephens, C. Saravanan, J. D. Kress: J. Vac. Sci. Technol. A **19**, 820 (2001)
346. D. S. Karpuzov: Nucl. Instrum. Methods B **19/20**, 109 (1987)
347. M. M. Jakas, D. E. Harrison, Jr.: Phys. Rev. B **32**, 2752 (1985)
348. N. Herbots, B. R. Appleton, T. S. Noggle, R. A. Zuhr, S. J. Pennycook: Nucl. Instrum. Methods B **13**, 250 (1986)

349. G. Ecke, R. Kosiba, V. Kharmalov, Y. Trushin, J. Pezoldt: Nucl. Instrum. Methods B **196**, 39 (2002)
350. T. S. Pugacheva, M. S. Saidov, A. S. Lutovich: Radiat. Eff. **105**, 117 (1987)
351. W. Eckstein, S. Hackel, D. Heinemann, B. Fricke: Z. Phys. D **24**, 171 (1992)
352. J. Sielanko, W. Szyszko: Surf. Sci. **161**, 101 (1985)
353. M. L. Roush, T. D. Andreadis, F. Davarya, O. F. Goktepe: J. Nucl. Mater. **191**, 135 (1981)
354. M. L. Roush, T. D. Andreadis, F. Davarya, O. F. Goktepe: Appl. Surf. Sci. **11/12**, 235 (1982)
355. Y. Kido, A. Kawano, J. Kawamoto: Preprint (1988)
356. Y. Yamamura, C. Mössner, H. Oechsner: Radiat. Eff. **103**, 25 (1987)
357. Y. Yamamura, C. Mössner, H. Oechsner: Radiat. Eff. **105**, 31 (1987)
358. M. L. Roush, T. D. Andreadis, F. Davarya, O. F. Goktepe: Radiat. Eff. **55**, 119 (1981)
359. T. Ishitani, R. Shimizu: Appl. Phys. **6**, 241 (1975)
360. T. Aoki, S. Chiba, J. Matsuo, I. Yamada, J. P. Biersack: Nucl. Instrum. Methods B **180**, 312 (2001)
361. J. Sielanko, W. Szyszko: Nucl. Instrum. Methods B **16**, 340 (1986)
362. K. Wittmaack: J. Vac. Sci. Technol. **3**, 1350 (1985)
363. A. M. Hassanein, D. L. Smith: Nucl. Instrum. Methods B **13**, 225 (1986)
364. R. Behrisch, G. Maderlechner, B. M. U. Scherzer, M. T. Robinson: In *Proc. SASP 78*, ed. by W. Lindinger, F. Howorka, F. Egger, (Institut für Atomphysik, Universität Innsbruck, Innsbruck 1978) pp. 33
365. L. G. Haggmark, J. P. Biersack: J. Nucl. Mater. **103& 104**, 345 (1981)
366. Y. Yamamura, K. Muraoka: Nucl. Instrum. Methods B **42**, 175 (1989)
367. V. M. Samoylov, A. H. Phillips, V. A. Eltekov, V. E. Yurasova: Nucl. Instrum. Methods B **18**, 243 (1987)
368. A. Barna, M. Menyhard, G. Zsolt, N. Q. Khanh, A. Zalar, P. Panjan: J. Vac. Sci. Technol. A **21**, 196 (2003)
369. Y. Yamamura, Y. Mizuno: J. Nucl. Mater. **128/129**, 559 (1984)
370. Y. Yamamura, Y. Mizuno: IPPJ-AM-40: Tech. Rpt., Nagoya (1985)
371. R. Becerra-Acevedo, J. Bohdansky, W. Eckstein, J. Roth: Nucl. Instrum. Methods B **2**, 631 (1984)
372. L. G. Haggmark, J. P. Biersack: J. Nucl. Mater. **93& 94**, 664 (1980)
373. W. Eckstein, J. P. Biersack: Nucl. Instrum. Methods B **2**, 550 (1984)
374. P. S. Chou, N.M. Ghoniem: J. Nucl. Mater. **117**, 55 (1983)
375. A. S. Mosunov, E. Yu. Zhukova, D. S. Colligon, S. A. Postnikov, V. E. Yurasova: Isvestia Akad. Nauk. Ser. Fiz. **68**, 313 (2004)
376. Yu. A. Ryzhov, A. A. Semyonov, I. I. Shkarban, A. S. Mosunov, V. E. Yurasova: Vopros Atom. Nauk. Tek. **2**, 54 (2004)
377. V. I. Nikiforov, V. I. Pavlenko, R. P. Slabopitskii, I. V. Khirnov: KhFTI 87-58 (1987)
378. L. B. Shelyakin, T. P. Martynenko, A. Bischoff, V. E. Yurasova, G. Shaarschmidt: Poverkhnost (USSR) **N 6**, 65 (1983)
379. V. E. Yurasova: In *Interaction of Charged Particles with Solids and Surfaces*, ed. by A. Gras-Marti, H. M. Urbassek, N. R. Arista, F. Flores, (Plenum, New York London 1991) pp. 505
380. W. Eckstein, H.-J. Barth, E. Mühlung: Nucl. Instrum. Methods B **14**, 507 (1986)

381. D. T. Goldman, D. E. Harrison, Jr., R. R. Coveyeau: Tech. Rpt. ORNL 2729, Oak Ridge (1959)
382. D. E. Harrison, Jr., M. M. Jakas: Nucl. Instrum. Methods B **15**, 25 (1986)
383. M. M. Jakas, D. E. Harrison, Jr.: Nucl. Instrum. Methods B **14**, 535 (1986)
384. M. Hou, M. T. Robinson: Appl. Phys. **18**, 381 (1979)
385. C. Coudray, G. Slodzian: Nucl. Instrum. Methods B **15**, 29 (1986)
386. M. H. Shapiro, D. Y. Lo, P. K. Haff, T. A. Tombrello: Nucl. Instrum. Methods B **13**, 348 (1986)
387. J. Likonen, M. Hautala: J. Phys. B **1**, 4697 (1989)
388. A. S. Mosunov, Yu. A. Ryzhov, A. A. Semenov, I. I. Shkarban, D. S. Colligon, V. E. Yurasova: Isvestia Akad. Nauk. Ser. Fiz. **68**, 1665 (2004)
389. R. N. Schlaug: "Sputtering Calculations from a Realistic Model"; Thesis, University of California, Berkeley (1965) (University Microfilms, Ann Arbor, MI 1966)
390. J. P. Biersack, A. Riccato, W. Kaczerowski: In *Proc. of the Workshop on Sputtering Caused by Plasma (Neutral Beam) Surface Interaction*, (CONF-790775, U.S.DOE, Washington, DC 1979) 16-1
391. S. M. Sotnikov: Pover. Fiz. Khim. Mekh. **8**, 45 (1989)
392. W. Eckstein, J. László: J. Nucl. Mater. **183**, 19 (1991)
393. M. D. Coventry, J. P. Allain, D. N. Ruzic: J. Nucl. Mater. **313 - 316**, 636 (2003)
394. E. Salonen, K. Nordlund, J. Keinonen, C. H. Wu: J. Nucl. Mater. **313 - 316**, 404 (2003)
395. V. I. Shulga: Nucl. Instrum. Methods B **174**, 423 (2001)
396. Y. Yamamura, Y. Kitazoe: Radiat. Eff. **39**, 251 (1978)
397. Y. Yamamura: Nucl. Instrum. Methods **194**, 515 (1982)
398. M. T. Robinson: Inst. Phys. Conf. Ser. **71**, 151 (1984)
399. V. K. Meyer, A. Güntherschulze: Z. Phys. **71**, 19 (1931)
400. T. P. Martynenko: Sov. Phys. - Solid State **9**, 2232 (1968)
401. G. K. Wehner: Phys. Rev. **108**, 35 (1957)
402. G. Holmén, O. Almén: Ark. Fys. **40**, 429 (1969)
403. H. Ismail: Rev. Phys. Appl. **5**, 759 (1970)
404. G. K. Wehner: Phys. Rev. **112**, 1120 (1958)
405. P. V. Pavlov, D. I. Tetelbaum, E. I. Zorin, V. I. Alekseev: Fiz. Tverd. Tela **8**, 2679 (1966), Sov. Phys. - Solid State **8**, 2141 (1967)
406. T. P. Martynenko: Sov. Phys. - Solid State **9**, 2887 (1968)
407. S. G. Askerov, L. A. Sena: Sov. Phys. - Solid State **11**, 288 (1969)
408. M. A. El Khakani, H. Jaffrezic, G. Marest, N. Montcoffre, J. Tousset: Nucl. Instrum. Methods B **50**, 406 (1990)
409. G. K. Wehner: J. Appl. Phys. **30**, 1762 (1959)
410. H. H. Andersen: Radiat. Eff. **19**, 257 (1973)
411. H. J. Smith: Radiat. Eff. **18**, 55 (1973)
412. W. Eckstein, J. Roth: Nucl. Instrum. Methods B **53**, 279 (1991)
413. K. Krieger, J. Roth: J. Nucl. Mater. **290-293**, 107 (2001)
414. N. Matsunami, M. Satake, A. Iwase, T. Inami, M. Kobiyama: J. Nucl. Mater. **302**, 206 (2002)
415. S. Ueda, T. Ohsaka, S. Kuwajima: J. Nucl. Mater. **283-287**, 1100 (2000)
416. S. S. Elovikov, V. A. Eltekov, N. N. Negrebetskaya, J. V. Sushkova, V. E. Yurasova, I. I. Shkarban, O. I. Buzhinskij, I. V. Opimach: J. Nucl. Mater. **212-215**, 1335 (1994)

417. E. E. Zhurkin, A. S. Kolesnikov: Nucl. Instrum. Methods B **193**, 822 (2002)
418. T. Mizutani, C. J. Dale, W. K. Chu, T. M. Mayer: Nucl. Instrum. Methods B **7/8**, 825 (1985)
419. E. F. C. Haddeman, B. J. Thijssse: Nucl. Instrum. Methods B **202**, 161 (2003)
420. V. A. Eltekov, V. E. Yurasova, N. N. Negrebetskaya, N. G. Vasichkina: Pover. Fiz. Khim. Mekh. **2**, 46 (1994)
421. S. P. Wolsky, E. J. Zdanuk: J. Appl. Phys. **32**, 782 (1961)
422. Y. Zhang, T. Zhang, Z. Xiao, H. J. Whitlow: Nucl. Instrum. Methods B **173**, 427 (2001)
423. V. M. Samoylov, A. H. Phillips, V. A. Eltekov, V. E. Yurasova: Vestn. Mosk. Univ. **27**, 87 (1986)
424. V. A. Eltekov, V. N. Samoylov, V. E. Yurasova, H. A. Motaweh: Nucl. Instrum. Methods B **13**, 443 (1986)
425. B. J. Garrison: J. Am. Chem. Soc. **105**, 373 (1983)
426. Z. B. Güvenc, Y. Hundur, R. Hippel: Nucl. Instrum. Methods B **164 - 165**, 854 (2000)
427. V. E. Yurasova, V. S. Chernysh, M. V. Kuvakin, L. B. Shelyakin: JETP (USSR) **21**, 197 (1975)
428. S. S. Elovikov, D. A. Konov, R. S. Gvosdover, L. B. Shelyakin, V. E. Yurasova: Poverknost **5**, 21 (2004)
429. K. Thiel, U. Sassmannshausen, H. Külzer, W. Herr: Radiat. Eff. **64**, 83 (1982)
430. M. M. Jakas, D. E. Harrison, Jr.: Phys. Rev. B **30**, 3573 (1984)
431. D. E. Harrison, Jr.: J. Appl. Phys. **52**, 4251 (1981)
432. D. E. Harrison, Jr., N. S. Levy, J. P. Johnson III, H. M. Effron: J. Appl. Phys. **39**, 3742 (1968)
433. D. E. Harrison, Jr., W. L. Moore, Jr., H. T. Holcombe: Radiat. Eff. **17**, 167 (1973)
434. D. E. Harrison, Jr., P. W. Kelly, B. J. Garrison, N. Winograd: Surf. Sci. **76**, 311 (1978)
435. B. J. Garrison, N. Winograd, D. E. Harrison, Jr.: Phys. Rev. B **18**, 6000 (1978)
436. N. Winograd, B. J. Garrison, T. Fleisch, W. N. Delgass, D. E. Harrison, Jr.: J. Vac. Sci. Technol. **16**, 629 (1979)
437. N. Winograd, K. E. Foley, B. J. Garrison, D. E. Harrison, Jr.: Phys. Lett. A **73**, 253 (1979)
438. L. P. Razvina, V. A. Eltekov, V. E. Yurasova: In Proc. 17th All-Union Conf. Emission Electronics, (Akad. NAUK SSSR, Moscow 1979) pp. 540
439. K. E. Foley, B. J. Garrison: J. Chem. Phys. **72**, 1018 (1980)
440. D. E. Harrison, Jr.: J. Appl. Phys. **52**, 1499 (1981)
441. V. A. Eltekov, V. N. Samoylov, V. E. Yurasova: Pover. Fiz. Khim. Mekh. **3**, 43 (1982)
442. V. I. Shulga: Radiat. Eff. **70**, 65 (1983)
443. J. Likonen, M. Hautala: Appl. Phys. A **45**, 137 (1988)
444. B. J. Garrison, N. Winograd: Chem. Phys. Lett. **97**, 381 (1983)
445. V. I. Shulga: Radiat. Eff. **82**, 169 (1984)
446. V. I. Shulga: Radiat. Eff. **84**, 1 (1985)
447. M. H. Shapiro, P. K. Haff, T. A. Tombrello, D. E. Harrison, Jr., R. P. Webb: Radiat. Eff. **89**, 243 (1985)
448. S. C. Park, R. A. Stansfield, D. C. Clary: J. Phys. D **20**, 880 (1987)
449. M. H. Shapiro, T. A. Tombrello: Nucl. Instrum. Methods B **18**, 355 (1987)

450. K. Broomfield, R. A. Stansfield, D. C. Clary: *Surf. Sci.* **202**, 320 (1988)
451. J. D. Kress, D. E. Hanson, A. F. Voter, C. L. Liu, X.-Y. Liu, D. G. Coronell: *J. Vac. Sci. Technol. A* **17**, 2819 (1999)
452. I. N. Iwanov, D. W. Ledyakin, I. F. Urazgil'din, V. E. Yurasova: *Fisika Tverd. - Solid State Phys.* **33**, 924 (1991)
453. V. E. Yurasova, I. F. Urazgil'din: *Radiat. Eff. Defects Sol.* **117**, 99 (1991)
454. A. A. Promokhov, V. A. Eltekov, V. E. Yurasova, J. S. Colligon, A. S. Mosunov: *Nucl. Instrum. Methods B* **115**, 544 (1996)
455. T. T. Nuver: *Proefschrift*, Groningen (2002)
456. M. H. Shapiro, T. A. Tombrello: *Nucl. Instrum. Methods B* **194**, 425 (2002)
457. V. I. Bachurin, E. S. Kharlamochkin, M. V. Kuvakin, V. E. Yurasova: In *Proc. 15th ICPIG*, Vol.1 (1981) 465
458. T. Michely, Ch. Teichert: *Phys. Rev. B* **50**, 11156 (2003)
459. A. Friedrich, H. M. Urbassek: *Surf. Sci.* **547**, 315 (2003)
460. Z.-Y. Ye, Q.-Y. Zhang: *Chin. Phys.* **10**, 329 (2001)
461. H. F. Lu, C. Zhang, Q. Y. Zhang: *Nucl. Instrum. Methods B* **206**, 22 (2003)
462. M. Hou: In *Proc. Symp. on Sputtering*, ed. by P. Varga, G. Betz, F. P. Viehböck, (Techn. Univ., Vienna 1980) pp. 101
463. M. M. Jakas, D. E. Harrison, Jr.: *Phys. Rev. Lett.* **55**, 1782 (1985)
464. M. A. Karolewski: *Nucl. Instrum. Methods B* **194**, 26 (2002)
465. T. Neidhart, Z. Toth, M. Hochhold, M. Schmid, P. Varga: *Nucl. Instrum. Methods B* **90**, 496 (1994)
466. N. Seifert, W. Husinsky, G. Betz, Q. Yan, N. H. Tolk: *Phys. Rev. B* **51**, 12202 (1995)
467. E. Gauthier, W. Eckstein, J. László, J. Roth: *J. Nucl. Mater.* **176& 177**, 438 (1990)
468. J. P. Biersack: *Fusion Technol.* **6**, 475 (1984)
469. S. S. Elovikov, E. Yu. Zykova, A. A. Promokhov, V. E. Yurasova: In *Non-destructive Testing and Computer Simulations in Science and Engineering*, Vol. 3687, A. I. Melker (ed.), (SPIE - The International Society for Optical Engineering)
470. A. A. Promokhov, A. S. Mosunov, S. S. Elovikov, V. E. Yurasova: *Vacuum* **56**, 247 (2000)
471. S. S. Elovikov, R. S. Gvosdover, E. Yu. Zykova, A. S. Mosunov, V. E. Yurasova: *Poverknost Rent. Synk. Netr.* **12**, 34 (2000)
472. S. S. Elovikov, E. Yu. Zykova, A. S. Mosunov, A. A. Semenov, I. I. Shkarban, V. E. Yurasova: *Bull. Russian Acad. Sci.* **66**, 608 (2002)
473. J. Bohdansky, J. Roth, F. Brossa: *J. Nucl. Mater.* **85 & 86**, 1145 (1979)
474. T. Nenadović, B. Perrailon, Z. Bogdanov, Z. Djordjević, M. Milić: *Nucl. Instrum. Methods B* **48**, 538 (1990)
475. G. Hayderer, S. Cernusca, V. Hoffmann, D. Niemann, N. Stolterfoht, M. Schmid, P. Varga, H. P. Winter, F. Aumayr: *Nucl. Instrum. Methods B* **182**, 143 (2001)
476. O. S. Oen, M. T. Robinson: *J. Nucl. Mater.* **76 & 77**, 370 (1978)
477. M. Kaminsky, R. Nielsen, P. Zschack: *J. Vac. Sci. Technol.* **20**, 1304 (1982)
478. J. A. Borders, G. C. Nelson: *J. Nucl. Mater.* **103 & 104**, 369 (1981)
479. K. Inoue, Y. Taga: *Surf. Sci.* **140**, 491 (1984)
480. B. Fritzsch, V. N. Samoylov, A. Zehe: *Solid State Commun.* **60**, 553 (1986)
481. H. von Seefeld, H. Schmidl, R. Behrisch, B. M. U. Scherzer: *J. Nucl. Mater.* **63**, 215 (1976)

482. B. Emmoth, M. Braun, T. Fried, J. Winter, F. Waelbroeck, P. Wienhold: *J. Nucl. Mater.* **103 & 104**, 393 (1981)
483. R. P. Schorn, E. Hintz, B. Baretzky, J. Bohdansky, W. Eckstein, J. Roth, E. Taglauer: *J. Nucl. Mater.* **162-164**, 924 (1989)
484. B. Baretzky, W. Eckstein, R. P. Schorn: *J. Nucl. Mater.* **224**, 50 (1995)
485. I. P. Soshnikov, Yu. A. Kudriavtsev, A. V. Lunev, N. A. Bert: *Nucl. Instrum. Methods B* **127-128**, 115 (1997)
486. J. P. Allain, D. N. Ruzic, M. R. Hendricks: *J. Nucl. Mater.* **290-293**, 33 (2001)
487. R. Bastasz, W. Eckstein: *J. Nucl. Mater.* **290-293**, 19 (2001)
488. W. Möller, W. Eckstein: IPP-Report 9/64, Garching (1988)
489. M. Taniguchi, K. Sato, K. Ezato, K. Yokoyama, M. Dairaku, M. Akiba: *J. Nucl. Mater.* **313-316**, 360 (2003)
490. O. F. Goktepe, T. D. Andreadis, M. L. Roush: University of Maryland, College Park (1979)
491. J. E. Griffith, R. A. Weller, L. E. Seiberling, T. A. Tombrello: *Radiat. Eff.* **51**, 223 (1980)

**Table 1.** Fitting values  $\lambda, q, \mu$  for the energy dependence of the sputtering yield  $Y(E_0)$  at normal incidence in (2). In addition, the threshold energy,  $E_{th}$ , the reduced energy,  $\varepsilon$ , the surface binding energy,  $E_{sb}$ , and  $E_{sb}/\gamma$  are given

ion	target	$\lambda$	q	$\mu$	$E_{th}$ (eV)	$\varepsilon$	$E_{sb}$ (eV)	$E_{sb}/\gamma$
H	Li	0.9540	0.0833	1.4705	5.6499	1.85375e+2	1.67	3.76
D	Li	1.4358	0.1321	1.2091	4.6359	2.08692e+2	1.67	2.40
T	Li	1.8839	0.1629	0.9741	4.8558	2.32243e+2	1.67	1.98
$^4$ He	Li	1.9370	0.3617	1.2501	6.5037	5.56715e+2	1.67	1.80
Li	Li	8.2237	0.5159	1.7546	5.5264	1.12841e+3	1.67	1.67
H	Be	0.8007	0.0564	1.5147	14.340	2.56510e+2	3.38	9.32
D	Be	1.7575	0.1044	1.9906	9.5059	2.82110e+2	3.38	5.67
T	Be	2.0794	0.1379	1.5660	9.4345	3.07966e+2	3.38	4.49
$^3$ He	Be	0.7725	0.3310	1.6036	12.8963	6.65344e+2	3.38	4.49
$^4$ He	Be	1.4745	0.3193	1.6989	12.3288	7.19545e+2	3.38	3.97
Be	Be	2.0334	0.8241	1.3437	16.9689	2.20796e+3	3.38	3.38
N	Be	5.2833	0.9334	2.5368	16.5425	5.46566e+3	3.38	3.55
O	Be	1.2209	1.2024	1.6881	22.6648	6.97104e+3	3.38	3.67
Ne	Be	2.5474	1.8309	1.9400	22.7750	1.06588e+4	3.38	3.96
Ar	Be	0.8082	3.2032	1.5058	37.1816	3.68450e+4	3.38	5.63
Kr	Be	0.3844	5.3588	1.9600	61.452	1.67028e+5	3.38	9.64
Xe	Be	0.4779	8.1740	1.8350	86.942	4.23834e+5	3.38	14.06
H	B	0.8989	0.0329	1.3689	28.5753	3.32864e+2	5.73	18.33
D	B	1.0068	0.0686	1.4105	20.255	3.61025e+2	5.73	10.84
T	B	2.0179	0.1107	1.3317	18.2282	3.89468e+2	5.73	8.39
$^3$ He	B	1.2373	0.2013	1.5394	20.829	8.35205e+2	5.73	8.39
$^4$ He	B	0.9493	0.2551	0.9796	23.533	8.94388e+2	5.73	7.27
B	B	3.1629	0.9355	1.5939	26.7860	3.71634e+3	5.73	5.73
O	B	0.8342	1.0128	1.1909	44.783	8.02325e+3	5.73	5.95
Ne	B	0.8654	1.3272	1.1180	47.0718	1.21179e+4	5.73	6.31
H	C	1.3533	0.0241	1.4103	38.630	4.14659e+2	7.41	25.89
D	C	1.2848	0.0539	1.1977	27.770	4.46507e+2	7.41	15.08
T	C	1.9050	0.0718	1.1512	23.617	4.78673e+2	7.41	11.54
$^3$ He	C	0.7341	0.2058	1.1956	29.883	1.02061e+3	7.41	11.54
$^4$ He	C	4.5910	0.1951	1.7852	19.124	1.08716e+3	7.41	9.88
C	C	13.9666	0.7015	2.0947	21.4457	5.68684e+3	7.41	7.41
N	C	5.4288	0.7481	1.7701	34.9372	7.37899e+3	7.41	7.45
O	C	9.6110	1.0171	2.0102	34.1293	9.29758e+3	7.41	7.56
Ne	C	2.5015	1.1912	1.6551	46.6904	1.39308e+4	7.41	7.92
Ar	C	1.2622	2.4576	1.3952	68.8460	4.57989e+4	7.41	10.42
Kr	C	1.3628	3.4372	2.2366	88.2918	1.99609e+5	7.41	16.90
Xe	C	0.4408	4.3004	1.7734	145.4236	4.98349e+5	7.41	24.13
Mg	Mg	0.2574	5.3651	1.6993	8.5706	2.86599e+4	1.54	1.54
Ar	Mg	0.2522	7.5660	1.8294	10.7751	6.10685e+4	1.54	1.64
Kr	Mg	0.2655	13.1219	2.1498	13.1728	2.37254e+5	1.54	2.21

**Table 2.** Fitting values  $\lambda, q, \mu$  for the energy dependence of the sputtering yield  $Y(E_0)$  at normal incidence in (2). In addition, the threshold energy,  $E_{th}$ , the reduced energy,  $\varepsilon$ , the surface binding energy,  $E_{sb}$ , and  $E_{sb}/\gamma$  are given

ion	target	$\lambda$	q	$\mu$	$E_{th}$ (eV)	$\varepsilon$	$E_{sb}$ (eV)	$E_{sb}/\gamma$
H	Al	0.4138	0.0469	1.6177	30.2224	1.05916e+3	3.36	24.15
D	Al	0.2912	0.1076	1.3913	18.4706	1.09700e+3	3.36	13.02
T	Al	0.3384	0.1628	1.3777	14.067	1.13522e+3	3.36	9.28
$^3\text{He}$	Al	0.2670	0.4034	2.2720	14.217	1.37037e+3	3.36	9.28
$^4\text{He}$	Al	0.2072	0.3889	1.3234	14.0994	2.44780e+3	3.36	7.47
N	Al	0.3513	2.0764	1.7955	13.6115	1.28804e+4	3.36	3.73
Ne	Al	0.3813	3.0949	1.7394	16.904	2.22732e+4	3.36	3.43
Al	Al	0.6008	3.9180	1.9550	16.0955	3.45451e+4	3.36	3.36
Ar	Al	0.4713	4.7928	2.0810	21.5497	6.28194e+4	3.36	3.49
Kr	Al	0.3085	8.4547	1.9648	28.6055	2.39411e+5	3.36	4.56
Xe	Al	0.2200	11.9561	1.9797	37.3796	5.63459e+5	3.36	5.94
H	Si	0.4819	0.0276	0.9951	49.792	1.16317e+3	4.70	35.07
D	Si	0.5326	0.0569	1.6537	24.543	1.20314e+3	4.70	18.85
T	Si	0.4112	0.0816	0.9325	21.298	1.24352e+3	4.70	13.41
$^3\text{He}$	Si	0.3065	0.1823	1.3953	21.405	2.59209e+3	4.70	13.41
$^4\text{He}$	Si	0.2524	0.2319	1.4732	18.899	2.67374e+3	4.70	10.77
N	Si	0.4888	1.4367	1.7970	16.6977	1.38909e+4	4.70	5.29
Ne	Si	0.2995	2.0693	1.5152	23.412	2.39034e+4	4.70	4.83
Si	Si	0.6726	2.6951	1.7584	20.035	4.10661e+4	4.70	4.70
Ar	Si	0.2770	3.2299	1.5284	32.8380	6.67979e+4	4.70	4.85
Kr	Si	0.3000	6.3659	1.7639	39.5819	2.52242e+5	4.70	6.25
Xe	Si	0.3076	8.4521	1.6342	45.1518	5.91044e+5	4.70	8.09
Ca	Ca	0.0968	6.6980	1.5276	10.679	9.43891e+4	1.83	1.83
Sc	Sc	0.3163	5.8720	1.7448	16.804	1.05770e+5	3.49	3.49
H	Ti	0.6214	0.0207	0.9427	77.1765	2.05415e+3	4.89	60.45
D	Ti	0.3491	0.0565	1.3957	39.259	2.09615e+3	4.89	31.63
T	Ti	0.3469	0.0887	1.1426	29.3389	2.13856e+3	4.89	21.91
$^3\text{He}$	Ti	0.3632	0.1456	1.1171	31.303	4.41677e+3	4.89	21.91
$^4\text{He}$	Ti	0.2053	0.2036	1.6310	24.5359	4.50177e+3	4.89	17.19
N	Ti	0.2321	1.8168	2.0297	16.5403	2.07557e+4	4.89	6.98
Ne	Ti	0.2317	2.6253	1.8113	19.564	3.39688e+4	4.89	5.86
Ar	Ti	0.3152	4.8957	1.8291	25.019	8.56428e+4	4.89	4.93
Ti	Ti	0.3217	4.9010	1.6929	24.356	1.17898e+5	4.89	4.89
Kr	Ti	0.4445	8.4878	2.2691	30.9784	2.89844e+5	4.89	5.28
Xe	Ti	0.2234	12.9890	1.8943	39.6382	6.42730e+5	4.89	6.24
H	V	0.7528	0.0234	1.7703	79.7078	2.17329e+3	5.33	69.90
D	V	0.6688	0.0606	1.6983	42.766	2.21513e+3	5.33	36.49
T	V	0.1885	0.0630	1.4064	33.343	2.25738e+3	5.33	25.22
$^3\text{He}$	V	0.5942	0.1590	1.2342	34.402	4.65839e+3	5.33	25.22
$^4\text{He}$	V	0.1705	0.2146	1.4230	29.0921	4.74299e+3	5.33	19.74
N	V	0.2801	1.9363	2.1837	18.4653	2.16246e+4	5.33	7.88
Ne	V	0.1444	3.3295	1.8660	23.1560	3.52128e+4	5.33	6.56
Ar	V	0.2139	5.2774	1.9274	29.797	8.78018e+4	5.33	5.41
V	V	0.3015	6.7315	1.6807	25.9840	1.30783e+5	5.33	5.33
Kr	V	0.3500	9.4796	2.2023	34.6199	2.93342e+5	5.33	5.67
Xe	V	0.2601	13.9197	2.0005	41.6428	6.45981e+5	5.33	6.62

**Table 3.** Fitting values  $\lambda, q, \mu$  for the energy dependence of the sputtering yield  $Y(E_0)$  at normal incidence in (2). In addition, the threshold energy,  $E_{th}$ , the reduced energy,  $\varepsilon$ , the surface binding energy,  $E_{sb}$ , and  $E_{sb}/\gamma$  are given

ion	target	$\lambda$	$q$	$\mu$	$E_{th}$ (eV)	$\varepsilon$	$E_{sb}$ (eV)	$E_{sb}/\gamma$
H	Cr	0.3673	0.0405	1.4998	65.8795	2.29573e+3	4.12	55.11
D	Cr	0.2899	0.1084	1.7152	35.024	2.33904e+3	4.12	28.75
T	Cr	0.2663	0.1776	1.8134	25.074	2.38278e+3	4.12	19.85
$^3\text{He}$	Cr	0.1869	0.2985	1.3060	28.803	4.91344e+3	4.12	19.85
$^4\text{He}$	Cr	0.3120	0.3508	1.8564	21.611	5.00096e+3	4.12	15.53
Ne	Cr	0.2550	5.8847	2.2414	18.550	3.68638e+4	4.12	5.11
Ar	Cr	0.3285	7.6222	2.3546	22.3536	9.15022e+4	4.12	4.19
Cr	Cr	0.3472	9.6358	2.1501	21.4357	1.44437e+5	4.12	4.12
Kr	Cr	0.3681	13.4719	2.4061	26.2860	3.04062e+5	4.12	4.36
Xe	Cr	0.0642	20.0590	1.7830	35.7764	6.67613e+5	4.12	5.07
H	Mn	0.5704	0.0774	2.5497	43.501	2.41819e+3	2.92	41.18
D	Mn	0.3203	0.2007	1.7627	25.5675	2.46141e+3	2.92	21.44
T	Mn	0.2140	0.3193	1.8198	18.5434	2.50506e+3	2.92	14.78
$^3\text{He}$	Mn	0.1201	0.5548	1.9758	19.7689	5.16191e+3	2.92	14.78
$^4\text{He}$	Mn	0.2061	0.6680	1.8364	16.4824	5.24919e+3	2.92	11.54
Ar	Mn	0.1275	14.2168	1.9572	17.9964	9.37995e+4	2.92	2.99
Kr	Mn	0.1164	24.5351	1.8377	21.0972	3.08095e+5	2.92	3.05
Xe	Mn	0.0978	32.8089	1.7796	23.9217	6.72160e+5	2.92	3.51
H	Fe	0.8696	0.0339	1.8635	67.2578	2.54382e+3	4.34	62.19
D	Fe	0.2743	0.0919	1.3489	40.8547	2.58856e+3	4.34	32.36
T	Fe	0.3131	0.1545	1.3250	28.9747	2.67374e+3	4.34	22.29
$^3\text{He}$	Fe	0.2630	0.2780	1.5947	29.6538	5.42342e+3	4.34	22.29
$^4\text{He}$	Fe	0.1836	0.3347	1.8574	24.2208	5.51371e+3	4.34	17.40
N	Fe	0.2590	2.7806	2.3278	16.6110	2.46747e+4	4.34	6.77
Ne	Fe	0.2608	4.4877	2.3857	18.7098	3.98491e+4	4.34	5.56
Ar	Fe	0.3517	7.5705	2.3822	22.5719	9.75914e+4	4.34	4.46
Fe	Fe	0.3409	11.0481	1.8048	13.7676	1.74096e+5	4.34	4.34
Kr	Fe	0.3296	13.8062	2.2461	27.8579	3.19107e+5	4.34	4.52
Xe	Fe	0.2492	19.8866	2.1631	32.2100	6.94435e+5	4.34	5.18
H	Co	0.4456	0.0396	1.7711	77.3535	2.66922e+3	4.43	66.85
D	Co	0.2832	0.1085	1.6859	42.1606	2.71375e+3	4.43	34.72
T	Co	0.3065	0.1689	1.4653	30.5090	2.75873e+3	4.43	23.88
$^3\text{He}$	Co	0.1762	0.3000	1.4515	33.4129	5.67719e+3	4.43	23.88
$^4\text{He}$	Co	0.1652	0.3649	1.8250	25.9871	5.76700e+3	4.43	18.61
Ne	Co	0.0828	5.1602	2.2943	20.8124	4.11463e+4	4.43	5.83
Ar	Co	0.2709	8.4019	2.3291	23.8571	9.98420e+4	4.43	4.60
Co	Co	0.3615	11.6517	2.3889	22.5211	1.90123e+5	4.43	4.43
Kr	Co	0.3021	14.5284	2.2207	28.5342	3.22806e+5	4.43	4.57
Xe	Co	0.2561	20.8948	2.1435	32.0848	6.98061e+5	4.43	5.18

**Table 4.** Fitting values  $\lambda, q, \mu$  for the energy dependence of the sputtering yield  $Y(E_0)$  at normal incidence in (2). In addition, the threshold energy,  $E_{th}$ , the reduced energy,  $\varepsilon$ , the surface binding energy,  $E_{sb}$ , and  $E_{sb}/\gamma$  are given

ion	target	$\lambda$	$q$	$\mu$	$E_{th}$ (eV)	$\varepsilon$	$E_{sb}$ (eV)	$E_{sb}/\gamma$
H	Ni	0.6039	0.0334	2.0121	72.9013	2.79866e+3	4.46	67.06
D	Ni	0.2649	0.0904	1.6534	42.0439	2.84552e+3	4.46	34.84
T	Ni	0.3185	0.1734	1.3881	30.7743	2.89285e+3	4.46	23.96
$^3\text{He}$	Ni	0.1421	0.3183	1.3582	33.9111	5.94964e+3	4.46	23.96
$^4\text{He}$	Ni	0.2024	0.3704	1.9128	25.3764	6.04409e+3	4.46	18.67
N	Ni	0.1941	2.9510	2.0380	18.4448	2.67793e+4	4.46	7.17
O	Ni	0.2107	3.4027	2.2297	18.3954	3.18555e+4	4.46	6.63
Ne	Ni	0.2478	4.5041	2.4046	18.7208	4.30554e+4	4.46	5.86
Ar	Ni	0.3068	7.9565	2.3102	23.3069	1.04416e+5	4.46	4.63
Ni	Ni	6.5700	11.8130	2.7875	11.7462	2.06960e+5	4.46	4.46
Kr	Ni	1.9541	13.5535	2.5909	18.1503	3.37355e+5	4.46	4.60
Xe	Ni	1.3490	20.8734	2.3649	21.2671	7.29221e+5	4.46	5.22
H	Cu	0.5015	0.0566	1.9914	61.7219	2.92563e+3	3.52	57.14
D	Cu	0.1989	0.1374	1.6642	35.5599	2.97095e+3	3.52	29.61
T	Cu	0.2904	0.2899	1.9648	24.2892	3.01673e+3	3.52	20.32
$^3\text{He}$	Cu	0.0750	0.7126	1.0303	28.4759	6.20088e+3	3.52	20.32
$^4\text{He}$	Cu	0.1639	0.6376	1.9937	21.5232	6.29218e+3	3.52	15.79
N	Cu	0.1595	3.4102	2.1567	15.6557	2.75601e+4	3.52	5.95
Ne	Cu	0.2009	5.0380	2.4014	15.5801	4.40689e+4	3.52	4.81
Ar	Cu	1.9417	14.8712	2.3907	12.9166	1.05525e+5	3.52	3.71
Cu	Cu	2.6044	14.5469	2.5577	10.7777	2.24619e+5	3.52	3.52
Kr	Cu	0.3072	16.6183	2.3257	21.3482	3.35590e+5	3.52	3.59
Xe	Cu	0.2781	24.4581	2.2393	23.6265	7.18907e+5	3.52	4.00
Ar	Zn	0.5168	35.7476	2.0349	7.6061	1.08696e+5	1.35	1.43
Zn	Zn	0.3077	30.3139	2.1318	6.5831	2.43109e+5	1.35	1.35
Kr	Zn	0.4951	34.1270	2.4413	6.9161	3.43442e+5	1.35	1.37
D	Ga	0.2292	0.1113	1.7674	29.5602	3.23166e+3	2.82	25.88
T	Ga	0.2369	0.1706	1.4510	21.3773	3.27716e+3	2.82	17.72
Ga	Ga	0.1105	16.5357	1.4877	16.8456	2.62439e+5	2.82	2.82
H	Ge	0.3938	0.0245	1.1582	88.3539	3.31932e+3	3.88	71.67
D	Ge	0.2327	0.0609	1.4101	44.6555	3.36441e+3	3.88	37.00
T	Ge	0.2998	0.0815	1.3007	30.8678	3.40997e+3	3.88	25.30
$^3\text{He}$	Ge	0.3206	0.2127	1.3195	32.3887	6.99838e+3	3.88	25.30
$^4\text{He}$	Ge	0.1446	0.2673	1.5062	26.2298	7.08909e+3	3.88	19.60
Ne	Ge	0.1485	3.5700	2.0064	14.1111	4.82268e+4	3.88	5.70
Ar	Ge	0.2357	6.2991	2.3935	15.5675	1.12992e+5	3.88	4.24
Ge	Ge	0.3535	11.8041	2.3480	17.2208	2.82619e+5	3.88	3.88
Kr	Ge	0.1769	12.8791	2.0150	23.9964	3.49421e+5	3.88	3.90
Xe	Ge	0.0838	18.2164	1.7290	28.5395	7.36368e+5	3.88	4.23
Ar	Se	0.1608	11.1577	2.2076	9.0783	1.18037e+5	2.14	2.40

**Table 5.** Fitting values  $\lambda, q, \mu$  for the energy dependence of the sputtering yield  $Y(E_0)$  at normal incidence in (2). In addition, the threshold energy,  $E_{th}$ , the reduced energy,  $\varepsilon$ , the surface binding energy,  $E_{sb}$ , and  $E_{sb}/\gamma$  are given

ion	target	$\lambda$	$q$	$\mu$	$E_{th}$ (eV)	$\varepsilon$	$E_{sb}$ (eV)	$E_{sb}/\gamma$
H	Zr	0.4518	0.0103	1.0406	182.7468	4.42211e+3	6.33	146.11
D	Zr	0.6485	0.0306	1.9944	80.1168	4.47714e+3	6.33	75.02
T	Zr	0.7209	0.0542	1.6586	54.9858	4.52564e+3	6.33	51.02
$^3\text{He}$	Zr	0.5744	0.1184	0.7719	66.7939	9.25829e+3	6.33	51.02
$^4\text{He}$	Zr	0.2633	0.1371	0.9538	53.1725	9.35457e+3	6.33	39.32
Ne	Zr	0.1101	2.5721	1.6851	23.4583	6.06862e+4	6.33	10.67
Ar	Zr	0.1601	5.0472	2.0223	24.0260	1.37106e+5	6.33	7.47
Kr	Zr	0.2163	9.2238	2.1484	33.5793	4.03685e+5	6.33	6.34
Zr	Zr	0.2699	10.8645	1.9248	29.9208	4.75691e+5	6.33	6.33
Xe	Zr	0.2943	12.8431	2.2275	37.8291	8.25496e+5	6.33	6.54
H	Nb	0.6259	0.0112	1.3327	210.8697	4.57351e+3	7.59	178.37
D	Nb	0.3858	0.0328	1.5253	106.8707	4.62220e+3	7.59	91.55
T	Nb	0.6475	0.0593	1.8826	68.8233	4.67139e+3	7.59	62.23
$^3\text{He}$	Nb	0.3872	0.1233	1.1568	79.8178	9.55327e+3	7.59	62.23
$^4\text{He}$	Nb	0.2626	0.1418	1.3089	62.2687	9.65087e+3	7.59	47.95
Ne	Nb	0.1307	2.4654	1.8441	28.0914	6.23657e+4	7.59	12.94
Ar	Nb	0.1913	5.3954	2.3033	28.6038	1.40484e+5	7.59	9.02
Kr	Nb	0.1964	9.5591	1.9919	42.3615	4.11932e+5	7.59	7.61
Nb	Nb	0.2284	10.4521	1.8885	37.3983	5.03904e+5	7.59	7.59
Xe	Nb	0.1998	13.4775	2.0015	49.0697	8.40173e+5	7.59	7.82
H	Mo	0.5124	0.0114	1.1469	201.4886	4.71832e+3	6.83	165.63
D	Mo	0.3241	0.0326	1.5410	97.7738	4.76698e+3	6.83	84.95
T	Mo	0.5078	0.0661	1.5955	67.1475	4.81614e+3	6.83	57.71
$^3\text{He}$	Mo	0.3541	0.1373	0.9926	75.3995	9.84614e+3	6.83	57.71
$^4\text{He}$	Mo	0.1537	0.1563	0.9989	59.3088	9.94365e+3	6.83	44.44
N	Mo	0.1157	1.7900	1.8032	28.2561	4.10879e+4	6.83	15.36
O	Mo	0.1762	2.1069	2.4821	23.9169	4.83320e+4	6.83	13.94
Ne	Mo	0.2205	2.8995	2.6514	23.6170	6.38956e+4	6.83	11.89
Ar	Mo	0.1339	6.3606	1.9562	28.2149	1.43274e+5	6.83	8.23
Kr	Mo	0.1412	11.9419	1.6911	38.6337	4.17411e+5	6.83	6.86
Mo	Mo	0.3580	12.2715	2.1844	31.4737	5.33049e+5	6.83	6.83
Xe	Mo	0.2401	32.5719	1.6694	47.4030	8.47848e+5	6.83	7.00
H	Ru	0.3912	0.0129	1.6744	194.6779	5.01173e+3	6.69	170.73
D	Ru	0.2887	0.0428	1.9612	97.5326	5.06083e+3	6.69	87.48
T	Ru	0.3922	0.0882	1.7061	68.6863	5.11042e+3	6.69	59.37
$^3\text{He}$	Ru	0.1990	0.1998	1.7831	72.7607	1.04414e+4	6.69	59.37
$^4\text{He}$	Ru	0.1617	0.2364	1.7290	57.4279	1.05397e+4	6.69	45.67
Ne	Ru	0.1389	3.1882	2.1092	26.1200	6.70985e+4	6.69	12.06
Ar	Ru	0.1872	6.8381	2.2039	27.4779	1.49334e+5	6.69	8.24
Kr	Ru	0.2419	13.1833	2.3683	35.6820	4.30460e+5	6.69	6.75
Xe	Ru	0.1828	18.9085	2.0945	43.4787	6.68372e+5	6.69	6.81

**Table 6.** Fitting values  $\lambda, q, \mu$  for the energy dependence of the sputtering yield  $Y(E_0)$  at normal incidence in (2). In addition, the threshold energy,  $E_{th}$ , the reduced energy,  $\varepsilon$ , the surface binding energy,  $E_{sb}$ , and  $E_{sb}/\gamma$  are given

ion	target	$\lambda$	$q$	$\mu$	$E_{th}$ (eV)	$\varepsilon$	$E_{sb}$ (eV)	$E_{sb}/\gamma$	
H	Rh	0.4883	0.0174	1.5635	173.8870	5.16041e+3	5.78	150.14	
	D	0.3593	0.0511	1.8715	85.5661	5.21007e+3	5.78	76.90	
	T	0.3510	0.1026	1.4508	61.9159	5.26022e+3	5.78	52.17	
	$^3$ He	0.1514	0.2049	1.5288	64.9824	1.07444e+4	5.78	52.17	
	$^4$ He	0.1038	0.2212	2.0736	49.0159	1.08438e+4	5.78	40.12	
	Ne	0.1310	3.7410	2.0601	23.2979	6.87945e+4	5.78	10.54	
	Ar	0.1519	7.8385	2.1666	24.8932	1.52692e+5	5.78	7.17	
	Kr	0.1467	15.4269	2.1139	33.6867	4.38429e+5	5.78	5.84	
	Xe	0.2480	21.6042	2.3157	34.9750	8.82222e+5	5.78	5.87	
	Pd	0.3805	0.0307	1.5679	119.3501	5.30935e+3	3.91	104.94	
D	Pd	0.1879	0.0875	1.7784	61.2249	5.35878e+3	3.91	53.72	
	T	0.2011	0.1654	1.5686	42.9267	5.40870e+3	3.91	36.42	
	$^3$ He	0.1429	0.3249	1.7971	44.0328	1.10446e+4	3.91	36.42	
	$^4$ He	0.1312	0.3839	1.8906	34.3297	1.11435e+4	3.91	27.99	
	Ne	0.1449	5.3982	2.3415	15.9494	7.03218e+4	3.91	7.29	
	Ar	0.1147	11.4507	2.1538	18.1505	1.55391e+5	3.91	4.93	
	Kr	0.1636	20.9141	2.3051	22.0273	4.43321e+5	3.91	3.97	
	Pd	0.2531	26.4367	2.3402	19.4305	6.59103e+5	3.91	3.91	
	Xe	0.1879	30.3470	2.1409	23.6613	8.88306e+5	3.91	3.95	
	H	Ag	0.4315	0.0568	1.9568	88.4899	5.46029e+3	2.97	80.79
T	D	Ag	0.1118	0.1421	1.7562	48.1788	5.51044e+3	2.97	41.35
	T	Ag	0.2015	0.2513	1.5178	33.7714	5.56109e+3	2.97	28.03
	$^3$ He	Ag	0.1344	0.4479	1.6924	34.1484	1.13527e+4	2.97	28.03
	$^4$ He	Ag	0.1136	0.5817	1.9719	26.4533	1.14531e+4	2.97	21.54
	N	Ag	0.1020	3.5600	2.2635	13.0433	4.66664e+4	2.97	7.30
	O	Ag	0.0839	4.5394	2.0010	13.4494	5.47544e+4	2.97	6.60
	O(Mol)	Ag	0.1711	5.6305	2.5908	13.4489	5.47544e+4	2.97	6.60
	Ne	Ag	0.0995	5.5124	2.7313	11.8829	7.20736e+4	2.97	5.59
	Ar	Ag	0.1650	18.8203	1.9424	13.9098	1.58921e+5	2.97	3.76
	Ar(KrC)	Ag	0.1178	13.6070	2.1743	13.5876	1.58921e+5	2.97	3.76
Ar	Ar(Mol)	Ag	0.2320	16.4201	2.4019	13.6547	1.58921e+5	2.97	3.76
	Ar(Mola)	Ag	0.1673	12.4010	2.3562	12.0571	1.58921e+5	2.97	3.76
	Ar(ZBL)	Ag	0.2100	13.9829	2.4962	14.0709	1.58921e+5	2.97	3.76
	Kr	Ag	0.1801	30.5548	2.4713	16.2072	4.51993e+5	2.97	3.02
	Ag	Ag	0.1687	36.6162	2.4091	15.2340	6.93021e+5	2.97	2.97
	Xe	Ag	0.2236	35.8737	2.2844	17.5897	9.03858e+5	2.97	3.00
	Ar	Cd	0.1235	25.3480	2.2793	5.4146	1.61276e+5	1.16	1.50
	Kr	Cd	0.1779	46.8071	2.6365	6.1572	4.55218e+5	1.16	1.19
	Cd	Cd	0.1861	66.4019	2.2778	5.7795	7.27916e+5	1.16	1.16
	H	In	0.4760	0.0408	1.7747	77.6070	5.76339e+3	2.49	72.02
D	D	In	0.1803	0.1049	1.4528	42.4095	5.81315e+3	2.49	36.82
	T	In	0.1745	0.1751	1.3489	29.0900	5.86340e+3	2.49	24.93
	Ne	In	0.0348	5.9422	1.3768	12.1811	7.51927e+4	2.49	4.90
	Kr	In	0.0996	23.4774	2.0666	13.4197	4.62260e+5	2.49	2.55
	In	In	0.1224	30.7665	1.9472	13.0986	7.63793e+5	2.49	2.49

**Table 7.** Fitting values  $\lambda, q, \mu$  for the energy dependence of the sputtering yield  $Y(E_0)$  at normal incidence in (2). In addition, the threshold energy,  $E_{th}$ , the reduced energy,  $\varepsilon$ , the surface binding energy,  $E_{sb}$ , and  $E_{sb}/\gamma$  are given

ion	target	$\lambda$	$q$	$\mu$	$E_{th}$ (eV)	$\varepsilon$	$E_{sb}$ (eV)	$E_{sb}/\gamma$
H	Sn	0.4702	0.0352	1.6669	104.1095	5.91631e+3	3.12	93.23
D	Sn	0.1829	0.0715	1.6497	53.8847	5.96574e+3	3.12	47.63
T	Sn	0.2917	0.1556	1.5871	36.4853	6.01566e+3	3.12	32.23
$^3$ He	Sn	0.1558	0.3227	1.5754	38.8436	1.22714e+4	3.12	32.23
$^4$ He	Sn	0.1102	0.3244	1.8523	29.6119	1.23702e+4	3.12	24.73
Ne	Sn	0.1152	4.5687	2.2682	11.5544	7.67367e+4	3.12	6.28
Ar	Sn	0.0746	9.2172	2.1869	11.9822	1.67157e+5	3.12	4.14
Kr	Sn	0.3289	17.5340	2.6550	13.6369	4.66941e+5	3.12	3.22
Sn	Sn	0.1494	27.3600	2.0140	15.7681	8.00660e+5	3.12	3.12
Xe	Sn	0.9767	25.3092	3.2145	14.2636	9.22556e+5	3.12	3.13
Kr	Sb	0.1171	22.1319	2.0888	13.5706	4.73059e+5	2.72	2.82
Ar	Te	0.0993	12.8971	2.2723	7.4376	1.72282e+5	2.02	2.78
Cs	Cs	0.1310	59.8329	1.7733	4.4983	1.00007e+6	0.82	0.82
Kr	Sm	0.1279	25.7558	2.4453	9.2611	5.50683e+5	2.16	2.35
H	Tb	0.4151	0.0245	1.4450	180.8106	8.32995e+3	3.89	154.97
D	Tb	0.2514	0.0764	1.4668	92.1545	8.38203e+3	3.89	78.85
T	Tb	0.2675	0.1140	1.7383	58.8710	8.43464e+3	3.89	53.14
$^3$ He	Tb	0.1970	0.2290	1.5498	62.3825	1.71555e+4	3.89	53.14
$^4$ He	Tb	0.1613	0.3219	1.5186	48.4940	1.72593e+4	3.89	40.61
Ar	Tb	0.0825	10.8668	2.0502	14.1521	2.15976e+5	3.89	6.06
H	Tm	0.3646	0.0525	1.6677	119.3908	9.00672e+3	2.52	106.64
D	Tm	0.1931	0.1483	1.5930	61.7026	9.05971e+3	2.52	54.22
T	Tm	0.2005	0.2252	1.7487	39.5783	9.11324e+3	2.52	36.51
$^3$ He	Tm	0.1329	0.4083	1.5808	42.9760	1.85244e+4	2.52	36.51
$^4$ He	Tm	0.1182	0.5425	1.8624	32.4379	1.86300e+4	2.52	27.88
Ar	Tm	0.1010	18.0207	2.1079	9.4852	2.29744e+5	2.52	4.07
H	Hf	0.6050	0.0106	1.3803	320.9804	9.52208e+3	6.31	281.94
D	Hf	0.2980	0.0303	1.8401	157.1012	9.57512e+3	6.31	143.26
T	Hf	0.2352	0.0507	1.3451	112.2792	9.62870e+3	6.31	96.42
$^3$ He	Hf	0.2596	0.1083	1.1964	115.5387	1.95639e+4	6.31	96.42
$^4$ He	Hf	0.1695	0.1230	1.7304	84.5645	1.96695e+4	6.31	73.58
Ne	Hf	0.0698	3.0827	1.6671	28.7970	1.15397e+5	6.31	17.29
Ar	Hf	0.0841	7.2844	1.9088	23.6839	2.39690e+5	6.31	10.56
Kr	Hf	0.0969	15.8759	1.9090	27.1771	6.21788e+5	6.31	7.26
Xe	Hf	0.1218	22.7796	2.0536	32.7651	1.16579e+6	6.31	6.46
H	Ta	0.5966	0.0078	0.7141	483.1426	9.69565e+3	8.10	366.86
D	Ta	0.6251	0.0218	0.7705	225.5901	9.74893e+3	8.10	186.37
T	Ta	0.2642	0.0284	1.0425	147.2448	9.80275e+3	8.10	125.42
$^3$ He	Ta	0.5951	0.0885	2.0793	131.9549	1.99149e+4	8.10	125.42
$^4$ He	Ta	0.1193	0.0989	1.3173	116.3022	2.00210e+4	8.10	95.70
Ne	Ta	0.0675	2.7626	2.0170	36.3551	1.17263e+5	8.10	22.43
Ar	Ta	0.1468	6.2661	2.3669	28.6179	2.43215e+5	8.10	13.67
Kr	Ta	0.1074	14.2018	2.0456	34.5045	6.29462e+5	8.10	9.36
Xe	Ta	0.1175	20.2166	2.0128	42.5105	1.17814e+6	8.10	8.31
Ta	Ta	0.1583	26.6919	1.9785	41.4906	1.93615e+6	8.10	8.10

**Table 8.** Fitting values  $\lambda, q, \mu$  for the energy dependence of the sputtering yield  $Y(E_0)$  at normal incidence in (2). In addition, the threshold energy,  $E_{th}$ , the reduced energy,  $\varepsilon$ , the surface binding energy,  $E_{sb}$ , and  $E_{sb}/\gamma$  are given

ion	target	$\lambda$	q	$\mu$	$E_{th}$ (eV)	$\varepsilon$	$E_{sb}$ (eV)	$E_{sb}/\gamma$
H	W	1.0087	0.0075	1.2046	457.42	9.86986e+3	8.68	399.36
D	W	0.3583	0.0183	1.4410	228.84	9.92326e+3	8.68	202.85
T	W	0.2870	0.0419	1.5802	153.8842	9.97718e+3	8.68	136.48
$^3\text{He}$	W	0.2424	0.0884	1.2439	164.3474	2.02666e+4	8.68	136.48
$^4\text{He}$	W	0.1692	0.1151	1.7121	120.56	2.03728e+4	8.68	104.13
N	W	0.0921	1.4389	2.0225	45.3362	7.90505e+4	8.68	32.98
O	W	0.0777	1.8824	1.7536	44.2135	9.19794e+4	8.68	29.46
Ne	W	0.0828	2.5520	1.9534	38.6389	1.19107e+5	8.68	24.35
Ar	W	0.2113	5.9479	2.3857	27.0503	2.46646e+5	8.68	14.80
Kr	W	0.1747	13.6917	2.5161	34.7592	6.36677e+5	8.68	10.09
Xe	W	0.1385	20.5321	2.0952	44.8701	1.18932e+6	8.68	8.93
W	W	2.2697	18.6006	3.1273	24.9885	1.99860e+6	8.68	8.68
H	Re	0.6547	0.0089	1.5919	410.7532	1.00450e+4	8.09	376.92
D	Re	0.3445	0.0262	1.6638	214.3341	1.00987e+4	8.09	191.42
T	Re	0.2667	0.0460	1.7325	143.8798	1.01529e+4	8.09	128.78
$^3\text{He}$	Re	0.2026	0.1092	1.5099	151.8603	2.06207e+4	8.09	128.78
$^4\text{He}$	Re	0.1179	0.1189	1.6235	115.5715	2.07275e+4	8.09	98.24
Ne	Re	0.0871	3.0197	1.9011	37.8276	1.20995e+5	8.09	22.93
Ar	Re	0.0922	8.1299	2.0957	32.2292	2.50221e+5	8.09	13.91
Kr	Re	0.1159	16.1742	2.1166	35.8918	6.44513e+5	8.09	9.45
Xe	Re	0.1345	23.6228	2.1797	42.6697	1.20203e+6	8.09	8.34
H	Os	0.5133	0.0089	1.3016	458.5624	1.02204e+4	8.13	386.83
D	Os	0.2692	0.0267	1.3190	232.7884	1.02739e+4	8.13	196.42
T	Os	0.3100	0.0507	1.5438	148.1225	1.03279e+4	8.13	132.10
$^3\text{He}$	Os	0.2226	0.1111	1.6367	152.6164	2.09735e+4	8.13	132.10
$^4\text{He}$	Os	0.1207	0.1315	1.9064	115.7747	2.10799e+4	8.13	100.75
Ne	Os	0.0816	3.0236	2.1827	37.7170	1.22785e+5	8.13	23.44
Ar	Os	0.0985	7.4153	2.2543	32.1090	2.53422e+5	8.13	14.17
Kr	Os	0.1140	16.3882	2.1619	36.1888	6.50625e+5	8.13	9.57
Xe	Os	0.1751	23.5196	2.4600	40.4010	1.21043e+6	8.13	8.41
H	Ir	0.4857	0.0108	1.7106	367.3325	1.03972e+4	6.90	331.72
D	Ir	0.2445	0.0332	1.6722	188.7811	1.04510e+4	6.90	168.42
T	Ir	0.2550	0.0640	1.6312	127.4106	1.05053e+4	6.90	113.26
$^3\text{He}$	Ir	0.1693	0.1387	1.4318	134.4943	2.13313e+4	6.90	113.26
$^4\text{He}$	Ir	0.1057	0.1664	1.6693	102.6618	2.14384e+4	6.90	86.37
Ne	Ir	0.0847	3.5828	2.0777	32.7658	1.24708e+5	6.90	20.06
Ar	Ir	0.1070	8.8295	2.2049	27.7592	2.57103e+5	6.90	12.11
Kr	Ir	0.1117	19.1063	2.2947	31.0366	6.58875e+5	6.90	8.16
Xe	Ir	0.1933	27.1913	2.5754	34.0523	1.22412e+6	6.90	7.15

**Table 9.** Fitting values  $\lambda, q, \mu$  for the energy dependence of the sputtering yield  $Y(E_0)$  at normal incidence in (2). In addition, the threshold energy,  $E_{th}$ , the reduced energy,  $\varepsilon$ , the surface binding energy,  $E_{sb}$ , and  $E_{sb}/\gamma$  are given

ion	target	$\lambda$	q	$\mu$	$E_{th}$ (eV)	$\varepsilon$	$E_{sb}$ (eV)	$E_{sb}/\gamma$
H	Pt	0.4428	0.0136	1.4981	325.0317	1.05744e+4	5.86	285.91
D	Pt	0.2020	0.0395	1.5601	166.7835	1.06283e+4	5.86	145.14
T	Pt	0.2492	0.0756	1.4307	112.6259	1.06828e+4	5.86	97.59
$^3$ He	Pt	0.1998	0.1482	1.5445	113.4769	2.16890e+4	5.86	97.59
$^4$ He	Pt	0.1214	0.1802	1.8192	85.5658	2.17963e+4	5.86	74.41
O	Pt	0.0785	2.8246	2.0224	31.5095	9.78987e+4	5.86	20.91
Ne	Pt	0.0949	5.0805	2.1232	28.0853	1.26583e+5	5.86	17.24
Ar	Pt	0.1380	13.7922	2.2949	23.3808	2.60590e+5	5.86	10.38
Kr	Pt	0.1087	29.4816	1.9534	27.9365	6.66218e+5	5.86	6.97
Xe	Pt	0.0658	41.7055	1.5076	34.0986	1.23553e+6	5.86	6.09
Pt	Pt	0.2616	42.2193	2.4689	28.0416	2.25981e+6	5.86	5.86
H	Au	0.3117	0.0286	1.8415	206.4074	1.07527e+4	3.80	187.17
D	Au	0.2082	0.0843	1.2739	112.9565	1.08070e+4	3.80	95.00
T	Au	0.1680	0.1560	1.4421	74.8582	1.08618e+4	3.80	63.88
$^3$ He	Au	0.1346	0.3759	1.6028	75.1673	2.20499e+4	3.80	63.88
$^4$ He	Au	0.0928	0.3406	1.6773	57.2732	2.21579e+4	3.80	48.70
N	Au	0.0934	3.6067	2.0278	22.0847	8.55290e+4	3.80	15.32
O	Au	0.0634	4.0269	1.9029	21.3321	9.94281e+4	3.80	13.67
Ne	Au	0.0758	5.9707	1.8885	19.0757	2.18526e+5	3.80	11.27
Ar	Au	0.0906	12.0104	2.3969	15.6192	2.64318e+5	3.80	6.78
Kr	Au	0.0940	30.2381	1.7709	18.7951	6.74618e+5	3.80	4.54
Xe	Au	0.1371	47.6103	2.5053	19.7602	1.24955e+6	3.80	3.96
Au	Au	0.1126	61.2607	1.7156	21.4123	2.32799e+6	3.80	3.80
Kr	Hg	0.0964	14.1592	2.1495	24.7454	6.81273e+5	6.36	7.65
Kr	Tl	0.0707	37.5934	2.3358	8.2027	6.87823e+5	1.88	2.28
He	Pb	0.0686	0.4081	1.6658	31.7654	2.32414e+4	2.03	27.31
Ne	Pb	0.0569	6.7337	2.1626	9.6887	1.34122e+5	2.03	6.27
Ar	Pb	0.0462	15.7003	1.9270	8.4298	2.74555e+5	2.03	3.74
Kr	Pb	0.0551	35.9566	2.0207	9.1375	6.95357e+5	2.03	2.48
Xe	Pb	0.0637	52.3584	2.0982	10.8209	1.28038e+6	2.03	2.14
Pb	Pb	0.1461	81.3238	2.1946	10.3121	2.53951e+6	2.03	2.03
Ar	Bi	0.0289	14.2020	1.5639	9.4013	2.78342e+5	2.17	4.03
Kr	Bi	0.0578	30.2017	2.0562	9.1764	7.03904e+5	2.17	2.66
$^4$ He	Th	0.1680	0.1524	1.5450	103.5217	2.61980e+4	5.93	88.99
Ne	Th	0.0592	2.9258	1.6073	30.7814	1.49508e+5	5.93	20.14
Ar	Th	0.0543	7.3739	1.6067	23.7676	3.02995e+5	5.93	11.83
Kr	Th	0.0767	16.5776	1.8831	22.9040	7.54519e+5	5.93	7.61
Xe	Th	0.1059	24.2490	1.9981	26.4766	1.37124e+6	5.93	6.42
H	U	0.5069	0.0144	1.4948	365.5917	1.31300e+4	5.42	322.05
D	U	0.1807	0.0266	1.2763	189.3173	1.31849e+4	5.42	163.18
$^4$ He	U	0.0839	0.1136	1.6784	95.3598	2.69513e+4	5.42	83.37
Ne	U	0.0449	3.0029	1.8839	28.5107	1.53434e+5	5.42	18.81
Ar	U	0.0584	7.6218	2.1314	21.6010	3.10275e+5	5.42	11.01
Kr	U	0.0592	18.0929	2.0957	22.5283	7.69792e+5	5.42	7.04
Xe	U	0.0694	26.9596	2.2075	25.9587	1.39494e+6	5.42	5.91
Rn	U	0.1709	40.4320	2.3889	30.1936	2.96732e+6	5.42	5.43
U	U	0.1932	56.2825	2.0420	26.7960	3.32167e+6	5.42	5.42

**Table 10.** Fitting values  $f, b, c$  for the angular dependence of the sputtering yield in (6). Furthermore, the values for the yield at normal incidence,  $Y(E_0, 0)$ , the binding energy,  $E_{\text{sp}}$ , for the projectiles, the value  $\theta_0^*$  (deg.), (7), and the angular position,  $\theta_{0m}$  (deg.), of the maximum yield, (8), are given

ion	target	$E_0$ (eV)	$f$	$b$	$c$	$Y(E_0, 0)$	$E_{\text{sp}}$ (eV)	$\theta_0^*$	$\theta_{0m}$
T	Li	100	7.2592	2.6907	0.8685	4.20e-2	1.00	95.71	74.53
T	Li	300	5.3765	1.5393	0.9380	4.52e-2	1.00	93.30	77.31
Li	Li	100	10.9922	5.1816	0.7382	9.48e-2	1.67	97.36	68.79
Li	Li	200	8.0198	3.3011	0.8089	1.50e-1	1.67	95.22	71.79
Li	Li	1000	4.8470	1.4003	0.8167	2.07e-1	1.67	92.34	79.36
H	Be	15	11.1512	10.4683	1.1501	2.39e-5	1.00	104.48	25.75
H	Be	17	16.2828	13.6595	0.5330	1.80e-4	1.00	103.63	23.40
H	Be	20	11.8530	9.7870	0.6069	8.03e-4	1.00	102.60	28.10
H	Be	22	9.9611	8.0685	0.6398	1.45e-3	1.00	102.04	31.29
H	Be	25	8.5822	6.5543	0.6820	2.57e-3	1.00	101.31	38.37
H	Be	30	6.2386	4.3193	0.8005	4.68e-3	1.00	100.35	48.80
H	Be	40	6.1156	3.5415	0.8961	8.46e-3	1.00	98.98	59.73
H	Be	50	5.9126	3.0661	0.9447	1.15e-2	1.00	98.05	64.11
H	Be	70	5.7275	2.5808	0.9899	1.54e-2	1.00	96.82	68.08
H	Be	100	5.3523	2.1181	1.0194	1.85e-2	1.00	95.71	70.71
H	Be	140	5.2036	1.8698	1.0226	1.98e-2	1.00	94.83	72.34
H	Be	200	4.9195	1.5975	1.0221	2.02e-2	1.00	94.04	73.90
H	Be	300	4.7651	1.4198	1.0017	1.93e-2	1.00	93.30	75.30
H	Be	500	4.5468	1.2312	0.9622	1.69e-2	1.00	92.56	77.19
H	Be	1000	4.3749	1.0536	0.8651	1.26e-2	1.00	91.81	81.10
D	Be	11	15.1382	12.5716	0.5871	2.61e-5	1.00	106.78	27.74
D	Be	12	12.2769	9.7520	0.4890	9.29e-5	1.00	106.10	28.24
D	Be	13	11.8349	9.1246	0.5030	2.32e-4	1.00	105.50	32.16
D	Be	14	11.1728	8.4156	0.5234	4.65e-4	1.00	104.96	35.47
D	Be	15	10.3229	7.5816	0.5573	8.10e-4	1.00	104.48	39.31
D	Be	17	9.3601	6.5239	0.6180	1.73e-3	1.00	103.63	45.94
D	Be	20	8.6777	5.6452	0.7059	3.64e-3	1.00	102.60	52.97
D	Be	25	8.5752	5.1717	0.7833	7.30e-3	1.00	101.31	58.26
D	Be	30	8.6869	4.9678	0.8221	1.08e-2	1.00	100.35	60.94
D	Be	40	8.3485	4.4220	0.8753	1.68e-2	1.00	98.98	63.92
D	Be	50	8.4098	4.2438	0.8948	2.09e-2	1.00	98.05	65.35
D	Be	70	7.8175	3.6199	0.9330	2.63e-2	1.00	96.82	67.56
D	Be	100	7.1106	3.0041	0.9611	3.10e-2	1.00	95.71	69.49
D	Be	140	6.6162	2.5702	0.9727	3.32e-2	1.00	94.83	71.06
D	Be	200	5.8071	2.0229	0.9890	3.51e-2	1.00	94.04	72.90
D	Be	300	5.3019	1.6773	0.9801	3.44e-2	1.00	93.30	74.52
D	Be	500	4.7090	1.3205	0.9559	3.24e-2	1.00	92.56	76.70
D	Be	1000	4.2992	1.0429	0.8839	2.53e-2	1.00	91.81	80.41
D	Be	3000	3.2495	0.4832	0.9270	1.25e-2	1.00	91.05	84.71
T	Be	10	11.3143	7.1581	0.5161	1.75e-5	1.00	107.55	54.13
T	Be	11	10.9347	6.8942	0.5346	7.08e-5	1.00	106.78	54.50
T	Be	12	11.3517	7.0538	0.5714	1.77e-4	1.00	106.10	56.20
T	Be	13	11.3297	6.9311	0.5920	3.49e-4	1.00	105.50	57.54
T	Be	15	11.8958	7.0949	0.6393	9.03e-4	1.00	104.48	59.55
T	Be	17	12.0355	7.0598	0.6734	1.74e-3	1.00	103.73	60.62
T	Be	20	12.3549	7.1299	0.7128	3.43e-3	1.00	102.60	61.29
T	Be	25	12.2645	6.9111	0.7510	6.83e-3	1.00	101.31	62.12

**Table 11.** Fitting values  $f, b, c$  for the angular dependence of the sputtering yield in (6). Furthermore, the values for the yield at normal incidence,  $Y(E_0, 0)$ , the binding energy,  $E_{sp}$ , for the projectiles, the value  $\theta_0^*$  (deg.), (7), and the angular position,  $\theta_{0m}$  (deg.), of the maximum yield, (8), are given

ion	target	$E_0$ (eV)	$f$	$b$	$c$	$Y(E_0, 0)$	$E_{sp}$ (eV)	$\theta_0^*$	$\theta_{0m}$
T	Be	30	11.9180	6.5619	0.7738	1.03e-2	1.00	100.35	62.87
T	Be	50	10.7247	5.4280	0.8473	2.11e-2	1.00	98.05	65.39
T	Be	100	8.7843	3.8375	0.9167	3.27e-2	1.00	95.71	68.86
T	Be	200	6.8472	2.5074	0.9558	4.00e-2	1.00	94.04	72.19
T	Be	300	6.0145	1.9963	0.9542	4.14e-2	1.00	93.30	73.94
T	Be	500	5.1690	1.5181	0.9354	4.05e-2	1.00	92.56	76.25
T	Be	1000	4.4884	1.1230	0.8709	3.38e-2	1.00	91.81	80.25
${}^4\text{He}$	Be	11	13.3115	7.4762	0.6483	1.59e-5	0.00	90.00	55.05
${}^4\text{He}$	Be	12	11.3837	5.9236	0.7450	4.18e-5	0.00	90.00	59.11
${}^4\text{He}$	Be	13	11.0954	5.5450	0.8004	8.92e-5	0.00	90.00	60.71
${}^4\text{He}$	Be	15	12.0126	6.1657	0.7756	3.08e-4	0.00	90.00	59.66
${}^4\text{He}$	Be	17	11.0765	5.5593	0.8258	8.21e-4	0.00	90.00	60.43
${}^4\text{He}$	Be	20	11.1672	5.7241	0.8209	2.27e-3	0.00	90.00	59.58
${}^4\text{He}$	Be	25	10.8794	5.6025	0.8297	6.28e-3	0.00	90.00	59.36
${}^4\text{He}$	Be	30	10.6545	5.4832	0.8281	1.16e-2	0.00	90.00	59.39
${}^4\text{He}$	Be	40	9.8918	4.9831	0.8487	2.35e-2	0.00	90.00	60.20
${}^4\text{He}$	Be	50	9.3707	4.6041	0.8623	3.42e-2	0.00	90.00	61.11
${}^4\text{He}$	Be	70	8.5526	3.9849	0.8863	5.03e-2	0.00	90.00	62.89
${}^4\text{He}$	Be	100	7.7207	3.3762	0.9077	6.76e-2	0.00	90.00	64.80
${}^4\text{He}$	Be	140	6.8183	2.7618	0.9309	8.31e-2	0.00	90.00	66.81
${}^4\text{He}$	Be	200	6.1209	2.2840	0.9469	9.60e-2	0.00	90.00	68.75
${}^4\text{He}$	Be	300	5.4354	1.8381	0.9580	1.06e-1	0.00	90.00	70.86
${}^4\text{He}$	Be	400	5.1109	1.6232	0.9604	1.09e-1	0.00	90.00	72.14
${}^4\text{He}$	Be	500	4.7756	1.4360	0.9609	1.10e-1	0.00	90.00	73.20
${}^4\text{He}$	Be	700	4.6688	1.3495	0.9432	1.09e-1	0.00	90.00	74.29
${}^4\text{He}$	Be	1000	4.5214	1.2552	0.9168	1.04e-1	0.00	90.00	75.61
${}^4\text{He}$	Be	2000	3.9996	0.9553	0.8655	8.70e-2	0.00	90.00	79.63
${}^4\text{He}$	Be	3000	2.9548	0.4527	0.9860	6.80e-2	0.00	90.00	81.59
${}^4\text{He}$	Be	5000	2.3689	0.2360	1.0133	5.93e-2	0.00	90.00	83.86
${}^4\text{He}$	Be	10000	2.3184	0.2110	0.9873	4.08e-2	0.00	90.00	85.21
Be	Be	12	35.8412	18.6635	0.4936	1.26e-5	3.38	117.96	78.65
Be	Be	13	36.3925	19.1900	0.5105	2.14e-5	3.38	117.02	76.76
Be	Be	15	36.6304	19.6402	0.5253	5.23e-5	3.38	115.39	74.15
Be	Be	17	35.6814	19.3245	0.5289	1.15e-4	3.38	114.03	72.38
Be	Be	20	33.7964	18.4992	0.5227	3.05e-4	3.38	112.35	70.38
Be	Be	25	30.3372	16.8120	0.5223	1.09e-3	3.38	110.19	67.94
Be	Be	30	27.7102	15.5065	0.5251	2.68e-3	3.38	108.55	66.10
Be	Be	40	24.3009	13.7865	0.5368	8.41e-3	3.38	106.21	63.58
Be	Be	50	22.2057	12.6890	0.5547	1.68e-2	3.38	104.57	62.14
Be	Be	70	19.4611	11.1466	0.5914	3.77e-2	3.38	102.39	60.93
Be	Be	100	16.6662	9.3775	0.6469	7.00e-2	3.38	100.42	61.30
Be	Be	200	12.0795	6.2040	0.7708	1.43e-1	3.38	97.41	64.55
Be	Be	300	9.7816	4.6056	0.8401	1.86e-1	3.38	96.06	67.06
Be	Be	500	7.6374	3.1692	0.8981	2.33e-1	3.38	94.70	69.96
Be	Be	700	6.6434	2.5351	0.9168	2.57e-1	3.38	93.97	71.61
Be	Be	1000	5.7378	1.9957	0.9261	2.74e-1	3.38	93.33	73.36
Be	Be	3000	4.1459	1.0784	0.8930	2.63e-1	3.38	91.92	79.02
Be	Be	5000	3.7580	0.8504	0.8638	2.27e-1	3.38	91.49	81.91

**Table 12.** Fitting values  $f, b, c$  for the angular dependence of the sputtering yield in (6). Furthermore, the values for the yield at normal incidence,  $Y(E_0, 0)$ , the binding energy,  $E_{\text{sp}}$ , for the projectiles, the value  $\theta_0^*$  (deg.), (7), and the angular position,  $\theta_{0m}$  (deg.), of the maximum yield, (8), are given

ion	target	$E_0$ (eV)	$f$	$b$	$c$	$Y(E_0, 0)$	$E_{\text{sp}}$ (eV)	$\theta_0^*$	$\theta_{0m}$
N	Be	20	48.9385	26.5720	0.5034	1.30e-5	1.00	102.60	64.91
N	Be	25	40.8964	22.5484	0.5362	1.32e-4	1.00	101.31	62.92
N	Be	27	39.8702	22.1580	0.5309	2.23e-4	1.00	100.89	62.01
N	Be	30	37.4299	20.9914	0.5363	4.97e-4	1.00	100.35	60.99
N	Be	40	32.2237	18.4203	0.5534	2.72e-3	1.00	98.98	58.78
N	Be	50	27.1013	15.5100	0.5983	7.94e-3	1.00	98.05	58.46
N	Be	70	23.2661	13.3500	0.6312	2.53e-2	1.00	96.82	56.99
N	Be	100	18.5794	10.4007	0.6958	6.02e-2	1.00	95.71	58.90
N	Be	140	14.9483	8.0322	0.7602	1.08e-1	1.00	94.83	60.25
N	Be	200	11.8204	5.9812	0.8224	1.72e-1	1.00	94.04	62.81
N	Be	500	7.1837	2.9571	0.9262	3.38e-1	1.00	92.56	68.30
N	Be	1000	5.3902	1.8661	0.9559	4.48e-1	1.00	91.81	71.80
Ne	Be	22	37.8307	19.0105	0.6044	1.54e-5	0.00	90.00	61.56
Ne	Be	25	35.8007	18.1513	0.6087	4.73e-5	0.00	90.00	61.02
Ne	Be	30	32.6599	16.7384	0.6188	1.99e-4	0.00	90.00	60.35
Ne	Be	35	30.1281	15.5617	0.6274	5.66e-4	0.00	90.00	59.88
Ne	Be	40	27.8302	14.4241	0.6390	1.28e-3	0.00	90.00	59.64
Ne	Be	45	25.8448	13.4144	0.6510	2.44e-3	0.00	90.00	59.52
Ne	Be	50	24.3632	12.6735	0.6597	4.08e-3	0.00	90.00	59.37
Ne	Be	60	21.5727	11.1858	0.6815	9.11e-3	0.00	90.00	59.47
Ne	Be	70	19.3093	9.9345	0.7037	1.63e-2	0.00	90.00	59.79
Ne	Be	100	15.1087	7.5705	0.7520	4.51e-2	0.00	90.00	60.82
Ne	Be	150	12.1657	5.8694	0.7943	9.80e-2	0.00	90.00	62.20
Ne	Be	200	10.3791	4.8187	0.8263	1.50e-1	0.00	90.00	63.45
Ne	Be	300	8.4375	3.6736	0.8644	2.40e-1	0.00	90.00	65.34
Ne	Be	500	6.6629	2.6321	0.9027	3.72e-1	0.00	90.00	67.84
Ne	Be	700	5.8331	2.1425	0.9218	4.58e-1	0.00	90.00	69.49
Ne	Be	1000	5.1859	1.7686	0.9333	5.44e-1	0.00	90.00	71.07
Ar	Be	30	35.7128	17.2562	0.6278	1.18e-5	0.00	90.00	63.48
Ar	Be	35	32.4561	15.7178	0.6419	5.22e-5	0.00	90.00	63.23
Ar	Be	40	30.6583	14.9605	0.6464	1.48e-4	0.00	90.00	62.79
Ar	Be	45	28.8311	14.1259	0.6530	3.43e-4	0.00	90.00	62.53
Ar	Be	50	27.0273	13.2560	0.6634	6.98e-4	0.00	90.00	62.39
Ar	Be	60	24.1964	11.8526	0.6801	2.02e-3	0.00	90.00	62.32
Ar	Be	70	21.9850	10.7572	0.6948	4.36e-3	0.00	90.00	62.27
Ar	Be	100	17.3823	8.3702	0.7353	1.83e-2	0.00	90.00	62.69
Ar	Be	150	13.3017	6.1743	0.7841	5.72e-2	0.00	90.00	63.81
Ar	Be	200	11.1755	4.9841	0.8183	1.01e-1	0.00	90.00	64.98
Ar	Be	300	9.0871	3.8726	0.8510	1.91e-1	0.00	90.00	66.18
Ar	Be	500	7.1160	2.7974	0.8891	3.49e-1	0.00	90.00	68.15
Ar	Be	700	6.1626	2.2693	0.9109	4.71e-1	0.00	90.00	69.59
Ar	Be	1000	5.3790	1.8371	0.9295	6.07e-1	0.00	90.00	71.10

**Table 13.** Fitting values  $f, b, c$  for the angular dependence of the sputtering yield in (6). Furthermore, the values for the yield at normal incidence,  $Y(E_0, 0)$ , the binding energy,  $E_{\text{sp}}$ , for the projectiles, the value  $\theta_0^*$  (deg.), (7), and the angular position,  $\theta_{0m}$  (deg.), of the maximum yield, (8), are given

ion	target	$E_0$ (eV)	$f$	$b$	$c$	$Y(E_0, 0)$	$E_{\text{sp}}$ (eV)	$\theta_0^*$	$\theta_{0m}$
D	B	30	9.8225	6.6573	0.7286	1.17e-3	1.00	100.35	49.15
D	B	50	7.3199	3.8871	0.9134	6.66e-3	1.00	98.05	63.17
D	B	100	6.5102	2.7189	0.9959	1.46e-2	1.00	95.71	69.50
D	B	400	5.0009	1.4855	0.9885	2.05e-2	1.00	92.86	75.34
D	B	500	5.0131	1.4255	0.9687	1.87e-2	1.00	92.56	76.18
D	B	8000	2.9214	0.3459	0.9361	5.43e-3	1.00	90.64	85.95
B	B	1000	7.1514	2.8161	0.8867	2.12e-1	5.73	94.33	71.41
B	B	2000	5.4626	1.8079	0.9049	2.50e-1	5.73	93.06	74.71
H	C	40	19.9809	13.5817	0.8381	9.00e-6	1.00	98.98	49.97
H	C	50	12.0758	8.1489	0.7350	1.75e-4	1.00	98.05	48.45
H	C	70	5.4383	3.1284	0.9195	1.23e-3	1.00	96.82	58.82
H	C	100	3.9021	1.5976	1.0451	2.92e-3	1.00	95.71	69.59
H	C	140	4.0027	1.3367	1.0590	4.42e-3	1.00	94.83	73.42
H	C	200	3.8151	1.0804	1.0649	5.84e-3	1.00	94.04	75.69
H	C	300	3.8086	0.9751	1.0455	7.05e-3	1.00	93.30	77.01
H	C	500	4.1077	1.0059	0.9884	6.76e-3	1.00	92.56	78.24
H	C	1000	4.4299	1.0578	0.8756	5.68e-3	1.00	91.81	80.93
H	C	2000	4.1024	0.8166	0.9397	4.44e-3	1.00	91.28	81.26
D	C	30	18.7533	13.3928	0.6303	8.58e-5	1.00	102.60	43.62
D	C	40	10.5178	6.5616	0.7465	7.35e-4	1.00	98.98	54.48
D	C	50	7.5874	4.1326	0.8655	1.96e-3	1.00	98.05	62.05
D	C	70	6.1109	2.7764	0.9695	4.79e-3	1.00	96.82	67.95
D	C	100	5.4981	2.1396	1.0110	8.18e-3	1.00	95.71	71.23
D	C	140	5.1852	1.8064	1.0205	1.10e-2	1.00	94.83	73.06
D	C	200	5.1235	1.6777	1.0074	1.32e-2	1.00	94.04	73.95
D	C	300	4.9019	1.4719	0.9931	1.47e-2	1.00	93.30	75.31
D	C	350	4.9419	1.4793	0.9963	1.62e-2	1.00	93.06	75.12
D	C	500	4.9952	1.4436	0.9320	1.44e-2	1.00	92.56	76.64
D	C	1000	4.4895	1.1320	0.8660	1.30e-2	1.00	91.81	80.25
D	C	2000	4.5151	1.0312	0.8022	1.02e-1	1.00	91.28	83.72
T	C	25	19.6619	13.0973	0.5723	4.70e-5	1.00	101.31	47.74
T	C	30	14.1788	8.6868	0.6507	2.44e-4	1.00	100.35	55.39
T	C	35	12.8594	7.3628	0.7278	6.90e-4	1.00	99.59	60.04
T	C	40	10.8275	5.8369	0.7969	1.23e-3	1.00	98.98	63.13
T	C	50	9.4042	4.6780	0.8682	2.76e-3	1.00	98.05	66.04
T	C	70	7.8716	3.4803	0.9388	6.05e-3	1.00	96.82	69.07
T	C	100	7.3284	2.9473	0.9618	9.44e-3	1.00	95.71	70.90
T	C	140	6.5713	2.4171	0.9798	1.28e-2	1.00	94.83	72.35
T	C	200	6.2607	2.1538	0.9746	1.54e-2	1.00	94.04	73.39
T	C	300	5.9195	1.9209	0.9502	1.75e-2	1.00	93.30	74.51
T	C	500	5.4224	1.6330	0.9126	1.87e-2	1.00	92.56	76.23
T	C	1000	5.0328	1.3613	0.8358	1.68e-2	1.00	91.81	79.77

**Table 14.** Fitting values  $f, b, c$  for the angular dependence of the sputtering yield in (6). Furthermore, the values for the yield at normal incidence,  $Y(E_0, 0)$ , the binding energy,  $E_{sp}$ , for the projectiles, the value  $\theta_0^*$  (deg.), (7), and the angular position,  $\theta_{0m}$  (deg.), of the maximum yield, (8), are given

ion	target	$E_0$ (eV)	$f$	$b$	$c$	$Y(E_0, 0)$	$E_{sp}$ (eV)	$\theta_0^*$	$\theta_{0m}$
${}^4\text{He}$	C	25	14.6404	8.8559	0.6282	4.20e-5	0.00	90.00	50.27
${}^4\text{He}$	C	27	12.0307	6.8705	0.7074	1.00e-4	0.00	90.00	54.32
${}^4\text{He}$	C	30	13.1803	7.2609	0.7109	2.40e-4	0.00	90.00	56.28
${}^4\text{He}$	C	35	10.6979	5.5485	0.7917	7.20e-4	0.00	90.00	59.15
${}^4\text{He}$	C	40	9.2954	4.4707	0.8724	1.50e-3	0.00	90.00	61.85
${}^4\text{He}$	C	50	8.8544	4.1314	0.8858	3.83e-3	0.00	90.00	62.85
${}^4\text{He}$	C	60	8.2705	3.7475	0.8993	6.84e-3	0.00	90.00	63.74
${}^4\text{He}$	C	70	7.7165	3.3800	0.9141	1.01e-2	0.00	90.00	64.69
${}^4\text{He}$	C	100	7.0586	2.8816	0.9323	1.83e-2	0.00	90.00	66.58
${}^4\text{He}$	C	140	6.5107	2.4872	0.9451	2.63e-2	0.00	90.00	68.19
${}^4\text{He}$	C	200	6.0474	2.1599	0.9522	3.45e-2	0.00	90.00	69.73
${}^4\text{He}$	C	300	5.5877	1.8616	0.9536	4.28e-2	0.00	90.00	71.26
${}^4\text{He}$	C	400	5.2835	1.6741	0.9516	4.75e-2	0.00	90.00	72.34
${}^4\text{He}$	C	500	5.0843	1.5587	0.9464	5.05e-2	0.00	90.00	73.10
${}^4\text{He}$	C	700	5.0583	1.5204	0.9217	5.17e-2	0.00	90.00	73.97
${}^4\text{He}$	C	1000	4.6895	1.3191	0.9059	5.19e-2	0.00	90.00	75.61
${}^4\text{He}$	C	2000	4.5101	1.1834	0.8292	4.69e-2	0.00	90.00	79.01
${}^4\text{He}$	C	3000	4.0905	0.9440	0.8126	4.24e-2	0.00	90.00	81.98
${}^4\text{He}$	C	5000	3.7153	0.7059	0.7928	3.40e-2	0.00	90.00	85.98
${}^4\text{He}$	C	10000	2.6820	0.2986	0.9802	2.43e-2	0.00	90.00	91.35
${}^4\text{He}$	C	20000	2.0022	0.1082	1.0128	1.66e-2	0.00	90.00	86.45
C	C	30	42.3520	22.5877	0.5107	1.83e-5	7.41	116.43	75.33
C	C	40	37.6060	20.3491	0.5157	1.35e-4	7.41	113.29	71.99
C	C	50	32.0236	17.1592	0.5118	5.21e-4	7.41	111.06	71.44
C	C	70	26.5068	14.2187	0.5267	2.57e-3	7.41	108.02	69.37
C	C	100	22.0310	11.8066	0.5552	8.84e-3	7.41	105.23	67.62
C	C	140	18.7261	9.9820	0.5946	2.13e-2	7.41	102.96	66.50
C	C	200	15.8273	8.2671	0.6395	4.14e-2	7.41	100.90	66.38
C	C	300	13.1991	6.6409	0.6938	7.16e-2	7.41	98.93	66.97
C	C	500	10.5675	4.9405	0.7630	1.16e-1	7.41	96.94	68.62
C	C	1000	7.7788	3.1823	0.8291	1.78e-1	7.41	94.92	71.47
C	C	300	13.0293	6.6396	0.7021	8.05e-2	7.40	98.93	66.24
C	C	1000	8.0328	3.4041	0.7226	1.79e-1	7.40	94.92	71.84
C	C	3000	4.9485	1.5045	0.7311	2.49e-1	7.40	92.85	81.25
N	C	40	46.4143	25.1992	0.5238	1.81e-5	1.00	98.98	62.64
N	C	50	41.1533	22.6413	0.5434	1.23e-4	1.00	98.05	61.08
N	C	70	33.5042	18.5624	0.5864	1.11e-3	1.00	96.82	59.92
N	C	100	26.2400	14.2958	0.6513	5.53e-3	1.00	95.71	60.43
N	C	140	20.3476	10.7156	0.7195	1.63e-2	1.00	94.83	61.73
N	C	200	15.5449	7.7646	0.7867	3.68e-2	1.00	94.04	63.53
N	C	300	11.9070	5.5403	0.8432	6.94e-2	1.00	93.30	65.56
N	C	500	8.9090	3.7472	0.8908	1.21e-1	1.00	92.56	68.04
N	C	1000	6.7186	2.4884	0.9106	1.96e-1	1.00	91.81	70.84
N	C	15000	3.1017	0.5614	0.9345	2.64e-1	1.00	90.47	81.85
N	C	30000	2.4599	0.3007	0.9258	2.15e-1	1.00	90.33	85.79

**Table 15.** Fitting values  $f, b, c$  for the angular dependence of the sputtering yield in (6). Furthermore, the values for the yield at normal incidence,  $Y(E_0, 0)$ , the binding energy,  $E_{sp}$ , for the projectiles, the value  $\theta_0^*$  (deg.), (7), and the angular position,  $\theta_{0m}$  (deg.), of the maximum yield, (8), are given

ion	target	$E_0$ (eV)	$f$	$b$	$c$	$Y(E_0, 0)$	$E_{sp}$ (eV)	$\theta_0^*$	$\theta_{0m}$
Ne	C	45	42.4911	21.3692	0.6065	1.07e-5	0.00	90.00	61.50
Ne	C	50	39.2571	19.9517	0.6096	3.41e-5	0.00	90.00	60.88
Ne	C	60	34.9544	17.7437	0.6312	1.48e-4	0.00	90.00	60.82
Ne	C	70	30.5197	15.4178	0.6536	4.59e-4	0.00	90.00	60.95
Ne	C	100	23.0552	11.4059	0.7070	3.25e-3	0.00	90.00	61.66
Ne	C	140	17.8207	8.5421	0.7551	1.18e-2	0.00	90.00	62.74
Ne	C	200	13.9445	6.4094	0.7992	3.03e-2	0.00	90.00	64.05
Ne	C	300	10.9291	4.7545	0.8387	6.50e-2	0.00	90.00	65.64
Ne	C	500	8.4196	3.3744	0.8761	1.26e-1	0.00	90.00	67.77
Ne	C	1000	6.3131	2.2510	0.9033	2.32e-1	0.00	90.00	70.51
Ne	C	2000	5.1757	1.6622	0.9003	3.36e-1	0.00	90.00	73.01
Ne	C	5000	4.3556	1.2290	0.8572	4.16e-1	0.00	90.00	76.75
Ne	C	10000	3.6410	0.8456	0.8528	4.21e-1	0.00	90.00	80.50
Ne	C	20000	2.8697	0.4814	0.8953	3.81e-1	0.00	90.00	83.58
Ar	C	70	33.8798	16.4564	0.6471	6.64e-5	0.00	90.00	63.02
Ar	C	100	26.2324	12.6103	0.6901	8.27e-4	0.00	90.00	63.14
Ar	C	140	20.3486	9.5425	0.7354	4.62e-3	0.00	90.00	63.83
Ar	C	200	15.8749	7.1967	0.7784	1.66e-2	0.00	90.00	64.78
Ar	C	300	12.3051	5.3108	0.8200	4.54e-2	0.00	90.00	66.11
Ar	C	500	9.2928	3.7250	0.8616	1.09e-1	0.00	90.00	67.95
Ar	C	1000	6.6196	2.3464	0.9035	2.47e-1	0.00	90.00	70.65
Ar	C	30000	2.4175	0.3179	0.9919	8.57e-1	0.00	90.00	82.69
Xe	C	150	30.7260	13.6835	0.6070	4.50e-5	0.00	90.00	67.97
Xe	C	170	29.2745	12.9894	0.6384	1.24e-4	0.00	90.00	67.57
Xe	C	200	25.3437	11.1859	0.6259	4.15e-4	0.00	90.00	68.05
Xe	C	250	22.4002	9.7749	0.6740	1.70e-3	0.00	90.00	67.72
Xe	C	300	19.5075	8.3043	0.7070	4.24e-3	0.00	90.00	68.20
Xe	C	500	13.2878	5.3847	0.7239	2.76e-2	0.00	90.00	69.80
Xe	C	1000	8.5390	3.0860	0.7752	1.27e-1	0.00	90.00	72.57
Xe	C	3000	5.1292	1.4472	0.7645	4.66e-1	0.00	90.00	79.52
Xe	C	10000	3.8051	0.8756	0.9244	1.02e-0	0.00	90.00	78.55
Xe	C	30000	2.4297	0.3057	1.0023	1.46e-0	0.00	90.00	82.70
Xe	C	100000	1.9300	0.1564	1.0042	1.69e-0	0.00	90.00	85.21
Ar	Al	100	14.7601	8.5471	0.6703	1.17e-1	0.00	90.00	53.34
Ar	Al	500	6.7055	3.4612	0.8024	9.10e-1	0.00	90.00	59.33
Ar	Al	1000	5.4733	2.5849	0.8298	1.37e-0	0.00	90.00	62.79
Ar	Al	1050	4.4893	1.7504	0.8913	1.17e-0	0.00	90.00	68.35
Ar	Al	10000	3.3890	1.0004	0.8667	2.39e-0	0.00	90.00	75.57
D	Si	30	44.6047	26.3734	0.3164	1.52e-4	1.00	100.35	52.21
D	Si	50	25.2643	14.1721	0.5693	3.09e-3	1.00	98.05	59.73
D	Si	100	12.7099	6.0832	0.6848	1.15e-2	1.00	95.71	67.42
D	Si	500	6.3060	2.0569	0.8725	2.48e-2	1.00	92.56	75.30
D	Si	1000	4.6790	1.2020	0.8521	2.36e-2	1.00	91.81	80.31
${}^4\text{He}$	Si	200	3.3626	1.1091	0.9879	7.68e-2	0.00	90.00	70.92
${}^4\text{He}$	Si	2000	2.3967	0.4284	0.9844	1.08e-1	0.00	90.00	80.12
${}^4\text{He}$	Si	3000	2.5727	0.4683	0.9532	9.56e-2	0.00	90.00	80.80
Ar	Si	4500	3.1385	0.8328	0.9440	1.28e-0	0.00	90.00	75.79

**Table 16.** Fitting values  $f, b, c$  for the angular dependence of the sputtering yield in (6). Furthermore, the values for the yield at normal incidence,  $Y(E_0, 0)$ , the binding energy,  $E_{sp}$ , for the projectiles, the value  $\theta_0^*$  (deg.), (7), and the angular position,  $\theta_{0m}$  (deg.), of the maximum yield, (8), are given

ion	target	$E_0$ (eV)	$f$	$b$	$c$	$Y(E_0, 0)$	$E_{sp}$ (eV)	$\theta_0^*$	$\theta_{0m}$
Si	Si(KrC)	200	11.0479	6.1405	0.6299	2.13e-1	4.70	98.72	61.01
Si	Si(Mo)	200	10.5874	6.1453	0.6210	2.86e-1	4.70	98.72	58.02
Si	Si(ZBL)	200	11.0834	5.9494	0.6393	1.73e-1	4.70	98.72	63.26
Si	Si(SiSi)	200	7.9001	3.8139	0.6017	1.70e-1	4.70	98.72	65.35
Si	Si	500	7.4656	3.6011	0.8032	4.40e-1	4.70	95.54	65.97
Si	Si	2000	4.7498	1.8181	0.8645	8.96e-1	4.70	92.78	71.39
He	Ti	100000	1.9229	0.1065	0.9665	1.63e-2	0.00	90.00	88.09
Ne	Ti	38	7.8592	4.0707	0.8577	1.12e-2	0.00	90.00	59.06
Ne	Ti	380	4.1989	1.9114	0.9136	5.33e-1	0.00	90.00	63.48
Ne	Ti	3800	3.3212	1.1093	0.8712	1.08e-0	0.00	90.00	72.68
Ar	Ti	1050	3.9753	1.6427	0.8942	1.12e-0	0.00	90.00	66.65
Ar	Ti	150000	1.7921	0.1849	0.9639	1.24e-0	0.00	90.00	85.29
Ar	Ti	900000	1.4988	0.0650	0.9866	6.30e-1	0.00	90.00	88.02
H	V	100	4.3828	3.2190	0.8990	1.01e-4	1.00	95.71	43.98
H	V	120	3.3311	2.2723	0.9700	4.49e-4	1.00	95.22	49.41
H	V	140	2.8610	1.8516	0.9921	1.03e-3	1.00	94.83	52.28
H	V	200	2.1946	1.0807	1.0293	3.09e-3	1.00	94.04	63.12
H	V	400	2.0664	0.5226	1.0687	7.87e-3	1.00	92.86	76.39
H	V	1000	2.3097	0.3954	1.0493	1.04e-2	1.00	91.81	80.48
H	V	3000	2.3607	0.2866	1.0250	8.30e-3	1.00	91.05	83.24
H	V	10000	2.6833	0.3268	0.9415	4.88e-3	1.00	90.57	85.48
D	V	55	5.1320	4.2287	0.8769	2.54e-4	1.00	97.68	34.89
D	V	60	4.7591	3.8345	0.8881	5.51e-4	1.00	97.36	37.10
D	V	70	4.0378	3.1247	0.9217	1.47e-3	1.00	96.82	40.94
D	V	100	2.8895	1.8739	0.9819	5.49e-3	1.00	95.71	52.57
D	V	200	1.9899	0.6708	1.0998	1.70e-2	1.00	94.04	72.10
D	V	500	2.4386	0.5933	1.0536	2.68e-2	1.00	92.56	76.97
D	V	1000	2.3231	0.4408	1.0423	2.85e-2	1.00	91.81	79.60
D	V	3000	2.3990	0.3768	0.9870	2.31e-2	1.00	91.05	82.28
D	V	10000	2.3706	0.2715	0.9614	1.24e-2	1.00	90.57	85.23
T	V	40	6.3376	5.3953	0.8382	3.49e-4	1.00	98.98	31.03
T	V	50	4.7448	3.8690	0.8969	1.79e-3	1.00	98.05	36.46
T	V	70	3.5720	2.5052	0.9398	6.60e-3	1.00	96.82	48.19
T	V	100	2.4950	1.3038	1.0454	1.43e-2	1.00	95.71	62.15
T	V	300	2.7891	0.8677	1.0445	3.78e-2	1.00	93.30	73.79
T	V	1000	2.3834	0.4768	1.0372	4.53e-2	1.00	91.81	79.14
T	V	3000	2.3246	0.3700	0.9891	3.71e-2	1.00	91.05	82.10
T	V	10000	2.2078	0.2396	0.9737	2.03e-2	1.00	90.57	85.17
<sup>4</sup> He	V	35	1.7453	2.6763	0.9355	5.04e-4	0.00	90.00	0.00
<sup>4</sup> He	V	40	2.1705	2.6154	0.9342	1.63e-3	0.00	90.00	0.00
<sup>4</sup> He	V	50	2.5628	2.4407	0.9078	5.65e-3	0.00	90.00	15.76
<sup>4</sup> He	V	70	1.9394	1.4203	0.9787	1.68e-2	0.00	90.00	42.65
<sup>4</sup> He	V	100	2.2659	1.2170	1.0013	3.35e-2	0.00	90.00	57.51
<sup>4</sup> He	V	300	2.6903	0.9304	1.0086	8.98e-2	0.00	90.00	69.65
<sup>4</sup> He	V	1000	2.2475	0.5217	1.0161	1.24e-1	0.00	90.00	76.23
<sup>4</sup> He	V	3000	2.1180	0.3668	1.0015	1.17e-1	0.00	90.00	79.99
<sup>4</sup> He	V	10000	1.9835	0.2272	0.9958	7.55e-2	0.00	90.00	83.55

**Table 17.** Fitting values  $f, b, c$  for the angular dependence of the sputtering yield in (6). Furthermore, the values for the yield at normal incidence,  $Y(E_0, 0)$ , the binding energy,  $E_{sp}$ , for the projectiles, the value  $\theta_0^*$  (deg.), (7), and the angular position,  $\theta_{0m}$  (deg.), of the maximum yield, (8), are given

ion	target	$E_0$ (eV)	f	b	c	$Y(E_0, 0)$	$E_{sp}$ (eV)	$\theta_0^*$	$\theta_{0m}$
H	Fe	4000	2.2066	0.2560	1.0265	1.22e-2	1.00	90.49	82.98
H	Fe	8000	2.3317	0.2544	0.9961	8.87e-3	1.00	90.64	84.46
H	Ni	150	3.2117	2.2893	0.9835	2.00e-3	1.00	94.67	46.65
H	Ni	200	2.7207	1.6060	1.0171	4.30e-3	1.00	94.04	56.30
H	Ni	400	2.1098	0.6960	0.9564	1.16e-2	1.00	92.86	73.69
H	Ni	450	1.8895	0.4824	1.0956	1.42e-2	1.00	92.70	75.64
H	Ni	1000	2.0731	0.3479	1.0856	1.52e-2	1.00	91.81	79.80
H	Ni	4000	2.5028	0.3836	0.9871	1.33e-2	1.00	90.91	82.38
H	Ni	8000	2.3038	0.2492	1.0029	9.39e-3	1.00	90.64	84.29
H	Ni	50000	1.7324	0.0610	1.0093	2.70e-3	1.00	90.26	87.89
D	Ni	1000	2.2389	0.4761	1.0506	4.51e-2	1.00	91.81	78.13
D	Ni	4000	1.9552	0.2335	1.0325	3.34e-2	1.00	90.91	83.00
D	Ni	8000	2.0430	0.2136	1.0102	2.37e-2	1.00	90.64	84.27
${}^4\text{He}$	Ni	100	2.0241	1.3441	0.9916	5.47e-2	0.00	90.00	48.32
${}^4\text{He}$	Ni	500	2.5267	0.8794	1.0066	1.68e-1	0.00	90.00	69.54
${}^4\text{He}$	Ni	1000	2.4668	0.7284	0.9950	1.90e-1	0.00	90.00	72.91
${}^4\text{He}$	Ni	4000	1.9873	0.3420	1.0072	1.67e-1	0.00	90.00	79.90
${}^4\text{He}$	Ni	8000	2.0723	0.3149	0.9841	1.32e-1	0.00	90.00	81.72
${}^4\text{He}$	Ni	100000	1.8360	0.0921	0.9937	2.23e-2	0.00	90.00	87.36
Ne	Ni	1000	4.7811	2.7093	0.7414	1.47e-0	0.00	90.00	54.86
Ar	Ni	40	20.4675	11.2697	0.6240	2.88e-3	0.00	90.00	56.17
Ar	Ni	50	14.8926	8.1426	0.7142	1.20e-2	0.00	90.00	56.68
Ar	Ni	70	10.5289	5.9310	0.7567	5.35e-2	0.00	90.00	55.22
Ar	Ni	100	7.6304	4.4032	0.7971	1.53e-1	0.00	90.00	54.13
Ar	Ni	200	5.5978	3.4646	0.7233	7.65e-1	0.00	90.00	49.79
Ar	Ni(ZBL)	290	5.1631	3.2541	0.7388	7.80e-1	0.00	90.00	48.85
Ar	Ni	300	5.0306	2.9919	0.8059	7.78e-1	0.00	90.00	52.63
Ar	Ni	1000	3.9887	2.1644	0.7780	1.97e-0	0.00	90.00	57.09
Ar	Ni	3000	2.8656	1.1258	0.9315	2.81e-0	0.00	90.00	67.63
Ar	Ni	30000	1.9547	0.3494	0.9924	3.23e-0	0.00	90.00	79.90
Ni	Ni	100	14.1078	8.8411	0.5677	1.13e-1	4.46	101.92	53.21
Ni	Ni	500	5.8343	3.5339	0.8012	1.24e-0	4.46	95.40	54.74
Ni	Ni	1000	4.8757	2.7113	0.8474	2.03e-0	4.46	93.82	58.40
Ni	Ni	2500	3.9820	1.8894	0.8896	2.90e-0	4.46	92.42	63.91
Ni	Ni	5000	3.4691	1.4129	0.9121	3.74e-0	4.46	91.71	68.14
Ni	Ni	10000	2.6717	0.8456	0.9678	4.34e-0	4.46	91.21	73.05
Kr	Ni	45000	2.7039	0.6843	0.9179	5.61e-0	0.00	90.00	77.21

**Table 18.** Fitting values  $f, b, c$  for the angular dependence of the sputtering yield in (6). Furthermore, the values for the yield at normal incidence,  $Y(E_0, 0)$ , the binding energy,  $E_{sp}$ , for the projectiles, the value  $\theta_0^*$  (deg.), (7), and the angular position,  $\theta_{0m}$  (deg.), of the maximum yield, (8), are given

ion	target	$E_0$ (eV)	f	b	c	$Y(E_0, 0)$	$E_{sp}$ (eV)	$\theta_0^*$	$\theta_{0m}$
H	Cu	50000	1.9195	0.0855	1.0004	3.01e-3	1.00	90.26	87.68
D	Cu	50	4.4937	4.2207	0.8591	1.47e-3	1.00	98.05	18.41
D	Cu	100	1.7910	1.2622	1.0565	1.64e-2	1.00	95.71	48.67
D	Cu	300	2.1337	0.6577	1.1002	4.34e-2	1.00	93.30	70.56
D	Cu	1000	2.1945	0.4894	1.0319	5.39e-2	1.00	91.81	76.41
D	Cu	3000	2.6275	0.5238	0.9010	3.93e-2	1.00	91.05	81.26
D	Cu	10000	2.2766	0.2868	0.9299	2.47e-2	1.00	90.57	85.09
${}^4\text{He}$	Cu	1000	2.3431	0.6903	0.9933	2.30e-1	0.00	90.00	72.98
Ne	Cu	1000	2.5361	1.1735	0.9540	1.84e-0	0.00	90.00	62.70
Ne	Cu	45000	2.0420	0.3165	0.9773	1.62e-0	0.00	90.00	81.74
Ar	Cu	16	23.7198	11.9382	0.6384	2.12e-5	0.00	90.00	61.24
Ar	Cu	18	22.1882	11.3333	0.6891	7.78e-5	0.00	90.00	60.20
Ar	Cu	20	21.4383	11.0751	0.6527	1.80e-4	0.00	90.00	59.76
Ar	Cu	25	19.9619	10.5883	0.6529	8.40e-4	0.00	90.00	58.33
Ar	Cu	30	17.3814	9.4935	0.6603	3.12e-3	0.00	90.00	56.69
Ar	Cu	40	14.1287	8.0673	0.6709	1.54e-2	0.00	90.00	54.17
Ar	Cu	50	11.7916	6.8970	0.6891	3.96e-2	0.00	90.00	52.86
Ar	Cu	100	5.8601	3.5052	0.8223	2.71e-1	0.00	90.00	52.43
Ar	Cu	300	3.4966	2.0419	0.8881	1.05e-0	0.00	90.00	53.90
Ar	Cu	1050	2.8705	1.4081	0.9193	2.45e-0	0.00	90.00	60.93
Ar	Cu	20000	2.4430	0.6188	0.9469	3.99e-0	0.00	90.00	76.49
Ar	Cu	27000	2.4527	0.5926	0.9391	3.90e-0	0.00	90.00	77.43
Ar	Cu	30000	2.5535	0.6295	0.9259	3.84e-0	0.00	90.00	77.44
Ar	Cu	37000	2.6151	0.6326	0.9153	3.68e-0	0.00	90.00	78.01
Ar	Cu	100000	2.3985	0.4287	0.9369	2.93e-0	0.00	90.00	81.47
Ar	Cu	300000	2.1945	0.2936	0.9252	2.05e-0	0.00	90.00	84.76
Ar	Cu	1000000	1.7152	0.1116	0.9744	1.17e-0	0.00	90.00	87.20
Cu	Cu	20	32.1005	17.5504	0.5452	1.90e-4	3.52	112.76	70.78
Cu	Cu	50	18.4043	10.9887	0.5362	2.45e-2	3.52	104.86	58.42
Cu	Cu	100	12.6246	8.0725	0.5792	1.87e-1	3.52	100.63	51.08
Cu	Cu	300	6.5005	4.0702	0.7677	9.47e-1	3.52	96.18	52.93
Cu	Cu	1000	4.0103	2.1565	0.8836	2.40e-0	3.52	93.40	59.67
Cu	Cu	3000	3.4447	1.5309	0.9067	3.80e-0	3.52	91.96	65.70
Cu	Cu	10000	3.1653	1.1604	0.8892	5.14e-0	3.52	91.07	70.87
Cu	Cu	100000	2.7838	0.6638	0.9178	4.66e-0	3.52	90.34	78.47
Kr	Cu	1050	3.5413	1.7566	0.8719	2.50e-0	0.00	90.00	60.71
Kr	Cu	45000	2.0693	0.4034	0.9762	6.65e-0	0.00	90.00	79.37
Xe	Cu	550	4.4365	2.2223	0.8477	1.37e-0	0.00	90.00	60.43
Xe	Cu	1050	3.9040	1.8736	0.8561	2.31e-0	0.00	90.00	62.02
Xe	Cu	1500	3.8896	1.8648	0.8579	2.32e-0	0.00	90.00	62.05
Xe	Cu	2050	3.5977	1.6054	0.8667	3.48e-0	0.00	90.00	64.51
Xe	Cu	5000	2.8734	1.0386	0.9247	5.17e-0	0.00	90.00	69.84
Xe	Cu	9500	2.8168	0.9214	0.9274	6.33e-0	0.00	90.00	72.10
Xe	Cu	30000	2.6217	0.7036	0.9293	8.10e-0	0.00	90.00	75.93
Xe	Cu	50000	2.1291	0.4332	0.9697	8.70e-0	0.00	90.00	79.03

**Table 19.** Fitting values  $f, b, c$  for the angular dependence of the sputtering yield in (6). Furthermore, the values for the yield at normal incidence,  $Y(E_0, 0)$ , the binding energy,  $E_{sp}$ , for the projectiles, the value  $\theta_0^*$  (deg.), (7), and the angular position,  $\theta_{0m}$  (deg.), of the maximum yield, (8), are given

ion	target	$E_0$ (eV)	$f$	$b$	$c$	$Y(E_0, 0)$	$E_{sp}$ (eV)	$\theta_0^*$	$\theta_{0m}$
Ga	Ga	100	11.5816	7.0037	0.6206	2.37e-1	2.97	99.78	55.67
Ga	Ga	150	9.1207	5.4708	0.6617	4.43e-1	2.97	98.01	55.69
Ga	Ga	200	7.9098	4.6934	0.6991	6.33e-1	2.97	96.95	56.11
Ga	Ga	300	6.5454	3.7692	0.7209	9.46e-1	2.97	95.68	57.32
Ga	Ga	900	4.6037	2.3725	0.7691	2.08e-0	2.97	93.29	61.67
Ga	Ga	1000	4.4426	2.2574	0.7917	2.22e-0	2.97	93.12	62.13
Ar	Zr	1050	3.1470	1.2965	0.9014	1.00e-0	0.00	90.00	66.66
Ar	Zr	150000	1.9591	0.2715	0.9305	1.28e-0	0.00	90.00	84.26
Ar	Zr	900000	1.5211	0.0854	0.9871	6.60e-1	0.00	90.00	87.25
D	Nb	12200	2.3944	0.2938	0.9234	8.91e-3	1.00	90.52	86.03
He	Nb	36500	2.1121	0.2220	0.9265	3.25e-2	0.00	90.00	86.55
Nb	Nb	60000	3.1234	0.9023	0.8518	3.86e-0	7.59	90.64	76.94
H	Mo	230	2.5308	1.5589	0.9749	6.45e-5	1.00	93.77	54.02
H	Mo	250	2.4814	1.4465	0.9794	1.36e-4	1.00	93.62	56.47
H	Mo	300	1.9363	1.0499	1.0147	4.51e-4	1.00	93.30	59.26
H	Mo	400	1.7189	0.7725	1.0282	1.32e-3	1.00	92.86	65.13
H	Mo	700	1.4682	0.3142	1.0664	3.72e-3	1.00	92.16	78.02
H	Mo	1400	1.8628	0.2690	1.0462	5.79e-3	1.00	91.53	81.76
H	Mo	2000	1.8885	0.2330	1.0410	5.99e-3	1.00	91.28	82.88
H	Mo	3000	2.0833	0.2444	1.0274	6.04e-3	1.00	91.05	83.28
H	Mo	4000	2.2339	0.2605	1.0147	5.55e-3	1.00	90.91	83.69
H	Mo	7000	2.4427	0.2922	0.9822	4.82e-3	1.00	90.68	84.32
H	Mo	8000	2.4361	0.2873	0.9759	4.70e-3	1.00	90.64	84.78
H	Mo	50000	2.2285	0.1283	0.9825	1.36e-3	1.00	90.26	87.59

**Table 20.** Fitting values  $f, b, c$  for the angular dependence of the sputtering yield in (6). Furthermore, the values for the yield at normal incidence,  $Y(E_0, 0)$ , the binding energy,  $E_{\text{sp}}$ , for the projectiles, the value  $\theta_0^*$  (deg.), (7), and the angular position,  $\theta_{0m}$  (deg.), of the maximum yield, (8), are given

ion	target	$E_0$ (eV)	$f$	$b$	$c$	$Y(E_0, 0)$	$E_{\text{sp}}$ (eV)	$\theta_0^*$	$\theta_{0m}$
D	Mo	110	3.6499	2.6095	0.9457	4.86e-5	1.00	95.45	46.36
	Mo	120	3.2952	2.3286	0.9466	1.57e-4	1.00	95.22	47.01
	Mo	200	1.9634	1.1456	1.0224	2.83e-4	1.00	94.04	56.81
	Mo	300	1.4416	0.5467	1.0712	6.97e-3	1.00	93.30	69.42
	Mo	450	1.4557	0.3418	1.0933	1.14e-2	1.00	92.70	76.80
	Mo	2000	2.0337	0.3153	1.0220	1.84e-2	1.00	91.28	81.62
	Mo	8000	2.0631	0.2276	0.9909	1.36e-2	1.00	90.64	84.55
	Mo	50000	2.1611	0.1359	0.9794	3.50e-3	1.00	90.26	87.40
	Mo	100000	1.8823	0.0773	0.9826	2.50e-3	1.00	90.18	88.49
T	Mo	75	5.7190	4.3244	0.8477	4.99e-5	1.00	96.59	41.28
	Mo	80	4.4191	3.3686	0.8953	1.40e-4	1.00	96.38	41.46
	Mo	90	3.7017	2.7864	0.9114	4.73e-4	1.00	96.02	42.54
	Mo	100	3.0735	2.2637	0.9516	1.00e-3	1.00	95.71	44.59
	Mo	170	1.9057	1.0592	1.0260	6.88e-3	1.00	94.39	59.00
	Mo	300	1.5224	0.4495	1.0976	1.66e-2	1.00	93.30	73.90
	Mo	1000	1.9541	0.3696	1.0454	3.03e-2	1.00	91.81	79.57
	Mo	3000	1.8690	0.2429	1.0270	3.03e-2	1.00	91.05	82.70
	Mo	10000	1.9745	0.2106	0.9852	2.09e-2	1.00	90.57	84.89
${}^3\text{He}$	Mo	90	2.2907	2.0843	0.9297	4.75e-4	0.00	90.00	22.98
	Mo	100	2.2428	1.9581	0.9243	1.12e-3	0.00	90.00	27.62
	Mo	140	1.6236	1.2028	0.9934	5.50e-3	0.00	90.00	42.11
	Mo	300	1.4534	0.5258	1.0395	2.59e-2	0.00	90.00	68.31
	Mo	1000	1.8915	0.4184	1.0215	5.66e-2	0.00	90.00	76.74
	Mo	3000	1.9766	0.3390	1.0012	6.41e-2	0.00	90.00	80.09
	Mo	10000	1.8416	0.2120	0.9975	5.29e-2	0.00	90.00	83.47
${}^4\text{He}$	Mo	70	2.1772	2.1982	0.9302	4.82e-4	0.00	90.00	0.00
	Mo	80	2.3636	2.1575	0.9161	1.44e-3	0.00	90.00	22.26
	Mo	100	1.6240	1.4009	0.9877	4.56e-3	0.00	90.00	30.15
	Mo	140	1.4173	0.9332	1.0098	1.28e-2	0.00	90.00	48.90
	Mo	1500	1.9254	0.3901	1.0151	8.56e-2	0.00	90.00	77.95
	Mo	4000	2.0918	0.3877	0.9785	8.73e-2	0.00	90.00	79.89
	Mo	8000	2.0587	0.3226	0.9598	7.73e-2	0.00	90.00	82.17
	Mo	50000	1.8652	0.1239	0.9958	2.64e-2	0.00	90.00	86.34
	Mo	100000	1.9021	0.1135	0.9788	1.67e-2	0.00	90.00	87.36
Ar	Mo	160	4.8275	2.6130	0.8934	2.12e-1	0.00	90.00	57.22
	Mo	1601	3.1027	1.3279	0.9136	1.37e-0	0.00	90.00	65.40
	Mo	16010	2.9182	0.9421	0.8367	2.23e-0	0.00	90.00	74.24
	Mo	27500	1.7967	0.3351	0.9851	2.52e-0	0.00	90.00	79.64
Mo	Mo	300	10.1673	5.9485	0.6592	3.15e-1	6.83	98.58	57.67
	Mo	350	9.4843	5.5342	0.6670	3.90e-1	6.83	97.95	57.34
	Mo	1000	5.9822	3.2443	0.7442	1.12e-0	6.83	94.72	60.11
	Mo	2000	4.7935	2.4008	0.7783	1.76e-0	6.83	93.34	62.97
Xe	Mo	9500	3.3127	1.2332	0.8500	3.77e-0	0.00	90.00	70.26
Xe	Mo	30000	2.9323	0.8811	0.8899	4.96e-0	0.00	90.00	74.66

**Table 21.** Fitting values  $f, b, c$  for the angular dependence of the sputtering yield in (6). Furthermore, the values for the yield at normal incidence,  $Y(E_0, 0)$ , the binding energy,  $E_{sp}$ , for the projectiles, the value  $\theta_0^*$  (deg.), (7), and the angular position,  $\theta_{0m}$  (deg.), of the maximum yield, (8), are given

ion	target	$E_0$ (eV)	f	b	c	$Y(E_0, 0)$	$E_{sp}$ (eV)	$\theta_0^*$	$\theta_{0m}$
Ar	Pd	1050	2.3568	1.1640	0.9286	2.32e-0	0.00	90.00	60.65
D	Ag	100	1.6699	1.1575	0.9596	6.25e-3	0.00	90.00	45.70
Ne	Ag	45000	2.1511	0.4426	0.9044	2.10e-0	0.00	90.00	80.73
Na	Ag	30000	2.2411	0.4338	0.7345	2.34e-0	0.00	90.00	88.48
Ar	Ag	1050	2.1556	1.0385	0.9298	2.82e-0	0.00	90.00	61.50
Ar	Ag	150000	2.2567	0.4090	0.9091	3.50e-0	0.00	90.00	82.21
Ar	Ag	900000	1.6226	0.1125	0.9708	1.56e-0	0.00	90.00	87.08
K	Ag	30000	2.5838	0.7509	0.8372	4.76e-0	0.00	90.00	76.65
Kr	Ag	45000	2.6001	0.7415	0.8747	8.56e-0	0.00	90.00	76.09
H	In	2000	2.1191	0.3247	0.9816	1.65e-2	1.00	91.28	82.88
In	In	100	9.7358	5.6869	0.6304	2.97e-1	2.52	99.02	57.82
In	In	200	6.8624	3.9483	0.6930	7.49e-1	2.52	96.40	57.66
In	In	1000	3.8772	1.9659	0.7756	2.76e-0	2.52	92.87	62.12
H	Ta	25000	2.2410	0.1662	0.9913	1.95e-3	1.00	90.36	86.39
${}^4\text{He}$	Ta	100000	1.8527	0.1291	0.9751	2.05e-2	0.00	90.00	86.90
Ne	Ta	45000	2.0106	0.4231	0.9077	1.04e-0	0.00	90.00	80.32
Ar	Ta	1050	2.4778	1.1269	0.9297	9.69e-1	0.00	90.00	63.40
Kr	Ta	45000	2.3799	0.7121	0.8775	5.01e-0	0.00	90.00	75.03
H	W	500	2.5871	1.3240	0.9573	1.18e-5	1.00	92.56	60.99
H	W	550	2.0951	1.0881	0.9637	4.25e-5	1.00	92.44	60.36
H	W	600	2.1147	1.0569	0.9534	8.88e-5	1.00	92.34	61.71
H	W	700	1.5690	0.7245	0.9963	2.42e-4	1.00	92.16	64.02
H	W	800	1.9786	0.8800	0.9555	4.18e-4	1.00	92.02	65.34
H	W	900	1.3549	0.5469	0.9980	6.72e-4	1.00	91.91	67.62
H	W	1000	1.3708	0.4824	1.0067	8.64e-4	1.00	91.81	70.70
H	W	2000	1.3195	0.1490	1.0566	2.42e-3	1.00	91.28	83.01
H	W	4000	1.7762	0.1779	1.0283	3.46e-3	1.00	90.91	84.21
D	W	250	4.2860	2.9471	0.7250	2.34e-5	1.00	93.62	44.77
D	W	270	2.6708	1.6256	0.9398	7.63e-5	1.00	93.48	54.23
D	W	300	2.0195	1.1760	0.9927	2.08e-4	1.00	93.30	56.36
D	W	350	1.9721	1.1169	0.9762	5.98e-4	1.00	93.06	57.35
D	W	400	1.6044	0.8545	1.0054	1.11e-3	1.00	92.86	59.65
D	W	500	1.3909	0.6348	1.0216	2.20e-3	1.00	92.56	64.51
D	W	600	0.9409	0.3319	1.0655	3.39e-3	1.00	92.34	70.32
D	W	700	1.1523	0.3351	1.0523	4.22e-3	1.00	92.16	73.95
D	W	1000	1.1544	0.1901	1.0824	6.55e-3	1.00	91.81	80.04
T	W	170	4.0524	2.7547	0.8673	3.77e-5	1.00	94.39	48.03
T	W	180	2.0906	1.4464	0.9946	9.81e-5	1.00	94.26	48.35
T	W	200	2.1916	1.4650	0.9693	3.03e-4	1.00	94.04	49.93
T	W	250	1.6394	1.0231	1.0104	1.23e-3	1.00	93.62	53.51
T	W	300	1.5437	0.8764	1.0206	2.41e-3	1.00	93.30	57.48
T	W	400	1.2873	0.5691	1.0391	4.89e-3	1.00	92.86	65.52
T	W	500	1.1505	0.3777	1.0626	7.22e-3	1.00	92.56	71.95
T	W	700	1.0887	0.2120	1.0927	1.11e-2	1.00	92.16	78.51
T	W	1000	1.1499	0.1573	1.1050	1.49e-2	1.00	91.81	80.97

**Table 22.** Fitting values  $f, b, c$  for the angular dependence of the sputtering yield in (6). Furthermore, the values for the yield at normal incidence,  $Y(E_0, 0)$ , the binding energy,  $E_{sp}$ , for the projectiles, the value  $\theta_0^*$  (deg.), (7), and the angular position,  $\theta_{0m}$  (deg.), of the maximum yield, (8), are given

ion	target	$E_0$ (eV)	f	b	c	$Y(E_0, 0)$	$E_{sp}$ (eV)	$\theta_0^*$	$\theta_{0m}$
${}^4\text{He}$	W	130	3.9913	3.1578	0.8285	3.21e-5	0.00	90.00	34.58
${}^4\text{He}$	W	140	3.2148	2.5337	0.8598	1.32e-4	0.00	90.00	35.53
${}^4\text{He}$	W	150	2.0005	1.6150	0.9398	3.10e-4	0.00	90.00	35.12
${}^4\text{He}$	W	170	2.0656	1.6420	0.9004	9.50e-4	0.00	90.00	35.63
${}^4\text{He}$	W	200	1.2584	0.9604	0.9999	2.33e-3	0.00	90.00	40.25
${}^4\text{He}$	W	250	1.1950	0.8161	1.0037	5.42e-3	0.00	90.00	49.96
${}^4\text{He}$	W	300	1.1907	0.6873	1.0087	8.61e-3	0.00	90.00	54.77
${}^4\text{He}$	W	350	0.9696	0.4845	1.0304	1.21e-2	0.00	90.00	59.94
${}^4\text{He}$	W	400	1.2471	0.5171	1.0235	1.47e-2	0.00	90.00	65.30
${}^4\text{He}$	W	500	1.1760	0.3783	1.0397	2.03e-2	0.00	90.00	70.65
${}^4\text{He}$	W	600	1.3199	0.3561	1.0396	2.42e-2	0.00	90.00	73.61
${}^4\text{He}$	W	700	1.2670	0.3010	1.0461	2.88e-2	0.00	90.00	75.30
${}^4\text{He}$	W	1000	1.4993	0.3257	1.0302	3.78e-2	0.00	90.00	76.77
${}^4\text{He}$	W	1400	1.6342	0.3388	1.0143	4.57e-2	0.00	90.00	77.70
${}^4\text{He}$	W	2000	1.7995	0.3688	0.9903	5.15e-2	0.00	90.00	78.41
${}^4\text{He}$	W	5000	2.0005	0.3776	0.9353	5.91e-2	0.00	90.00	80.91
${}^4\text{He}$	W	10000	2.0468	0.3395	0.8989	5.63e-2	0.00	90.00	83.58
${}^4\text{He}$	W	20000	1.5332	0.1238	1.0084	4.78e-2	0.00	90.00	85.08
${}^4\text{He}$	W	50000	1.6774	0.1195	0.9966	3.23e-2	0.00	90.00	86.03
N	W	48	2.9557	5.8879	0.9465	1.82e-5	1.00	98.21	0.00
N	W	50	1.7735	4.3144	0.9468	5.70e-5	1.00	98.05	0.00
N	W	52	1.2707	3.6458	0.8840	1.35e-4	1.00	97.90	0.00
N	W	55	1.1002	3.3751	0.9604	3.60e-4	1.00	97.68	0.00
N	W	60	0.4622	2.5095	1.0118	9.73e-4	1.00	97.36	0.00
N	W	70	3.5011	4.1573	0.8630	3.26e-3	1.00	96.82	0.00
N	W	80	2.7960	3.4029	0.8841	7.00e-3	1.00	96.38	0.00
N	W	90	2.1152	2.6541	0.9226	1.17e-2	1.00	96.02	0.00
N	W	100	1.7312	2.1735	0.9489	1.72e-2	1.00	95.71	0.00
N	W	120	1.6230	1.6737	1.0004	2.77e-2	1.00	95.22	0.00
N	W	140	1.7195	1.5092	1.0176	3.99e-2	1.00	94.83	30.54
N	W	200	2.0738	1.3460	1.0316	7.57e-2	1.00	94.04	51.98
N	W	300	2.2531	1.2151	1.0310	1.32e-1	1.00	93.30	59.47
N	W	500	2.4324	1.1313	1.0171	2.13e-1	1.00	92.56	62.20
N	W	1000	2.4383	0.9940	0.9936	3.39e-1	1.00	91.81	66.00
Ne	W	45	1.4835	3.8004	0.8094	1.64e-5	0.00	90.00	0.00
Ne	W	50	0.2818	2.3919	0.9244	7.38e-5	0.00	90.00	0.00
Ne	W	60	0.1490	1.7027	0.9423	3.61e-4	0.00	90.00	0.00
Ne	W	70	1.0487	1.9268	0.8972	8.44e-3	0.00	90.00	0.00
Ne	W	80	0.4630	1.3150	0.9399	1.58e-2	0.00	90.00	0.00
Ne	W	100	0.7008	1.0256	0.9957	3.15e-2	0.00	90.00	0.00
Ne	W	140	1.3407	1.0746	0.9942	6.97e-2	0.00	90.00	36.63
Ne	W	200	1.9700	1.1784	0.9844	1.23e-1	0.00	90.00	53.20
Ne	W	300	2.1649	1.1382	0.9810	2.02e-1	0.00	90.00	58.30
Ne	W	400	2.3287	1.1413	0.9754	2.67e-1	0.00	90.00	60.74
Ne	W	500	2.4225	1.1426	0.9688	3.24e-1	0.00	90.00	62.01
Ne	W	700	2.2943	1.0333	0.9668	4.25e-1	0.00	90.00	63.45
Ne	W	1000	2.2664	0.9602	0.9638	5.33e-1	0.00	90.00	65.24

**Table 23.** Fitting values  $f, b, c$  for the angular dependence of the sputtering yield in (6). Furthermore, the values for the yield at normal incidence,  $Y(E_0, 0)$ , the binding energy,  $E_{\text{sp}}$ , for the projectiles, the value  $\theta_0^*$  (deg.), (7), and the angular position,  $\theta_{0m}$  (deg.), of the maximum yield, (8), are given

ion	target	$E_0$ (eV)	f	b	c	$Y(E_0, 0)$	$E_{\text{sp}}$ (eV)	$\theta_0^*$	$\theta_{0m}$
Ar	W	30	18.8008	14.3233	0.5298	1.03e-5	0.00	90.00	29.59
Ar	W	35	6.8215	6.2803	0.5504	1.17e-4	0.00	90.00	10.89
Ar	W	40	0.0399	1.2328	0.8651	4.63e-4	0.00	90.00	0.00
Ar	W	45	0.0200	0.9444	0.9324	1.26e-3	0.00	90.00	0.00
Ar	W	50	0.0092	0.7256	1.0034	2.85e-3	0.00	90.00	0.00
Ar	W	55	0.0177	0.5887	1.0523	5.23e-3	0.00	90.00	0.00
Ar	W	60	0.4625	0.7963	1.0148	8.40e-3	0.00	90.00	0.00
Ar	W	70	1.1976	1.1420	0.9778	1.75e-2	0.00	90.00	17.06
Ar	W	80	1.5694	1.2543	0.9772	2.86e-2	0.00	90.00	36.57
Ar	W	100	1.9354	1.3595	0.9674	5.60e-2	0.00	90.00	45.02
Ar	W	140	2.4932	1.5322	0.9542	1.16e-1	0.00	90.00	51.84
Ar	W	200	2.8464	1.6178	0.9437	2.01e-1	0.00	90.00	55.25
Ar	W	300	2.7481	1.4845	0.9442	3.36e-1	0.00	90.00	57.30
Ar	W	500	2.6042	1.3461	0.9401	5.62e-1	0.00	90.00	58.98
Ar	W	700	2.6193	1.3056	0.9333	7.25e-1	0.00	90.00	60.31
Ar	W	1000	2.4763	1.1745	0.9366	9.26e-1	0.00	90.00	62.00
Ar	W	1005	2.4753	1.1700	0.9371	9.39e-1	0.00	90.00	62.11
Ar	W	1050	2.4911	1.1739	0.9341	9.61e-1	0.00	90.00	62.22
Ar	W	30000	1.5166	0.2967	0.9875	2.59e-0	0.00	90.00	79.04
Xe	W	9500	2.1148	0.7406	0.9329	4.25e-0	0.00	90.00	70.47
Xe	W	30000	2.2644	0.7036	0.9115	5.94e-0	0.00	90.00	73.50
W	W	35	32.1495	16.2298	0.4627	2.13e-5	8.68	116.47	80.98
W	W	40	31.5560	16.1944	0.4990	5.60e-5	8.68	114.98	77.95
W	W	50	31.1720	16.3715	0.5115	1.92e-4	8.68	112.62	74.22
W	W	50	29.1892	14.9454	0.4922	1.77e-4	8.68	112.62	76.62
W	W	a 50	31.1660	16.1845	0.5159	1.92e-4	8.68	112.62	75.18
W	W	60	28.4556	15.0978	0.5159	5.89e-4	8.68	110.82	72.13
W	W	70	25.7454	13.7699	0.5175	1.51e-3	8.68	109.40	70.52
W	W	80	23.3907	12.5813	0.5156	3.15e-3	8.68	108.23	69.29
W	W	100	19.8712	10.8397	0.5208	9.54e-3	8.68	106.42	66.95
W	W	100	20.1422	10.9606	0.5241	9.26e-3	8.68	106.42	67.16
W	W	120	17.5207	9.6863	0.5251	2.04e-2	8.68	105.05	64.98
W	W	140	15.8372	8.8582	0.5403	3.58e-2	8.68	103.98	63.43
W	W	200	12.9717	7.4152	0.5705	9.68e-2	8.68	101.77	60.57
W	W	300	10.2481	5.9264	0.6168	2.28e-1	8.68	99.65	58.79
W	W	350	9.5022	5.4740	0.6363	2.92e-1	8.68	98.95	58.78
W	W	400	8.9966	5.1930	0.6532	3.59e-1	8.68	98.38	58.41
W	W	500	8.1383	4.6991	0.6674	4.97e-1	8.68	97.51	60.21
W	W	800	6.1837	3.4586	0.7349	8.47e-1	8.68	95.95	59.20
W	W	1000	5.6049	3.0949	0.7587	1.07e-0	8.68	95.32	59.35
W	W	1000	5.8226	3.2309	0.7429	1.04e-0	8.68	95.32	59.26
W	W	2000	4.4556	2.3233	0.7594	1.81e-0	8.68	93.77	61.45
W	W	2500	4.0991	2.0502	0.8270	2.10e-0	8.68	93.37	62.84
W	W	5000	3.6732	1.7278	0.8289	3.11e-0	8.68	92.39	64.62

**Table 24.** Fitting values  $f, b, c$  for the angular dependence of the sputtering yield in (6). Furthermore, the values for the yield at normal incidence,  $Y(E_0, 0)$ , the binding energy,  $E_{sp}$ , for the projectiles, the value  $\theta_0^*$  (deg.), (7), and the angular position,  $\theta_{0m}$  (deg.), of the maximum yield, (8), are given

ion	target	$E_0$ (eV)	f	b	c	$Y(E_0, 0)$	$E_{sp}$ (eV)	$\theta_0^*$	$\theta_{0m}$
H	Au	1000	1.1436	0.1758	1.0340	7.55e-3	0.00	90.00	80.23
H	Au	4000	1.7553	0.1874	1.0068	1.10e-2	0.00	90.00	83.65
D	Au	130	2.8168	2.1780	0.8276	2.44e-4	1.00	95.01	38.42
D	Au	140	2.1529	1.6150	0.9556	4.92e-4	1.00	94.83	42.96
D	Au	150	2.0274	1.5209	0.9366	7.96e-4	1.00	94.67	42.59
D	Au	160	1.9649	1.3976	0.9776	1.14e-3	1.00	94.52	46.64
D	Au	200	1.7254	1.1440	0.9847	3.05e-3	1.00	94.04	50.51
D	Au	250	1.9522	1.1324	0.9057	5.45e-3	1.00	93.62	56.45
D	Au	300	1.2658	0.5848	1.0421	7.84e-3	1.00	93.30	64.55
D	Au	500	0.9402	0.1928	1.1191	1.60e-2	1.00	92.56	77.78
D	Au	1000	1.3545	0.2159	1.0734	2.51e-2	1.00	91.81	80.27
D	Au	3000	1.6865	0.2338	0.9943	3.12e-2	0.00	90.00	82.20
Na	Au	30000	2.2786	0.6106	0.8236	2.20e-0	1.00	90.33	79.04
Ne	Au	6000	1.9240	0.6608	0.9121	2.18e-0	0.00	90.00	71.27
Ne	Au	14000	1.6611	0.4130	0.9587	2.31e-0	0.00	90.00	76.51
Ar	Au	1050	1.8345	0.9363	0.9395	2.24e-0	0.00	90.00	59.44
Ar	Au	3000	1.7776	0.7560	0.9330	3.52e-0	0.00	90.00	65.41
Ar	Au	6000	1.4391	0.4722	0.9762	4.28e-0	0.00	90.00	71.21
Ar	Au	10000	1.5072	0.4461	0.9697	4.74e-0	0.00	90.00	73.33
Ar	Au	30000	1.8818	0.5059	0.9221	5.11e-0	0.00	90.00	76.07
K	Au	30000	2.2529	0.3512	0.8527	4.72e-0	1.00	90.33	86.35
Xe	Au	10000	2.3259	0.9589	0.8569	8.88e-0	0.00	90.00	67.16
Kr	Hg	762	3.0516	1.4476	0.8695	1.06e-0	0.00	90.00	62.37
H	U	2000	1.2788	0.1275	1.0504	4.13e-3	1.00	91.28	82.73
Kr	U	17900	1.6156	0.4821	0.9436	5.76e-0	0.00	90.00	73.68

**Table 25.** Elemental targets for which measurements and static calculations (low fluence), not included in fits and figures, have been performed

target	ion	energy (keV)	angle (deg.)	meas.	calc.
Li	D,Li	0.075,0.125,0.2	0 - 89		[328]
Li	D,T,Li	0.01 - 10	0 - 85		[329]
Li	D, <sup>4</sup> He,Li	0.1 - 1	45	[46]	[46]
Li	D, <sup>4</sup> He,Li	0.7	45	[330]	[330]
Li	T	0.01 - 1	0 - 85		[331]
Li	Li	0.05 - 50	0		[332]
Be	D	0.01 - 0.7	45	[333]	[333]
Be	T	0.015 - 1	0 - 85		[331]
Be	Be	0.05 - 50	0		[332]
Be	Be	1, 3	0 - 85		[334]
B	B	1	0 - 85		[334]
C	H	0.3	0, 60		[335]
C	H,D,T	0.05 - 10	0		[336]
C	H,D,T, <sup>3</sup> He, <sup>4</sup> He	0.02 - 10	0 - 85		[331]
C	H, Xe	0.4,1,10,40	0,60,80		[28]
C	<sup>4</sup> He	0.1 - 9	0		[337]
C	C	0.03 - 10	0 - 85		[332,338]
C	C	0.1, 0.3	0 - 75		[335]
C	Ar	0.4, 10, 40	0, 60		[339]
C	Ar	1	0 - 85		[340]
C	Ar <sub>n</sub>	0.1/atom	0		[341]
C	C + Pt	0.3 - 1	0		[342]
Al	O	10	0	[158]	
Al	O	5	0	[343]	
Al	Ne,Al,Ar,Kr,Xe	10-50	0		[344]
Al	Al	0.025 - 0.09	0 - 90		[345]
Al	Ar	40	0 - 85		[346]
Al	Ar	3	0		[347]
Si	O	10	0	[158]	
Si	O	5	0	[343]	
Si	O,Ar	4.5,9	0 - 60	[242]	
Si	Ne	0.2 - 0.62	0		[348]
Si	Ne,Ar,Xe	0.5,1,5	60	[349]	[349]
Si	Si	0.05 - 100	0		[332]
Si	Si	0.5 - 5	0		[350]
Si	Si	0.03 - 10	0 - 89		[351]
Si	Si,Ar,Kr	0.04, 0.6	0		[348]
Si	Ar	3,5,10	0,45,60		[124]
Si	Ar	0.4,1	0		[339]
Si	Ar	0.2 - 100	0		[352]
Si	Ar	3	51		[353,354]
Si	Ar	0.15 - 3	0		[355]
Si	Ar	1.05	0 - 85		[356,357]
Si	Ar	5,10	0		[358,359]
Si	Ar	0.05 - 2			[360]
Si	Ar,Kr	1	0		[361]
Si	Xe	2 - 12	0	[362]	

**Table 26.** Elemental targets for which measurements and static calculations (low fluence), not included in fits and figures, have been performed

target	ion	energy (keV)	angle (deg.)	meas.	calc.
Ti	O	10	0	[158]	
Ti	$^4\text{He}$	0.15 - 10	0		[337]
V	O	10	0	[158]	
V	$^4\text{He}$	0.2 - 10	0		[363]
Cr	O	10	0	[158]	
Mn	O	10	0	[158]	
Fe	H,D,T, $^4\text{He}$	0.6 - 10	0		[270,364]
Fe	D	0.06 - 200	0		[365]
Fe	D	50,100,200	60,75,85		[365]
Fe	O	10	0	[158]	
Fe	Ar	0.3 - 5	0		[366]
Co	O	10	0	[158]	
Co	Ar	0.2 - 10			[367]
Co	Ar	1	0 - 85		[368]
Ni	H	50	0 - 85		[135]
Ni	H	0.45,1,4	0 - 80		[257]
Ni	H	0.1,0.2,0.45,1	0 - 85		[369,370]
Ni	H	1	0 - 80		[318]
Ni	H	4	80		[371]
Ni	H,D,T, $^4\text{He}$	0.1 - 10	0 - 85		[372]
Ni	H,D,T, $^4\text{He}$	0.05 - 8	0		[336]
Ni	H,D, $^4\text{He}$ ,Ne,Ar	0.15 - 100	0-87.5		[28,373]
Ni	D	0.08 - 50	0		[28,373]
Ni	D	1	0 - 85		[365]
Ni	$^4\text{He}$	100	0 - 80		[135]
Ni	$^4\text{He}$	0.03,0.1,1	0		[370]
Ni	$^4\text{He}$	4	0 - 85		[374]
Ni	$^4\text{He}$ ,Ne	1	0 - 80		[318]
Ni	$^4\text{He}$ ,Ne	0.1 - 100	0		[318]
Ni	Li,B,N,Ne,Al	0.15	0		[375,376]
Ni	O	10	0	[158]	
Ni	Ca,Ni,Ga,Kr,Xe	0.15	0		[375,376]
Ni	Ne	1	0-87.5		[28]
Ni	Ne	0.1 - 100	0 - 85		[377]
Ni	Ar	40	0 - 85		[346]
Ni	Ar	0.1 - 0.5	0		[134]
Ni	Ar	0.2	0	[378,379]	
Ni	Ar	0.5, 1	0 - 85		[340]
Ni	Ni	0.03 - 100	0 - 80		[332,380]
Ni	Ni	0.03,0.1,1	0		[370]
Ni	Xe	0.07 - 100	0-87.5		[28,318]

**Table 27.** Elemental targets for which measurements and static calculations (low fluence), not included in fits and figures, have been performed

target	ion	energy (keV)	angle (deg.)	meas.	calc.
Cu	H	50	0 - 78		[135]
Cu	D	30 - 300	0		[381]
Cu	<sup>4</sup> He	0.08 - 50	0		[337]
Cu	<sup>4</sup> He, Ne, Xe	3	0		[382,383]
Cu	<sup>4</sup> He, Ne, Kr, Xe	1	0		[352,358]
Cu	<sup>4</sup> He, N, Ne, Ar, Kr, Xe	0.5 - 2	0 - 70		[384]
Cu	O	10	0	[158]	
Cu	Ne	10	0		[385]
Cu	Ne, Xe	3	0		[382]
Cu	Ar	1 - 30	0		[383]
Cu	Ar	1.05	0 - 85		[356]
Cu	Ar	0.01 - 1	0 - 85		[370]
Cu	Ar	0.1 - 1.4	0		[352]
Cu	Ar	40	0 - 85		[346]
Cu	Ar	3,30,300	0		[382]
Cu	Ar	5	0		[386]
Cu	Ar	5	0		[387]
Cu	Ar	1	0 - 85		[368]
Cu	Ar	0.3	0 - 60		[388]
Cu	Ar, Cu	0.5 - 10	0		[389]
Cu	Ar, Xe	0.4,10,40	0,60		[339]
Cu	Cu	1	0		[358]
Zn	O, Ar	1	70	[210]	
Ga	D,T,Ga	0.02 - 10	0 - 80		[329]
Ga	D,Ga	0.075,0.125,0.2	0 - 89		[328]
Ga	O	5	0	[343]	
Ge	O a	10	0	[158]	
Ge	O	5	0	[343]	
Ge	Ar	0.4,1	0		[339]
Ge	Ar	1.05	0 - 85		[356,357]
Ge	Ge,Kr	0.1 - 0.62	0		[348]
Nb	H	16400	0		[186,390]
Nb	O	10	0	[158]	
Nb	Ar	20	0,45,77,85		[391]
Mo	H, <sup>4</sup> He	0.1 - 10	0		[270]
Mo	H,D, <sup>4</sup> He	50,100	0 - 75		[135]
Mo	H, D, T	2	0 - 85		[365,372]
Mo	D	0.06 - 200	0,60,75,85		[365]
Mo	D,T, <sup>4</sup> He	0.15 - 9	0		[336]
Mo	D,T,Mo	0.03 - 100	0 - 85		[392]
Mo	O	10	0	[158]	
Mo	Mo	0.05 - 100	0		[332]
Ag	<sup>4</sup> He,O,Ar,Xe	1	70	[210]	
Ag	O	10	0	[158]	
Ag	Ar	0.015,0.1,1	0		[370]
Ag	Ar	1.05	0 - 85		[356]
Ag	Xe	0.4,10	0		[339]

**Table 28.** Elemental targets for which measurements and static calculations (low fluence), not included in fits and figures, have been performed

target	ion	energy (keV)	angle (deg.)	meas.	calc.
Cd	O	5	0	[343]	
Cd	Ar, Xe	0.4,10,40	0		[339]
In	D,T,In	0.02 - 10	0 - 80		[329]
In	Ar	1	70	[210]	
Sn	H,D, <sup>4</sup> He	0.3 - 1	45	[393]	[393]
Sn	O	10	0	[158]	
Sn	O	5	0	[343]	
Ta	H	25	0 - 70		[135]
Ta	Ar	1.05	0 - 85		[356,357]
Ta	Li,B,N,Ne,Al	0.15	0		[375,376]
Ta	Ca,Ni,Ga,Kr,Xe	0.15	0		[375,376]
W	D	0.06 - 200	0,60,75,85		[365]
W	D,T,W	0.03 - 50	0 - 85		[392]
W	O	10	0	[158]	
W	W	0.03 -100	0 - 80		[332]
W	W	10	70		[358]
W	W	0.15 - 1	0, 20		[394]
Pt	Ne	0.03,0.1,1	0		[370]
Pt	Ar	0.2 - 50	0		[395]
Au	H, D, T	1	0 - 83		[372]
Au	D	0.15 - 20	0		[337]
Au	D,T, <sup>4</sup> He	0.1 - 8	0		[336]
Au	<sup>4</sup> He	0.15 - 9	0		[337]
Au	O	10	0	[158]	
Au	Ar	1	70	[210]	
Au	Ar	0.4,10	0,60		[339]
Au	Ar	0.02,0.1,1	0		[370]
Au	Xe	0.4,10	0,60		[339]
Au	Au	100	0		[396]
Au	Au	10 - 10000	0		[397]
U	U	0.05 - 9	0 - 85		[300]
U	U	0.1 - 10	0		[398]
U	U	0.05 - 100	0		[332]

**Table 29.** Elemental targets bombarded with metal ions for which experiments and/or static calculations (low fluence) have been performed

target	ion	energy (keV)	angle (deg.)	exp.	calc.
Be	C	3	0-70		[334]
Be	Hg	1	0	[399]	
C	Cd	0.1 - 0.5	0	[400]	
C	W	100	0	[290]	[290]
C	Hg	0.05-0.5	0	[401]	
C	Hg	5 - 100	0-60	[402]	
C	Hg	10 - 25	0	[403]	
C	Hg	0.4 - 10	0		[370,25]
Al	Au	50	0	[237]	
Al	Hg	0.5 - 3	0	[399]	
Al	Hg	0.125-0.35	0	[401,404]	
Al	Hg	0.4	0	[63]	
Al	Hg	20	0	[403]	
Al	Hg	0.07,0.2,1	0		[370]
Si	B	20,40,60	0		[405]
Si	Al	25,50,100,150	0		[405]
Si	P	25,50,100,150	0		[405]
Si	Ge	0.04 - 0.2	0		[348]
Si	As	25,50,100,150	0		[405]
Si	Cs	2 - 12	0-60	[362]	
Si	Au	50	0	[237]	
Si	Hg	1	0	[399]	
Si	Hg	0.125-0.35	0	[401]	
Si	Hg	0.4	0	[63]	
Si	Pb	25 - 500	0	[114]	
Si	Pb	0.03 - 20	0		[25,370]
Ti	Cd	0.1 - 0.5	0	[400,406]	
Ti	Hg	0.1 - 0.5	0	[401,404]	
Ti	Hg	4 - 14	0	[211]	
Ti	Hg	0.4	0	[63]	
Ti	Hg	0.04-0.28	0	[407]	
Ti	Hg	15,20,25	0	[403]	
V	Hg	0.125-0.35	0	[401]	
V	Hg	4 - 15	0	[211]	
V	Hg	0.4	0	[63]	
Cr	Hg	1	0	[399]	
Cr	Hg	0.1 - 0.3	0	[401,404]	
Cr	Hg	0.025-0.35	0	[142]	
Cr	Hg	0.05-0.23	0	[407]	
Mn	Hg	1	0	[399]	
Fe	Ti	110	0	[408]	
Fe	Ni	90	0	[139]	
Fe	Hg	0.5 - 4	0	[399]	
Fe	Hg	0.4,0.8	0-75	[409]	
Fe	Hg	1-100	0-60	[402]	
Fe	Hg	0.1 - 0.4	0	[401,404]	
Fe	Hg	4 - 15	0	[211]	
Fe	Hg	0.04-0.3	0	[407]	
Fe	Hg	20	0	[403]	

**Table 30.** Elemental targets bombarded with metal ions for which experiments and/or static calculations (low fluence) have been performed

target	ion	energy (keV)	angle (deg.)	exp.	calc.
Ni	Cu	90	0	[139]	[369,370]
	Hg	0.5 - 4	0	[399]	
	Hg	0.07-0.4	0	[401]	
	Hg	0.2,0.8	0-62	[409]	
	Hg	4 - 15	0	[211]	
	Hg	0.02-0.25	0	[407]	
	Hg	10 - 25	0	[403]	
	Hg	0.03 - 0.1	0-85		
Co	Hg	1	0	[399]	
	Hg	0.125-0.35	0	[401]	
	Hg	4 - 15	0	[211]	
	Hg	0.04-0.25	0	[407]	
Cu	Be	0.5, 1	0		[384]
	Na,Si,P,S,Cl,K	5-20	0	[262]	
	V,Bi	45	0	[410]	
	Ni	90	0	[139]	
	Zn,Cd,I,Hg,Tl	5-20	0-53	[262]	
	Co,Ni,Cd	39	0	[173,411]	
	Cd, Hg	0.1 - 0.5	0	[400]	
	Ag	0.5, 1	0		
	Hg	1	0	[399]	
	Hg	0.06-0.3	0	[401]	
	Hg	4 - 15	0	[211]	
	Hg	0.03-0.25	0	[407]	
	Hg	10 - 25	0-45	[403]	
	U	30	0	[108]	
Zn	Ni,Co,Cu,Cd	39	0	[173,176,411]	
Ge	Hg	0.125-0.4	0	[401]	
As	Ag	45,90	0	[139]	
Zr	Cd	0.1 - 0.5	0	[400,406]	
	Hg	1	0	[399]	
	Hg	0.1-0.4	0	[401]	
	Hg	0.04-0.28	0	[407]	
Nb	Br	100,70000	0	[193]	
	Hg	0.2 - 0.4	0	[401]	
	Hg	0.05-0.25	0	[407]	
Mo	Cd	0.1 - 0.5	0	[400]	
	Hg	0.5 - 4	0	[399]	
	Hg	0.15-0.8	0-65	[401,409]	
	Hg	4 - 15	0	[211]	
	Hg	0.04-0.26	0	[407]	
	Hg	15,20,25	0	[403]	
Rh	Hg	0.075-0.3	0	[401]	
	Hg	4 - 15	0	[211]	
Pd	Hg	1	0	[399]	
	Hg	0.075-0.3	0	[401]	
	Hg	4 - 15	0	[211]	

**Table 31.** Elemental targets bombarded with metal ions for which experiments and/or static calculations (low fluence) have been performed

target	ion	energy (keV)	angle (deg.)	exp.	calc.
Ag	Hg	1	0	[399]	[397]
	Hg	0.05-0.25	0-60	[401]	
	Hg	0.125	0-60	[409]	
	Hg	4 - 15	0	[211]	
	Hg	0.03-0.2	0	[407]	
	Hg	10 - 25	0	[403]	
	Bi	30	0		
Cd	Ni	39	0	[411]	
In	Hg	20	0	[403]	
Sn	Co,Cu,Cd	39	0	[411]	
Ho	Hg	20	0	[403]	
Hf	Hg	0.12-0.4	0	[401]	
Ta	Cd	0.1 - 0.5	0	[400]	
	Hg	1	0	[399]	
	Hg	0.11-0.35	0	[401]	
	Hg	0.4	0-70	[409]	
	Hg	4 - 15	0	[211]	
	Hg	0.04-0.26	0	[407]	
	Hg	10 - 25	0	[403]	
W	C	1, 6	0-70		[412]
	C	2.4	0	[413]	
	CH <sub>3</sub>	3.0	0	[413]	
	Cd	0.1 - 0.5	0	[400]	
	Hg	0.5 - 2	0	[399]	
	Hg	0.04-0.4	0	[401]	
	Hg	0.2-0.8	0-65	[409]	
	Hg	4 - 15	0	[211]	
	Hg	0.05-0.29	0	[407]	
Re	Hg	0.125-0.35	0	[401]	
Ir	Hg	0.1 - 0.3	0	[401]	
Pt	Hg	1	0	[399]	
	Hg	0.2	0-70	[409]	
	Hg	4 - 15	0	[211]	
	Hg	0.03-0.29	0	[407]	
Au	Al	50	0	[237]	[397]
	S	80000	0	[414]	
	Ni	69000	0	[414]	
	I	99000,198000	0	[414]	
	Hg	0.05-0.25	0	[401]	
	Hg	4 - 15	0	[211]	
	Hg	0.02-0.19	0	[407]	
	Bi	30	0		
Pb	Ni	39	0	[411]	
Th	Hg	0.1-0.42	0	[401]	
U	Hg	0.075-0.35	0	[401]	

**Table 32.** Crystalline targets for which experiments and/or static calculations (low fluence) have been performed

single crystal target	ion	energy (keV)	angle (deg.)	exp.	calc.
Be(001),(010),(110)	D, <sup>4</sup> He	0.1	0-80		[415]
Bn(0001)	Ar,Xe	0.3 - 3	0	[416]	[416]
Al(100)	Al	0.1 - 1.3	0		[417]
Al(111)	Al	0.025-0.15	0-90		[345]
Al(111)	Ar	3	0		[347]
Si	Ar	1	0-50	[418]	
Si(100)	Ar	0.5	45		[419]
Si(100),(110),(111)	Ar	40	0	[122]	
Si(111)	Ar	0.04 - 8	0		[420]
Si(111)	Ar	0.05-0.8	0	[421]	
Si(111)	Ar	1-5	0	[146]	
Si(111)	V,Co,Ni,Er	40	0	[422]	
Fe(001)	Ar	1	65		[311]
Ni(100)	Ar	0.2	0		[423]
Ni(100)	Ar	0.2	0		[424]
Ni(100)	Ar	1	0		[425]
Ni(100)	Ar	0.02-0.04	0		[426]
Ni(001)	Ar	1	0-75		[311]
Ni(001)	Ne	10	0-85		[312]
Ni(110)	Ar	15	30	[379,427]	
Ni(111)	Al	0.025-0.15	0-90		[345]
Ni <sub>3</sub> Al(100)	Al	0.5,1.3	0		[417]
Ni <sub>0.35</sub> Fe <sub>0.65</sub> (111)	Ne	10	45	[428]	
minerals(001)	<sup>4</sup> He,N,Ne,Ar,Xe	50	0-60	[429]	

**Table 33.** Crystalline targets for which experiments and/or static calculations (low fluence) have been performed

single crystal target	ion	energy (keV)	angle (deg.)	exp.	calc.
Cu(111)	<sup>4</sup> He,B,Ne,Ar,Xe	3	0		[347,430]
Cu(111)	Ne,Ar	0.6, 5	0		[431]
Cu(100),(110),(111)	Ar	1-20	0		[432]
Cu(100)	Ar	5	0		[433]
Cu(100)	Ar	20	29-61		[433]
Cu(100),(110),(111)	Ar	0.6	0		[434]
Cu(100)	Ar	0.6	0		[435]
Cu(100),(111)	Ar	0.6-20	0		[436,437]
Cu(100)	Ar	5	0		[438]
Cu(100)	Ar	0.6	0-60		[439]
Cu(100),(111)	Ar,Kr,Xe	0.6,5	0		[440]
Cu(111)	Ar	1-10	0		[358]
Cu(100)	Ar	40	1-8		[441]
Cu(100)	Ar	27	0-75		[442]
Cu(100)	Ar	1.05,5	0-85		[443]
Cu(100)	Ar	0.1,0.5	0		[444]
Cu(100)	Ar	27	0-87		[445,446]
Cu(100),(110),(111)	Ar	0.2,5	0		[447]
Cu(100)	Ar	0.5,5	0-85		[279]
Cu(001)	Ar	0.05-0.6	0		[448]
Cu(100)	Ar	0.05-1	0		[449]
Cu(100),(110),(111)	Ar	0.5-5	0		[278]
Cu(122)	Ar	0.5-5	0		[278]
Cu(001)	Ar	0.06-0.6	0		[450]
Cu(111),(113),(122)	Ar	0.5-5	0	[146]	
Cu(123),(011),001)	Ar	0.5-5	0	[146]	
Cu(012)	Ar	0.5-5	0	[146]	
Cu(111)	Ar,Cu	0-0.25	0-85		[451]
Cu(001)	Ar	20, 30	0-41		[452,453]
Cu(001)	Ar	0.01-2.5	0		[454]
Cu(100)	Ar,Kr,Xe	5	60-70		[455]
Cu(100)	Ar	5	0-48		[456]
Zn(1000),(1010),(1120)	Ar	3	0		[278]
Ge(100),(110),(111)	Ar	1-5	0	[146]	
Ge(100),(110),(111)	Ar	40	0	[122]	
Ge(100),(110),(111)	Ge	50	0	[402]	
Gd(0001)	Ne	20	30	[379,457]	
Pt(111)	Ne,Ar,Xe	0.04-5	0		[458]
Pt(111)	Xe	5	0-85		[459]
Pt(100)	Pt	0.1-200	0		[460]
Pt(111)	Pt	0.1-200	0		[461]
Au(100)	Be,N,Ne,Cu	0.1 - 2	0		[462]
Au(111)	Ar	3	0		[347]
Au(100)	Mo,Xe,Er,Au	0.1 - 2	0		[462]
Au(111),(001)	Au	0.5-500/nucl.	0		[463]
Pb/CU(100)	Ar	3	0		[464]

**Table 34.** Compound targets for which experiments and/or static calculations (low fluence) have been performed

compound	ion	energy (keV)	angle (deg.)	exp.	calc.
LiF	Ar	0.01-5	0	[129,465]	[466]
Be <sub>4</sub> B	H,D, <sup>4</sup> He	0.05-4	0	[27,467]	
Be <sub>2</sub> C	D	0.02-2	0		[47]
Be-C	Be	0.3-5	0	[62]	
Be-W	Be	0.3-5	0	[62]	
<sup>10</sup> B <sub>0.2</sub> <sup>11</sup> B <sub>0.8</sub>	<sup>4</sup> He,Ar,Kr,Xe	0.07-2	60		[293]
B <sub>4</sub> C	H	0.06-8	0	[69]	
B <sub>4</sub> C	H,D, <sup>4</sup> He	0.1-4	0	[27,72]	[27]
B <sub>4</sub> C	H,D, <sup>4</sup> He	0.06-8	0-75	[27,51,111]	
B <sub>4</sub> C	H,D, <sup>4</sup> He	0.025-8	0-85		[27,36]
B <sub>4</sub> C	D, <sup>4</sup> He	0.03-10	0		[468]
B <sub>4</sub> C	Ne	0.15-10	0	[27,66]	
B <sub>4</sub> C	C,O, Ne	0.015-3	0-80		[27,36]
B <sub>4</sub> C	Cd	0.1-0.5	0	[400]	
BN	Ar	0.3-5	0,45	[469]	[469]
BN	Ar	0.3-10	0,45		[470,471]
BN	B,N,Ne,Ar,Kr,Xe	0.15-10	0,45	[472]	[472]
BN	Li,B,N,Ne,Al	0.2-2	0		[375,376]
BN	Ca,Ni,Ga,Kr,Xe	0.2-2	0		[375,376]
BeO	H,D, <sup>4</sup> He	0.05-4	0	[27,50,51,252]	
BeO	D	0.33-3.33	0	[75]	
BeO	O	0.1-10	0-85		[27,36]
B <sub>2</sub> O <sub>3</sub>	O	0.15-3	0		[27,36]
B(OH) <sub>3</sub>	O	0.15-3	0		[36]
C/USB15	D	0.01-3	0-80	[27]	[27]
SAP	H,D, <sup>4</sup> He	0.25-8	0	[51,473]	
MgO	Ar	3-25	0	[474]	
MgO	Ar	0.05-1	0	[129]	
AlN	Ar	0.3-5	0,45	[469]	[469]
AlN	Ar	0.3-10	0,45		[470,471]
Al <sub>2</sub> O <sub>3</sub>	H,D, <sup>4</sup> He	0.10-8	0	[27,51,473]	
Al <sub>2</sub> O <sub>3</sub>	Ar	3-25	0	[474]	
Al <sub>2</sub> O <sub>3</sub>	Xe <sup>q+</sup>	0.1-1.5	0	[475]	
Al on metals	<sup>4</sup> He,Ne,Ar,Kr,Xe	0.3,0.5	0		[288]
SiC	H	0.6-20	0	[69]	
SiC	H	5, 7.5	0	[68]	
SiC	H,D, <sup>4</sup> He	0.10-8	0-80	[27,51,72,111]	
SiC	H,D, <sup>4</sup> He	0.10-8	0	[52]	
SiC	D, <sup>4</sup> He	0.02-10	0		[468]
SiC	O,Ne	0.15-10	0	[27,78]	
SiC	Ar,Xe	0.5-5	60,80	[349]	[349]
Si <sub>3</sub> N <sub>4</sub>	H	0.1-1	0	[127]	
Si <sub>3</sub> N <sub>4</sub>	Ar,Kr	0.5-2.5	0?	[126]	
SiO <sub>2</sub>	H,D, <sup>4</sup> He	0.06-8	0	[27,51]	
SiO <sub>2</sub>	Ar	3-40	0-70	[474]	
SiO <sub>2</sub>	Ar	0.06-1	0	[129]	
SiO <sub>2</sub>	Ar,CF <sub>4</sub>	0.07-1.5	0	[125]	
SiO <sub>2</sub>	Ar,Kr	0.5-2.5	0?	[126]	

**Table 35.** Compound targets for which experiments and/or static calculations (low fluence) have been performed

compound	ion	energy (keV)	angle (deg.)	exp.	calc.
TiH <sub>2</sub>	H	0.1	0		[476]
TiB <sub>2</sub>	H,D, <sup>4</sup> He	0.20-8	0	[27]	
TiB <sub>2</sub>	<sup>4</sup> He	3-20	0	[477]	
TiB <sub>2</sub>	<sup>4</sup> He	0.02-25	0		[468]
TiB <sub>2</sub>	Cd	0.1-0.5	0	[406]	
TiC	H,D, <sup>4</sup> He	0.10-8	0	[27,72]	
TiC	H,D, <sup>4</sup> He	0.10-8	0-80	[27,51,111]	
TiC	D	0.02-40	0		[398]
TiC	D	0.4-10	0	[478]	
TiC	D	2	0	[132]	
TiC	D, <sup>4</sup> He	1.5-60	0	[477]	
TiC	D, <sup>4</sup> He	0.02-80	0		[468]
TiC	O,Ne	0.15-10	0	[27,78]	
TiC	Cd	0.1 - 0.5	0	[400]	
Ti <sub>x</sub> C <sub>y</sub>	H	0.5,6	0,30		[36]
TiN	N,Ar	0.4-0.7	0	[138]	[138]
TiN	Cd	0.1-0.5	0	[406]	
Ti <sub>x</sub> Al <sub>y</sub>	O	9.25	0	[479]	
VC	Cd	0.1 - 0.5	0	[400]	
VN	Cd	0.1 - 0.5	0	[406]	
VSi <sub>2</sub>	Kr	0.2	0		[480]
Cr <sub>3</sub> C <sub>2</sub>	Cd	0.1 - 0.5	0	[400]	
FeH, FeH <sub>2</sub> , FeT	H	0.1, 0.5	0		[476]
SS	H	0.6-20	0	[69]	
SS	H	0.5-7.5	0	[68]	
SS	H	0.4-1	0	[154]	
SS	H,D, <sup>4</sup> He	0.10-8	0	[27,51,153]	
SS	D	0.33-10	0	[75]	
SS	D	5-30	0	[220]	
SS	O	0.10-10	0	[27,78]	
SS	H,D, <sup>4</sup> He	0.08-10	0	[145]	
SS304	H,D, <sup>4</sup> He,Ne,Ar	1-20	0	[481]	
SS	N,Ne,Ar	25	0	[99]	
SS	Ar	1-5	0	[146]	
Inconel	H,D, <sup>4</sup> He	0.07-8	0	[51,153]	
Inconel	D, <sup>4</sup> He	0.10-10	0	[145]	
Inconel	Hg	0.1-0.3	0	[404]	
K-Monel	Hg	0.15-0.3	0	[404]	
S-Monel	Hg	0.1-0.3	0	[404]	
NiCroFer	H,D, <sup>4</sup> He	0.07-8	0	[51,153]	
B <sub>20</sub> Fe <sub>40</sub> Ni <sub>40</sub>	<sup>4</sup> He	2-20	0	[482]	
Cu/Li	D, <sup>4</sup> He,Ne,Ar	0.1-8	0	[483,484]	[483,484]

**Table 36.** Compound targets for which experiments and/or static calculations (low fluence) have been performed

compound	ion	energy (keV)	angle (deg.)	exp.	calc.
GaN	Ar	0.15-0.6	0	[485]	
	Ar	0.3-10	0,45		[470]
	Ar	0.3-3	0,45	[471]	[471]
	Li,B,N,Ne,Al	0.2-2	0		[376]
	Ca,Ni,Ga,Kr,Xe	0.2-2	0		[376]
GaP	Ar	0.15-0.6	0	[485]	
GaAs	Ar	0.15-0.6	0	[485]	
	Ar	0.03-1	0	[129]	
	Ar	0.3	0-85		[355]
	Cs	8	0-60	[362]	
GaSb	Ar	0.15-0.6	0	[485]	
ZrB <sub>2</sub>	Cd	0.1-0.5	0	[406]	
	H,D, <sup>4</sup> He	0.12-8	0	[27,51]	
	Cd	0.1-0.5	0	[400]	
	Cd	0.1-0.5	0	[406]	
NbB <sub>2</sub>	D	0.40-8	0-70	[257]	[257]
NbC	Cd	0.1-0.5	0	[400]	
MoSi <sub>2</sub> <sup>92</sup> Mo <sup>100</sup> Mo MoW	Cd	0.1-0.5	0	[406]	
	Ar,Xe	5,10	0-85		[189]
	Cd	0.1-0.5	0	[406]	
InP	Ar	0.15-0.6	0	[485]	
InAs	Ar	0.15-0.6	0	[485]	
Sn-Li Sn <sub>0.8</sub> Li <sub>0.2</sub>	D, He,Li	0.2-1	45	[486]	[486]
	D	0.5	0		[487]
LaB <sub>6</sub>	Cd	0.1-0.5	0	[406]	
TaC	H,D, <sup>4</sup> He	0.40-8	0	[27,51,111]	
	<sup>4</sup> He	0.15-10	0,30		[34]
	<sup>4</sup> He	1	0		[294]
	Ne	0.07-50	0-90		[293,488]
	Cd	0.1-0.5	0	[400]	
	H,D, <sup>4</sup> He	0.50-8	0	[27,51]	
Ta <sub>2</sub> O <sub>5</sub>	H,D, <sup>4</sup> He,Ne	2-15	0	[10]	
WC WC W <sub>x</sub> C <sub>1-x</sub> WC WC W <sub>x</sub> C <sub>1-x</sub> W <sub>x</sub> C <sub>1-x</sub> WN WO <sub>3</sub> WO <sub>3</sub> W <sub>x</sub> O <sub>y</sub>	H,D, <sup>4</sup> He	0.20-8	0	[27,51,111]	
	<sup>4</sup> He	0.02-15	0		[293,468]
	<sup>4</sup> He	1	30		[293]
	<sup>4</sup> He	0.20-15	0		[27]
	<sup>4</sup> He,Xe	0.07-15	30		[293]
	D	0.07-0.2	0		[489]
	<sup>4</sup> He	1	30		[293]
	N	10	0,45,70		[490]
	O,Ne,Kr	0.05-10	0-85		[36]
	O	0.50-6	0		[36]
	O	0.10-5	0		[36]
UF <sub>4</sub>	O,F,Ne	100,1.2-3 MeV	0	[491]	
glasses minerals	<sup>4</sup> He,N,Ne,Ar,Xe	50, 70, 100	0-60	[429]	
	<sup>4</sup> He,N,Ne,Ar,Xe	50	0-60	[429]	



# Index

- adatom, 67
- adsorption of
  - oxygen, 2
  - water, 2
- angular dependence of the sputtering yield
  - Ag, 86
  - Al, 72
  - Au, 89–91
  - Be, 70
  - C, 70–72
  - Cu, 77–81, 94
  - Fe, 73
  - Mo, 83–85
  - Nb, 82
  - Ni, 74–76
  - Pd, 87
  - Si, 72
  - Ta, 87
  - Ti, 73
  - W, 88
  - Zr, 82
- annealing, 99
- backscattering, 3
- Bayesian statistics, 7
- BCA program
  - ACAT, 3, 101
  - MARLOWE, 93, 101
  - Monte Carlo (MC), 91, 99–101
  - TRIDYN, 4, 96
  - TRIM, 101
  - TRIM.SP, 3, 68, 100
- binary collision approximation (BCA), 3
- catcher foils, 2
- channeling, 8, 99
- composition
  - change, 5, 94
- compound formation, 94
- crater
  - depth, 2
- depth
  - distribution, 95, 96
- depth of origin, 101
- diffusion, 94–96, 99
- electrical resistivity, 2
- electron microprobe, 2
- energy dependence of the sputtering yield
  - Ag, 3, 4, 45, 46
  - Al, 15, 16
  - Au, 61, 62
  - B, 11
  - Be, 9, 10
  - Bi, 63
  - C, 12, 13
  - Ca, 18
  - Cd, 47
  - Co, 27, 28
  - Cr, 23, 24
  - Cs, 49
  - Cu, 31, 32
  - Fe, 25, 26
  - Ga, 33
  - Ge, 33, 34
  - Hf, 51
  - Hg, 63
  - In, 47
  - Ir, 58, 60
  - Li, 8
  - Mg, 14
  - Mn, 24

- Mo, 7, 39, 40
- Nb, 37, 38
- Ni, 5, 29, 30
- Os, 57
- Pb, 64
- Pd, 43, 44
- Pt, 59, 60
- Re, 56
- Rh, 42
- Ru, 41
- Sb, 49
- Sc, 18
- Se, 36
- Si, 17, 18
- Sm, 50
- Sn, 48
- Ta, 52, 53
- Tb, 50
- Te, 49
- Th, 65
- Ti, 19, 20
- Tl, 63
- Tm, 50
- U, 66, 67
- V, 21, 22
- W, 54, 55
- Zn, 33
- Zr, 35, 36
- energy loss
  - electronic, 3, 4, 6, 67
- Lindhard-Scharff model, 3
- Oen-Robinson model, 3
- escape time, 101
- evaporation, 99
- field ion microscopy (FIM), 3
- fluctuation, 100
- fluence, 4, 6, 94–97
- fractionation, 98, 99
- heat of sublimation, 3, 92, 99
- implantation, 96
- interaction potential, 3, 4, 6, 67, 99
  - Nakagawa-Yamamura, 3
  - power, 98, 101
  - screened Coulomb
    - KrC (WHB), 3, 6
    - Molière, 3
- ZBL, 3
- isotope sputtering, 98, 99
- lattice vibration, 99
- mass change, 2
- molecular dynamics, 99
- negative binomial distribution, 100, 101
- neutron activation, 3
- oscillations, 96
- partial sputtering yield, 94
- planetary science, 99
- Poisson distribution, 100
- preferential sputtering, 96, 97
- projectile binding energy, 69
- reduced energy, 6
- reflection coefficient, 94, 95
- refraction, 68
- regime
  - deposition, 95
  - erosion, 95, 96
- screening length, 3, 6
- segregation, 94, 96, 99
- selfsputtering, 68, 69, 95, 96
- sheath potential, 97
- simultaneous bombardment, 97
- solid-liquid transition, 99
- spike
  - elastic collision, 68
- sputtering yield, 2–4
- sputtering yield oscillations, 96
- state
  - charge, 97
  - ferromagnetic, 99
  - magnetic, 99
  - paramagnetic, 99
  - steady, 1, 94–98
- sticking, 3
- stoichiometry, 96
- stopping power
  - nuclear, 6
- surface
  - roughness, 2, 6, 67, 91, 95, 100
- surface binding energy, 3, 67, 92, 97, 99

- target
    - amorphous, 3, 8
    - composition, 97
    - compound, 96, 97
    - multicomponent, 94, 99
    - polycrystalline, 3, 8
    - randomized, 99
    - single crystal, 3, 8, 94, 99
  - target structure
    - amorphous, 1
  - crystalline, 1
  - polycrystalline, 1
- threshold energy, 6, 69, 92, 93
- tunneling microscope, 91
- vaporization, 99
- Wehner spot, 99
- x-ray analysis, 2